National Library of Canada
Bibliothèque nationale du Canada

Canadian Theses Service
Service des thèses canadiennes

Ottawa, Canada
K1A 0N4

NOTICE

The quality of this microform is heavily dependent upon the quality of the original thesis submitted for microfilming. Every effort has been made to ensure the highest quality of reproduction possible.

If pages are missing, contact the university which granted the degree.

Some pages may have indistinct print especially if the original pages were typed with a poor typewriter ribbon or if the university sent us an inferior photocopy.

Reproduction in full or in part of this microform is governed by the Canadian Copyright Act, R.S.C. 1970, c. C-30, and subsequent amendments.

AVIS

La qualité de cette microforme dépend grandement de la qualité de la thèse soumise au microfilmage. Nous avons tout fait pour assurer une qualité supérieure de reproduction.

S'il manque des pages, veuillez communiquer avec l'université qui a conféré le grade.

La qualité d'impression de certaines pages peut laisser à désirer, surtout si les pages originales ont été dactylographiées à l'aide d'un ruban usé ou si l'université nous a fait parvenir une photocopie de qualité inférieure.

La reproduction, même partielle, de cette microforme est soumise à la Loi canadienne sur le droit d'auteur, SRC 1970, c. C-30, et ses amendements subséquents.

NL-339 (r. 88/04) c

Canada

THE UNIVERSITY OF ALBERTA

REACTIVITY AT ADJACENT METAL CENTERS: MODELS FOR BINUCLEAR HYDROGENATION CATALYSTS

by

Brian Anthony Vaartstra

A THESIS

SUBMITTED TO THE FACULTY OF GRADUATE STUDIES AND RESEARCH IN PARTIAL FULFILMENT OF THE REQUIREMENTS FOR THE DEGREE OF DOCTOR OF PHILOSOPHY

DEPARTMENT OF CHEMISTRY

EDMONTON, ALBERTA

SPRING, 1989

National Library of Canada
Bibliothèque nationale du Canada

Canadian Theses Service
Service des thèses canadiennes

Ottawa, Canada
K1A 0N4

The author has granted an irrevocable non-exclusive licence allowing the National Library of Canada to reproduce, loan, distribute or sell copies of his/her thesis by any means and in any form or format, making this thesis available to interested persons.

L'auteur a accordé une licence irrévocable et non exclusive permettant à la Bibliothèque nationale du Canada de reproduire, prêter, distribuer ou vendre des copies de sa thèse de quelque manière et sous quelque forme que ce soit pour mettre des exemplaires de cette thèse à la disposition des personnes intéressées.

The author retains ownership of the copyright in his/her thesis. Neither the thesis nor substantial extracts from it may be printed or otherwise reproduced without his/her permission.

L'auteur conserve la propriété du droit d'auteur qui protège sa thèse. Ni la thèse ni des extraits substantiels de celle-ci ne doivent être imprimés ou autrement reproduits sans son autorisation.

ISBN 0-315-52976-8

Canada

THE UNIVERSITY OF ALBERTA

RELEASE FORM

NAME OF AUTHOR: Brian Anthony Vaartstra

TITLE OF THESIS: Reactivity at Adjacent Metal Centers: Models for Binuclear Hydrogenation Catalysts

DEGREE: Ph.D.

YEAR THIS DEGREE GRANTED: 1989

Permission is hereby granted to THE UNIVERSITY OF ALBERTA LIBRARY to reproduce single copies of this thesis and to lend or sell such copies for private, scholarly or scientific research purposes only.

The author reserves other publication rights, and neither the thesis nor extensive extracts from it may be printed or otherwise reproduced without the author's written permission.

(Signed) B.A. Vaartstra

Permanent Address:

7809 - 102 avenue

Edmonton, Alberta, Canada

Date: 19 April 1989

THE UNIVERSITY OF ALBERTA

FACULTY OF GRADUATE STUDIES AND RESEARCH

The undersigned certify that they have read, and recommend to the Faculty of Graduate Studies and Research for acceptance, a thesis entitled Reactivity at Adjacent Metal Centers: Models for Binuclear Hydrogenation Catalysts submitted by Brian Anthony Vaartstra in partial fulfilment of the requirements for the degree of Doctor of Philosophy.

Martin Cowie
(Supervisor)

Alan L Balch

Janet Ibers

Richard Puddephatt

Byron Kratochvil

Date: 14 April 1989

To my wife, Bev.

ABSTRACT

The complexes, $[Ir_2I_2(CO)(\mu\text{-}CO)(DPM)_2]$, $[Ir_2(CO)_2(\mu\text{-}I)(DPM)_2][BF_4]$, $[RhIrCl_2(CO)_2(DPM)_2]$, $[RhIr(CO)_2(\mu\text{-}Cl)(DPM)_2][BF_4]$ and $[RhIr(CO)_2(\mu\text{-}S)(DPM)_2]$ (DPM = bis(diphenylphosphino)methane) have been prepared and their reactions with CO and alkynes investigated. The X-ray structure determination of $[Ir_2I_2(CO)(\mu\text{-}CO)(DPM)_2]$ reveals an unusual unsymmetrical geometry. All of the above complexes react reversibly with CO, yielding tricarbonyls, and an additional unstable tetracarbonyl complex results in the case of $[RhIrCl_2(CO)_2(DPM)_2]$ and $[RhIr(CO)_2(\mu\text{-}Cl)(DPM)_2][BF_4]$. Reactions with activated alkynes, dimethylacetylenedicarboxylate (DMA) or hexafluoro-2-butyne (HFB), give products which contain one molecule of the alkyne, bridging the metals as a cis-dimetallated olefin.

The sulfide-bridged complexes, $[Ir_2(CO)_2(\mu\text{-}S)(DPM)_2]$ and $[RhIr(CO)_2(\mu\text{-}S)(DPM)_2]$ react reversibly with DMA and HFB yielding complexes in which the alkyne moiety is terminally bound at an iridium center. The X-ray structure of $[Ir_2(CO)(\eta^2\text{-}HFB)(\mu\text{-}S)(\mu\text{-}CO)(DPM)_2]$ confirms this structural assignment.

The reactions of neutral and cationic binuclear complexes with dihydrogen are studied, with the results leading to a proposed mechanism for hydride rearrangement in A-frame complexes. The reaction of $[Ir_2(CO)_2(\mu\text{-}S)(DPM)_2]$ with H_2 reveals the formation of three dihydride products over time. These products correspond to stepwise rearrangement of the hydrido ligands from the pocket of the A-frame (between the metals) to the outsides, adjacent to the sulfide-bridge. The complexes,

$[RhIrCl_2(CO)_2(DPM)_2]$, $[RhIr(CO)_2(\mu\text{-}Cl)(DPM)_2][BF_4]$ and $[RhIr(CO)_2(\mu\text{-}S)(DPM)_2]$, react with H_2 yielding dihydrides in which the hydrido ligands are primarily bound to iridium, as substantiated by the crystal structure determination of $[RhIr(H)_2(CO)_2(\mu\text{-}Cl)(DPM)_2][BF_4]$. The iodo complexes do not exhibit hydride rearrangement upon reaction with H_2, with $[Ir_2I_2(CO)(\mu\text{-}CO)(DPM)_2]$ giving an equilibrium mixture of two dihydrides, $[Ir_2I_2(H)_2(CO)_2(DPM)_2]$ and $[Ir_2(H)_2(CO)(\mu\text{-}I)(DPM)_2][I]$. Reaction of $[Ir_2(CO)_2(\mu\text{-}I)(DPM)_2][BF_4]$ with excess H_2 yields a tetrahydride, but undergoes facile loss of both HI and H_2.

Reaction of $[Ir_2(H)_2(CO)_2(\mu\text{-}Cl)(DPM)_2][BF_4]$ with DMA in THF yields $[Ir_2(CH_3CO_2C{=}C(H)CO_2CH_3)_2(CO)_2(\mu\text{-}Cl)(DPM)_2][BF_4]$, which subsequently adds H_2 giving the structurally characterized dihydrido-dialkenyl species, $[Ir_2(H)_2Cl(CH_3CO_2C{=}C(H)CO_2CH_3)_2(CO)_2(DPM)_2][BF_4]$. Although this species does not eliminate the hydrogenated substrate, the same reaction using phenylacetylene does produce styrene. Based on these data, a mechanism is proposed by which the hydrogenation occurs. The same reaction with 2-butyne or ethylene immediately gives hydrogenated products by an intermolecular pathway.

Reaction of $[Ir_2I_2(CO)(\mu\text{-}CO)(DPM)_2]$ with atmospheric oxygen yields $[Ir_2I_2(CO)_2(\mu\text{-}O_2)(DPM)_2]$. An X-ray structure determination reveals a peroxo-bridged metal-metal bond. This peroxo species is reactive toward H^+, NO_2 and SO_2.

Acknowledgements

I wish to express my gratitude to Professor Martin Cowie for his expert direction during the course of this work, for his enthusiasm toward research, and for his "lighter side" which contributed to an enjoyable working environment.

I thank my fellow coworkers in the group and in the department for many helpful discussions, technical assistance and friendship, especially the following: Jim Jenkins, Bob McDonald, Dr. Steve Sherlock, Dr. Al Hunter, Dietmar Kennepohl, Gord Nicol, and Richard Krentz.

I thank my family, especially my parents, for their prayers, support and encouragement over the many years of my education.

I also thank the Sandstra family for their prayers and support.

Special thanks goes to my son, Matthew, for that extra joy which he brought into my life, from the miracle of his birth, to the excitement and love he expressed after patiently waiting for Daddy to come home.

Very special thanks and appreciation go to my dear wife, Bev, who provided me with so much encouragement and support, and took on the added load at home. Her patience and determination were a great asset to the success of this work, and her faith and prayers were sustaining.

Finally, I give thanks to God for those whom I have just mentioned, for the talents He has given me, and for the wonder of His creation which manifests itself in the field of chemistry.

TABLE OF CONTENTS

CHAPTER 1

INTRODUCTION 1

References and Footnotes 19

CHAPTER 2

BINUCLEAR IODOCARBONYL COMPLEXES OF IRIDIUM: REACTIVITIES WITH CARBON MONOXIDE AND DIMETHYL-ACETYLENEDICARBOXYLATE, AND THE UNUSUAL STRUCTURE OF $[Ir_2I_2(CO)(\mu\text{-}CO)(DPM)_2]\cdot CH_2Cl_2$ 27

Introduction 27

Experimental Section 28

General Experimental Conditions 28

Preparation of Compounds 29

Reactions with Carbon Monoxide 32

Reactions with Dimethylacetylenedicarboxylate 33

X-ray Data Collection 34

Structure Solution and Refinement 37

Results and Discussion 41

(a) Description of Structure 41

(b) Description of Chemistry 48

Conclusions 58

References and Footnotes 60

CHAPTER 3

THE PREPARATION OF HETEROBINUCLEAR RHODIUM/IRIDIUM

COMPLEXES AND THEIR REACTIONS WITH CARBON MONOXIDE AND ACTIVATED ALKYNES 63
Introduction 63
Experimental Section 65
Preparation of Compounds 65
Reactions with CO 71
Reaction of Compound 3 with Activated Akynes 72
Results and Discussion 72
Conclusions 87
References and Footnotes 89
CHAPTER 4
BINUCLEAR DIIRIDIUM AND MIXED-METAL RHODIUM-IRIDIUM COMPLEXES CONTAINING TERMINAL η^2-ALKYNES: THE STRUCTURE OF $[Ir_2(CO)(\eta^2\text{-}F_3CC{\equiv}CCF_3)(\mu\text{-}S)(\mu\text{-}CO)(DPM)_2]\cdot CH_2Cl_2$ 92
Introduction 92
Experimental Section 94
Preparation of Compounds 95
X-ray Data Collection 97
Structure Solution and Refinement 98
Results and Discussion 98
(a) Description of Structure 98
(b) Description of Chemistry 111
Conclusions 119
References and Footnotes 121

CHAPTER 5

FACILE HYDRIDE REARRANGEMENTS IN A-FRAME AND RELATED COMPLEXES AND THE STRUCTURE OF $[RhIr(H)_2(CO)_2(\mu\text{-}Cl)(DPM)_2][BF_4]\cdot CH_2Cl_2$, THE PRODUCT OF H_2 ADDITION AT ONE METAL CENTER IN THE A-FRAME POCKET.....123

Introduction 123

Experimental Section 125

H/D Exchange Promoted by Compounds 1 and 5c.....125

Preparation of Compounds 126

Reaction of $[Ir_2(CO)_2(\mu\text{-}S)(DPM)_2]$ (4) with Dihydrogen.....131

X-ray Data Collection 131

Structure Solution and Refinement 132

Results and Discussion 135

(a) A-frame Complexes 135

(b) Neutral, Non-A-frame Complexes 166

Conclusions 170

References and Footnotes 172

CHAPTER 6

MODELLING BINUCLEAR HYDROGENATION CATALYSTS: THE STRUCTURE OF $[Ir_2(H)_2Cl(CH_3O_2CC{=}C(H)CO_2CH_3)_2(CO)_2(DPM)_2]$-$[BF_4]\cdot 3THF$, A STABLE COMPLEX CONTAINING MUTUALLY ADJACENT ALKENYL AND HYDRIDO LIGANDS.....175

Introduction 175

Experimental Section 176

Preparation of Compounds 177

X-ray Data Collection 178
Structure Solution and Refinement 179
Results and Discussion 182
(a) Description of Structure 182
(b) Description of Chemistry 194
Conclusions 214
References and Footnotes 217
CHAPTER 7
CONCLUSIONS 219
APPENDIX I
REACTION OF A BINUCLEAR IODOCARBONYL COMPLEX WITH MOLECULAR OXYGEN: THE STRUCTURE OF $[Ir_2I_2(CO)_2(\mu\text{-}O_2)(DPM)_2]$, A COMPOUND CONTAINING A PEROXO-BRIDGED METAL-METAL BOND 225
Introduction 225
Experimental Section 226
Preparation of Compounds 227
X-ray Data Collection 228
Structure Solution and Refinement 229
Results and Discussion 232
(a) Description of Structure 232
(b) Description of Chemistry 242
References and Footnotes 246
APPENDIX II
SOLVENTS AND DRYING AGENTS 249

LIST OF TABLES

CHAPTER 2

Table 2.1 Spectroscopic Data for the Compounds of Chapter 2 30

Table 2.2 Summary of Crystal Data and Details of Intensity Collection 35

Table 2.3 Positional Parameters and Isotropic Thermal Parameters 38

Table 2.4 Selected Distances (Å) in $[Ir_2I_2(CO)(\mu\text{-}CO)(DPM)_2]$ 43

Table 2.5 Selected Angles (deg) in $[Ir_2I_2(CO)(\mu\text{-}CO)(DPM)_2]$ 44

CHAPTER 3

Table 3.1 Infrared Spectral Data for the Compounds of Chapter 3 67

Table 3.2 NMR Spectral Data for the Compounds of Chapter 3 68

CHAPTER 4

Table 4.1 Spectroscopic Data for the Compounds in Chapter 4 96

Table 4.2 Summary of Crystal Data and Details of Intensity Collection 99

Table 4.3 Positional Parameters and Isotropic Thermal Parameters ..101

Table 4.4 Selected Distances (Å) in $[Ir_2(CO)(\eta^2\text{-}HFB)(\mu\text{-}S)(\mu\text{-}CO)(DPM)_2]$ 106

Table 4.5 Selected Angles (deg) in $[Ir_2(CO)(\eta^2\text{-}HFB)(\mu\text{-}S)(\mu\text{-}CO)(DPM)_2]$ 107

CHAPTER 5

Table 5.1 Spectroscopic Data for the Compounds in Chapter 5 127

Table 5.2 Summary of Crystal Data and Details of Intensity Collection 133

Table 5.3 Positional Parameters and Isotropic Thermal Parameters ..136

Table 5.4 Selected Distances (Å) in $[RhIr(H)_2(CO)_2(\mu\text{-}Cl)(DPM)_2][BF_4]$ 153

Table 5.5 Selected Angles (deg) in $[RhIr(H)_2(CO)_2(\mu\text{-}Cl)(DPM)_2][BF_4]$ ..154

CHAPTER 6

Table 6.1 Summary of Crystal Data and Details of Intensity Collection 180

Table 6.2 Positional Parameters and Isotropic Thermal Parameters ..183

Table 6.3 Distances (Å) in $[Ir_2(H)_2Cl(CH_3O_2CC{=}C(H)CO_2CH_3)_2(CO)_2(DPM)_2]^+$ 189

Table 6.4 Angles (deg) in $[Ir_2(H)_2Cl(CH_3O_2CC{=}C(H)CO_2CH_3)_2(CO)_2(DPM)_2]^+$ 190

APPENDIX I

Table A.1 Summary of Crystal Data and Details of Intensity Collection 230

Table A.2 Positional Parameters and Isotropic Thermal Parameters ..233

Table A.3 Bond Distances (Å) in $[Ir_2I_2(CO)_2(\mu\text{-}O_2)(DPM)_2]$ 237

Table A.4 Angles (deg) in $[Ir_2I_2(CO)_2(\mu\text{-}O_2)(DPM)_2]$ 238

LIST OF FIGURES

Figure 2.1 A perspective view of $[Ir_2I_2(CO)(\mu\text{-}CO)(DPM)_2]$, showing the numbering scheme 42

Figure 3.1 The $^{13}C\{^1H\}$ NMR spectrum of Compound **4c** 78

Figure 4.1 A perspective view of $[Ir_2(CO)(\eta^2\text{-}F_3CC{\equiv}CCF_3)(\mu\text{-}S)(\mu\text{-}CO)\text{-}(DPM)_2]$ showing the numbering scheme 105

Figure 5.1 The $^{31}P\{^1H\}$ NMR and corresponding hydride region of the ^1H NMR spectrum of compound **4** under H_2 showing the three products 142

Figure 5.2 The $^{31}P\{^1H\}$ NMR spectrum and ^1H NMR spectra (hydride region) of compound **9**, including selective ^{31}P decoupling of the ^1H NMR spectrum 148

Figure 5.3 A perspective view of the $[RhIr(H)_2(CO)_2(\mu\text{-}Cl)(DPM)_2]^+$ cation showing the numbering scheme 152

Figure 5.4 The $^{31}P\{^1H\}$ NMR spectrum and ^1H NMR spectra (hydride region) of compounds **11b** and **15**, also showing selective ^{31}P decoupled ^1H NMR spectra 168

Figure 6.1 Perspective view of the $[Ir_2(H)_2Cl(CH_3O_2CC{=}C(H)CO_2CH_3)_2\text{-}(CO)_2(DPM)_2]^+$ cation showing the numbering scheme 187

Figure 6.2 View of the approximate equatorial plane of the complex, including some relevant distances 188

Figure 6.3 The $^{31}P\{^1H\}$ NMR spectrum and ^1H NMR spectra (hydride region) of compounds **3** at -80 °C, also showing selective ^{31}P decoupled ^1H NMR spectra 197

Figure A.1 Ortep plot of $[Ir_2I_2(CO)_2(\mu\text{-}O_2)(DPM)_2]$ showing the numbering scheme 235

Figure A.2 A view of the approximate equatorial plane of the complex, including some relevant parameters 236

List of Abbreviations and Symbols

anal	analyses
av	average
ca	circa (approximately)
calcd	calculated
coeff	coefficient
DMA	dimethylacetylenedicarboxylate
DPM	bis(diphenylphosphino)methane
Et	ethyl
fw	formula weight
h	hours
HFB	hexafluoro-2-butyne
IR	infrared
L	ligand
M	molar (moles/liter)
Me	methyl
MeOH	methanol
min	minutes
mL	milliliters
NMR	nuclear magnetic resonance
Ph	phenyl
ppm	parts per million
t-Bu	tertiary butyl
THF	tetrahydrofuran

Crystallographic Abbreviations and Symbols

a, b, c	respective lengths of x, y, and z axes of the unit cell
B	isotropic thermal parameter
deg (or °)	degrees
F_c	calculated structure factor
F_o	observed structure factor
h, k, l	indices defining lattice planes, expressed as reciprocals of the fraction of a, b, and c being intersected
p	ignorance factor (accounts for instrumental inaccuracies in measurement of intensity)
R	residual index (measure of agreement between observed and calculated structure factors)
R_w	weighted residual index
w	weighting factor (applied to structure factor)
Z	number of formula weights per unit cell
Å	Angstroms (1 Å = 10^{-10} meters)
α	angle between the b and c axes of the unit cell
β	angle between the a and c axes of the unit cell
γ	angle between the a and b axes of the unit cell
2θ	diffraction angle
ρ	density
λ	wavelength
σ	standard deviation

CHAPTER 1

INTRODUCTION

It is well known that catalysts play an important role in many modern industrial scale chemical processes.[1] Examples such as the hydrogenation of edible fats using Rainey nickel, the hydrogenation of fine organic chemicals using palladium on carbon, and chemical oxidation using 90%Pt-10%Rh wire gauze are only a few among many useful processes which are catalytically driven.[1a] It is therefore not surprising that there is considerable interest in the development of improved and more efficient catalyst systems.

Catalysts can be broadly classified into two groups, heterogeneous and homogeneous, where the latter type refers to catalysts which are soluble in the reaction medium, while the former are not. Heterogeneous catalysts tend to be metals or metal oxides which promote chemical reactivity on their surfaces, whereas homogeneous catalysts are most often transition metal complexes dissolved in appropriate solvents.

Although heterogeneous catalysts are by far the more important type industrially, an increasing interest in homogeneous catalysts is arising due to their capacity for high catalytic activity under mild conditions and especially for their high selectivity toward specific functional groups in the substrates.[2] Homogeneous catalysts also offer the advantages of being better understood, mainly due to the ease by which spectroscopic characterization can be applied *in situ*. Techniques such as infrared (IR)

and nuclear magnetic resonance (NMR) spectroscopy have proven to be very useful in characterizing transition metal intermediates which are potentially involved in catalytic cycles. Further information can be gained by crystallization of organometallic complexes (which may be catalyst precursors or related complexes designed to model catalytic intermediates) and using X-ray crystallography for a complete structural analysis.

Transition metal complexes have already been utilized in many types of catalytic reactions including hydrogenation, hydroformylation, oxidation, polymerization, hydrocyanation, hydrosilation and olefin metathesis.[2] Among these reactions, homogeneous hydrogenation has drawn substantial interest in chemical research, much of which has been summarized in a number of text books and reviews.[2,3] This field continues to receive much attention and has been marked by impressive achievements, such as the asymmetric hydrogenation of prochiral olefins, in which stereoselectivity has been found to rival enzymic catalysts.[4] This process is being applied to the commercial production of L-DOPA (3,4-dihydroxyphenylalanine),[5] a drug used in the treatment of Parkinson's Disease. This and other highly stereoselective hydrogenations are achieved by Rh(I) complexes which contain chiral diphosphine ligands,[4] and represent an excellent example of the advantage that homogeneous systems can have over heterogeneous ones.

Since alkenes have been and remain an important feedstock for the chemical industry,[2a] investigations in the area of catalytic hydrogenation of unsaturated organic substrates have been extensive. The reactivity of hydrogen sources and unsaturated compounds toward metal centers is

therefore of considerable interest. This thesis will deal with cases in which the hydrogen source is molecular hydrogen and will be concerned with the hydrogenation of unsaturated C-C bonds of organic substrates.

Much of the current understanding about homogeneous hydrogenation of unsaturated organic substrates stems from investigations of mononuclear rhodium phosphine complexes, the most extensively studied of these complexes being $RhCl(PPh_3)_3$, often referred to as "Wilkinson's Catalyst".[3d] For this Group-VIII complex and many others like it, hydrogenation evidently occurs by initial oxidative addition of H_2 to the metal center, yielding a dihydride species as outlined in Scheme 1.1. Subsequent alkene coordination, followed by hydride migration to the alkene and finally reductive elimination of the alkane, complete the catalytic cycle.[6] The scheme shown is somewhat simplified, as mechanistic studies have revealed this reaction system to be more complex than was originally supposed.[7] The general reaction scheme is often referred to as the "hydride route" of catalytic hydrogenation since metal hydrides are formed first, followed by olefin coordination. For many transition metal complexes the "olefin route" (or more generally, "unsaturate route")[3k] can be important as well, or may be the dominant pathway. By this route, olefin coordination precedes hydrogen activation in the catalytic cycle.

The olefin route is often followed in cases where the active catalyst is a transition-metal hydride complex. For example, $HRh(CO)(PPh_3)_3$ catalyzes the hydrogenation of alkynes and olefins under mild conditions (25 °C, <1 atm H_2).[8] The high selectivity of this complex toward hydrogenation of terminal alkenes is attributed to the spacial restrictions imposed

Scheme 1.1

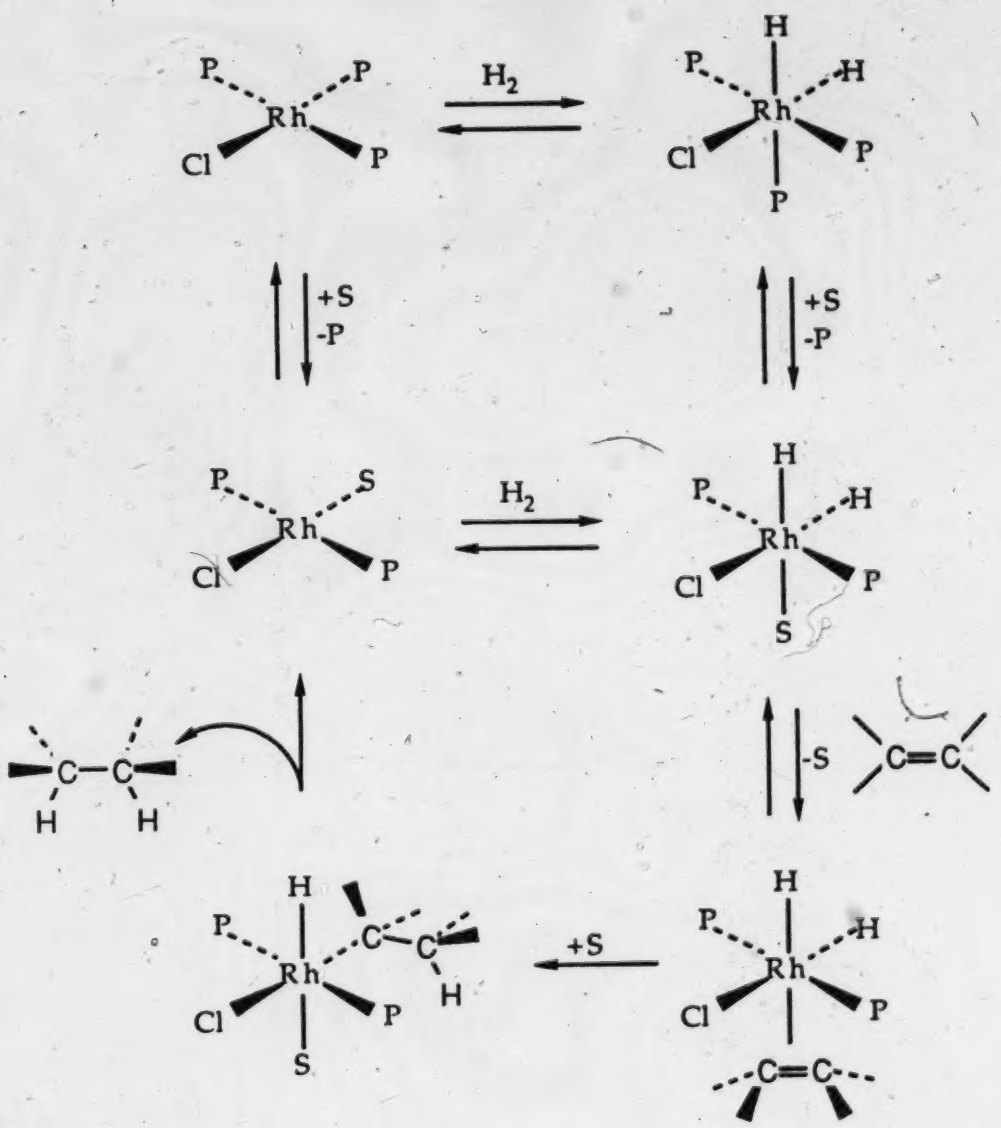

(S = solvent ; P = phosphine)

by the steric bulk of the phosphine ligands. Olefin hydrogenation by this rhodium hydride has been shown to proceed by olefin coordination and hydride migration before oxidative addition of H_2, as outlined in Scheme 1.2. The related ruthenium complex, $HRuCl(PPh_3)_3$, likewise exhibits a

Scheme 1.2.

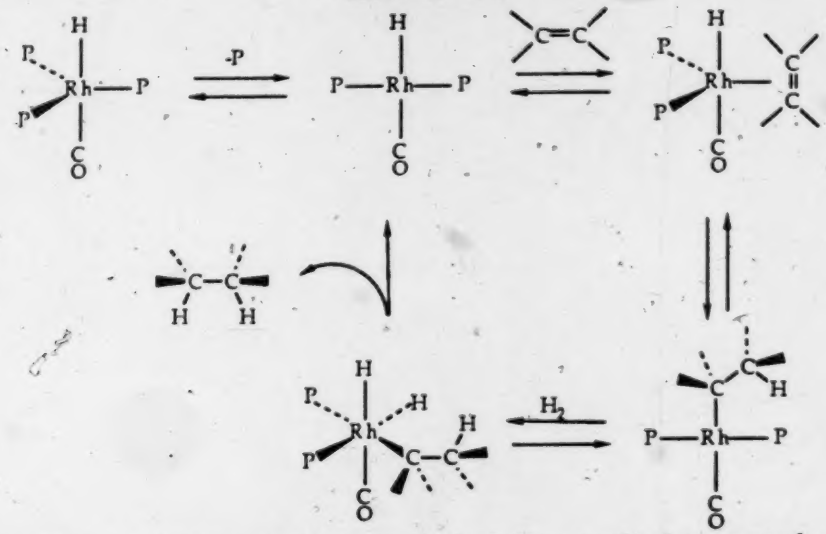

remarkable selectivity whereby terminal olefins are hydrogenated at a rate 10^4 times faster than the corresponding internal olefins.[9]

Homogeneous hydrogenation has also been observed to occur by radical processes. An example is the hydrogenation of α-methylstyrene by $HMn(CO)_5$,[10] which was established to proceed by a free radical path based

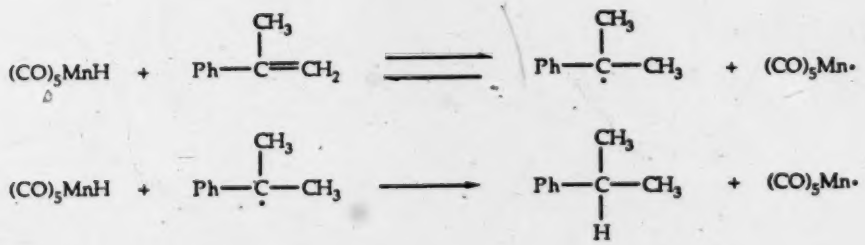

on the observation of CIDNP (Chemically Induced Dynamic Nuclear Polarization) in the NMR spectra. Polarization of the methyl resonance of the hydrogenated product was attributed to competition, involving the radical pair, between product formation and reversion to reactants. Unlike the previous routes, such a radical mechanism need not proceed by prior coordination of the olefin to the metal. This pathway is often favored by conjugated olefins like styrene and butadiene due to the stability of the resulting radicals.[11]

Alkynes tend to undergo hydrogenation in much the same way as do alkenes, but have not been nearly as extensively studied. Being somewhat more π-acidic than their alkene counterparts, once the alkyne is bound, oxidative addition of H_2 tends to be more difficult.[3b] There is also a tendency for alkynes to oligomerize and polymerize, especially at high temperatures, and one must also be aware that further hydrogenation to alkanes is possible. Catalysts are known which preferentially reduce alkynes,[3b] but often the reaction products need to be monitored so that the reaction can be stopped if the alkene is desired. For example, $HRuCl(PPh_3)_3$ selectively hydrogenates 1-hexyne in the presence of 1-octene, which is attributed to stronger binding of the alkyne. Individually, however, the alkene is hydrogenated at a faster rate due to a slower rate-determining oxidative-addition of H_2 for the alkyne complex.[3k]

The need for a catalyst in the hydrogenation of an unsaturated carbon-carbon bond is realized upon considering the reaction without the aid of a catalyst. Although the reaction is thermodynamically favorable, hydrogen is very stable toward polarization and therefore will not

normally undergo a typical addition reaction with alkenes via heterolytic bond cleavage. Two other conceivable routes involving homolytic bond cleavage are diagrammed below. Route A describes a concerted addition

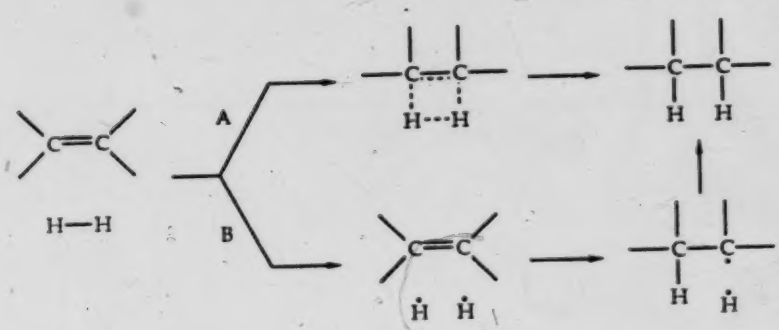

involving a four-centered transition state. However, the required interactions between highest occupied molecular orbitals (HOMO) of one reactant and the lowest unoccupied molecular orbital (LUMO) on the other is forbidden by orbital symmetry rules.[12] Homolysis of the hydrogen molecule (Route B) to form hydrogen atoms is also difficult due to the substantial bond dissociation energy that must be overcome.[3j] The conclusion is that the activation barrier for uncatalyzed hydrogenation is unfavorably high. On the other hand, transition metal complexes are conveniently well suited for reducing this activation barrier by reacting with each of the necessary components in succession.

If the formation of a metal-dihydride complex is favored thermodynamically, hydrogen activation is accomplished by a concerted process. Interaction of a metal "d" orbital and the σ^* molecular orbital of H_2 causes

a reduction in the activation energy for cleaving the H-H bond by simultaneously forming two M-H bonds, favorable by virtue of the fact that twice the bond energy of a transition metal-hydride bond is normally in the range comparable to the bond dissociation enthalpy of H_2.[13] This similarity in net bond strengths, along with the positive entropy associated with reductive elimination, often makes H_2 addition reversible.

The presumed intermediate in H_2 activation is the dihydrogen complex (illustrated below), which has only been recognized as a viable

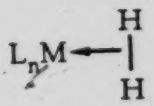

species since 1984.[14] Since that time, many examples of polyhydride complexes containing the η^2-H_2 ligand have been recognized[15] and are routinely distinguished from classical hydrides by T_1 measurements in the NMR experiment.[16] The attractive forces in such complexes are described to be dominated by a donation of σ-bonding electrons of H_2 toward an appropriate metal "d" orbital, while metal(d_π)-H_2(σ^*) backbonding is very limited.[15a]

An early observation of the reversible binding of H_2 was that of *trans*-[IrCl(CO)(PPh_3)$_2$], commonly referred to as "Vaska's Complex".[17] The dihydride formed by H_2 addition to this complex has been characterized[18] by infrared and NMR spectroscopy. Infrared bands due to Ir-H stretching

vibrations are observed at 2222 cm^{-1} and 2098 cm^{-1} and the ^1H NMR spectrum displays distinctive resonances at δ -7.3 and δ -18.4, each signal being a 1:2:1 triplet due to ^1H-^{31}P coupling. A kinetic study of the reaction suggests a concerted addition of H_2 to the complex via a non-polar transition state, and a relatively small deuterium isotope effect indicates that Ir-H bond formation is more important than H-H bond cleavage.[19] The dependence of the reactivity of such complexes upon the ancillary ligands has been demonstrated in this case by changing the halide to bromide and iodide,[20] and the rate of reaction with hydrogen is found to increase in the order Cl<Br<I. Reaction with hydrogen is also found to be enhanced by introduction of electron donating substituents on the phosphine phenyl groups.[21] These observations indicate another advantage that homogeneous complexes have over heterogeneous catalysts, that is, their ability to be "tailored" to change their reactivity.

Although the term "hydride" is used in discussing these complexes, the M-H bond is normally considered a covalent bond, and is not remarkably polar.[3i] Nevertheless, a considerable range of bond polarities exists in transition metal hydrides, dependent upon the metal and upon the nature of the ligands. The hydridic nature of such complexes has been measured by their propensities to reduce ketones,[22] while acidities, based on acid dissociation constants, have also been used to characterize the nature of the M-H bond.[23]

Due to the potential differences in the M-H bond strengths, it is an important consideration that the metal hydride complex involved in catalytic hydrogenation not have overly strong metal-hydrogen bonds. In

that case the hydride migration step to give the metal-alkyl intermediate may be difficult. On the other hand, complexes which are modified to have stronger M-H bonds may be useful as models for catalysis by providing stability to intermediates.

Formation of the metal alkyls by reaction of the metal hydride with alkene can also be reversible, and the reverse reaction, β-hydride elimination, has been extensively studied.[3b] Evidence for β-hydride elimination is acknowledged in the commonly observed isomerization of organic substrates under catalytic conditions, and can be explained by the equilibria shown below, involving alternate β-hydride elimination and hydride

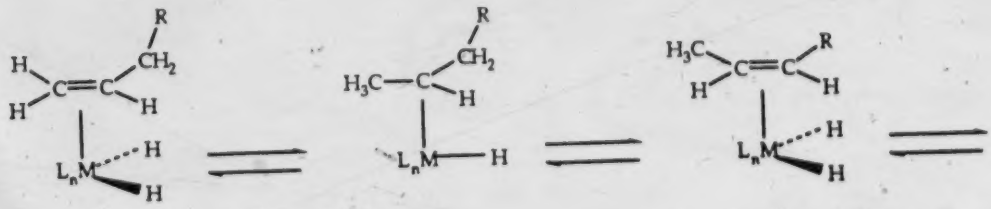

migration steps. In the same way that transition metal catalysts can be highly specific for terminal olefins, isomerization can also be inhibited by the presence of bulky ligands on the metal. The hydride migration step itself typically occurs with cis addition of M-H across the C=C bond as required by the postulated transition state, shown below (left). Following the olefin route, oxidative addition of H_2 would then be possible due to coordinative unsaturation generated by the hydride migration. Finally, hydride transfer through a 3-centered transition state (below, right) is considered to occur very rapidly, so that dihydrido alkyl complexes have,

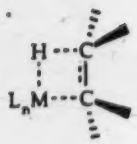

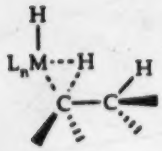

in fact, not been detected.[3b] Complexes containing "agostic"[24] C-H interactions with metal centers, such as those shown below (two additional chloride ligands on each complex, above and below the plane shown, are omitted)[25] containing β-agostic and α-agostic C-H interactions, respectively, represent models of the above transition states. This class of compounds is more often discussed in connection with dehydrogenation, or C-H activation.[15a]

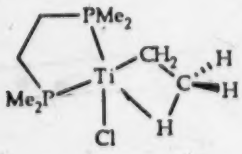

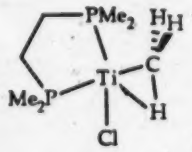

Although homogeneous catalysts have demonstrated the advantages of specificity and selectivity, there are some drawbacks to the use of homogeneous systems, leading to consideration of combining the attributes of both homogeneous and heterogeneous systems. A major disadvantage of homogeneous catalysts is that they are difficult to separate from the reaction mixture, which is especially of concern in large scale processes. Because of this problem, research has branched into the area of

supported metal complexes,[26,27] where the metal complex is chemically bound to solid supports such as organic polymers or inorganic oxides. Another question which arises with respect to homogeneous catalysts is whether there is an advantage to be gained by having metal atoms near one another, as is the case in heterogeneous systems. For example, a number of metal cluster complexes have been described wherein the bonding of ligands to the cluster framework is often postulated to represent the bonding on metal surfaces.[26] It has been pointed out that although metal-metal bonds are weaker in clusters than they are in bulk metals, the binding modes of ligands such as hydrogen, carbon monoxide and acetylenes should be quite analogous.[28] Bonding of ligands and reactive substrates can therefore involve more than one metal center, which is normally not available in mononuclear systems. Another potential advantage is the capability for ligand migration around the cluster framework rather than the necessity for ligand dissociation in order to create open coordination sites.[29] Such discussion prompts the study of possible cooperation between closely situated metals in transition-metal complexes as a means by which reactivity of homogeneous catalysts could be enhanced.

The simplest molecular unit capable of displaying metal-metal cooperativity is the binuclear complex which has two adjacent metal centers, and a great deal of interesting reactivity has already been observed in this type of system.[30] Several strategies have been employed in order to maintain the integrity of such complexes, normally using some type of bridging ligand to hold the metals in close proximity.[31] As was evident in the

previously discussed mononuclear hydrogenation catalysts, tertiary phosphines are effective as ligands because of the ease by which electronic and steric properties can be controlled.[32] A related diphosphine ligand suitable for binuclear systems is bis(diphenylphosphino)methane, often abbreviated "dppm" or simply "DPM". Its success as a bridging-ligand in binuclear complexes has been surveyed in recent reviews,[33] and arises from its reluctance to form a strained, four-membered chelate ring at one metal, therefore being more likely to act as a bidentate ligand across two metals.

The analogy between a pair of closely situated molecules of the mononuclear phosphine complex, "Vallerino's compound",[34] and a DPM-bridged dirhodium complex, $[RhCl(CO)(DPM)]_2$, is illustrated below. This

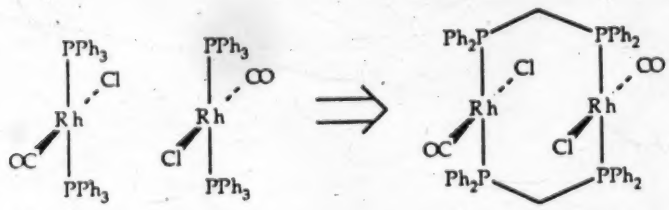

was the first DPM-bridged binuclear complex reported,[35] and was later structurally characterized,[36] revealing the trans relationship between the two chloro and the two carbonyl ligands. Since that time it has been shown that DPM can coordinate to many different metals to yield a variety of homobinuclear complexes and more recently, heterobinuclear complexes.[33] Within this class of compounds there are examples which contain one, two, or three bridging DPM groups per dimer, but most

common to Group VIII metals are binuclear complexes that contain two trans DPM ligands.[33]

DPM often forms strong bonds to metal atoms and is also flexible enough to span a wide range of metal-metal distances.[33b] In addition, the DPM ligand offers the advantages of good solubility and crystallizability afforded to complexes containing the ligand. These properties are considered to be a function of the phenyl groups, which allow solubility in a variety of organic solvents and promote efficient packing of molecules in crystals suitable for X-ray diffraction studies. Another important advantage is that DPM bonds directly to the metal centers through its phosphorus atoms , so that information about the environment at both metals is readily obtained using ^{31}P NMR. For example, in a binuclear complex with two trans DPM ligands it is rather straightforward to identify species which have four equivalent phosphorus atoms and therefore equivalent metal environments. The spectra can be further simplified by broad-band decoupling of the proton signals ($^{31}P\{^{1}H\}$ NMR).

The reactivity of binuclear DPM-bridged rhodium complexes with small molecules has been extensively studied.[37-95] More specifically, the complexes **I**,[79] **II**[62,64] and **III**,[45] shown below, were found to be alkyne hydro-

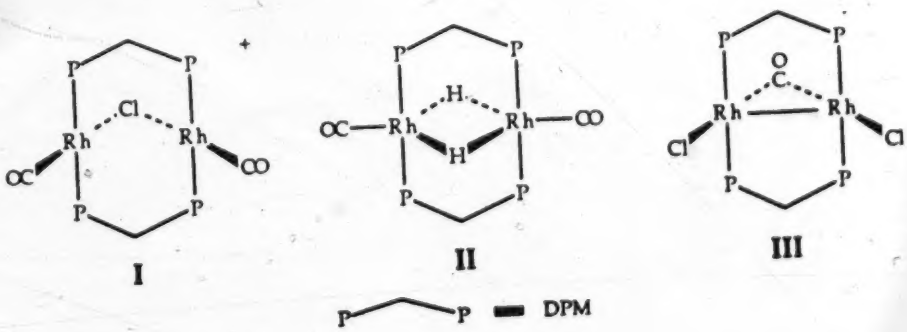

genation catalysts under mild conditions. Although the possibility of metal-metal cooperativity in the catalysis involving these species was suggested,[66,96] attempts to observe potential intermediates in the reactions failed, leaving no evidence to substantiate such cooperativity. In order to understand how two metals could cooperate in the hydrogenation of unsaturated substrates, suitable model complexes were required which would be likely to react in similar fashion, but which would yield stable and characterizable intermediates. The obvious choices in this case were analogous binuclear iridium complexes, since the third-row congeners of the Group VIII transition metals are believed to give generally more stable hydride and alkyl complexes than those of the second row.[97]

An alternate bonding mode which is available to halides and related ligands in binuclear complexes is demonstrated in the "A-frame" structure of species **I**. Not only can the halide function, in its usual mode, as a terminal ligand on one metal, it can also be a four-electron donor, bridging two metal atoms. Note that the A-frame complex retains a square-planar geometry at the metal centers as was the case in *trans*-$[RhCl(CO)(DPM)]_2$, but now with one ligand shared by two metals. This would also appear to present an open site between the two metals; the so-called "pocket" of the A-frame complex, which has proved to be the site of attack by a number of small-molecule reactants.[33b]

Subsequent studies into related binuclear DPM-bridged iridium complexes have also been reported.[80,81,98-107] Of relevance to this thesis are reactions of binuclear iridium complexes with dihydrogen and unsaturated organic substrates as models for catalytic hydrogenation at adjacent

metal centers. A project was initiated to model the alkyne hydrogenation by the A-frame complex, **I**, using the diiridium analogue. Preliminary studies[102] had revealed that, in general, activated alkynes were required in order to induce reactivity with the model diiridium complexes. However, in the absence of H_2, relatively stable binuclear species resulted in which the alkyne was bound as a cis-dimetallated olefin, and further reaction was not observed, at least under moderate conditions. It was therefore apparent that the hydride route for modelling the catalysis by **I** might be more productive.

Reaction of both the diiridium analogue of **I** and the neutral dichloro precursor, *trans*-$[IrCl(CO)(DPM)]_2$ with H_2 yielded significantly different dihydride products,[104] (shown below as **IV** and **V** respectively).

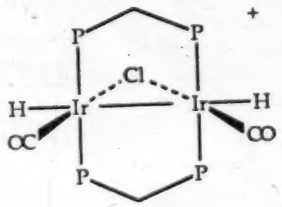

IV

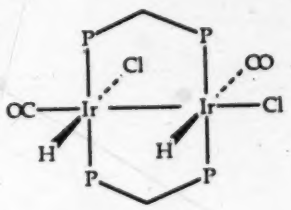

V

Furthermore, the reactions of these dihydrides with the activated alkyne, dimethylacetylenedicarboxylate (DMA), gave insertion of the substrate into both Ir-H bonds of **IV** (although the resulting complex reacted with chloride ion, presumably from the CH_2Cl_2 solvent, yielding **VI**), but into only one of the Ir-H bonds of **V**, to give **VII**. No additional reactivity of these neutral dichloro species could be induced in either case, presumably due to coordinative saturation at the metals. An additional feature of

complex IV was the formation of a tetrahydride species upon reaction with excess H_2, whereas V did not react further with H_2.[104]

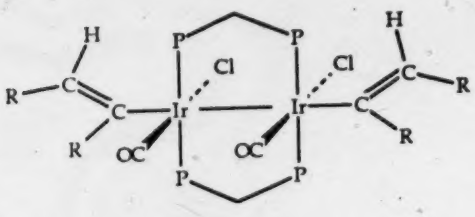

VI

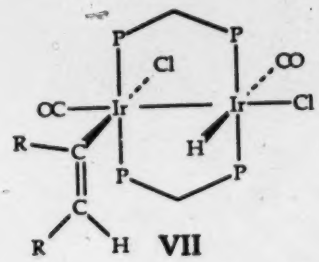

VII

The objective of this thesis is to extend the above study in an effort to obtain a better understanding of how the adjacent metals interact with substrate molecules. The focus of these studies will be: (a) to explain the result of the formation of complex IV in which a presumed concerted oxidative addition of H_2 has led to non-adjacent hydrido ligands, (b) to investigate the effect of the anionic bridging ligand and ligand mobility on H_2 activation and substrate coordination, and (c) to further investigate the possibility of metal-metal cooperativity and successfully model the hydrogenation of unsaturated organic substrates at adjacent metal centers.

One of the major difficulties with the use of homogeneous catalysts in large-scale processes is the sensitivity of transition metal complexes to traces of impurities, notably oxygen. Nevertheless, oxygenated species can also be of value to catalytic oxidation reactions. The reaction of one of the DPM-bridged binuclear complexes (herein reported) with molecular oxygen leads to an interesting new species. The structure determination and subsequent chemistry of this dioxygen complex is appended to this

thesis as an additional study into metal-metal cooperativity effects in binuclear complexes.

References and Footnotes

1. (a) Satterfield, C. N. *Heterogeneous Catalysis in Practice*, McGraw-Hill, New York, **1980**. (b) Davis, B. H.; Hettinger, W. P. Jr., eds., *Heterogeneous Catalysis*, American Chemical Society, Washington, DC, **1983**. (c) Leach, B. E., ed., *Applied Industrial Catalysis*, Academic Press, New York, **1983**, Vol 1-3. (d) Grasselli, R. K.; Brazdil, J. F., eds., *Solid State Chemistry in Catalysis*, American Chemical Society, Washington, DC, **1985**. (e) Lee, H. H. *Heterogeneous Reactor Design*, Butterworth, Boston, **1985**.

2. (a) Mortreux, A.; Petit, F. eds. *Industrial Applications of Homogeneous Catalysis*, D. Reidel, Dordrecht, **1988**. (b) Nakamura, A.; Tsutsui, M. *Principles and Applications of Homogeneous Catalysis*, Wiley, New York, **1980** and references therein. (c) Parshall, G. W,; Putscher, R. E. *J. Chem. Ed.* **1986**, *63*, 189.

3. (a) Dickson, R. S. *Homogeneous Catalysis with Compounds of Rhodium and Iridium*, Ugo, R.; James, B. R., eds., D. Reidel, Dordrecht, **1985**. (b) James, B. R. in *Comprehensive Organometallic Chemistry*, Wilkinson, G.; Stone, F. G. A.; Abel, E. W. eds., Pergamon Press, Oxford, **1982**, *Vol. 8*, p 285. (c) Brothers, P. J. *Prog. Inorg. Chem.* **1981**, *28*, 1. (d) Jardine, F. H. *Prog. Inorg. Chem.* **1981**, *28*, 63. (e) Halpern, J. *J. Organomet. Chem.* **1980**, *200*, 133. (f) James, B. R. *Adv. Organomet. Chem.* **1979**, *17*, 319. (g) Rylander, P. N. *Catalytic Hydrogenation in Organic Synthesis*, Academic Press, New

York, **1979**. (h) Valentine, D.; Scott, J. W. *Synthesis* **1978**, 329. (i) Birch, A. J.; Williamson, D. H. *Org. React.* **1978**, *24*, 1. (j) McQuillin, F. J. *Homogeneous Hydrogenation in Organic Chemistry*, D. Reidel, Dordrecht, **1976**. (k) James, B. R. *Homogeneous Hydrogenation*, Wiley, New York, **1972**. (l) Coffey, R. S. *Aspects of Homogeneous Catalysis*, **1970**, *1*, 3. (m) Dolcetti, G.; Hoffman, N. W. *Inorg. Chim. Acta* **1974**, *9*, 269. (n) Pignolet, L. H. ed., *Homogeneous Catalysis with Metal Phosphine Complexes*, Plenum Press, New York, **1983**.

4. Leading references in this field are: (a) Halpern, J. *Science (Washington, DC)* **1982**, *217*, 401, and references therein. (b) Kagan, H. B. in *Comprehensive Organometallic Chemistry*, Wilkinson, G.; Stone, F. G. A.; Abel, E. W. eds., Pergamon Press, Oxford, **1982**,*Vol. 8*, pp 463-498. (c) Knowles, W. S.; Chrisopfel, W. S.; Koenig, K. E.; Hobbs, C. F. *Adv. Chem. Ser.* **1982**, *196*, 325. (d) Bosnich, B.; Fryzuk, M. D. *Top. Stereochem.* **1981**, *12*, 119.

5. Knowles, W. S. *Acc. Chem. Res.* **1983**, *16*, 106, and references therein.

6. Osborne, J. A.; Jardine, F. H.; Young, J. F.; Wilkinson, G. *J. Chem. Soc. A* **1966**, 1711.

7. (a) Tolman, C. A.; Meakin, P. Z.; Lindner, D. L.; Jesson, J. P. *J. Am. Chem. Soc.* **1972**, *94*, 3240. (b) Halpern, J. *Trans. Am. Crystallogr. Assoc.* **1978**, *14*, 59. (c) Halpern, J.; Okamoto, T.; Zakhariev, A. *J. Mol. Catal.* **1976**, *2*, 65. (d) Halpern, J. *Inorg. Chim. Acta* **1981**, *50*, 11.

8. Ref. 3a, p 57, and references therein.

9. (a) Hallman, P. S.; McGarvey, B. R.; Wilkinson, G. *J. Chem. Soc. A* **1968**, 3143. (b) Evans, D.; Osborne, J. A.; Jardine, F. H.; Wilkinson, G. *Nature (London)* **1965**, *208*, 1203.

10. Sweany, R. L.; Halpern, J. *J. Am. Chem. Soc.* **1977**, *99*, 8335.

11. Collman, J. P.; Hegidus, L. S.; Norton, J. R.; Finke, R. G. *Principles and Applications of Organotransition Metal Chemistry*, University Science Books, Mill Valley, California, **1987**, p 527.

12. Woodward, R. B.; Hoffmann, R. *Angew. Chem. Int. Ed. Engl.* **1969**, *8*, 781.

13. Yamamoto, A. *Organotransition Metal Chemistry*, Wiley, New York, **1986**.

14. Kubas, G. J.; Ryan, R. R.; Vergamini, P. J.; Wasserman, H. J. *J. Am. Chem. Soc.* **1984**, *106*, 451.

15. (a) Crabtree, R. H.; Hamilton, D. G. *Adv. Organomet. Chem.* **1988**, *28*, 299 and references therein. (b) Chinn, M. S.; Heinekey, D. M. *J. Am. Chem. Soc.* **1987**, *109*, 5865. (c) Bianchini, C.; Mealli, C.; Peruzzini, M.; Zanobini, F. *J. Am. Chem. Soc.* **1987**, *109*, 5548. (d) Bautista, M.; Earl, K. A.; Morris, R. H.; Sella, A. *J. Am. Chem. Soc.* **1987**, *109*, 3780. (e) Kubas, G. J.; Ryan, R. R.; Unkefer, C. J. *J. Am. Chem. Soc.* **1987**, *109*, 8113. (f) Bautista, M.; Earl, K. A.; Morris, R. H. *Inorg. Chem.* **1988**, 27, 1124. (g) Fontaine, X. L. R.; Fowles, E. H.; Shaw, B. L. *J. Chem. Soc., Chem. Commun.* **1988**, 482. (h) Cotton, F. A.; Luck, R. L. *J. Chem. Soc., Chem. Commun.* **1988**, 1277. (i) Bianchini, C.; Peruzzini, M.; Zanobini, F. *J. Organomet. Chem.* **1988**,

354, C19. (j) Bautista, M. T.; Earl, K. A.; Maltby, P. A.; Morris, R. H.; Schweitzer, C. T.; Sella, A. *J. Am. Chem. Soc.* **1988**, *110*, 7031.

16. Hamilton, D. G.; Crabtree, R. H. *J. Am. Chem. Soc.* **1988**, *110*, 4126.
17. Vaska, L.; Diluzio, J. W. *J. Am. Chem. Soc.* **1962**, *84*, 679.
18. (a) Vaska, L. *J. Am. Chem. Soc.* **1966**, *88*, 4100. (b) Vaska, L.; Rhodes, R. E. *J. Am. Chem. Soc.* **1965**, *87*, 4970. (c) Taylor, R. C.; Young, J. F.; Wilkinson, G. *Inorg. Chem.* **1966**, *5*, 20.
19. Hyde, E. M.; Shaw, B. L. *J. Chem. Soc., Dalton Trans.* **1975**, 765.
20. Vaska, L.; Werneke, M. F. *Trans. New York Acad. Sci.* **1971**, *31*, 70.
21. (a) Strohmeier, W.; Onoda, T. Z. *Naturforsch.* **1968**, *23b*, 1927. (b) Strohmeier, W.; Onoda, T. Z. *Naturforsch.* **1969**, *24b*, 515, 931.
22. Labinger, J. A.; Komadina, K. H. *J. Organomet. Chem.* **1978**, *155*, C25.
23. Ref. 11, p 91, and references therein.
24. Brookhart, M.; Green, M. L. H. *J. Organomet. Chem.* **1983**, *250*, 395.
25. Dawoodi, Z.; Green, M. L. H.; Mtetwa, V. S. B.; Prout, K. *J. Chem. Soc., Chem. Commun.* **1982**, 802, 1410.
26. Hartley, F. R. *Supported Metal Complexes*, D. Reidel, Dordrecht, **1985** and references therein.
27. Iwasawa, Y. ed., *Tailored Metal Catalysts*, D. Reidel, Dordrecht, **1986**.
28. Muetterties, E. L. *Science* **1977**, *196*, 839.
29. Johnson, B. F., ed., *Transition Metal Clusters*, Wiley, New York, **1980**.
30. Chisholm, M. H., ed., *Reactivity of Metal-Metal Bonds*, A.C.S. Symposium Series 155, Washington, DC, **1981**.

31. (a) Muetterties, E. L.; Stein, J. *Chem. Rev.* **1979**, *79*, 479. (b) Collman, J. P.; Rothrock, R. K.; Finke, R. G.; Rose Munch, E. J. *Inorg. Chem.* **1982**, *21*, 146, and references therein.

32. Tolman, C. A. *Chem. Rev.* **1977**, *77*, 313.

33. (a) Chaudret, B.; Delavaux, B.; Poilblanc, R. *Coord. Chem. Rev.* **1988**, *86*, 191. (b) Puddephatt, R. J. *Chem. Soc. Rev.* **1983**, 99.

34. Vallarino, L. J. Chem. Soc. 1957, 2287.

35. Mague, J. T.; Mitchener, J. P. *Inorg. Chem.* **1969**, *8*, 119.

36. Cowie, M.; Dwight, S. K. *Inorg. Chem.* **1980**, *19*, 2500.

37. Mague, J. T. *Inorg. Chem.* **1969**, *8*, 1975.

38. Balch, A. L. *J. Am. Chem Soc.* **1976**, *98*, 8049.

39. Balch, A. L.; Tulyathan, B. *Inorg. Chem.* **1977**, *16*, 2840.

40. Balch, A. L.; Labadie, J. W.; Delker, G. *Inorg. Chem.* **1979**, *18*, 1224.

41. Mague, J. T.; DeVries, S. H. *Inorg. Chem.* **1980**, *19*, 3743.

42. Sanger, A. R. *J. Chem. Soc., Dalton Trans.* **1981**, 228.

43. Gelmini, L.; Stephan, D. W.; Loeb, S. J. *Inorg. Chim. Acta* **1985**, *98*, L3.

44. Gelmini, L.; Stephan, D. W.; Loeb, S. J. *Organometallics* **1986**, *5*, 231.

45. Cowie, M.; Southern, T. G. *Inorg. Chem.* **1982**, *21*, 246.

46. McKeer, I. R.; Cowie, M. *Inorg. Chim. Acta* **1982**, *65*, L107.

47. Cowie, M.; Dickson, R. S.; Hames, B. W. *Organometallics* **1984**, *3*, 1879.

48. Sutherland, B. R.; Cowie, M. *Inorg. Chem.* **1984**, 23, 1290.

49. Gibson, J. A. E.; Cowie, M. *Organometallics* **1984**, 3, 722.

50. Gibson, J. A. E.; Cowie, M. *Organometallics* **1984**, 3, 984.

51. Sanger, A. R. *Inorg. Chim. Acta* **1985**, *99*, 95.

52. Mague, J. T.; DeVries, S. H. *Inorg. Chem.* **1982**, *21*, 1632.

53. Mague, J. T. *Inorg. Chem.* **1983**, *22*, 45.

54. Mague, J. T. *Inorg. Chem.* **1983**, *22*, 1158.

55. Deraniyagala, S. P.; Grundy, K. R. *Organometallics* **1985**, *4*, 424.

56. Cowie, M.; Loeb, S. J. *Organometallics* **1985**, *4*, 852.

57. Deraniyagala, S. P.; Grundy, K. R. *Inorg. Chem.* **1985**, *24*, 50.

58. Deraniyagala, S. P.; Grundy, K. R. *Inorg. Chim. Acta* **1984**, *84*, 205.

59. Deraniyagala, S. P.; Grundy, K. R. *Inorg. Chim. Acta* **1985**, *101*, 103.

60. Deraniyagala, S. P.; Grundy, K. R. *J. Chem. Soc., Dalton Trans* **1985**, 1577.

61. Kubiak, C. P.; Eisenberg, R. *J. Am. Chem. Soc.* **1980**, *102*, 3637.

62. Kubiak, C. P.; Woodcock, C.; Eisenberg, R. *Inorg. Chem.* **1982**, *21*, 2119.

63. Woodcock, C.; Eisenberg, R. *Organometallics* **1982**, *1*, 886.

64. Woodcock, C.; Eisenberg, R. *Inorg. Chem.* **1984**, *23*, 4207.

65. Woodcock, C.; Eisenberg, R. *Inorg. Chem.* **1985**, *24*, 1285.

66. Kubiak, C. P.; Eisenberg, R. *J. Am. Chem. Soc.* **1977**, *99*, 6129.

67. Berry, D. H.; Eisenberg, R. *J. Am. Chem. Soc.* **1985**, *107*, 7181.

68. Hommeltoft, S. I.; Berry, D. H.; Eisenberg, R. *J. Am. Chem. Soc.* **1986**, *108*, 5345.

69. Woodcock, C.; Eisenberg, R. *Organometallics* **1985**, *4*, 4.

70. Ladd, J. A.; Olmstead, M. M.; Balch, A. L. *Inorg. Chem.* **1984**, *23*, 2318.

71. Womack, D. R.; Enlow, P. D.; Woods, C. *Inorg. Chem.* **1983**, *22*, 2653.

72. Enlow, P. D.; Woods, C. *Inorg. Chem.* **1985**, *24*, 1273.

73. Oro, L. A.; Carmona, D.; Perez, P. L.; Esteban, M.; Tiripicchio, A.; Tiripicchio-Camellini, M. *J. Chem. Soc., Dalton Trans.* **1985**, 973.

74. Lahoz, F. J.; Tiripicchio, A.; Tiripicchio-Camellini, M.; Oro, L. A.; Pinillos, M. T. *J. Chem. Soc., Dalton Trans.* **1985**, 1487.

75. Faraone, F.; Bruno, G.; Lo Shiavo, S.; Bombieri, G. *J. Chem. Soc., Dalton Trans.* **1984**, 533.

76. Bruno, G.; Lo Shiavo, S.; Piraino, P.; Faraone, F. *Organometallics* **1985**, *4*, 1098.

77. Lo Shiavo, S.; Bruno, G.; Piraino, P.; Faraone, F. *Organometallics* **1986**, *5*, 1400.

78. Mann, B. E.; Meanwell, N. J.; Spencer, C. M.; Taylor, B. F.; Maitlis, P. M. *J. Chem. Soc., Dalton Trans.* **1985**, 1555.

79. Sanger, A. R. *Prepr. -Can. Symp. Catal.* **1979**, *6th*, 37.

80. Cowie, M.; Mague, J. T.; Sanger, A. R. *J. Am. Chem. Soc.* **1978**, *100*, 3628.

81. Mague, J. T.; Sanger, A. R. *Inorg. Chem.* **1979**, *18*, 2060.

82. Sanger, A. R. *J. Chem. Soc., Dalton Trans.* **1977**, 120.

83. Sanger, A. R. *J. Chem. Soc., Dalton Trans.* **1977**, 1971.

84. Sanger, A. R. *J. Chem. Soc., Chem. Commun.* **1975**, 893.

85. Cowie, M.; Dwight, S. K.; Sanger, A. R. *Inorg. Chim. Acta* **1978**, *31*, L407.

86. Sanger, A. R. *Can. J. Chem.* **1982**, *60*, 1363.

87. Kubiak, C. P.; Eisenberg, R. *Inorg. Chem.* **1980**, *19*, 2726.

88. Cowie, M. *Inorg. Chem.* **1979**, *18*, 286.

89. Cowie, M.; Dwight, S. K. *Inorg. Chem.* **1979**, *18*, 2700.

90. Cowie, M.; Dwight, S. K. *Inorg. Chem.* **1980**, *19*, 209.

91. Cowie, M.; Dwight, S. K. *Inorg. Chem.* **1980**, *19*, 2508.

92. Cowie, M.; Dwight, S. K. *J. Organomet. Chem.* **1980**, *198*, C20.

93. Cowie, M.; Dwight, S. K. *J. Organomet. Chem.* **1981**, *214*, 233.

94. Cowie, M.; Southern, T. G. *J. Organomet. Chem.* **1980**, *193*, C46.

95. Cowie, M.; Dickson, R. S. *Inorg. Chem.* **1981**, *20*, 2682.

96. Poilblanc, R. Inorg. Chim. Acta 1982, 62, 75.

97. Ref. 11, p 82, 100 and references therein.

98. Mague, J. T.; DeVries, S. H. *Inorg. Chem.* **1982**, *21*, 1632.

99. Mague, J. T.; Klein, C. L.; Majeste, R. J.; Stevens, E. D. *Organometallics* **1984**, *3*, 1860.

100. Eisenberg, R.; Kubiak, C. P.; Woodcock, C. *Inorg. Chem.* **1980**, *19*, 2733.

101. Sutherland, B. R.; Cowie, M. *Inorg. Chem.* **1984**, 23, 2324.

102. Sutherland, B. R.; Cowie, M. *Organometallics* **1984**, 3, 1869.

103. Sutherland, B. R.; Cowie, M. *Organometallics* **1985**, 4, 1637.

104. Sutherland, B. R.; Cowie, M. *Organometallics* **1985**, 4, 1801.

105. Sutherland, B. R.; Cowie, M. *Can. J. Chem.* **1986**, *64*, 464.

106. Cowie, M.; Vasapollo, G.; Sutherland, B. R.; Ennett, J. P. *Inorg. Chem.* **1986**, *25*, 2648.

107. McDonald, R.; Sutherland, B. R.; Cowie, M. *Inorg. Chem.* **1987**, *26*, 3333.

CHAPTER 2

BINUCLEAR IODOCARBONYL COMPLEXES OF IRIDIUM: REACTIVITIES WITH CARBON MONOXIDE AND DIMETHYL-ACETYLENEDICARBOXYLATE, AND THE UNUSUAL STRUCTURE OF $[Ir_2I_2(CO)(\mu\text{-}CO)(DPM)_2]\cdot CH_2Cl_2$

Introduction

In attempts to gain an understanding of ligand migrations in binuclear complexes, the chemistry of DPM-bridged diiridium complexes having different anionic groups has been under investigation.[1,2] It appears that an important aspect affecting ligand mobility is the ability of these bridging anionic groups to move back and forth, from one metal to another, in a "windshield-wiper" motion. In later chapters the differing tendencies of the bridging chloride and sulfide groups in $[Ir_2(CO)_2(\mu\text{-}Cl)(DPM)_2]^+$ and $[Ir(CO)_2(\mu\text{-}S)(DPM)_2]$ to undergo this windshield-wiper motion, and the subsequent effect on the chemistries of these species will be discussed.

In this chapter the effect of the larger I^- anion on A-frame reactivity is studied, with the assumption that the increased size of this anion over the chloride and sulfide groups should significantly influence its tendency to bridge the two metals, particularly in metal-metal bonded species, which have been shown to be important intermediates in hydrogenation reactions.[1,2] Furthermore, this large anion is expected to influence the

preferred site of attack by incoming substrates, and should also enhance the basicity of the metal centers by virtue of its π-donor ability (*c.f.* its position in the spectrochemical series), thus promoting the reactivity of these complexes.

Experimental Section

General Experimental Conditions

All solvents were appropriately dried and distilled prior to use (see Appendix II) and were stored under dinitrogen. Reactions were carried out under standard Schlenk conditions using dinitrogen which had been passed through columns containing Ridox and 4A molecular sieves in order to remove traces of oxygen and water, respectively. Hydrated iridium trichloride was obtained from Johnson-Matthey and bis(diphenylphosphino)methane (DPM) was purchased from Strem Chemicals. Dimethylacetylenedicarboxylate (DMA) and silver tetrafluoroborate were purchased from Aldrich Chemical Company. Carbon monoxide (Matheson) and dihydrogen (Linde) were used as received. The compound *trans*-$[IrCl(CO)(DPM)]_2$ was prepared by the previously reported procedure.[3] The $^{31}P\{^1H\}$, ^1H, and $^1H\{^{31}P\}$ NMR spectra were run on a Bruker WH-400 spectrometer. Infrared spectra were recorded on a Nicolet 7199 Fourier transform IR spectrometer either as solids in Nujol mulls on KBr plates or as solutions in KCl cells with 0.5 mm window path lengths. Elemental analyses were performed by the

microanalytical service within the department (low carbon analyses in some cases were ascribed to metal-carbide formation during combustion). Conductivity measurements were made on 10^{-3} M solutions using a Yellow Springs Instrument Co. Model 31 conductivity bridge.

Preparation of Compounds

(a) $[Ir_2I_2(CO)(\mu\text{-}CO)(DPM)_2]\cdot CH_2Cl_2$ (**1**).

The compound *trans*-$[IrCl(CO)(DPM)]_2$ (200 mg, 0.156 mmol) was suspended in 20 mL of CH_2Cl_2, to which was added an excess of KI (260 mg, 10 equiv) in a minimum volume of methanol. The suspension immediately changed color from deep purple to orange, and after stirring for 30 min the solvent was removed *in vacuo* and the product redissolved in approximately 10 mL of CH_2Cl_2. To remove the potassium salts, this solution was filtered and washed with several portions of degassed distilled water. The product was then precipitated by the addition of 25 mL of diethyl ether. The resulting microcrystalline orange solid was collected and dried *in vacuo*, giving typical yields of 80-85%. Compound **1** was determined to be non-conducting in CH_2Cl_2 solutions (Λ_m = 1.78 $\Omega^{-1}cm^2$ $mole^{-1}$).[4] Spectroscopic data for this and all subsequent compounds are given in Table 2.1. Anal. calcd for $Ir_2I_2Cl_2P_4O_2C_{53}H_{46}$: C, 41.12%; H, 3.00%; I, 16.40%. Found: C, 40.96%; H, 3.00%; I, 16.58%. In this case the amount of solvent was confirmed in the crystallographic study (*vide infra*). In other compounds that crystallized with solvent molecules the amount of solvent was confirmed by ^1H NMR.

Table 2.1. Spectroscopic Data for the Compounds in Chapter 2.[a]

compound	infrared(cm^{-1}) solid[c]	infrared(cm^{-1}) solution[d]	NMR[b] $^{31}P\{^1H\}$ δ[e]	NMR[b] ^1H δ
$[Ir_2I_2(CO)(\mu\text{-}CO)(DPM)_2]$ (1)	1948(vs),1741(vs)	1960(vs),1742(st)	7.32(m), -10.13(m)[f]	7.1-7.8(m, 40H), 4.71(m, 2H), 4.56(m, 2H)
$[Ir_2(CO)_2(\mu\text{-}I)(DPM)_2][BF_4]$ (2)	1966(vs),1937(st)	1971(st),1957(vs)	13.93(s)	6.9-7.9(m, 40H), 4.21(m, 2H), 3.80(m, 2H)
$[Ir_2(CO)_2(\mu\text{-}CO)(\mu\text{-}I)(DPM)_2][I]$ (3a)	1991(st),1949(vs,br), 1815(st)	1977(vs,br), 1872(med)	-4.46(s)	6.9-7.8(m, 40H), 4.63(m, 2H), 4.13(m, 2H)
$[Ir_2(CO)_2(\mu\text{-}CO)(\mu\text{-}I)(DPM)_2][BF_4]$ (3b)	1954(vs,br), 1804(med)	1970(vs),1950(st) 1825(w)	-4.81(s)	7.0-7.9(m, 40H), 4.50(m, 2H), 4.21(m, 2H)
$[Ir_2I_2(CO)_2(\mu\text{-}DMA)(DPM)_2]$ (4a)	2025(vs)[g]	2040(vs), 2008(st)[g], 1689(sh)[h],1548(w)[i]	-4.08(s)	4.78(m, 4H), 3.51(s, 6H)[j]
$[Ir_2I_2(CO)_2(\mu\text{-}DMA)(DPM)_2]$ (4b)	1996(st),1977(med)[g]	1961(vs,br),1728(vs,br)[g] 1705(med)[h],1635(med)[i]	-23.53(s)	2.45(m, 4H), 1.71(s, 6H)

Table 2.1. (Continued)

$[Ir_2I_2(CO)_2(\mu\text{-DMA})(DPM)_2]$ (4c)	2071(vs)[g], 1685(med)[h],1632(med)[i]	2063(st)[g]	-29.22(s)	4.94(m, 2H), 4.08(m, 2H), 2.89(s, 6H)
$[Ir_2I_2(CO)_2(\mu\text{-DMA})(DPM)_2]$ (4d)	2042(vs),1983(vs)[g] 1695(med), 1669(med)[h], 1554(med)[i]	2033(vs), 2006(st), 1932(st),1703(st)[g], 1683(med),1662(med)[h] 1555(med),1539(w)[i]	-35.87(m)	5.08(m, 2H), 4.43(m, 2H), 3.53(s, 3H), 2.54(s, 3H)
$[Ir_2(CO)_2(\mu\text{-I})(\mu\text{-DMA})(DPM)_2][BF_4]$ (5)	1987(vs,br)[g], 1705(med)[h],1613(w)[i]	1998(vs)[g],1704(med) 1690(med)[h], 1613(w)[i]	-16.86(s)	6.8-8.1(m, 40H), 4.29(m, 2H), 3.97(m, 2H), 2.95(s, 6H)

[a] Abbreviations used: st = strong, vs = very strong, med = medium, w = weak, sh = shoulder, s = singlet, m = multiplet, br = broad. [b] In CD_2Cl_2 except compound 2 ($THF\text{-}d_8$). [c] Nujol mull. [d] CH_2Cl_2 solution except compounds 2 and 3b (THF). [e] Vs 85% H_3PO_4. [f] -40C. [g] ν(CO). [h] ν(C=O) of CO_2Me. [i] ν(C=C) of coordinated alkyne. [j] Phenyl resonances for compounds **4a-4d** were combined together in the range 7.0-8.0.

(b) $[Ir_2(CO)_2(\mu\text{-}I)(DPM)_2][BF_4]\cdot THF$ (**2**).

The compound $[Ir_2I_2(CO)(\mu\text{-}CO)(DPM)_2]$ (**1**) (80.0 mg, 0.055 mmol), which had previously been recrystallized from THF/diethylether, was suspended in 10 mL of THF. To the suspension was added $AgBF_4$ (10.0 mg, 0.055 mmol) in 5 mL of THF, causing an immediate color change to dark red. The solution was stirred for an additional 30 min after which time it was filtered to remove the silver salts. The solution was concentrated to approximately 5 mL with rapid dinitrogen flow and 10 mL of diethyl ether was added, resulting in the precipitation of a brick-red microcrystalline solid. The solid was collected and washed with two 5-mL portions of diethyl ether and dried *in vacuo*, giving typical isolated yields of 75-80%. Compound **2** was determined to be weakly conducting in THF solutions (Λ_m = 16.4 $\Omega^{-1}cm^2mole^{-1}$), but a normal 1:1 electrolyte in acetone (Λ_m = 147 $\Omega^{-1}cm^2mole^{-1}$). Anal. calcd for $Ir_2IP_4F_4O_3C_{56}BH_{52}$: C, 44.99%; H, 3.51%; I, 8.49%. Found: C, 44.54%; H, 3.34%; I, 7.24%.

Reactions with Carbon Monoxide

For each of compounds **1** and **2**, a sample of the compound was dissolved in a minimum volume of CH_2Cl_2 and THF, respectively, under dinitrogen. The dinitrogen atmosphere was then replaced by carbon monoxide and in each case caused an immediate color change to light yellow. Only in the case of **1** was the resulting compound isolable without CO loss. Compound **3a**, $[Ir_2(CO)_2(\mu\text{-}CO)(\mu\text{-}I)(DPM)_2][I]$, was obtained by layering the CH_2Cl_2 solution with 10 mL of diethyl ether under CO atmosphere and allowing slow diffusion for 17 h to precipitate a yellow

microcrystalline solid. The solvent was removed and the solid was dried by rapid dinitrogen flow giving compound **3a** in 90% yield. Compound **3a** was determined to be a 1:1 electrolyte in CH_2Cl_2 solutions (Λ_m = 56.3 $\Omega^{-1}cm^2$ $mole^{-1}$). Anal. calcd for $Ir_2I_2P_4O_3C_{53}H_{44}$: C, 42.69%; H, 2.97%; I, 17.02%. Found: C, 42.43%; H, 3.06%; I, 16.72%.

Reactions with Dimethylacetylenedicarboxylate (DMA)

For each of compounds **1** and **2**, a 50.0 mg sample of the compound was dissolved in 10 mL of CH_2Cl_2, and THF, respectively, and one equivalent of dimethylacetylenedicarboxylate (DMA) was added. After the reaction was complete (as monitored by $^{31}P\{^1H\}$ NMR) the solution was concentrated to one half its original volume with rapid N_2 flow, and the products precipitated by the addition of 10 mL of diethyl ether. The solid was then collected, washed with diethyl ether and dried *in vacuo*.

In the case of compound **1**, four products were observed over time, the final product being $[Ir_2I_2(CO)_2(\mu\text{-DMA})(DPM)_2]$ (**4d**) obtained in 95% yield. Compound **4d** was found to be non-conducting in CH_2Cl_2 solutions (Λ_m = 2.3 $\Omega^{-1}cm^2mole^{-1}$). Anal. calcd for $Ir_2I_2Cl_2P_4O_6C_{59}H_{52}$: C, 42.82%; H, 3.17%; I, 15.23%. Found: C, 42.82%; H, 2.93%; I, 16.12%.

In the case of compound **2**, one product was formed immediately, accompanied by a color change to light orange-yellow, and was isolated in 95% yield. Compound **5**, $[Ir_2(CO)_2(\mu\text{-I})(\mu\text{-DMA})(DPM)_2][BF_4]$, was determined to be a 1:1 electrolyte in CH_2Cl_2 solutions (Λ_m = 57.4 $\Omega^{-1}cm^2mole^{-1}$). Anal. calcd for $Ir_2IP_4F_4O_6C_{58}BH_{50}$: C, 45.54%; H, 3.29%; I, 8.30%. Found: C, 44.57%; H, 3.10%; I, 8.11%.

X-ray Data Collection

Crystals of $[Ir_2I_2(CO)(\mu\text{-}CO)(DPM)_2]\cdot CH_2Cl_2$ (**1**) suitable for an X-ray diffraction study were obtained by slow diffusion of diethyl ether into a saturated CH_2Cl_2 solution of complex **1**. Due to the sensitivity of the crystals to air, one was wedged into a dinitrogen-filled glass capillary which was flame sealed. Unit cell parameters were obtained from a least-squares refinement of the setting angles of 25 reflections, in the range $22.0° \leq 2\theta \leq 25.2°$, which were accurately centered on an Enraf-Nonius CAD4 diffractometer using graphite monochromated MoKα radiation. The systematic absences (h0l, l = odd; 0k0, k = odd) were consistent with the space group $P2_1/c$.

Intensity data were collected on the CAD4 diffractometer in the bisecting mode employing the $\theta/2\theta$ scan technique up to $2\theta = 50.00°$. The scan range was determined as a function of θ to compensate for α_1-α_2 wavelength dispersion and backgrounds were scanned for 25% of the peak width on either end of the peak scan. The intensities of three standard reflections were measured every 1 h of exposure time in order to monitor crystal and electronic stability. The mean decrease in the intensity of the standards was 6.3% and a correction was applied assuming linear decay. The data were processed in the usual manner with a value of 0.04 used for p to downweight intense reflections.[5] Corrections for Lorenz and polarization effects and for absorption, using the method of Walker and Stuart,[6] were applied to the data. See Table 2.2 for pertinent crystal data and details of intensity collection.

Table 2.2. Summary of Crystal Data and Details of Intensity Collection.

compd	$[Ir_2I_2(CO)(\mu\text{-}CO)(DPM)_2]\cdot CH_2Cl_2$
formula	$Ir_2I_2Cl_2P_4O_2C_{53}H_{46}$
fw	1547.97
crystal shape	monoclinic prism
crystal size, mm	$0.34 \times 0.24 \times 0.048$
space group	$P2_1/c$ (No. 14)
cell parameters	
a, Å	20.241(4)
b, Å	14.153(2)
c, Å	20.446(2)
β, deg	112.76(1)
V, Å^3	5400.7
Z	4
ρ(calcd), g/cm^3	1.904
temp, °C	22
radiation (λ, Å)	graphite monochromated MoKα (0.71069)
receiving aperture, mm	3.00+(tanθ) wide × 4.00 high, 173 from crystal
take off angle, deg	3.00
scan speed, deg/min	variable between 6.67 and 0.91
scan width, deg	0.75 + (0.347 tanθ) in θ

Table 2.2. (Continued)

2θ limits, deg	$0.6 \leq 2\theta \leq 50.0$
no. of unique data collected	9599 (h, k, ±l)
no. of unique data used ($F_o^2 \geq 3\sigma(F_o^2)$)	5949
linear absorption coeff, μ, cm^{-1}	62.91
range of transmission factors	0.818-1.574
final no. of parameters refined	346
error in observation of unit weight	1.454
R	0.041
R_w	0.049

Structure Solution and Refinement

The crystal structure was solved in the space group $P2_1/c$ by using a combination of direct methods and Patterson techniques to locate the metals and the iodine atoms. All other atoms were located after subsequent least-squares and difference Fourier calculations. Electron densities in the regions of the CH_2Cl_2 solvent atoms were somewhat smeared out, giving rise to high thermal parameters for these atoms. All hydrogen atoms were located, but were assigned idealized positions based on the geometry of their attached carbon atom and using C-H distances of 0.95 Å; thermal parameters were fixed at 1.2 times that of their attached carbon atom. The hydrogen atoms were included as fixed contributions in the least-squares calculations but were not refined.

Refinement was carried out using full-matrix least-squares techniques,[7] minimizing the function $\Sigma w(|F_o|-|F_c|)^2$, with $w = 4F_o^2/\sigma^2(F_o^2)$. The neutral atom scattering factors[8,9] and anomalous dispersion terms[10] used in the structure determination programs were obtained from the usual sources.

The final model with 346 parameters varied refined to R = 0.041 and $R_w = 0.049$.[11] In the final difference Fourier map, the 10 highest residual peaks were in the range 1.09-0.80 e/Å^3, and were located in the vicinities of the iridium and iodine atoms and the DPM ligands. The positional and thermal parameters for the individual non-hydrogen atoms are given in Table 2.3.

Table 2.3. Positional Parameters and Isotropic Thermal Parameters.[a]

Atom	x	y	z	B (Å^2)
Ir(1)	0.23486(2)	0.46273(3)	0.41553(2)	2.002(8)
Ir(2)	0.22573(2)	0.63648(3)	0.47848(2)	2.100(8)
I(1)	0.24372(4)	0.29948(5)	0.35289(4)	3.62(2)
I(2)	0.37284(4)	0.66399(6)	0.51473(4)	3.83(2)
Cl(1)[b]	0.4963(4)	0.5845(5)	0.1089(4)	14.2(3)
Cl(2)[b]	0.5827(5)	0.6723(5)	0.2387(5)	20.7(3)
P(1)	0.2307(1)	0.5358(2)	0.3130(1)	2.37(6)
P(2)	0.2028(2)	0.7191(2)	0.3731(1)	2.36(6)
P(3)	0.2685(1)	0.3840(2)	0.5221(1)	2.23(6)
P(4)	0.2592(1)	0.5705(2)	0.5917(1)	2.37(6)
O(1)	0.0957(4)	0.5136(5)	0.4111(4)	3.3(2)
O(2)	0.1421(5)	0.7824(7)	0.5182(4)	5.9(2)
C(1)	0.1587(5)	0.5317(7)	0.4283(4)	1.9(2)
C(2)	0.1754(6)	0.7295(8)	0.5044(6)	3.7(3)
C(3)	0.2472(5)	0.6632(7)	0.3213(5)	2.6(2)
C(4)	0.3087(5)	0.4619(8)	0.5991(5)	2.7(2)
C(5)[b]	0.533(1)	0.687(1)	0.151(1)	13.0(9)
C(11)	0.1486(5)	0.5257(7)	0.2330(5)	2.7(2)*
C(12)	0.0909(6)	0.4803(8)	0.2377(6)	3.5(2)*
C(13)	0.0253(7)	0.4782(9)	0.1784(6)	4.5(3)*
C(14)	0.0205(7)	0.519(1)	0.1167(7)	5.1(3)*
C(15)	0.0769(7)	0.563(1)	0.1105(7)	5.0(3)*
C(16)	0.1422(6)	0.5689(9)	0.1692(6)	4.0(3)*
C(21)	0.3054(6)	0.4962(8)	0.2905(6)	3.1(2)*
C(22)	0.3723(7)	0.5090(9)	0.3421(6)	4.2(3)*
C(23)	0.4339(7)	0.477(1)	0.3329(7)	5.3(3)*
C(24)	0.4258(9)	0.438(1)	0.2693(8)	7.3(4)*
C(25)	0.3596(8)	0.426(1)	0.2165(8)	6.5(4)*

Table 2.3. (Continued)

C(26)	0.2955(7)	0.4548(9)	0.2257(6)	4.5(3)*
C(31)	0.1102(5)	0.7321(7)	0.3130(5)	2.7(2)*
C(32)	0.0951(7)	0.7711(9)	0.2452(6)	4.4(3)*
C(33)	0.0242(7)	0.782(1)	0.1984(7)	5.0(3)*
C(34)	-0.0308(7)	0.758(1)	0.2189(7)	5.2(3)*
C(35)	-0.0172(7)	0.7212(9)	0.2853(6)	4.4(3)*
C(36)	0.0533(6)	0.7088(9)	0.3315(6)	4.0(3)*
C(41)	0.2345(6)	0.8420(8)	0.3845(5)	2.8(2)*
C(42)	0.1930(7)	0.9092(9)	0.4012(6)	4.3(3)*
C(43)	0.2200(7)	1.005(1)	0.4104(7)	5.2(3)*
C(44)	0.2811(8)	1.025(1)	0.4041(7)	5.8(4)*
C(45)	0.3215(8)	0.962(1)	0.3890(8)	6.1(4)*
C(46)	0.2984(7)	0.8662(9)	0.3780(6)	4.5(3)*
C(51)	0.3442(6)	0.3040(8)	0.5356(5)	2.9(2)*
C(52)	0.3411(6)	0.2094(9)	0.5464(6)	3.8(3)*
C(53)	0.3991(8)	0.150(1)	0.5496(7)	5.9(4)*
C(54)	0.4566(8)	0.189(1)	0.5428(7)	5.5(3)*
C(55)	0.4623(8)	0.284(1)	0.5348(7)	5.7(3)*
C(56)	0.4056(7)	0.3442(9)	0.5309(6)	4.7(3)*
C(61)	0.2027(6)	0.3156(8)	0.5424(5)	3.0(2)*
C(62)	0.2160(6)	0.2798(8)	0.6101(6)	3.6(2)*
C(63)	0.1632(7)	0.232(1)	0.6241(7)	4.9(3)*
C(64)	0.0983(8)	0.215(1)	0.5702(7)	5.8(3)*
C(65)	0.0847(8)	0.247(1)	0.5023(8)	6.0(4)*
C(66)	0.1377(7)	0.2992(9)	0.4892(6)	4.5(3)*
C(71)	0.1872(5)	0.5415(7)	0.6125(5)	2.7(2)*
C(72)	0.1158(6)	0.5528(9)	0.5764(6)	3.8(3)*
C(73)	0.0614(7)	0.527(1)	0.5998(7)	5.0(3)*
C(74)	0.0784(7)	0.4921(9)	0.6634(7)	4.6(3)*
C(75)	0.1492(7)	0.4813(9)	0.7113(7)	4.7(3)*

Table 2.3. (Continued)

C(76)	0.2046(6)	0.5042(9)	0.6888(6)	3.8(3)*
C(81)	0.3207(6)	0.6417(8)	0.6649(5)	3.0(2)*
C(82)	0.3137(6)	0.7413(9)	0.6603(6)	3.9(3)*
C(83)	0.3627(7)	0.797(1)	0.7168(6)	4.7(3)*
C(84)	0.4152(7)	0.754(1)	0.7752(7)	5.4(3)*
C(85)	0.4214(7)	0.658(1)	0.7785(7)	4.8(3)*
C(86)	0.3741(6)	0.5998(9)	0.7233(6)	3.8(3)*

[a] Estimated standard deviations in this and other tables are given in parentheses and correspond to the least significant digits. Starred atoms were refined isotropically. Anisotropically refined atoms are given in the form of the isotropic equivalent displacement parameter defined as: $(4/3)[a^2\beta(1,1) + b^2\beta(2,2) + c^2\beta(3,3) + ab(\cos \text{gamma})\beta(1,2) + ac(\cos \text{beta})\beta(1,3) + bc(\cos \text{alpha})\beta(2,3)]$.

[b] Atoms Cl(1), Cl(2) and C(5) are those of the CH_2Cl_2 solvent molecule.

Results and Discussion

(a) Description of Structure

The complex $[Ir_2I_2(CO)(\mu\text{-}CO)(DPM)_2]$ (**1**) crystallizes in the space group $P2_1/c$ with one complex molecule and one CH_2Cl_2 solvent molecule in the asymmetric unit. The solvent molecule displays the expected geometry with no unusual contacts to the complex molecule. A perspective view of the complex, including the numbering scheme is shown in Figure 2.1. Selected distances and angles are given in Tables 2.4 and 2.5, respectively.

The complex has the bridging DPM ligands in a normal trans arrangement,[12] but having the DPM methylene groups tilted toward the side of the molecule containing the large iodine atoms. Such an arrangement is atypical of A-frame-like complexes, in which the DPM methylenes usually bend toward the group which bridges the metals. However, in this complex the present geometry appears to minimize the potentially more severe steric interactions between the phenyl hydrogens and the iodo ligands. Within the diphosphine ligands the parameters are as expected.[1,3,13,14] Even the slightly longer Ir-P distances involving Ir(2) are not unexpected, reflecting the greater crowding at this metal center.

In the equatorial plane the ligand arrangement is unusual in two significant ways. First, both of the carbonyl and both of the iodo ligands are mutually cis on adjacent metals, even though the two chloro and two carbonyl ligands in the precursor, $[IrCl(CO)(DPM)]_2$, were mutually trans.

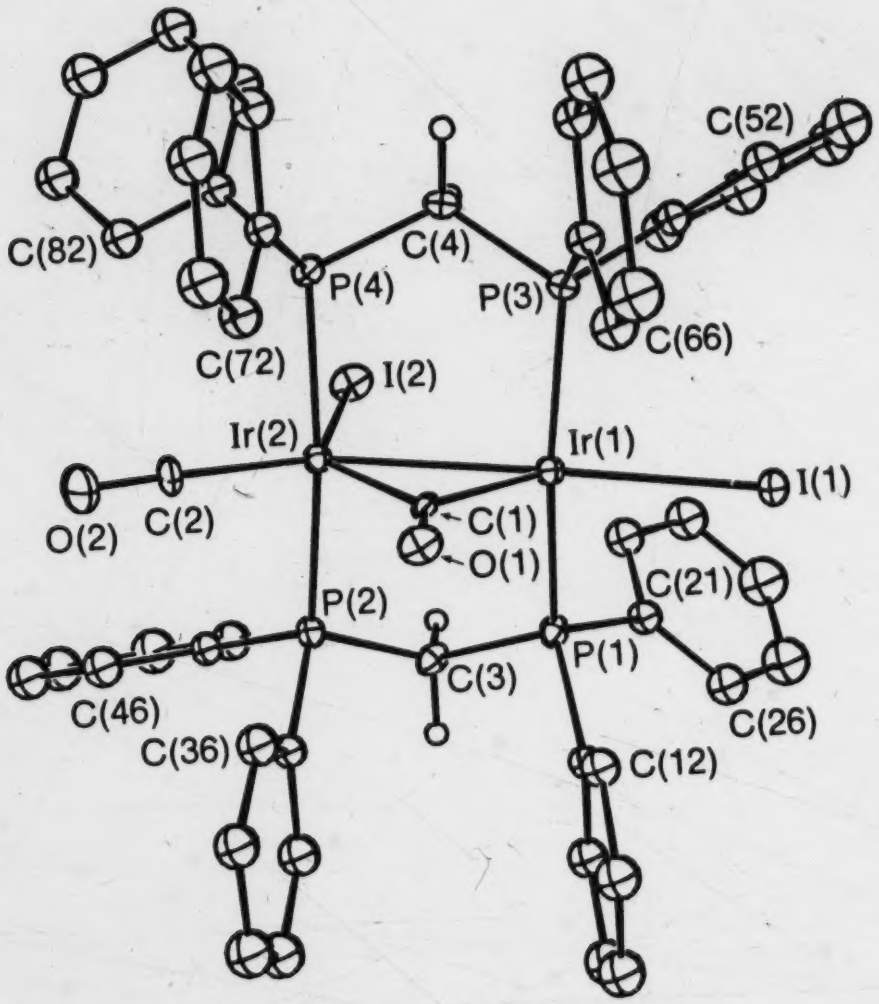

Figure 2.1. A perspective view of $[Ir_2I_2(CO)(\mu\text{-}CO)(DPM)_2]$, showing the numbering scheme. Thermal ellipsoids are shown at the 20% level except for the methylene hydrogens, which are shown artificially small and the phenyl hydrogens, which are omitted.

Table 2.4. Selected Distances (Å) in $[Ir_2I_2(CO)(\mu\text{-}CO)(DPM)_2]$.

Ir(1)-Ir(2)	2.8159(5)	P(1)-C(21)	1.84(1)
Ir(1)-I(1)	2.6811(7)	P(2)-C(3)	1.814(9)
Ir(1)-P(1)	2.310(2)	P(2)-C(31)	1.811(9)
Ir(1)-P(3)	2.303(2)	P(2)-C(41)	1.838(9)
Ir(1)-C(1)	1.926(8)	P(3)-C(4)	1.835(9)
Ir(2)-I(2)	2.8032(8)	P(3)-C(51)	1.84(1)
Ir(2)-P(2)	2.334(2)	P(3)-C(61)	1.82(1)
Ir(2)-P(4)	2.340(2)	P(4)-C(4)	1.808(9)
Ir(2)-C(1)	2.005(9)	P(4)-C(71)	1.831(9)
Ir(2)-C(2)	1.86(1)	P(4)-C(81)	1.83(1)
P(1)-C(3)	1.830(9)	O(1)-C(1)	1.22(1)
P(1)-C(11)	1.830(9)	O(2)-C(2)	1.11(1)

Table 2.5. Selected Angles (deg) in $[Ir_2I_2(CO)(\mu\text{-}CO)(DPM)_2]$.

Ir(2)-Ir(1)-I(1)	178.60(2)	P(4)-Ir(2)-C(1)	95.2(2)
Ir(2)-Ir(1)-P(1)	92.18(6)	P(4)-Ir(2)-C(2)	88.9(3)
Ir(2)-Ir(1)-P(3)	92.17(6)	C(1)-Ir(2)-C(2)	109.4(4)
Ir(2)-Ir(1)-C(1)	45.4(3)	Ir(1)-P(1)-C(3)	114.6(3)
I(1)-Ir(1)-P(1)	86.43(6)	Ir(1)-P(1)-C(11)	118.6(3)
I(1)-Ir(1)-P(3)	89.16(6)	Ir(1)-P(1)-C(21)	110.3(3)
I(1)-Ir(1)-C(1)	134.9(3)	C(3)-P(1)-C(11)	103.3(4)
P(1)-Ir(1)-P(3)	165.70(9)	C(3)-P(1)-C(21)	100.7(4)
P(1)-Ir(1)-C(1)	98.4(2)	C(11)-P(1)-C(21)	107.7(4)
P(3)-Ir(1)-C(1)	94.3(2)	Ir(2)-P(2)-C(3)	110.8(3)
Ir(1)-Ir(2)-I(2)	89.48(2)	Ir(2)-P(2)-C(31)	117.4(3)
Ir(1)-Ir(2)-P(2)	92.28(6)	Ir(2)-P(2)-C(41)	114.9(3)
Ir(1)-Ir(2)-P(4)	93.31(6)	C(3)-P(2)-C(31)	105.4(4)
Ir(1)-Ir(2)-C(1)	43.1(2)	C(3)-P(2)-C(41)	105.2(4)
Ir(1)-Ir(2)-C(2)	152.5(4)	C(31)-P(2)-C(41)	102.0(4)
I(2)-Ir(2)-P(2)	89.21(6)	Ir(1)-P(3)-C(4)	113.1(3)
I(2)-Ir(2)-P(4)	85.53(6)	Ir(1)-P(3)-C(51)	111.4(3)
I(2)-Ir(2)-C(1)	132.6(2)	Ir(1)-P(3)-C(61)	120.0(3)
I(2)-Ir(2)-C(2)	118.0(4)	C(4)-P(3)-C(51)	100.0(4)
P(2)-Ir(2)-P(4)	172.28(8)	C(4)-P(3)-C(61)	104.2(4)
P(2)-Ir(2)-C(1)	92.6(2)	C(51)-P(3)-C(61)	106.2(4)
P(2)-Ir(2)-C(2)	88.6(3)	Ir(2)-P(4)-C(4)	111.3(3)

Table 2.5. (Continued)

Ir(2)-P(4)-C(71)	117.1(3)	Ir(1)-C(1)-O(1)	131.4(7)
Ir(2)-P(4)-C(81)	115.7(3)	Ir(2)-C(1)-O(1)	137.1(7)
C(4)-P(4)-C(71)	105.4(4)	Ir(2)-C(2)-O(2)	176.(1)
C(4)-P(4)-C(81)	102.7(4)	P(1)-C(3)-P(2)	111.7(5)
C(71)-P(4)-C(81)	103.1(4)	P(3)-C(4)-P(4)	113.0(5)
Ir(1)-C(1)-Ir(2)	91.5(4)		

The observed arrangement for the diiodo complex is perhaps unexpected based on steric arguments, which would appear to favour a trans arrangement, having the bulky iodo ligands widely separated. The second unusual feature is the unsymmetrical structure adopted by the complex, in which both metals have a terminal iodo and a bridging carbonyl group attached, with one metal having an additional terminal carbonyl ligand. Based on the stoichiometry, a symmetric structure in which each metal is bound to one CO and one iodo ligand, as observed in the dichloro analogue,[3] would appear more likely. In addition, the movement of one carbonyl group to the bridging position is accompanied by metal-metal bond formation, a feature which should destabilize the structure by bringing the bulky iodo ligands closer together.

The most likely rationale for the adopted structure, particularly the presence of the bridging carbonyl group, is that it serves to relieve the metal centers of some excess electron density, put upon them by the good electron-donor iodo ligands. Bridging carbonyl groups are recognized as better π-acids than terminal carbonyls,[15] and of relevance to the present case, conversion of terminal CO ligands into bridging ones has been observed in metal-carbonyl clusters[15] and in related binuclear complexes[16] upon substitution of carbonyl groups for electron-donating groups. Such a role for the bridging CO ligand in compound **1** is supported by the low infrared stretching frequency of the group (1741 cm^{-1}), although this value is not outside of the range displayed by similar diiridium chlorocarbonyls.[3] The unsymmetrical geometry has previously been observed in a related dirhodium complex, $[Rh_2Cl_2(CO)(\mu\text{-}CO)((MeO)_2PNEtP(OMe)_2)_2]$.[17] Here

too, the carbonyl groups are adjacent to one another, as are the two chloro ligands. In this case it would seem unlikely that the geometry is dictated by steric effects, since the methoxy substituents are smaller than the phenyl groups in the present compound. Furthermore, one should compare this methoxydiphosphane-bridged complex with its phenoxy-substituted analogue, $[RhCl(CO)((PhO)_2PNEtP(OPh)_2)]_2$,[17] which does have the symmetric trans structure. The structures of these two species would appear consistent with previous arguments regarding compound **1**, based on the greater electron-donating ability of the methoxy group compared to the phenoxy group.[18] An analogous geometry has been proposed for $[Rh_2I_2(CO)(\mu\text{-}CO)(DPM)_2]$[19] and is also suggested for one isomer of the heterobinuclear complex, $[RhIrCl_2(CO)_2(DPM)_2]$ (Chapter 3), as well as for $[RhIrI_2(CO)(\mu\text{-}CO)(DPM)_2]$.[20] For the mixed-metal species the terminal CO groups reside on the iridium centers, thus it would appear that the carbonyl-bridged structures are also favored by the greater tendency of the more basic iridium center to bind carbonyl groups.

The geometries at each of the iridium centers in compound **1** are reminiscent of two known DPM-bridged complexes. At Ir(1) the geometry resembles that observed in $[Rh_2X_2(\mu\text{-}CO)(DPM)_2]$ (X = Cl,[21] Br[22]), except that in **1** the iodo ligand is almost colinear with the Ir-Ir bond (178.60(2)°), whereas the analogous Rh-Rh-Br and Rh-Rh-Cl angles averaged 166.26° and 161.5°, respectively. This difference is probably a consequence of steric repulsions involving I(1) and the proximate phenyl groups in **1**. The geometry about Ir(2) closely resembles that observed in $[Ir_2Cl_2(CO)_2(\mu\text{-}CO)\text{-}(DPM)_2]$,[3] and here again the slight differences in the angles at Ir appear to

be steric in origin. The entire structure of compound **1** is closely related to that of the above dichlorotricarbonyl species, merely lacking one carbonyl group on Ir(1).

The Ir(1)-Ir(2) separation of 2.8159(5) Å corresponds to a normal single bond,[1,3,13,14] and the relatively acute Ir(1)-C(1)-Ir(2) angle (91.5(4)°) is typical for a carbonyl group which is bridging a metal-metal bond. The bonding of this carbonyl is unsymmetrical, being significantly closer to Ir(1) than Ir(2) (1.926(8) Å *vs* 2.005(9) Å). This difference may be due either to electronic or steric factors. The π back-donation to C(1)-O(1) should be somewhat lower from Ir(2) due to competition from C(2)-O(2), and may partially account for the longer Ir(2)-C(1) distance. It also appears that the proximate phenyl group (ring 7) forces the bridging carbonyl away from Ir(2) as seen in Figure 2.1. Consistent with this suggestion the H(72)-O(1) distance is rather short, at 2.43 Å.

As was observed for the Rh-Cl distances in $[Rh_2Cl_2(CO)(\mu\text{-}CO)\text{-}\{(MeO)_2PNEtP(OMe)_2\}_2]$,[17] the Ir(2)-I(2) bond adjacent to the metal-metal bond is longer (2.8032(8) Å) than the one opposite the metal-metal bond (Ir(1)-I(1) = 2.6811(7) Å). Since metal-metal bonds have been shown to cause a "trans lengthening" in such complexes,[13,23-25] the observed reversal in this case must again reflect the greater crowding about Ir(2).

(b) Description of Chemistry

Solutions of *trans*-$[IrCl(CO)(DPM)]_2$ react immediately with KI yielding compound **1**. The orange microcrystalline solid isolated from the

solution displays a terminal carbonyl band in the infrared spectrum at 1948 cm^{-1} and a bridging CO band at 1741 cm^{-1}. A low conductivity in CH_2Cl_2 and the solution IR data indicate that there is little difference between the structure of **1** in solution and its structure in the solid state. The $^{31}P\{^1H\}$ NMR spectrum at -40 °C displays two sets of complex multiplets, also consistent with an unsymmetrical species having an AA'BB' spin system by virtue of the two sets of chemically inequivalent phosphorus nuclei. Note that these spectroscopic data are in agreement with the structure previously discussed. As the sample is warmed, the resonances in the $^{31}P\{^1H\}$ NMR spectrum broaden and coalesce at approximately +35 °C, indicating a fluxional process which exchanges the phosphorus environments. This could possibly occur via iodide dissociation to yield a cationic A-frame species. However the low conductivity of **1** in solution and the instability of the iodide A-frame species in CH_2Cl_2 (vide infra) suggests that the fluxionality does not result from iodide loss, but instead occurs by exchange of the carbonyl groups between bridging and terminal sites, as shown.

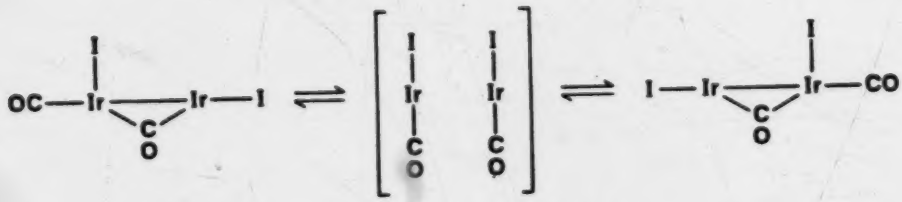

Iodide abstraction from **1** using $AgBF_4$ immediately yields a dark-red solution. The isolated solid displays two terminal carbonyl bands (1966,

1937 cm^{-1}) in the infrared spectrum and elemental analyses indicate the presence of only one iodine atom per dimer. This information, along with the $^{31}P\{^1H\}$ NMR spectrum (δ 13.93(s)) which indicates that all four phosphorus atoms are chemically equivalent, leads to the A-frame formulation for **2**, analogous to the chloro- and sulfido-bridged complexes of

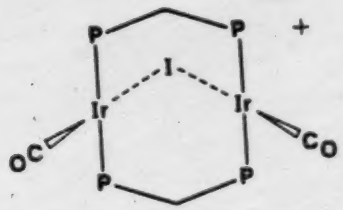

2

both rhodium[26-28] and iridium.[3,14] In the infrared spectrum, the carbonyl stretches for compound **2** are at lower frequency than those of the chloro analogue (1989, 1964 cm^{-1}),[3] reflecting the higher π-donor ability of iodine over chlorine. However the values are still higher than the neutral sulfido-bridged species (1918, 1902 cm^{-1}),[14] presumably owing, in part, to the cationic nature of **2**. In THF the low conductivity of compound **2** (16.4 $\Omega^{-1}cm^2mole^{-1}$) suggests rather tight ion pairing; in acetone, however, **2** behaves as a normal 1:1 electrolyte (147 $\Omega^{-1}cm^2mole^{-1}$).[4b] Although the low conductivity in THF suggests the possibility of weak interactions between the fluorine atoms of BF_4^- and one or both metal centers, no indication of such is observed in either the infrared or the ^{19}F NMR spectra. Compound **2** is also found to readily scavenge Cl^- from CH_2Cl_2 yielding at least two unidentified unsymmetrical complexes which are presumed to be mixed-halide species; the use of this solvent was subsequently avoided.

Addition of one equivalent of CO to a solution of $[Ir_2I_2(CO)(\mu\text{-}CO)(DPM)_2]$ (**1**) causes an immediate color change from orange to yellow. The $^{31}P\{^1H\}$ NMR spectrum reveals a single symmetric species, and the infrared spectrum displays terminal (1977 cm^{-1}) and bridging (1872 cm^{-1}) carbonyl stretches. The broadness of the terminal CO stretch would suggest that another band is beneath it. No further change is observed upon addition of excess CO to the solution. This information, together with the conductivity measurements (which indicate a 1:1 electrolyte) leads to the formulation, $[Ir_2(CO)_2(\mu\text{-}I)(\mu\text{-}CO)(DPM)_2][I]$ (**3a**), having the doubly-bridged A-frame geometry previously observed for the chloro-bridged dirhodium

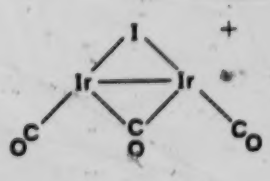

3a

analogue[27,29] and the sulfido-bridged diiridium complex.[14] In contrast, the analogous neutral chloro compound, *trans*-$[IrCl(CO)(DPM)]_2$, did not lose chloride upon reaction with one equivalent of CO, but gave a neutral dichloro-tricarbonyl species, $[Ir_2Cl(CO)_3(\mu\text{-}Cl)(DPM)_2]$,[3] which subsequently reacted further with CO to yield a cationic tetracarbonyl species through substitution of Cl^- by CO. Although the structure proposed for **3a** is not totally unexpected, attack at the open coordination site on Ir(1) of **1** would yield a product analogous to the above neutral dichloride species, if I^- loss did not occur. Apparently the steric demands in such a complex are too

great, promoting iodide dissociation. Subsequent CO attack, to give a cationic tetracarbonyl complex, as observed for the chloride, also does not appear to occur, again probably for steric reasons. Notably, iodide loss and coordination of an additional carbonyl ligand raises the infrared stretching frequency of the bridging carbonyl in **3a** considerably compared to **1**.

The cationic iodo-bridged A-frame, **2**, also reacts with one equivalent of CO yielding a product which is very similar in most respects to compound **3a** and is accordingly formulated as $[Ir_2(CO)_2(\mu\text{-}I)(\mu\text{-}CO)\text{-}(DPM)_2][BF_4]$ (**3b**). A significant difference, however, is that CO loss from **3b** is very facile, occurring simply upon N_2 purge over a solid sample of **3b**, whereas **3a** requires 10 min under reflux in THF and N_2 purge to recover compound **1** quantitatively.[30] The reasons for the different labilities of **3a** and **3b** are not readily understood since one might expect the incoming iodide ligand to make CO loss more facile from **3a**. Furthermore, these results are inconsistent with slightly higher frequency infrared stretches for the carbonyls in **3a** (see Table 2.1), which would suggest weaker Ir-CO bonds compared to those of **3b**.

Each of compounds **1** and **2** reacts with dimethylacetylenedicarboxylate (DMA), yielding complexes having the organic substrate bound parallel to the Ir-Ir axis as a cis-dimetallated olefin. Compound **1** reacts over a 2 h period with one equivalent of DMA to yield two isomers **4a** and **4b** in nearly equal concentrations. Both **4a** and **4b** are symmetric species as judged by the $^{31}P\{^1H\}$ NMR spectrum (singlets at δ -4.08 and -23.53, respectively). Over an additional 18 h period another symmetric species, **4c** (δ -29.22), and an unsymmetrical one, **4d** (δ -35.87), appear. No changes in the

$^{31}P\{^1H\}$ NMR resonances of the four products is observed over the temperature range from 20°C to -80°C. Compound **4d** is apparently the thermodynamically favoured species, obtained quantitatively by refluxing the mixture of four isomers in CH_2Cl_2 for 2 h. The yellow solid finally obtained displays two terminal CO bands in the infrared spectrum (2042, 1983 cm^{-1}) and a band at 1554 cm^{-1}, which is assigned to the C-C stretch of the coordinated acetylene. The similarity of the spectral parameters of compound **4d** and the structurally characterized dichloro species, $[Ir_2Cl_2(CO)_2(\mu\text{-DMA})(DPM)_2]$,[13] suggests an analogous formulation for **4d**. However, in solution compound **4d** is significantly different as evidenced by additional terminal CO bands in the infrared spectrum (2033, 2006, 1982 cm^{-1}), as well as a low frequency stretch at 1703 cm^{-1} which is distinguishable from the carboxylate bands by its intensity. Two acetylenic stretches are also observed (1555, 1539 cm^{-1}). The solution characteristics may indicate a facile fluxionality in which one carbonyl group moves from a terminal to a bridging position. Furthermore, the carbonyl-bridged form

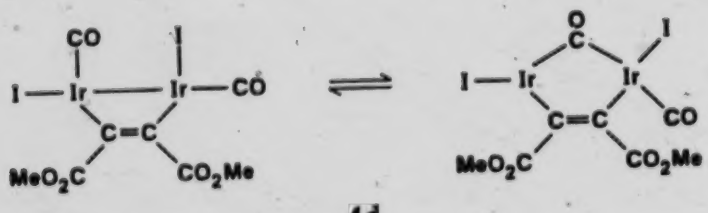

4d

of **4d** should not be unexpected, being rather analogous to the geometry adopted by compound **1**. Although CO bridge-formation might also be electronically favorable, as previously discussed for **1**, this transformation

retains hexa-coordination at one metal center, while reducing the coordination number at the other metal from six to five. Further alleviation of steric crowding could presumably occur by loss of I^-, however, there is no evidence for this, with conductivities in CH_2Cl_2 being very low (Λ_m = 2.3 $\Omega^{-1}cm^2mole^{-1}$). Furthermore, introduction of more polar solvents in an attempt to induce iodide loss only causes precipitation of the complex. Clearly, the iodide loss noted earlier upon CO addition to **1** cannot be solely sterically induced since such loss is not observed upon addition of the bulkier alkyne ligands. Loss of CO is also apparently unfavourable, and in contrast to the chloro analogue of **4d**, refluxing under N_2 purge in higher boiling solvents does not produce a monocarbonyl species, but eventually leads to decomposition of **4d**.

The symmetric intermediates leading to **4d** could not be unequivocally identified. However, based on previous studies[1,13] and upon spectroscopic data monitored during progress of the reaction their natures can be confidently assigned as shown in Scheme 2.1. Although the solid-state structure of **1** suggests that attack at the 16-electron iridium center should occur (site 2), the fluxionality of **1** in solution must be recalled, and thus the exact nature of the reactive intermediates giving rise to **4a** and **4b** is not clear. The methylene proton resonances in the ^1H NMR (see Table 2.1) were assignable to each of **4a-4d** by selective ^{31}P decoupling which causes each resonance in turn to lose coupling to their respective phosphorus atoms. The carboxylate methyl resonances were then easily assigned by comparing their integrations with those of the methylene protons. Due to the similarity in the concentrations of **4a** and **4b**, the infrared bands

Scheme 2.1

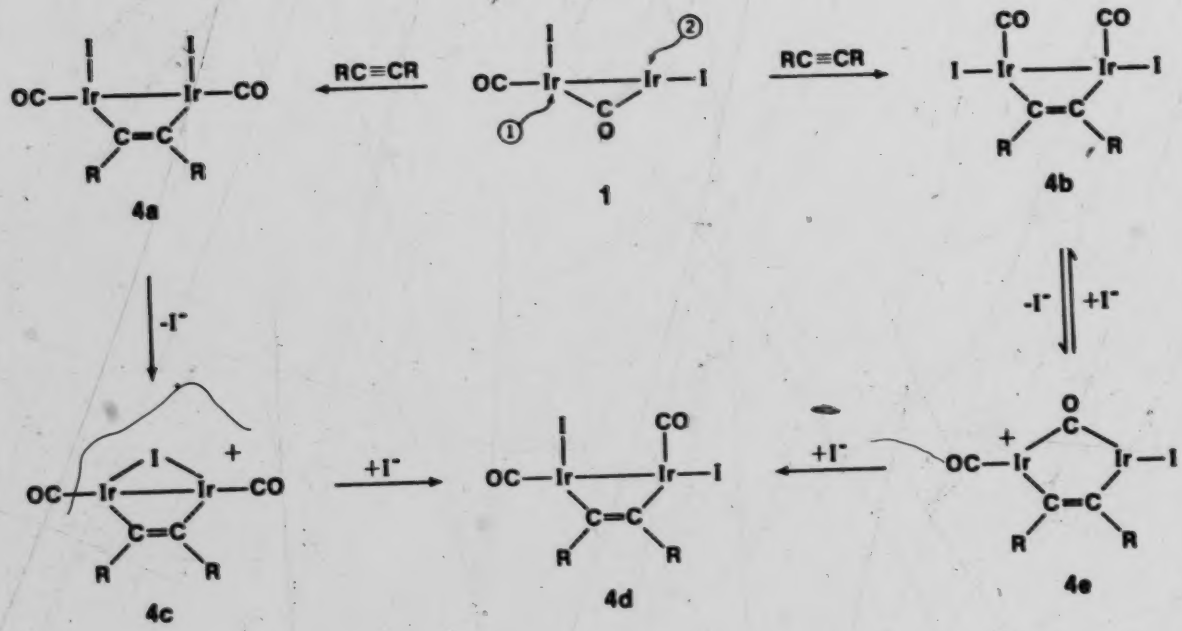

corresponding to each of these species can not be unambiguously assigned. However, they are tentatively assigned according to the previously discussed chloro analogue of **4d**,[13] where the carbonyl ligand opposite the Ir-Ir bond displayed a higher CO stretch (2023 cm^{-1}) than the one opposite the Ir-DMA linkage (1999 cm^{-1}). Furthermore, of the two species, only **4b** appears capable of exhibiting a bridging carbonyl stretch in solution (1728 cm^{-1}), by the mechanism described earlier for **4d**. An equilibrium with species **4e** might be suggested based on the broadness of the two infrared bands attributed to **4b** (possibly due to overlapping bands) and by the slight conductivity (Λ_m = 8.84 $\Omega^{-1}cm^2mole^{-1}$) measured in solutions containing only **4a** and **4b**. Furthermore, iodide loss from both of these species is the most reasonable route to **4d**. In the case of **4a**, iodide loss apparently gives the symmetric species **4c**, observed in the $^{31}P\{^1H\}$ NMR. In support of this scheme, addition of one equivalent of $AgBF_4$ to a THF solution containing all four isomers yields only two products as revealed by $^{31}P\{^1H\}$ NMR: a symmetrical species (δ -16.86) which corresponds exactly to compound **5**, the product of DMA addition to the A-frame complex $[Ir_2(CO)_2(\mu\text{-}I)(DPM)_2][BF_4]$ (**2**) (vide infra), and an unsymmetrical species (δ -0.04, δ -29.07) which must be the analogue of **4e**. The ratio of the symmetrical to unsymmetrical products indicates that all of the **4d** originally present was converted to the unsymmetrical product upon reaction with $AgBF_4$, which is consistent with labilization of the iodide ligand on the more sterically congested iridium center in the carbonyl-bridged form of **4d**. Subsequent addition of excess KI to these products gave only **4d**.

The cationic A-frame complex $[Ir_2(CO)_2(\mu\text{-}I)(DPM)_2][BF_4]$ (**2**) also

reacts slowly with DMA, producing a yellow solution over 2 h. The $^{31}P\{^1H\}$ NMR spectrum reveals a single product, **5**, having four chemically equivalent phosphorus atoms (δ -16.86(singlet)). The solid isolated from the reaction displays a single terminal carbonyl stretch in the infrared spectrum at 1987 cm^{-1}, and a C-C stretch of the coordinated acetylenic moiety at 1613 cm^{-1}. From this information the compound is formulated as $[Ir_2(CO)_2(\mu\text{-}I)(\mu\text{-}DMA)(DPM)_2][BF_4]$ (**5**), the analogue of **4c**. Although there are some differences in the spectroscopic parameters of **4c** and **5**, their similarity is particularly evident in the ^1H NMR spectra (see Table 2.1).

It is important to note that compound **5** appears to result from alkyne attack in the "pocket" of **2**. In contrast, the analogous chloro- and acetate-bridged A-frames, $[Ir_2(CO)_2(\mu\text{-}Cl)(DPM)_2]^+$ and $[Rh_2(CO)_2(\mu\text{-}O_2CCH_3)(DPM)_2]^+$, yielded products which indicated that alkyne attack occurred on the "outsides" of the complexes, adjacent to the bridging anionic groups.[13,31] Such proposals have also been confirmed by an X-ray structure determination of $[Ir_2(CO)(CF_3C_2CF_3)(\mu\text{-}S)(\mu\text{-}CO)(DPM)_2]$ (Chapter 4), which shows the hexafluorobutyne group bound to one metal, adjacent to sulfur on the outside of the complex. Apparently, the presence of the large iodo group in **2** inhibits attack at an adjacent site and instead directs attack to the A-frame pocket on the opposite face of the dimer. It appears that in both **1** and **2** the bulky iodo ligands exert a significant steric influence as shown by the contrasts noted between the chemistry of these species and the chloro analogues, and by the relatively slow rate of reaction with DMA in both cases.

Conclusions

Significant differences between the diiridium iodocarbonyl complexes reported herein, and their chloro and sulfido analogues, appear to result from both the added electron donating ability of the iodo ligand and its increased steric requirements. The good electron-donor iodo ligands cause an increased tendency for the complexes to form carbonyl bridges, compared to analogous chloro species. This is consistent with the greater ability of a bridging CO group (*vs* terminal CO) to relieve the metals of excess electron density. The highest carbonyl-containing species in these complexes is a tricarbonyl cation, which is evidently restricted from additional CO coordination by the size of the iodo ligand. The large iodo ligand also appears to inhibit attack of the alkyne, particularly evident in the reaction of the cationic A-frame complex, $[Ir_2(CO)_2(\mu\text{-}I)(DPM)_2][BF_4]$, with DMA, which yields a symmetric product corresponding to addition of alkyne in the pocket of the A-frame, opposite the iodide-bridge. In contrast, chloride, sulfide and related A-frames have indicated a preference for alkyne attack at the outside sites of the complexes (see also Chapter 4). Nevertheless, the product reveals the expected cis-dimetallated olefin geometry for the bridging DMA, as is commonly observed in these species. Up to this point, the investigations of the binuclear iodocarbonyl complexes does not seem to indicate a reduced tendency for the large iodo ligand to occupy the bridge-position, even in metal-metal bonded situations.

Supplementary Material Available: Listings of the observed and calculated structure factors, bond lengths and angles involving the solvent and phenyl groups, anisotropic thermal parameters, and hydrogen atom parameters for this and subsequent structures are available from Dr. M. Cowie, Department of Chemistry, University of Alberta, Edmonton, Alberta, Canada. T6A 2G2.

References and Footnotes

1. Sutherland, B. R.; Cowie, M. *Organometallics* **1985, 4,** 1801.
2. See Chapter 5.
3. Sutherland, B. R.; Cowie, M. *Inorg. Chem.* **1984,** 23, 2324.
4. (a) Typically a 1:1 electrolyte such as $[Rh_2(CO)_2(\mu\text{-}Cl)(\mu\text{-}CO)(DPM)_2][BF_4]$ gives a value of *ca.* 45 $\Omega^{-1}cm^2mole^{-1}$. (b) See also Geary, W. J. *Coord. Chem. Rev.* **1971,** 7, 81.
5. Doedens, R. J.; Ibers, J. A. *Inorg. Chem.* **1967,** 6, 204.
6. Walker, N.; Stuart, D. *Acta Crystallogr., Sect. A: Cryst. Phys., Diffr., Theor. Gen. Crystallogr.* **1983,** *A*39, 1581.
7. Programs used were those of the Enraf-Nonius Structure Determination Package by B. A. Frenz, in addition to some local programs by R. G. Ball.
8. Cromer, D. T.; Waber, J. F. *International Tables for X-Ray Crystallography*; Kynock: Birmingham, England, 1974; Vol. IV, Table 2.2A.
9. Stewart, R. F.; Davidson, E. F.; Simpson, W. T. *J. Chem. Phys.* **1965,** 42, 3175.
10. Cromer, D. T.; Liberman, D. *J. Chem. Phys.* **1970,** 53, 1891.
11. $R = \Sigma||F_o|-|F_c||/\Sigma|F_o|$; $R_w = [\Sigma w(|F_o|-|F_c|)^2/\Sigma wF_o^2]^{1/2}$.
12. Puddephatt, R. J. *Chem. Soc. Rev.* **1983,** 12, 98.
13. Sutherland, B. R.; Cowie, M. *Organometallics* **1984,** 3, 1869.
14. Eisenberg, R.; Kubiak, C. P.; Woodcock, C. *Inorg. Chem.* **1980,** 19, 2733.

15. Collman, J. P.; Hegedus, L. S.; Norton, J. R.; Finke, R. G. *Principles and Applications of Organotransition Metal Chemistry*, University Science Books, Mill Valley, California, **1987**, p 112.

16. Cowie, M.; Vasapollo, G.; Sutherland, B. R.; Ennett, J. P. *Inorg. Chem.* **1986**, *25*, 2648.

17. Haines, R. J.; Laing, M.; Meintjies, E.; Sommerville, P. J. *Organomet. Chem.* **1981**, *215*, C17.

18. Koskikallio, J. *Acta Chem. Scand.* **1969**, *23*, 1477.

19. Cowie, M.; Dwight, S. K. *Inorg. Chem.* **1980**, *19*, 2500.

20. Vaartstra, B. A.; Jenkins, J. A.; Cowie, M. to be submitted for publication.

21. Gelmini, L.; Stephan, D. W.; Loeb, S. J. *Inorg. Chim. Acta* **1985**, *98*, L3.

22. Cowie, M.; Dwight, S. K. *Inorg. Chem.* **1980**, *19*, 2508.

23. Cowie, M.; Dwight, S. K. *Inorg. Chem.* **1980**, *19*, 209.

24. Cowie, M.; Gibson, J. A. E. *Organometallics* **1984**, *3*, 984.

25. Farr, J. P.; Olmstead, M. M.; Balch, A. L. *Inorg. Chem.* **1983**, *22*, 1229 and references therein.

26. Herde, J. L.; Lambert, J. C.; Senoff, C. V. *Inorg. Synth.* **1974**, *15*, 18.

27. Cowie, M.; Mague, J. T.; Sanger, A. R. *J. Am. Chem. Soc.* **1978**, *100*, 3628.

28. Kubiak, C. P.; Eisenberg, R. *Inorg. Chem.* **1980**, *19*, 2726.

29. Cowie, M. *Inorg. Chem.* **1979**, *18*, 286.

30. Reflux in CH_2Cl_2 proved insufficient to remove an equivalent of CO from **3a**.

31. (a) Mague, J. T.; DeVries, S. H. *Inorg. Chem.* **1982**, *21*, 1632. (b) Mague, J. T. *Inorg. Chem.* **1983**, *22*, 1158.

CHAPTER 3

THE PREPARATION OF HETEROBINUCLEAR RHODIUM/IRIDIUM COMPLEXES AND THEIR REACTIONS WITH CARBON MONOXIDE AND ACTIVATED ALKYNES.

Introduction

Binuclear DPM-bridged complexes of iridium, discussed throughout this thesis and elsewhere,[1-4] are found to exhibit chemistry which generally complements that of related dirhodium complexes.[5-8] Many of the differences which are found can be related to the expected trends encountered as one descends a transition-metal triad. For example, diiridium complexes are found[1,2] to bind CO more strongly than analogous dirhodium species,[5-8] and generally display higher coordination numbers. Although alkynes tend to bind similarly (as cis-dimetallated olefins) in both cases, the rhodium complexes tend to also contain bridging carbonyl ligands,[7,8] while carbonyl groups in the iridium complexes remain terminal.[2] Reactions of the complexes, $[M_2Cl_2(CO)_2(DPM)_2]$ (M = Rh, Ir) with hydride sources produce a variety of polyhydrides for iridium,[3] while an unstable dihydride is the only product for rhodium.[9] Of significance to this thesis, oxidative addition of H_2 leads to stable hydrides for the diiridium species,[4,10] while hydrides are not observed in the analogous dirhodium system.[7,11,12] These differences are also manifested in the catalytic activity displayed by some dirhodium complexes,[7,11,12] while

related diiridium species are not catalysts under the same mild conditions (see Chapter 6 and elsewhere[10]).

Although diiridium complexes have been found to serve as useful models of reactive intermediates in the rhodium chemistry by virtue of the greater stability of the iridium species (see Chapters 5 and 6), exact parallels between analogues of the two metals cannot always be drawn because they do not behave identically. In an effort to bridge the gap between the chemistries of the dirhodium and diiridium complexes a study was initiated into the chemistry of mixed-metal binuclear "RhIr" complexes. Such mixed-metal complexes present the opportunity for metal-specific attack by incoming ligands and perhaps subsequent metal-specific reactivity. It would also appear reasonable to expect novel bonding modes for small molecules between two <u>different</u> metals in close proximity, perhaps leading to enhanced activation of substrates.

Homogeneous bimetallic complexes are also of interest based on the success of bimetallic systems in industrial heterogeneous catalysis, where a variety of mixed-metal systems have proven themselves highly active as catalysts, offering increased selectivity over other systems.[13] Furthermore, although the catalytic reactivity of rhodium is well known, iridium has also been shown to exhibit remarkable activity in certain cases.[14] Herein are described the syntheses of some DPM-bridged heterobinuclear "RhIr" complexes and their reactivities with carbon monoxide and activated alkynes.

Experimental Section

General experimental conditions are as described in Chapter 2. Carbon monoxide (Matheson), sodium sulfide hydrate (MCB), dimethylacetylenedicarboxylate (Aldrich) and hexafluoro-2-butyne (PCR Inc.) were used as received. The compounds, $[Ir(DPM)_2(CO)][Cl]$[15] and $[RhCl(CO)_2]_2$[16] were prepared by the reported procedures. $[RhIrCl_2(CO)_2(DPM)_2]$ (**1**), as reported herein, was prepared by a modification of a previously reported procedure.[17] The $^{31}P\{^1H\}$ NMR spectra were run on Bruker HFX-90 (with Fourier transform capability) and Bruker WH-400 spectrometers. ^1H, $^{13}C\{^1H\}$ and ^{19}F NMR spectra were recorded on the Bruker WH-400 spectrometer.

$^{13}C\{^1H\}$ NMR spectra were obtained on ^{13}CO enriched products which were derived from enrichment of the starting material, $[RhIrCl_2(CO)_2(DPM)_2]$ (**1**). Nearly quantitative ^{13}CO enrichment of **1** was obtained by allowing a CH_2Cl_2 solution of **1** to stir under ^{13}CO for 24 h, followed by reflux under ^{13}CO for approximately 1 h, and finally refluxing under N_2 purge for 2-3 h.

Preparation of Compounds

(a) $[RhIrCl_2(CO)_2(DPM)_2]$ (**1**).

The dry solids $[Ir(DPM)_2(CO)][Cl]$ (200 mg, 0.195 mmol) and $[RhCl(CO)_2]_2$ (38.0 mg, 0.098 mmol) were combined, dissolved in 25 mL of CH_2Cl_2 and the resulting solution stirred for 18 h. During this time the

color of the solution changed from yellow to orange. The solution was refluxed under dinitrogen flow for 1 h which caused the orange color to intensify. A 40-mL volume of diethyl ether was added, resulting in the precipitation of a bright orange microcystalline solid, which was collected, washed with diethyl ether and dried *in vacuo*. Typical isolated yields were 75-80%. Compound **1** was found to be a non-electrolyte in CH_2Cl_2 solutions (Λ_m = 4.8 $\Omega^{-1}cm^2mole^{-1}$). Spectroscopic data for this and subsequent compounds are given in Tables 3.1 and 3.2. Anal. calcd for $IrRhCl_2P_4O_2C_{52}H_{44}$: C, 52.45; H, 3.72; Cl, 5.95. Found: C, 51.57; H, 3.77; Cl, 5.37.

(b) $[RhIr(CO)_2(\mu\text{-}Cl)(DPM)_2][BF_4]$ (**2**).

Compound **1** (200 mg, 0.168 mmol) was suspended in 20 mL of THF, then $AgBF_4$ (32.7 mg, 0.168 mmol), dissolved in 5 mL of THF, was added to the suspension. An immediate color change to dark orange occurred and after stirring for an additional 30 min the volume was reduced to approximately 15 mL, followed by the addition of 30 mL of diethyl ether to cause complete precipitation. The solvent was removed, then the product was redissolved in 10 mL of CH_2Cl_2 and filtered to remove the silver salts. The product was reprecipitated by the addition of 30 mL of diethyl ether, collected and dried *in vacuo*. Yields were approximately 80% of a dark orange microcrystalline solid. Compound **2** was determined to be a 1:1 electrolyte in CH_2Cl_2 solutions (Λ_m = 59.7 $\Omega^{-1}cm^2mole^{-1}$).[18] Anal. calcd for $IrRhClP_4O_2F_4C_{52}BH_{44}$: C, 50.28; H, 3.57; Cl, 2.85. Found: C, 50.02; H, 3.53; Cl, 3.20.

Table 3.1. Infrared Spectral Data for the Compounds of Chapter 3.[a]

compound	Stretching Frequencies (cm^{-1}) solid[b]	solution[c]
$[RhIrCl_2(CO)_2(DPM)_2]$ (1)	1968(sh), 1960(vs)[d]	1980(vs), 1970(vs), 1756(st)[d]
$[RhIr(CO)_2(\mu\text{-}Cl)(DPM)_2][BF_4]$ (2)	1993(vs), 1974(vs)[d]	2002(st), 1982(vs)[d]
$[RhIr(CO)_2(\mu\text{-}S)(DPM)_2]$ (3)	1932(vs), 1906(vs)[d]	1948(st), 1920(vs)[d]
$[RhIrCl_2(CO)_2(\mu\text{-}CO)(DPM)_2]$ (4a & 4b)	2062(w), 2039(w), 1985(sh) 1845(w), 1786(m), 1760(m)[d]	2068(w), 2053(w), 2000(sh) 1850(m), 1755(w)[d]
$[RhIrCl(CO)_2(\mu\text{-}CO)(DPM)_2][BF_4]$(5a)	2010(st), 2004(st), 1951(vs,br) 1863(w), 1835(st)[d]	2053(w), 1981(vs), 1851(m) 1797(w)[d]
$[RhIr(CO)_2(\mu\text{-}CO)(\mu\text{-}S)(DPM)_2]$ (6)		1934(vs,br), 1799(m)[d]
$[RhIrCl_2(CO)(\mu\text{-}CO)(\mu\text{-}DMA)(DPM)_2]$ (7)	2043(vs), 1645(st)[d] 1698(sh),[e] 1563(w)[f]	2054(vs), 1660(st)[d] 1702(st),[e] 1558(w)[f]
$[RhIrCl(CO)_2(\mu\text{-}DMA)(DPM)_2][BF_4]$ (9a)		2099(st), 2060(vs)[d]
$[RhIrCl(CO)_2(\mu\text{-}DMA)(DPM)_2][BF_4]$ (9b)	2095(vs), 2054(vs)[d] 1686(st), 1701(w)[e]	2083(st), 2045(vs)[d] 1727(st), 1701(st)[e]
$[RhIrCl(CO)_2(\mu\text{-}HFB)(DPM)_2][BF_4]$ (10a)		2084(st), 2048(st)[d]
$[RhIrCl(CO)_2(\mu\text{-}HFB)(DPM)_2][BF_4]$ (10b)	2093(st), 2056(vs)[d] 1608(m)[f]	2102(st), 2064(vs)[d] 1605(m)[f]

[a] Abbreviations used: st = strong, vs = very strong, m = medium, w = weak, sh = shoulder. [b] Nujol mull. [c] CH_2Cl_2. [d] ν(CO). [e] ν(C=O) of CO_2Me. [f] ν(C=C) of coordinated alkyne.

Table 3.2. .NMR Spectral Data for the Compounds of Chapter 3.[a]

compound	$^{31}P\{^1H\}$ δ[b]	^1H δ[c]	$^{13}C\{^1H\}$ δ[c]
$[RhIrCl_2(CO)_2(DPM)_2]$ (1)	17.16(dm, $^1J_{Rh-P}$=125.7 Hz) -6.96(m)	6.8-8.0(m,40H) 4.29(m,2H), 4.01(m,2H)	
$[RhIr(CO)_2(\mu\text{-}Cl)(DPM)_2][BF_4]$ (2)	17.66(dm, $^1J_{Rh-P}$=111.0 Hz) 12.76(m)	7.2-7.8(m,40H) 4.14(m,2H), 3.65(m,2H)	
$[RhIr(CO)_2(\mu\text{-}S)(DPM)_2]$ (3)	14.42(dm, $^1J_{Rh-P}$=131.3 Hz) 6.88(m)	7.0-7.9(m,40H) 5.20(m,2H), 3.41(m,2H)	
$[RhIrCl_2(CO)_2(\mu\text{-}CO)(DPM)_2]$ (4a)	13.27(m) -4.16(m)	4.42(m,2H), 4.24(m,2H)	222.03(m), 187.99(dm)[d] 171.61(br,s)
$[RhIr(CO)_2(\mu\text{-}Cl)(\mu\text{-}CO)(DPM)_2]$ [Cl](4b)	27.88(m) 0.55(m)	5.01(m,2H), 4.47(m,2H)	190.26(dm)[e], 186.14(dm)[f] 172.75(br,s)
$[RhIrCl(CO)_3(\mu\text{-}CO)(DPM)_2]$ [Cl](4c)	27.71(m) -13.63(m)	4.07(m,2H), 3.66(m,2H)	212.07(dm)[g], 185.59(dm)[h] 170.66(m), 168.20(br,s)
$[RhIrCl(CO)_2(\mu\text{-}CO)(DPM)_2][BF_4]$(5a)	28.61(m) 1.01(m)	7.1-7.8(m,40H) 3.85(br,4H)	
$[RhIr(CO)_2(\mu\text{-}CO)(\mu\text{-}S)(DPM)_2]$ (6)	19.78(dm, $^1J_{Rh-P}$=130.5 Hz) -3.78(m)	7.1-7.8(m,40H) 4.59(m,2H), 2.52(m,2H)	
$[RhIrCl_2(CO)(\mu\text{-}CO)(\mu\text{-}DMA)(DPM)_2]$ (7)	8.94(dm, $^1J_{Rh-P}$=140.6 Hz) -12.16(m)	4.36(m,2H), 2.53(m,2H) 3.17(s,3H), 1.81(s,3H)	198.56(dm, $^1J_{Rh-C}$=28.9 Hz) 169.68(t, $^2J_{P-C}$=7.2 Hz)
$[RhIrCl(CO)_2(\mu\text{-}DMA)(DPM)_2][BF_4]$ (9a)	15.58(dm, $^1J_{Rh-P}$=103.3 Hz) -17.57(m)	2.62(s,3H), 2.30(s,3H)	188.09(dm, $^1J_{Rh-C}$=57.09 Hz) 153.44(br,m)

Table 3.2 (Continued)

compound	$^{31}P\{^1H\}$ δ^b	^1H δ^c	$^{13}C\{^1H\}$ δ^c
$[RhIrCl(CO)_2(\mu\text{-DMA})(DPM)_2][BF_4]$ (9b)	11.58(dm, $^1J_{Rh\text{-}P}$=114.3 Hz) -22.08(m)	3.92(m,2H), 3.52(m,2H) 2.86(s,3H), 2.42(s,3H)	173.81(t, $^2J_{P\text{-}C}$=5.1 Hz) 146.49(br,d, $^2J_{Rh\text{-}C}$=7.9 Hz)
$[RhIrCl(CO)_2(\mu\text{-HFB})(DPM)_2][BF_4]$ (10b)	10.40(dm, $^1J_{Rh\text{-}P}$=109.6 Hz) -26.82(m)	6.8-8.0(m,40H) 3.70(m,2H), 3.64(m,2H)	[i]

[a] Abbreviations used: dm = doublet of multiplets, m = multiplet, s = singlet, br = broad, t = triplet, q = quartet [b] In CD_2Cl_2; vs. 85% H_3PO_4 [c] In CD_2Cl_2; vs. TMS. [d] ($^1J_{Rh\text{-}C}$=39.5 Hz). [e] ($^1J_{Rh\text{-}C}$=39.5 Hz). [f] ($^1J_{Rh\text{-}C}$=70.8 Hz). [g] ($^1J_{Rh\text{-}C}$=45.3 Hz). [h] ($^1J_{Rh\text{-}C}$=72.4 Hz). [i] ^{19}F NMR(δ, vs. $CFCl_3$): -48.06(q, $^5J_{F\text{-}F}$ = 10.6 Hz), -50.21(q, $^5J_{F\text{-}F}$ = 10.6 Hz).

(c) $[RhIr(CO)_2(\mu\text{-}S)(DPM)_2]$ (3).

To a solution of $[RhIrCl_2(CO)_2(DPM)_2]$ (1) (50.0 mg, 0.0420 mmol) in 5 mL of CH_2Cl_2 was added $Na_2S{\cdot}9H_2O$ (12.0 mg, approx. 10% excess) dissolved in 5 mL of methanol. The color of the solution immediately turned dark red. After stirring for 15 min the solution was concentrated to 5 mL whereupon a dark red microcrystalline solid precipitated. The solid was collected and recrystallized from CH_2Cl_2/MeOH, washed with MeOH and then with diethyl ether. Isolated yields were 90-95%. Anal. calcd for $IrRhSP_4O_2C_{52}H_{44}$: C, 54.22%; H, 3.85%. Found: C, 53.58%; H, 3.96%.

(d) $[RhIrCl_2(CO)(\mu\text{-}CO)(\mu\text{-}DMA)(DPM)]$ (7).[19]

Compound 1 (50.0 mg, 0.042 mmol) was dissolved in 10 mL of CH_2Cl_2 under dinitrogen. To the resulting orange solution was added 5.2 μL (0.042 mmol) of dimethylacetylenedicarboxylate (DMA) causing an immediate color change to yellow. After 15 min the solution was concentrated to 5 mL with rapid N_2 flow and the product precipitated with a 10 mL volume of diethyl ether. The resulting yellow solid was isolated and dried *in vacuo*, giving 7 in 90% yield. Compound 7 was found to be nonconducting in CH_2Cl_2 solutions ($\Lambda_m \leq 0.5\ \Omega^{-1}cm^2mol^{-1}$). Anal. calcd for $IrRhCl_2P_4O_6C_{58}H_{50}$: C, 52.26%; H, 3.78%; Cl, 5.32%. Found: C, 51.90%; H, 3.63%; Cl, 5.76%.

(e) $[RhIrCl(CO)_2(\mu\text{-}DMA)(DPM)_2][BF_4]$ (9b)

Compound 2 (50.0 mg, 0.040 mmol) was dissolved in 10 mL of CH_2Cl_2 under dinitrogen. To this orange solution was added 5.0 μL (0.040

mmol) of DMA which caused an immediate color change to red-violet. Upon stirring for 30 min the solution became predominantly dark red. Concentrating to 5 mL under dinitrogen flow and addition of 15 mL of diethyl ether caused precipitation of a flocculent red-brown solid. This solid was collected, washed with a 5 mL portion of diethyl ether and dried *in vacuo*. Isolated yield: 92%. Compound **9b** was found to be a normal 1:1 electrolyte in CH_2Cl_2 solutions (Λ_m = 40.0 $\Omega^{-1}cm^2mol^{-1}$). Anal. calcd for $IrRhClP_4F_4O_6C_{58}BH_{50}$: C, 50.32%; H, 3.64%; Cl, 2.56%. Found: C, 48.56%; H, 3.57%; Cl, 2.66%.

(f) $[RhIrCl(CO)_2(\mu\text{-HFB})(DPM)_2][BF_4]$ **(10b)**

Compound **2** (25.0 mg, 0.020 mmol) was dissolved in 4 mL of CH_2Cl_2 under dinitrogen. Hexafluoro-2-butyne (HFB) was then bubbled into the solution causing an immediate color change to dark red-violet. The solution was left under HFB for 30 min whereupon little change in color had occurred. The solution was sampled for infrared analysis, then the product was precipitated by addition of 10 mL of diethyl ether. The resulting pale-pink solid was collected and dried *in vacuo*.

Reactions with CO

For each of compounds **1-3**, approximately 10 mg of sample was dissolved in CH_2Cl_2 in a 3-necked round bottom flask (or in CD_2Cl_2 in an NMR tube) under dinitrogen. One equivalent of carbon monoxide (typically *ca.* 0.25 mL) was then bubbled into the solution using a gas-tight syringe, followed by recording of IR, $^{31}P\{^1H\}$ and $^{13}C\{^1H\}$ NMR spectra.

Then excess CO was bubbled into the solution and the sample left under CO atmosphere for a repeated spectroscopic characterization.

Reaction of Compound 3 with Activated Alkynes

Compound 3 was also reacted with both DMA and HFB, however, it was found that a significant excess of reactant was required in order to yield the products. The reactions were found to be easily reversible and the products have been formulated as terminal η^2-alkyne complexes. These compounds will be discussed in Chapter 4.

Results and Discussion

A study of the A-frame complex, $[Ir_2(CO)_2(\mu\text{-}Cl)(DPM)_2][BF_4]$,[1,4] was initiated, in part, with the hope of modelling alkyne hydrogenation reactions which are catalyzed by the rhodium analogue, $[Rh_2(CO)_2(\mu\text{-}Cl)(DPM)_2][BF_4]$.[11] In these modelling studies it became evident that the cationic A-frame complex exhibited additional reactivity over its neutral precursor, *trans*-$[IrCl(CO)(DPM)]_2$, and this reactivity appeared to be a function of the incipient coordinative unsaturation afforded by the bridging halide ligand.[4] This function was further investigated by substitution of the chloride ligand by iodide (as described in Chapter 2) and by sulfide in the complex $[Ir_2(CO)_2(\mu\text{-}S)(DPM)_2]$ (see Chapter 5). It was therefore obvious that extension of these studies into heterobinuclear rhodium-iridium complexes should include the analogous neutral dichloride and cationic chloride-bridged A-frame complexes and also the

sulfide-bridged A-frame. Investigations of the mixed-metal iodides are left to future studies.

The mixed-metal analogue of *trans*-[MCl(CO)(DPM)]$_2$ (M = Rh, Ir) appeared to have been previously observed,[17] however, complete characterization of the complex was not provided and its formulation as a cationic chloro-bridged species was uncertain. The desired compound is obtained in high purity by the reaction of [Ir(DPM)$_2$CO][Cl] and [RhCl(CO)$_2$]$_2$ in CH_2Cl_2 for 18 h followed by reflux under N_2 purge to eliminate CO from the higher carbonyl-containing species. As previously noted,[17] the reaction between the iridium monomer and the rhodium dimer is rather slow and appears to require at least 12 h for complete reaction under the conditions used. The isolated orange solid, [RhIrCl$_2$(CO)$_2$(DPM)$_2$] (**1**), displays an infrared spectrum containing two terminal carbonyl stretches (1960, 1968 cm^{-1}). However, in solution **1** displays three carbonyl bands (1980, 1970, 1756 cm^{-1}), suggesting the formation of an additional species containing a bridging CO ligand. This infrared data, along with the low conductivity in CH_2Cl_2 (4.8 Ω^{-1}cm^{2}mol^{-1}), are inconsistent with the previously proposed cationic formulation for **1**,[17] and instead suggests a neutral species which exists as two isomers in solution but as a single species in the solid state. The solid state geometry is presumed to have a trans arrangement of terminal chloro and carbonyl ligands (**1a**) around the two metal centers, based on the trend within the homobinuclear analogues[1,20] and as observed in a related dirhodium complex, [RhCl(CO)(EtSCH$_2$SEt)]$_2$.[21] Certainly, the two CO stretches observed for **1a** are consistent with the proposed geometry.

In solution, the three carbonyl stretches suggest the presence of **1a** together with at least one additional species, which is proposed to have a geometry as shown (**1b**). Such coordination geometry has been confirmed

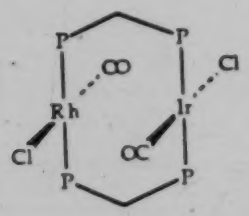

1a

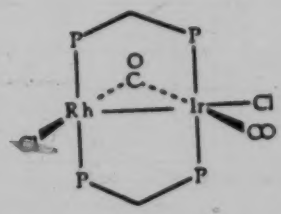

1b

for the diiodo complex, $[Ir_2I_2(CO)(\mu\text{-}CO)(DPM)_2]$ (Chapter 2), which exhibits carbonyl stretches (1960, 1742 cm^{-1}) in the same regions as those observed for **1**, but at slightly lower frequencies due to more electron-rich metal centers. The structure proposed for **1b** is furthermore in agreement with an observed trend within heterobinuclear "RhIr" complexes, described in this account (*vide infra*) and elsewhere,[22] that geometries appear to be favored in which the rhodium center retains a sixteen-electron configuration, while iridium has an eighteen-electron configuration.[23] The two broad terminal CO stretching bands observed for **1** in solution apparently obscure the third expected band. It appears that in solution compounds **1a** and **1b** are rapidly interconverting on the NMR timescale since the $^{31}P\{^1H\}$ NMR spectrum reveals only one species, even down to -80 °C. This spectrum is consistent with an AA'BB'X spin system and clearly distinguishes the iridium-bound phosphorus signals (δ -6.96) from those of the rhodium-bound phosphorus signals (δ 17.16), with the latter displaying obvious coupling to ^{103}Rh ($^1J_{Rh\text{-}P}$ = 125.7 Hz).

The cationic mixed-metal A-frame complex, $[RhIr(CO)_2(\mu\text{-}Cl)(DPM)_2][BF_4]$ (2), is easily obtained from 1 by chloride abstraction, using one equivalent of $AgBF_4$. All evidence suggests the expected A-frame geometry as observed for homobinuclear halide-bridged analogues.[1,6] Its infrared spectrum dislays two carbonyl stretches (1993, 1974 cm^{-1}) which are in the ranges expected for terminal carbonyls on Rh(I) and Ir(I), respectively. Compound 2 behaves as a normal 1:1 electrolyte (Λ_m = 59.7 $\Omega^{-1}cm^2mol^{-1}$ in CH_2Cl_2) and elemental analyses indicate one chlorine atom per dimer.

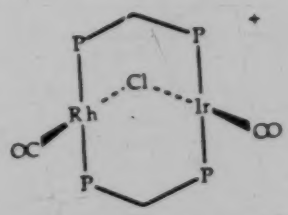

2

The sulfido-bridged A-frame complex, $[RhIr(CO)_2(\mu\text{-}S)(DPM)_2]$ (3), is obtained in high yield by reaction of $[RhIrCl_2(CO)_2(DPM)_2]$ (1) with excess $Na_2S{\cdot}9H_2O$. The infrared spectrum of the isolated dark red solid displays two terminal CO stretches at 1932 cm^{-1} and 1906 cm^{-1}, concordant with the respective dirhodium[24] and diiridium[10] analogues. As in the homobinuclear complexes, the sulfido-bridged species has lower carbonyl stretching frequencies than the chloro-bridged species, indicating more electron-rich metal centers. The $^{31}P\{^1H\}$ NMR spectrum is again typical of the heterobinuclear "RhIr" complexes, with $^1J_{Rh\text{-}P}$ = 131.3 Hz.

The reaction of $[RhIrCl_2(CO)_2(DPM)_2]$ (1) with CO yields two different tricarbonyl complexes, and a tetracarbonyl species. Reaction with one equivalent of CO causes an immediate color change to orange-yellow and the $^{31}P\{^1H\}$ NMR spectrum recorded at -40 °C reveals two species, **4a** (δ 13.27 (m), -4.16 (m)) and **4b** (δ 27.88 (m), 0.55 (m)), in a 1:2 ratio, respectively, along with some unreacted **1** . Rhodium-phosphorus coupling is evident in the low-field multiplet of each species, but the coupling constants are not readily separable from other couplings. Warming the solution to 22 °C results in the merging and broadening of these resonances to intermediate values of δ 21.6 and δ -2.9 for the rhodium- and iridium-bound phosphorus nuclei, respectively. This suggests that **4a** and **4b** are related by an equilibrium, which is sufficiently slowed down at -40°C to observe both species in the NMR spectrum. The $^{13}C\{^1H\}$ NMR spectrum obtained after addition of one equivalent of ^{13}CO to a ^{13}CO-enriched sample of **1** displays three distinct resonances for each of **4a** and **4b** and are easily assigned by integration of the peak areas. Compound **4a** shows a complex multiplet $^{13}C\{^1H\}$ NMR resonance at δ 222.03 ($^1J_{Rh\text{-}C}$ is not clearly distinguishable from other couplings), consistent with a bridging CO ligand, another at δ 187.99 (doublet of multiplets, $^1J_{Rh\text{-}C}$ = 53.4 Hz) due to a terminal CO on rhodium and one at δ 171.61 (broad singlet) which is readily assigned to a terminal position on iridium due to the absence of Rh-coupling. Compound **4b**, which was previously formulated as $[RhIr(CO)_2(\mu\text{-}CO)(\mu\text{-}Cl)(DPM)_2]^+$ from ^{31}P NMR and IR data,[17] exhibits ^{13}C resonances at δ 190.26 (doublet of multiplets, $^1J_{Rh\text{-}C}$ = 39.5 Hz), consistent with a bridging CO, δ 186.14 (doublet of multiplets, $^1J_{Rh\text{-}C}$ = 70.8 Hz),

consistent with a terminal CO on rhodium, and δ 172.75 (broad singlet) due to a terminal CO on iridium. The previous formulation[17] appears consistent with all spectroscopic evidence, and in accord with spectral parameters found for the homobinuclear tricarbonyls, $[M_2(CO)_2(\mu\text{-}CO)(\mu\text{-}Cl)(DPM)_2]^+$ (M = Rh,[6,25] Ir[1]).

Upon addition of excess CO to this solution, another species, **4c**, arises and upon stirring the solution under CO atmosphere for 5 h, **4c** is the only product present as identified by $^{31}P\{^1H\}$ NMR (δ 27.71 (m), δ -13.63 (m)). The $^{13}C\{^1H\}$ NMR spectrum (-40 °C) of a ^{13}CO-enriched sample of **4c** (see Figure 3.1) reveals that this final product is a tetracarbonyl species which contains a bridging CO ligand (δ 212.07, $^1J_{Rh\text{-}C}$ = 45.3 Hz), a terminal CO on rhodium (δ 185.59, $^1J_{Rh\text{-}C}$ = 72.4 Hz) and two terminal CO ligands on iridium (δ 170.66, 168.20). One of the carbonyls on iridium exhibits a five-line pattern which can be estimated as an overlapping doublet of triplets. There thus appears to be a coupling to rhodium of approximately 25 Hz, which is much lower than couplings observed for terminal carbonyls bonded directly to rhodium, but rather significant for a two-bond coupling in such systems. Resonances which appear very similar to this one are described in Chapters 5 and 6, wherein efficient transmission of coupling through as many as three bonds has been observed when the coupled nuclei are related by a colinear chain of bonded atoms. A similar colinear Rh-Ir-CO linkage in **4c** might be suggested. This tetracarbonyl complex proves to be very susceptible to CO loss, yielding **4a**, **4b**, and **1** upon exchange of the CO atmosphere for N_2, after which compound **1** can be quantitatively restored by mild reflux in CH_2Cl_2 solutions with N_2 purge.

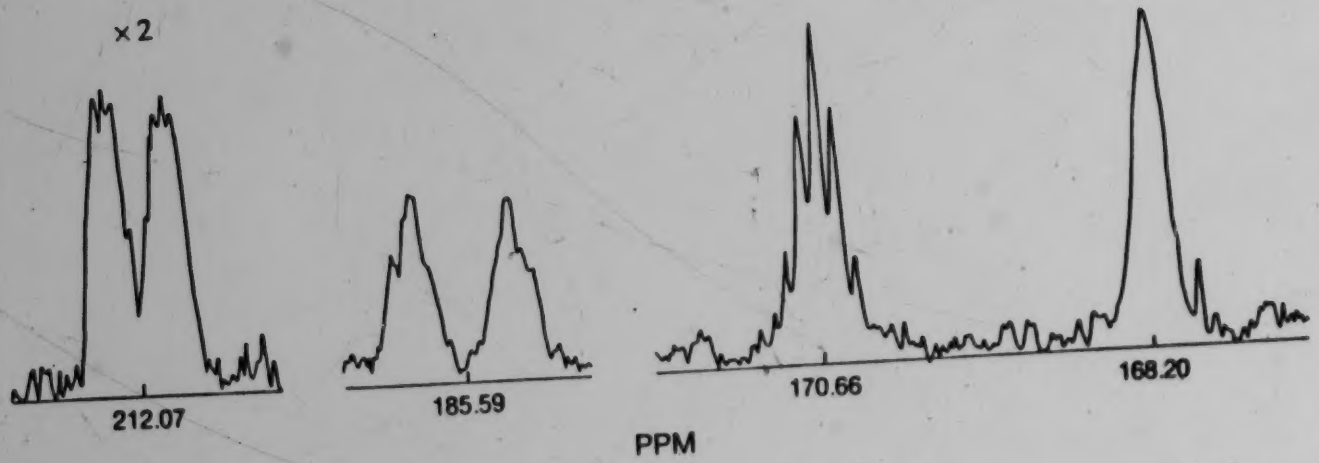

Figure 3.1. $^{13}C\{^{1}H\}$ NMR spectrum (-40 °C) of compound **4c**.

These observations along with the NMR data can be explained by the equilibria in Scheme 3.1 (diphosphine ligands are omitted for clarity), in which **4a** and **4b** are tricarbonyl species. The proposal that these

Scheme 3.1

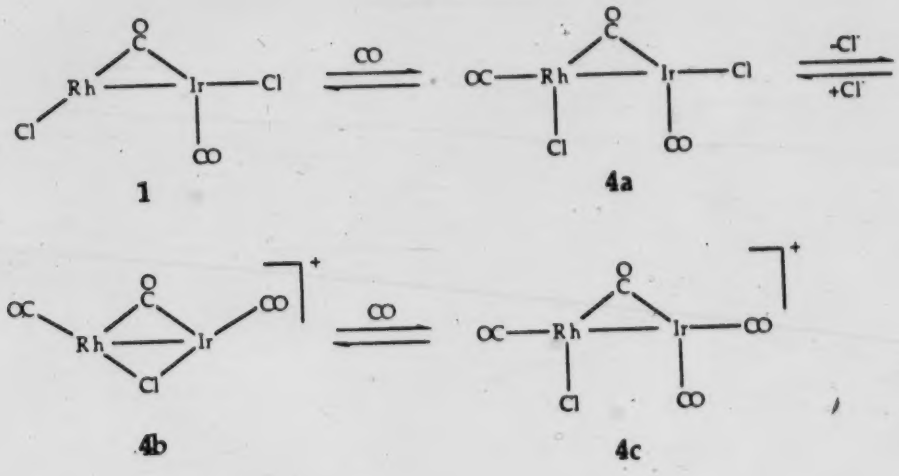

tricarbonyls are related by chloride loss as indicated in Scheme 3.1 is supported by the fact that addition of ethanol to a CH_2Cl_2 solution containing both isomers causes the conversion of all **4a** present into **4b**, as monitored by $^{31}P\{^1H\}$ NMR at low temperature. This observation is consistent with the tendency for the ionic species to be favored in more polar solvents.

The infrared spectrum of the isomeric tricarbonyls is somewhat obscured by compound **1**, but higher frequency CO bands (2068, 2053 cm^{-1}) are consistent with the cationic nature of **4b**. The stretches due to the bridging CO ligands which appear at 1755 cm^{-1} and 1850 cm^{-1} strongly

support the formulations of **4a** and **4b**, respectively, being comparable to values for the neutral diiridium analogues of **4a** (1731, 1717 cm^{-1})[1] and the cationic dirhodium analogue of **4b** (1873 cm^{-1}),[6] respectively. The presence of additional bands in the IR spectrum of the solid may indicate that **4a** also exists as an isomer having three mutually cis carbonyl ligands, as was the case in the diiridium analogue.[1]

Additional support for the natures of the species in Scheme 3.1 comes from the reaction of $[RhIr(CO)_2(\mu\text{-}Cl)(DPM)_2][BF_4]$ (**2**) with CO. Reaction with one equivalent of CO yields a single species, **5a**, which corresponds very well to compound **4b** with respect to its $^{31}P\{^1H\}$ NMR parameters (Table 3.2). Addition of excess CO to **2** immediately causes formation of another species, **5b**, which is identical in all respects to **4c**. Although **5b** is observable in the $^{31}P\{^1H\}$ NMR at -40 °C, warming to ambient shows only **5a**. The immediate formation of the tetracarbonyl complex is reasonable in this case, since there is no competing reaction for **5a** as there is for **4b**, namely chloride addition over carbonyl addition. Similarly, the tricarbonyl species **5a** is also significantly more stable toward CO loss compared to **4b**, and solutions of **5b** under N_2 purge yield **5a** almost exclusively, while any recovery of **2** requires additional slight warming.

The sulfido-bridged complex, $[RhIr(CO)_2(\mu\text{-}S)(DPM)_2]$ (**3**), also reacts with CO, however, an excess is required in order to successfully maintain the new complex, **6**, in solution. Under CO atmosphere, solutions of **3** change color from dark red to red-orange over several minutes. Displacing the CO atmosphere with N_2 rapidly restores the dark red color

of **3**, indicating facile CO loss from **6**. The $^{31}P\{^1H\}$ NMR spectrum indicates a single species having a pattern typical of the heterobinuclear DPM-bridged complexes (see Table 3.2). An IR spectrum of the solution reveals both terminal (1934 cm^{-1}) and bridging (1799 cm^{-1}) carbonyl stretches. All evidence suggests that **6** is a tricarbonyl species analogous to **4b** and **5a**. Failure to incorporate another equivalent of CO and the lability of **6** toward CO loss is consistent with the observation that the homobinuclear iridium analogue of **3** forms a stable tricarbonyl complex,[10] but the dirhodium analogue shows no apparent affinity for CO.[24]

The mixed-metal complexes **1-3** all react with activated alkynes, although only the reactions involving **1** and **2** will be discussed here, as compound **3**, the sulfido-bridged species, gives a different result and will be discussed in Chapter 4.

The neutral complex, $[RhIrCl_2(CO)_2(DPM)_2]$ (**1**), reacts with dimethylacetylenedicarboxylate (DMA) yielding a yellow compound, **7**. Spectral parameters for this species are almost identical to those reported by Mague.[19b] Although the previous report argued that this complex contained mutually cis carbonyl ligands, this species is herein formulated as shown below, where the chloro and carbonyl ligands remain mutually

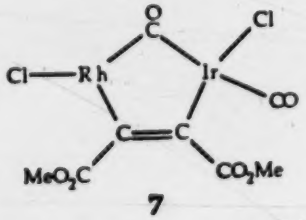

7

trans. The previously proposed cis geometry (having the terminal CO and Cl ligands on Ir interchanged) was assumed[19b] due to the absence of a trans coupling between the carbonyls in the ^{13}C NMR spectrum. It should be noted, however, that the steric requirements of the coordinated DMA group may not allow a direct trans arrangement of the carbonyls. Furthermore, the terminal carbonyl band in the infrared spectrum (2043 cm^{-1}) may be more indicative of a carbonyl which is in the position shown, rather than trans to the acetylenic moiety, where values near or below 2000 cm^{-1} appear typical in related diiridium complexes.[2] Consistent with the absence of a metal-metal bond in **7**, the bridging CO band displays a low stretching frequency in the IR spectrum (1647 cm^{-1}), similar to the "ketonic" carbonyls of related dirhodium complexes.[8] Evidence for the bridging carbonyl group is also clear in the $^{13}C\{^1H\}$ NMR spectrum which displays a doublet of multiplets at δ 198.56 with coupling to rhodium of 28.9 Hz. Another resonance in the $^{13}C\{^1H\}$ NMR spectrum at δ 169.68 (triplet, $^2J_{P\text{-}C}$ = 7.2 Hz), clearly results from the terminal CO on iridium.

The acetylenic stretching frequency in this and subsequent compounds are consistent with both the "perpendicular" and "parallel" bonding modes for alkynes coordinated to two metal centers.[26] The latter is the expected bonding mode in these complexes based on the observed trend in the reaction of alkynes with binuclear Rh(I) and Ir(I) complexes,[2,7,26-38] and is consistent with the observation of two separate ^1H NMR resonances for each carboxylate methyl group of the alkyne.

Although the homobinuclear counterparts of compound **1** yield slightly different results upon reaction with DMA, compound **7** appears to

adopt features of both. The carbonyl and chloro ligands are retained as was the result for the diiridium species, $[Ir_2Cl_2(CO)_2(\mu\text{-DMA})(DPM)_2]$,[2] whereas the analogous reaction for the dirhodium species yielded $[Rh_2Cl_2(\mu\text{-CO})(\mu\text{-DMA})(DPM)_2]$,[8] with coincident CO loss. In addition, the unusual "ketonic" carbonyl is observed for the mixed-metal species, as for the dirhodium case, whereas only terminal carbonyls were observed with the diiridium analogue. Facile CO loss from **7** occurs on mild reflux to yield species **8** (shown as characterized by Mague[19b]), where the carbonyl group

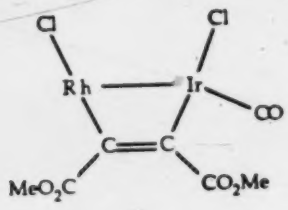

8

most closely associated with the rhodium center is lost. It is rather attractive to consider that CO loss occurs from **7** by a "windshield wiper" motion of the bridging carbonyl and the Ir-bound chloro ligands, toward the rhodium center, with subsequent carbonyl dissociation. It should be noted that additional chloride dissociation and recoordination would be required to yield the resulting species if the dicarbonyl precursor contained a cis arrangement of ligands. Although only CO loss from **7** was previously reported,[19b] it is found that refluxing CH_2Cl_2 solutions of **7** for 3 h with slow dinitrogen purge leads to competing chloride loss as well, yielding a compound identified in the $^{31}P\{^1H\}$ NMR spectrum to be analogous to **9b**, the product of DMA addition to $[RhIr(CO)_2(\mu\text{-Cl})$-

$(DPM)_2][BF_4]$ (2) (*vide infra*). Note that this is the result of chloride loss from the more sterically congested iridium center of **7**.

The A-frame complex, $[RhIr(CO)_2(\mu\text{-}Cl)(DPM)_2][BF_4]$ (2), reacts readily with DMA as evidenced by an immediate color change from orange to dark red-violet. The $^{31}P\{^1H\}$ NMR spectra reveal two isomers in a 5:1 ratio with the minor one, **9a**, disappearing within 30 min. The major species is characterized as $[RhIrCl(CO)_2(\mu\text{-}DMA)(DPM)_2][BF_4]$ (**9b**), which

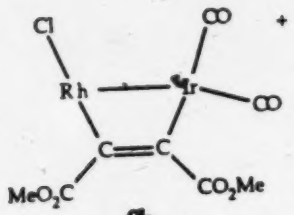

9b

has spectroscopic parameters which are virtually identical to the previously characterized perchlorate salt of the complex obtained by a different route.[19b] In solution, compound **9b** displays two terminal CO bands in the infrared spectrum (2083, 2045 cm^{-1}) and shows two distinct resonances in the $^{13}C\{^1H\}$ NMR spectrum for the CO groups; a triplet at δ 173.81 ($^2J_{P\text{-}C}$ = 5.1 Hz) and a broadened doublet at δ 146.49 ($^2J_{Rh\text{-}C}$ = 7.9 Hz). The latter coupling is too low to be due to a carbon bonded directly to rhodium and therefore is assigned to a two-bond coupling to Rh of the carbonyl ligand opposite the metal-metal bond. Note that this coupling is not as effective as was previously described for **4c**. Upon selective decoupling of the Rh-bound ^{31}P signal, the resonance at δ 146.49 in the $^{13}C\{^1H\}$ NMR spectrum resolves into an apparent quartet while that at δ 173.81 remains a triplet.

Selectively decoupling the iridium-bound ^{31}P signal yields a singlet at δ 173.81 and a doublet ($^2J_{Rh\text{-}C}$ = 7.9 Hz) for the ^{13}C resonance at δ 146.49, confirming that the high field quartet is actually an overlapping doublet of triplets ($^2J_{P\text{-}C} \approx {}^2J_{Rh\text{-}C}$ = 7.9 Hz).

The minor species, **9a**, formed initially in the reaction, displays two terminal CO stretches in the solution IR spectrum (2099, 2060 cm^{-1}) in addition to those of **9b**. Attempts to coprecipitate **9a** along with **9b** leads to the conversion of all the **9a** present and isolation of solid **9b** exclusively, as evidenced by the solid IR spectrum. Redissolving the solid reveals only **9b** in solution. The $^{13}C\{^1H\}$ NMR spectrum of a solution containing **9a** shows a doublet of multiplets (δ 188.09, $^1J_{Rh\text{-}C}$ = 57.09 Hz) for this species, corresponding to a terminal CO on rhodium. Although this chemical shift is not outside of the range representative of bridging CO ligands, the infrared spectrum clearly shows this is not the case, and the large Rh-C coupling is more typical of terminal carbonyls on rhodium than for those bridging. Each half of this resonance is in fact very close to being a triplet, but there is some apparent coupling to the distant phosphorus nuclei on iridium. The other ^{13}C resonance (δ 153.44) is a somewhat broad pseudo-quartet ($^2J_{Rh\text{-}C}$ = 9.1 Hz) not unlike the δ 146.49 resonance of **9b**. The conversion of **9a** to **9b** with time suggests that **9a** may be formed prior to **9b** and a mechanism consistent with this is outlined in Scheme 3.2. Compound **9a** appears analogous to the result of DMA addition to the diiridium analogue of compound **2**, $[Ir_2(CO)_2(\mu\text{-}Cl)(DPM)_2][BF_4]$.[2] As pointed out for the diiridium case, the product strongly suggests that attack of alkyne at an outer site occurs, rather than between the two metals. In the homo-

Scheme 3.2

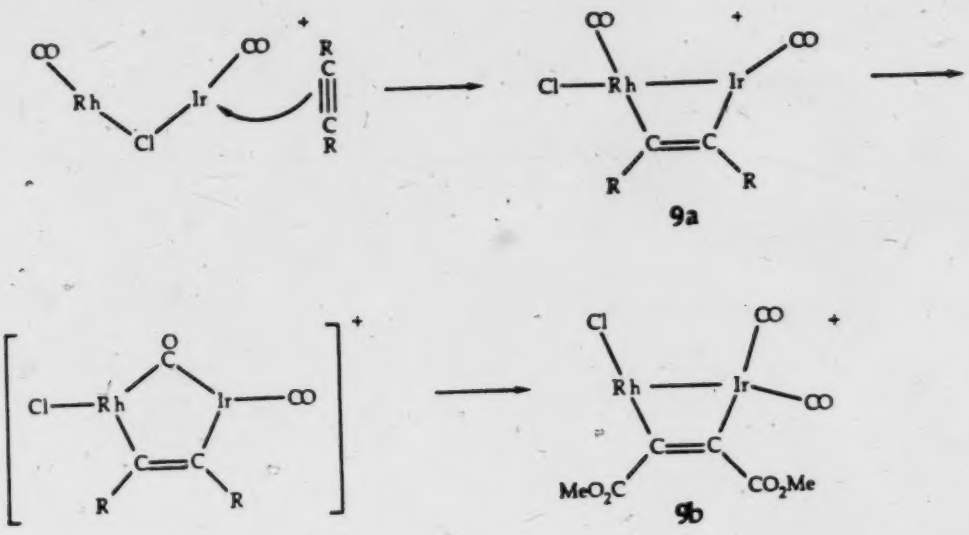

binuclear A-frame complex, $[Rh_2(CO)_2(\mu\text{-}Cl)(DPM)_2]^+$, attack by CO has also been shown to occur at this outside site,[6,25] and the geometry of the product upon reaction of $[Rh_2(CO)_2(\mu\text{-}O_2CCH_3)(DPM)_2]^+$ with hexaflouro-2-butyne (HFB) indicates the same.[27,29] Evidence for the initial attack at Ir on the outside of the complex has been obtained by reaction of sulfido-bridged complexes such as $[RhIr(CO)_2(\mu\text{-}S)(DPM)_2]$ (**3**) with activated alkynes (Chapter 4). In the sulfido-bridged complexes the reluctance of the initial product to rearrange to species such as **9a** appears to result from the barrier associated with cleavage of a metal-sulfur bond to form a dipolar intermediate (see also Chapter 5). Conversion of **9a** to **9b** might occur via a species such as the one shown, although there is no evidence for this intermediate.

Reaction of compound **2** with HFB appears to proceed much the same as the reaction with DMA, except that in this case, even after 30 min of reaction under HFB, the IR spectrum in solution reveals significant amounts of the species, $[RhIrCl(CO)_2(\mu\text{-HFB})(DPM)_2][BF_4]$ (**10a**), corresponding to **9a**. All carbonyl stretching frequencies (Table 3.1) are somewhat higher than for the DMA derivative, demonstrating the greater electron-withdrawing ability of the CF_3 groups in HFB over the carboxylates in DMA.[39] Perhaps this factor is also the reason for slower conversion of **10a** to **10b**, as the less electron-rich iridium center may not be as inclined to support additional π-acidic ligands. Here too, precipitation of the product reveals only species **10b**. A very distinct acetylenic stretch is observed in the IR spectrum at 1608 cm^{-1}, certainly in the acceptable range for a cis-dimetallated olefin. The ^{19}F NMR spectrum of **10b** displays two different environments for the CF_3 groups (δ -48.06, -50.21; $^5J_{F\text{-}F}$ = 10.6 Hz). The presence of two different ^{19}F resonances is consistent with a cis-dimetallated olefin coordination for the alkyne; the perpendicular bonding mode would render the environments equivalent.

Conclusions

In general, the reactivity of the heterobinuclear "RhIr" complexes appears to display attributes of <u>both</u> of the homobinuclear analogues. Addition of CO to $[RhIrCl_2(CO)_2(DPM)_2]$ (**1**) eventually gives a tetracarbonyl species as was observed for the diiridium species,[1] but the resulting product is very susceptible to CO loss, reflecting the presence of

rhodium, for which the highest carbonyl-containing species in the homobinuclear complex is the labile tricarbonyl cation.[5,6] This is also reflected in the observed stability of the cationic tricarbonyl species, **4b**, toward CO loss, which again falls between that of the related dirhodium and diiridium species.

Reactions with activated alkyne yield products which contain the now commonly encountered cis-dimetallated olefin geometry. Consistent with the diiridium case, the neutral dichloro species retains the ligands after alkyne coordination, but in accord with the dirhodium case, CO loss can be induced rather easily. Reaction of the A-frame complex, **2**, with alkyne gives a product analogous to that observed for the diiridium species, but transfer of a carbonyl ligand from rhodium to iridium occurs, demonstrating a greater affinity of iridium for the π-acidic ligand. Later chapters will describe attempts to utilize the attributes of both metals in these species for the activation of dihydrogen and subsequent reaction with unsaturated organic substrates.

References and Footnotes

1. Sutherland, B. R.; Cowie, M. *Inorg. Chem.* **1984**, 23, 2324.
2. Sutherland, B. R.; Cowie, M. *Organometallics* **1984**, 3, 1869.
3. McDonald, R.; Sutherland, B. R.; Cowie, M. *Inorg. Chem.* **1987**, 26, 3333.
4. Sutherland, B. R.; Cowie, M. *Organometallics* **1985**, 4, 1801.
5. Cowie, M. *Inorg. Chem.* **1979**, *18*, 286.
6. Cowie, M.; Mague, J. T.; Sanger, A. R. *J. Am. Chem. Soc.* **1978**, *100*, 3628.
7. Cowie, M.; Southern, T. G. *J. Organomet. Chem.* **1980**, 193, C46.
8. Cowie, M.; Southern, T. G. *Inorg. Chem.* **1982**, 21, 246.
9. Woodcock, C.; Eisenberg, R. *Inorg. Chem.* **1984**, 23, 4207.
10. Kubiak, C. P.; Woodcock, C.; Eisenberg, R. *Inorg. Chem.* **1980**, 19, 2733.
11. Sanger, A. R. *Prepr. -Can. Symp. Catal.* **1979**, *6th*, 37.
12. Kubiak, C. P.; Woodcock, C.; Eisenberg, R. *Inorg. Chem.* **1982**, 21, 2119.
13. Sinfelt, J. H. *Bimetallic Catalysts*, Wiley, New York, **1983**.
14. Crabtree, R. *Acc. Chem. Res.* **1979**, 12, 331.
15. Miller, J. S.; Caulton, K. G. *Inorg. Chem.* **1975**, 14, 1067.
16. McCleverty, J. A.; Wilkinson, G. *Inorg. Synth.* Vol. VIII, p 211.
17. Hutton, A. T.; Pringle, P. G.; Shaw, B. L. *Organometallics* **1983**, 2, 1889.

18. Typically, for a 1:1 electrolyte such as $[Rh_2(CO)_2(\mu\text{-}Cl)(\mu\text{-}CO)\text{-}(DPM)_2][BF_4]$, $\Lambda_m = 45\ \Omega^{-1}cm^2mol^{-1}$. See also: Geary, W. J. *Coord. Chem. Rev.* **1971**, *7*, 81.

19. (a) Compound **7** was reported while this work was underway. See: (b) Mague, J. T. *Organometallics* **1986**, *5*, 918.

20. (a) Mague, J. T.; Mitchener, J. P. *Inorg. Chem.* **1969**, *8*, 119. (b) Cowie, M.; Dwight, S. K. *Inorg. Chem.* **1980**, *19*, 2500.

21. Song, H.; Haltiwanger, R. C.; Rakowski DuBois, M. *Organometallics* **1987**. *6*, 2021.

22. McDonald, R.; Cowie, M. manuscripts in preparation.

23. For a description of the electron counting formalism see: Mitchell, P. R.; Parish, R. V. *J. Chem. Ed.* **1969**, *46*, 811.

24. Kubiak, C. P.; Eisenberg, R. *Inorg. Chem.* **1980**, *19*, 2726.

25. Mague, J. T.; Sanger, A. R. *Inorg. Chem.* **1979**, *18*, 2060.

26. A theoretical discussion of both bonding modes including many references is: Hoffman, D. M.; Hoffmann, R.; Fisel, C. R. J. Am. Chem. Soc. 1982, 104, 3858.

27. Mague, J. T.; DeVries, S. H. *Inorg. Chem.* **1982**, *21*, 1632.

28. Mague, J. T. *Inorg. Chem.* **1983**, *22*, 45.

29. Mague, J. T. *Inorg. Chem.* **1983**, *22*, 1158.

30. Mague, J. T.; Klein, C. L.; Majeste, R. J.; Stevens, E. D. *Organometallics* **1984**, *3*, 1860.

31. Cowie, M.; Dickson, R. S. *Inorg. Chem.* **1981**, *20*, 2682.

32. Cowie, M.; Dickson, R. S.; Hames, B. W. *Organometallics* **1984**, *3*, 1879.

33. Dickson, R. S.; Gatehouse, B. M.; Nesbit, M. C.; Pain, G. M. *J. Organomet. Chem.* **1981**, *215*, 97.

34. Devillers, J.; Bonnet, J. -J.; deMontauzon, D.; Galy, J.; Poilblanc, R. *Inorg. Chem.* **1980**, *19*, 154.

35. El Amane, M.; Mathieu, R.; Poilblanc, R. *Nouv. J. Chim.* **1982**, *6*, 191.

36. Lemoine, R.; Gross, M.; deMontauzon, D.; Poilblanc, R. *Inorg. Chim. Acta* **1983**, *71*, 15.

37. Guilmet, E.; Maisonnat, A.; Poilblanc, R. *Organometallics* **1983**, *2*, 1123.

38. El Amane, M.; Mathieu, R.; Poilblanc, R. *Organometallics* **1983**, *2*, 1618.

39. Kosower, E. M. *An Introduction to Physical Organic Chemistry*, Wiley, New York, **1968**, p 49.

CHAPTER 4

BINUCLEAR DIIRIDIUM AND MIXED-METAL RHODIUM-IRIDIUM COMPLEXES CONTAINING TERMINAL η^2-ALKYNES: THE STRUCTURE OF $[Ir_2(CO)(\eta^2\text{-}F_3CC{\equiv}CCF_3)(\mu\text{-}S)(\mu\text{-}CO)(DPM)_2]\cdot CH_2Cl_2$

Introduction

As described in Chapter 1, the coordination of unsaturated organic substrates to transition metal complexes is an important step in homogeneous catalytic hydrogenation. Although the bonding mode of such substrates to mononuclear complexes is essentially the same from one complex to the next, binuclear complexes offer additional coordination modes in which the unsaturated molecule may interact with both metal centers simultaneously. The previous two chapters of this thesis contain examples of such bonding by alkynes, and many related binuclear alkyne complexes have been reported.[1-13] Almost invariably the resulting complexes bind the acetylene moiety in one of two common bridging modes, either parallel(I) or perpendicular(II) to the metal-metal axis. Hoffmann and coworkers have presented a molecular orbital analysis of

I

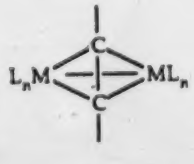

II

both types in an attempt to rationalize the geometries observed in the large number of complexes which have been structurally characterized.[2]

Alkynes which are found to coordinate to homobinuclear DPM-bridged complexes of rhodium and iridium are almost exclusively bound parallel to the metal-metal axis,[1-10] and more recent studies show that heterobinuclear "RhIr" analogues conform to the same trend (see Chapter 3 and elsewhere[11]). Although many related perpendicular acetylene complexes are known, especially for dicobalt species,[2] there are only a few examples of this bonding mode in the chemistry of homo- or hetero-binuclear DPM-bridged rhodium/iridium complexes.[12]

One alkyne coordination mode that has not yet been identified in binuclear DPM-bridged complexes is that in which the alkyne is bonded to only one metal center in an η^2 fashion. This would be analogous to the many well-known examples of mononuclear alkyne complexes. Such complexes have been proposed to precede the formation of the bridged species, as described for the reaction of alkynes with $[RhIr(CO)_2(\mu\text{-}Cl)(DPM)_2]^+$ in Chapter 3 and as shown below for the reaction of $[Ir_2(CO)_2(\mu\text{-}Cl)(DPM)_2]^+$ with alkynes.[1] With this chloro-bridged A-frame species rearrangement is apparently extremely facile since no evidence of an

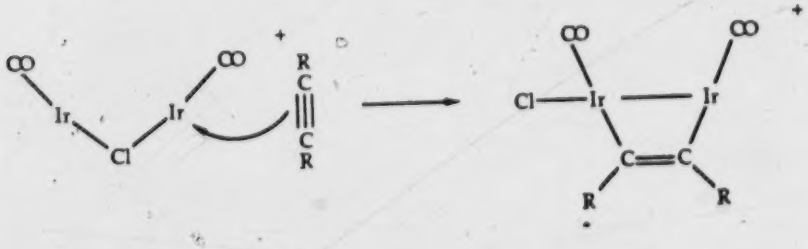

intermediate containing a terminal η^2-alkyne was ever observed. Nevertheless, the above route, in which coordination at one metal occurs first, followed by rearrangement, was proposed based on the stucture of the product obtained, in which the carbonyls were approximately trans to the alkyne group. If attack had occurred in the A-frame pocket, between the two metals, a symmetric product having both carbonyls adjacent to the alkyne would be expected.

Based on other studies (Chapter 5), in which rearrangement of the bridging sulfido ligand to a terminal position was found to be much less facile than for halide analogues, it was felt that in a reaction like the one diagrammed above, sulfide-bridged complexes might yield stable products having the alkyne bound at the initial site of attack. Furthermore, similar bridging thiolato groups were found to permit the isolation of a terminal η^2-alkyne complex, $[Ir_2(CO)_2(\eta^2\text{-}C_4F_6)(P(O\text{-}t\text{-}Bu)_3)_2(\mu\text{-}S\text{-}t\text{-}Bu)_2]$, which only slowly rearranged to give the alkyne-bridged form.[13]

Experimental Section

General experimental conditions were described in Chapter 2. The compounds, $[Ir_2(CO)_2(\mu\text{-}S)(DPM)_2]$[14] and $[RhIr(CO)_2(\mu\text{-}S)(DPM)_2]$ (See Chapter 3), were prepared according to the reported procedures. Hexafluoro-2-butyne (HFB) was purchased from PCR Incorporated and dimethylacetylenedicarboxylate (DMA) was obtained from Aldrich Chemical Company. The $^{31}P\{^1H\}$, ^1H, and ^{19}F NMR spectra were recorded on a Bruker WH-400 spectrometer.

Preparation of Compounds

(a) $[Ir_2(CO)(\eta^2\text{-}F_3CC{\equiv}CCF_3)(\mu\text{-}S)(\mu\text{-}CO)(DPM)_2]$ (2).

A 50.0 mg sample (0.040 mmol) of $[Ir_2(CO)_2(\mu\text{-}S)(DPM)_2]$ (1) was dissolved in 5 mL of CH_2Cl_2 under dinitrogen. Excess hexaflouro-2-butyne (HFB) was then bubbled through the solution, causing the deep purple solution to become yellow within 1 min. The solution was left under HFB for 10 min, then was concentrated to approximately 2 mL with a rapid flow of dinitrogen. The product was precipitated by the addition of 10 mL of diethyl ether, the solvent was removed by syringe and the solid dried with a rapid flow of dinitrogen. Compound 2 was isolated as an orange microcrystalline solid in 75% yield. Spectroscopic data for this and subsequent compounds are given in Table 4.1. Anal. calcd for $Ir_2SP_4F_6O_2C_{56}H_{44}$: C, 47.93%; H, 3.16%, Found: C, 47.08%; H, 2.98%.

(b) $[Ir_2(CO)(\eta^2\text{-}H_3CO_2CC{\equiv}CCO_2CH_3)(\mu\text{-}S)(\mu\text{-}CO)(DPM)_2]$ (3).

A 50.0 mg sample (0.040 mmol) of $[Ir_2(CO)_2(\mu\text{-}S)(DPM)_2]$ (1) was dissolved in 4 mL of CH_2Cl_2 under dinitrogen. To this solution was added excess dimethylacetylenedicarboxylate (DMA) (10 μL, approx. 2 equiv) which caused an immediate color change to orange. The compound was precipitated by the addition of 10 mL of hexanes, yielding an orange-yellow powder, which was washed with two 5-mL portions of diethyl ether and dried with dinitrogen flow. Isolated yield: 85%. Anal. calcd for $Ir_2SP_4F_6O_6C_{58}H_{50}$: C, 50.36%; H, 3.64%, Found: C, 49.52%; H, 3.64%.

Table 4.1. Spectroscopic Data for the Compounds in Chapter 4.[a]

compound	infrared(cm^{-1}) solid[c]	infrared(cm^{-1}) solution[d]	NMR[b] $^{31}P\{^1H\}$ δ[e]	NMR[b] ^1H δ	NMR[b] ^{19}F[f]
$[Ir_2(CO)(\eta^2\text{-HFB})(\mu\text{-S})(\mu\text{-CO})(DPM)_2]$ (2)	1943(vs),1780(vs)[g] 1744(st)[h]	1945(vs),1771(st)[g] 1747(med)[h]	-9.45(m), -10.91(m)	6.9-7.8(m, 40H), 4.71(m, 2H), 4.56(m, 2H)	-52.56(q), -52.74(q)[j] ($^5J_{F\text{-}F}$=4.5 Hz)
$[Ir_2(CO)(\eta^2\text{-DMA})(\mu\text{-S})(\mu\text{-CO})(DPM)_2]$ (3)	1933(vs),1770(vs)[g] 1753(st)[h],1679(st)[i]	1939(vs),1775(st)[g] 1680(med)[i]	-8.63(m), -10.06(m)	6.6-8.0(m, 40H), 4.21(m, 2H), 3.80(m, 2H)	
$[RhIr(CO)(\eta^2\text{-HFB})(\mu\text{-S})(\mu\text{-CO})(DPM)_2]$ (5)		1959(vs),1814(med)[g] 1753(med)[h]	15.98(dm),[k] -10.39(m)	6.8-8.1(m, 40H), 5.12(m, 2H), 2.64(m, 2H)	-52.04(q) -53.74(br) ($^5J_{F\text{-}F}$=5.0 Hz)

[a] Abbreviations used: st = strong, vs = very strong, med = medium, m = multiplet, dm = doublet of multiplets, q = quartet, br = broad. [b] CD_2Cl_2 solution. [c] Nujol mull. [d] CH_2Cl_2 solution. [e] Vs 85% H_3PO_4. [f] Vs $CFCl_3$. [g] ν(CO). [h] ν(C≡C) of coordinated alkyne. [i] -20 °C. [j] ν(C=O) of CO_2Me. [k] $^1J_{Rh\text{-}P}$ = 137.7 Hz.

(c) $[RhIr(CO)(\eta^2\text{-}F_3CC{\equiv}CCF_3)(\mu\text{-}S)(\mu\text{-}CO)(DPM)_2]$ (5)

A 10.0 mg sample of $[RhIr(CO)_2(\mu\text{-}S)(DPM)_2]$ (4) was dissolved in 1 mL of CH_2Cl_2 under dinitrogen. Hexafluoro-2-butyne (HFB) was bubbled through the solution, causing an immediate color change from dark red to orange-yellow. In the absence of an HFB atmosphere the solution regained a dark red color and infrared spectroscopy revealed only starting material. Compound 5 was characterized in solution (see Table 4.1) by saturating the solution with HFB and keeping it under an atmosphere of HFB.

X-ray Data Collection

Crystals of $[Ir_2(CO)(\eta^2\text{-}F_3CC{\equiv}CCF_3)(\mu\text{-}S)(\mu\text{-}CO)(DPM)_2]{\cdot}CH_2Cl_2$ (2) were obtained by slow diffusion of diethyl ether into a saturated CH_2Cl_2 solution of the complex. A suitable crystal was wedged into a capillary tube which was flame sealed as a precaution against loss of solvent of crystallization. Unit cell parameters were obtained from a least-squares refinement of the setting angles of 25 reflections, in the range $22.2° \leq 2\theta \leq 25.8°$, which were centered in both positive and negative θ on an Enraf-Nonius CAD4 diffractometer using graphite monochromated MoKα radiation. Automatic peak search and reflection indexing programs established a monoclinic crystal system. The systematic absences (h0l, l = odd; 0k0, k = odd) were consistent with the space group $P2_1/c$.

Intensity data were collected on the CAD4 diffractometer, and processed in the usual manner as described in Chapter 2. There was no

appreciable decrease in the intensities of the three standard reflections, so no correction was applied to the data. See Table 4.2 for crystal data and details of intensity collection.

Structure Solution and Refinement

The crystal structure was solved in the space group $P2_1/c$ using Patterson techniques to locate the metal atoms and by successive least-squares and difference Fourier calculations to obtain the other atom positions. The electron density in the vicinity of the solvent atoms appeared somewhat smeared out, indicating slight disorder in this group and giving rise to high thermal parameters. All hydrogen atoms were located but were assigned idealized positions as noted in Chapter 2.

The positional and isotropic thermal parameters for the final model are given in Table 4.3. In the final difference Fourier map, the 10 highest residual peaks were in the range 2.630-0.706 e/Å^3 and were located mainly in the vicinities of the CH_2Cl_2 solvent atoms. Refinement in the space group $P2_1/c$ converged at $R = 0.045$ and $R_w = 0.063$.[15]

Results and Discussion

(a) Description of Structure

The complex, $[Ir_2(CO)(\eta^2\text{-}F_3CC{\equiv}CCF_3)(\mu\text{-}S)(\mu\text{-}CO)(DPM)_2]$ (**2**), crystallizes in the space group $P2_1/c$ with one complex molecule and one

Table 4.2. Summary of Crystal Data and Details of Intensity Collection.

compd	$[Ir_2(CO)(\eta^2\text{-}C_4F_6)(\mu\text{-}S)(\mu\text{-}CO)(DPM)_2]\cdot CH_2Cl_2$
formula	$Ir_2Cl_2SP_4F_6O_2C_{57}H_{46}$
fw	1488.26
crystal shape	monoclinic prism
crystal size, mm	0.63 × 0.45 × 0.29
space group	$P2_1/c$ (No. 14)
cell parameters	
a, Å	20.614(7)
b, Å	15.348(3)
c, Å	19.890(5)
β, deg	117.84(2)
V, Å^3	5565.0
Z	4
ρ(calcd), g/cm^3	1.776
temp, °C	22
radiation (λ, Å)	graphite monochromated MoKα (0.71069)
receiving aperture, mm	3.00+(tanθ) wide × 4.00 high, 173 from crystal
take off angle, deg	3.00
scan speed, deg/min	variable between 6.67 and 1.54
scan width, deg	0.80 + (0.347 tanθ)in θ

Table 4.2. (Continued)

2θ limits, deg	$1.0 \leq 2\theta \leq 50.0$
no. of unique data collcd	9821 (h, k, ±l)
no. of unique data used ($F_o^2 \geq 3\sigma(F_o^2)$)	6806
linear absorption coeff, μ, cm^{-1}	50.66
range of transmission factors	0.723-1.169
final no. of parameters refined	412
error in observation of unit weight	2.027
R	0.045
R_w	0.063

Table 4.3. Positional Parameters and Isotropic Thermal Parameters[a]

Atom	x	y	z	B(Å^2)
Ir(1)	0.27694(2)	0.06539(2)	0.27614(2)	2.547(8)
Ir(2)	0.25690(2)	-0.07577(2)	0.17183(2)	2.689(8)
Cl(1)[b]	0.1947(4)	0.5243(6)	0.0840(5)	8.4(2)*
Cl(2)[b]	0.0952(7)	0.476(1)	0.1315(7)	14.2(4)*
S	0.3712(1)	-0.0101(2)	0.2554(1)	3.11(6)
P(1)	0.2669(1)	0.1666(2)	0.1832(1)	2.97(6)
P(2)	0.2623(1)	0.0143(2)	0.0809(1)	2.76(6)
P(3)	0.2878(1)	-0.0362(2)	0.3693(1)	2.92(6)
P(4)	0.2910(1)	-0.1805(2)	0.2657(2)	3.32(6)
F(1)	0.3944(5)	0.2884(5)	0.4120(5)	9.2(3)
F(2)	0.4552(5)	0.1837(7)	0.4147(6)	12.2(4)
F(3)	0.4080(7)	0.1904(7)	0.4865(5)	19.1(4)
F(4)	0.2392(6)	0.2500(7)	0.4212(5)	16.6(4)
F(5)	0.1909(5)	0.2897(6)	0.3096(5)	13.2(3)
F(6)	0.1529(5)	0.1866(7)	0.3451(6)	18.6(3)
O(1)	0.1239(3)	-0.0063(5)	0.1765(3)	3.8(2)
O(2)	0.1473(5)	-0.1960(6)	0.0537(4)	6.8(3)
C(1)	0.1864(5)	-0.0006(7)	0.2013(5)	3.3(2)
C(2)	0.1869(5)	-0.1483(7)	0.0993(5)	4.1(3)
C(3)	0.3944(8)	0.2029(8)	0.4190(7)	6.4(4)
C(4)	0.3286(6)	0.1600(6)	0.3624(5)	3.8(3)
C(5)	0.2588(6)	0.1634(7)	0.3365(5)	4.3(3)
C(6)	0.2084(7)	0.2198(9)	0.3505(7)	7.5(4)
C(7)	0.2982(5)	0.1246(6)	0.1173(5)	2.9(2)
C(8)	0.3326(5)	-0.1337(7)	0.3619(5)	3.7(3)
C(9)[b]	0.157(2)	0.562(2)	0.095(2)	11.(1)*
C(11)	0.3219(5)	0.2632(7)	0.2191(5)	3.6(2)*
C(12)	0.2931(6)	0.3410(8)	0.2257(6)	4.9(3)*

Table 4.3. (Continued)

C(13)	0.3415(7)	0.414(1)	0.2585(8)	6.6(3)*
C(14)	0.4142(7)	0.403(1)	0.2862(8)	6.5(3)*
C(15)	0.4455(7)	0.3277(9)	0.2818(7)	5.8(3)*
C(16)	0.3972(6)	0.2538(8)	0.2471(6)	5.0(3)*
C(21)	0.1746(5)	0.2091(7)	0.1180(5)	3.7(2)*
C(22)	0.1167(6)	0.1900(8)	0.1324(6)	4.6(3)*
C(23)	0.0471(7)	0.218(1)	0.0798(7)	6.4(3)*
C(24)	0.0354(7)	0.261(1)	0.0145(8)	6.9(4)*
C(25)	0.0939(7)	0.283(1)	0.0029(7)	6.7(3)*
C(26)	0.1641(6)	0.2548(8)	0.0532(6)	5.0(3)*
C(31)	0.3248(5)	-0.0254(6)	0.0466(5)	3.1(2)*
C(32)	0.3429(6)	-0.1124(8)	0.0544(6)	4.7(3)*
C(33)	0.3890(7)	-0.1453(9)	0.0259(7)	6.1(3)*
C(34)	0.4168(7)	-0.0891(9)	-0.0076(7)	5.9(3)*
C(35)	0.4008(7)	-0.0071(9)	-0.0154(7)	6.0(3)*
C(36)	0.3549(6)	0.0289(8)	0.0131(6)	4.4(2)*
C(41)	0.1746(5)	0.0332(6)	-0.0055(5)	3.0(2)*
C(42)	0.1104(6)	0.0211(8)	-0.0019(6)	4.7(3)*
C(43)	0.0434(7)	0.0386(9)	-0.0665(7)	6.0(3)*
C(44)	0.0408(6)	0.0644(7)	-0.1318(6)	4.5(2)*
C(45)	0.1035(6)	0.0763(7)	-0.1371(6)	4.4(2)*
C(46)	0.1713(5)	0.0611(7)	-0.0736(5)	3.6(2)*
C(51)	0.3444(5)	-0.0051(6)	0.4680(5)	2.9(2)*
C(52)	0.3139(6)	0.0435(7)	0.5038(6)	4.0(2)*
C(53)	0.3584(6)	0.0733(8)	0.5811(7)	5.2(3)*
C(54)	0.4301(6)	0.0527(8)	0.6168(6)	4.7(3)*
C(55)	0.4616(7)	0.0021(9)	0.5811(7)	5.7(3)*
C(56)	0.4168(6)	-0.0269(8)	0.5050(6)	4.7(3)*
C(61)	0.2045(5)	-0.0728(7)	0.3716(6)	3.6(2)*
C(62)	0.2047(6)	-0.1473(8)	0.4104(6)	5.2(3)*
C(63)	0.1404(7)	-0.172(1)	0.4123(7)	6.8(4)*

Table 4.3. (Continued)

C(64)	0.0792(7)	-0.122(1)	0.3788(7)	6.4(3)*
C(65)	0.0779(8)	-0.047(1)	0.3429(8)	6.8(4)*
C(66)	0.1434(6)	-0.0215(8)	0.3390(6)	4.6(2)*
C(71)	0.2194(5)	-0.2518(7)	0.2647(6)	4.0(2)*
C(72)	0.2401(7)	-0.3272(9)	0.3086(7)	6.1(3)*
C(73)	0.1842(8)	-0.376(1)	0.3139(8)	7.7(4)*
C(74)	0.1125(7)	-0.352(1)	0.2754(8)	7.1(4)*
C(75)	0.0920(7)	-0.280(1)	0.2316(7)	6.5(3)*
C(76)	0.1464(6)	-0.2292(8)	0.2258(6)	4.6(3)*
C(81)	0.3574(5)	-0.2567(7)	0.2664(6)	4.0(2)*
C(82)	0.4279(6)	-0.2656(9)	0.3280(7)	5.6(3)*
C(83)	0.4773(8)	-0.327(1)	0.3214(8)	7.1(4)*
C(84)	0.4571(7)	-0.373(1)	0.2571(8)	7.0(4)*
C(85)	0.3904(8)	-0.361(1)	0.1954(8)	7.7(4)*
C(86)	0.3389(7)	-0.302(1)	0.1995(7)	6.5(3)*

[a] Estimated standard deviations in this and other tables are given in parentheses and correspond to the least significant digits. Starred atoms were refined isotropically. Anisotropically refined atoms are given in the form of the isotropic equivalent displacement parameter defined as: $(4/3)[a^2\beta(1,1) + b^2\beta(2,2) + c^2\beta(3,3) + ab(\cos \text{gamma})\beta(1,2) + ac(\cos \text{beta})\beta(1,3) + bc(\cos \text{alpha})\beta(2,3)]$.

[b] Atoms Cl(1), Cl(2) and C(9) are those of the CH_2Cl_2 solvent molecule.

CH_2Cl_2 solvent molecule in the asymmetric unit. The solvent molecule displays the expected geometry, in spite of the apparent disorder (*vide supra*) and is not involved in any unusual contacts with the complex. A perspective view of the complex, including the numbering scheme, is shown in Figure 4.1. Selected bond distances and angles are given in Tables 4.4 and 4.5, respectively.

The complex molecule has the usual trans arrangement of DPM ligands and a doubly-bridged A-frame geometry in which the metals are bridged by sulfur and by CO. One iridium center has a terminal CO and the other has an η^2-bound hexafluoro-2-butyne (HFB) group. The overall geometry of the complex is very similar to that of $[Ir_2(CO)_2(\mu\text{-}S)(\mu\text{-}CO)(DPM)_2]$,[14] which is related to compound **2** by substitution of the alkyne by a terminal CO ligand. The DPM methylene groups are tilted toward the anionic bridging group as is most often the case in such A-frame complexes, minimizing interactions between the phenyl rings and atoms in the equatorial plane. The unsymmetrical structure results in somewhat different geometries at the metals.

The coordination at Ir(2) is very similar to both metal environments in $[Ir_2(CO)_2(\mu\text{-}S)(\mu\text{-}CO)(DPM)_2]$,[14] having a square pyramidal geometry with the two phosphorus atoms, the sulfur bridge-atom and C(2) at the base, and the bridging carbonyl group at the apex. Angles involving the pseudo trans-related basal groups (P(2)-Ir(2)-P(4) = 159.60(7)°; S-Ir(2)-C(2) = 162.0(3)°) are in better mutual agreement than are the corresponding angles in the tricarbonyl species (166.7(1)°; 151.5(4)°). The Ir-P distances at Ir(2) (2.320(2) Å, 2.311(2) Å) are virtually identical to those of the tricar-

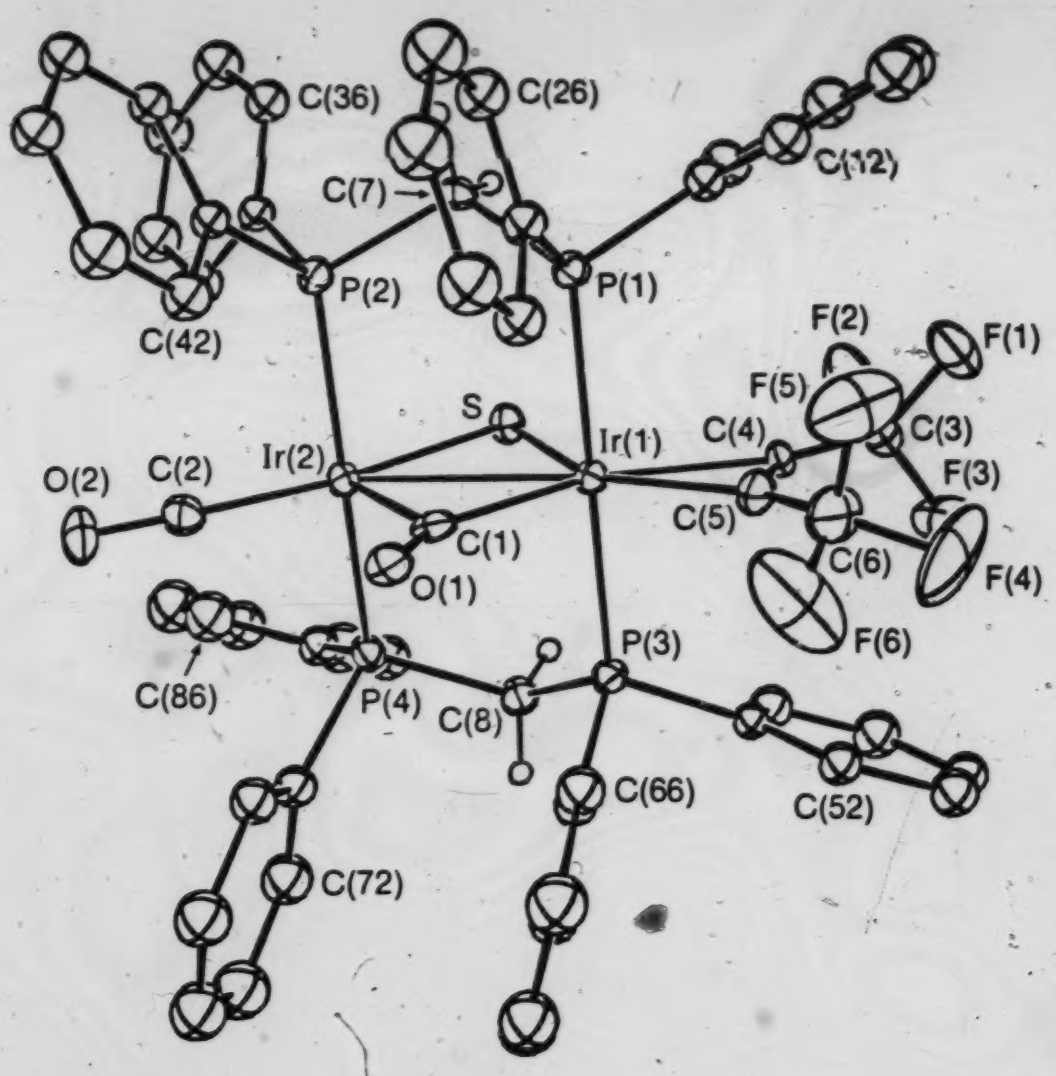

Figure 4.1 A perspective view of $[Ir_2(CO)(\eta^2\text{-}F_3CC{\equiv}CCF_3)(\mu\text{-}S)(\mu\text{-}CO)\text{-}(DPM)_2]$ showing the numbering scheme. Thermal ellipsoids are shown at the 20% level except for the methylene hydrogens, which are shown artificially small and the phenyl hydrogens, which are omitted.

Table 4.4. Selected Distances (Å) in $[Ir_2(CO)(\eta^2\text{-HFB})(\mu\text{-S})(\mu\text{-CO})(DPM)_2]$

Ir(1)-Ir(2)	2.8929(4)	P(3)-C(8)	1.799(8)
Ir(1)-S	2.457(2)	P(3)-C(51)	1.817(7)
Ir(1)-P(1)	2.350(2)	P(3)-C(61)	1.829(8)
Ir(1)-P(3)	2.351(2)	P(4)-C(8)	1.839(8)
Ir(1)-C(1)	2.032(8)	P(4)-C(71)	1.830(8)
Ir(1)-C(4)	2.117(7)	P(4)-C(81)	1.795(8)
Ir(1)-C(5)	2.065(8)	F(1)-C(3)	1.33(1)
Ir(2)-S	2.381(2)	F(2)-C(3)	1.33(1)
Ir(2)-P(2)	2.320(2)	F(3)-C(3)	1.26(1)
Ir(2)-P(4)	2.311(2)	F(4)-C(6)	1.33(1)
Ir(2)-C(1)	2.141(8)	F(5)-C(6)	1.29(1)
Ir(2)-C(2)	1.860(8)	F(6)-C(6)	1.21(1)
P(1)-C(7)	1.827(7)	O(1)-C(1)	1.148(8)
P(1)-C(11)	1.798(8)	O(2)-C(2)	1.155(9)
P(1)-C(21)	1.851(8)	C(3)-C(4)	1.45(1)
P(2)-C(7)	1.854(7)	C(4)-C(5)	1.28(1)
P(2)-C(31)	1.822(7)	C(5)-C(6)	1.47(1)
P(2)-C(41)	1.845(7)		

Table 4.5. Selected Angles (deg) in $[Ir_2(CO)(\eta^2\text{-HFB})(\mu\text{-S})(\mu\text{-CO})(DPM)_2]$

Ir(2)-Ir(1)-S	52.09(4)	P(2)-Ir(2)-P(4)	159.60(7)
Ir(2)-Ir(1)-P(1)	90.01(5)	P(2)-Ir(2)-C(1)	100.2(2)
Ir(2)-Ir(1)-P(3)	89.85(5)	P(2)-Ir(2)-C(2)	93.2(3)
Ir(2)-Ir(1)-C(1)	47.7(2)	P(4)-Ir(2)-C(1)	98.2(2)
Ir(2)-Ir(1)-C(4)	160.8(3)	P(4)-Ir(2)-C(2)	92.5(3)
Ir(2)-Ir(1)-C(5)	163.5(3)	C(1)-Ir(2)-C(2)	98.9(3)
S-Ir(1)-P(1)	88.03(7)	Ir(1)-S-Ir(2)	73.43(5)
S-Ir(1)-P(3)	91.57(7)	Ir(1)-P(1)-C(7)	113.6(2)
S-Ir(1)-C(1)	99.8(2)	Ir(1)-P(1)-C(11)	115.1(3)
S-Ir(1)-C(4)	108.8(3)	Ir(1)-P(1)-C(21)	117.9(3)
S-Ir(1)-C(5)	144.4(3)	C(7)-P(1)-C(11)	102.1(3)
P(1)-Ir(1)-P(3)	179.58(7)	C(7)-P(1)-C(21)	102.4(3)
P(1)-Ir(1)-C(1)	92.3(2)	C(11)-P(1)-C(21)	103.8(4)
P(1)-Ir(1)-C(4)	90.6(2)	Ir(2)-P(2)-C(7)	113.3(2)
P(1)-Ir(1)-C(5)	90.2(2)	Ir(2)-P(2)-C(31)	113.1(2)
P(3)-Ir(1)-C(1)	87.9(2)	Ir(2)-P(2)-C(41)	115.9(2)
P(3)-Ir(1)-C(4)	89.4(2)	C(7)-P(2)-C(31)	103.3(3)
P(3)-Ir(1)-C(5)	90.1(2)	C(7)-P(2)-C(41)	105.0(3)
C(1)-Ir(1)-C(4)	151.4(3)	C(31)-P(2)-C(41)	105.2(3)
C(1)-Ir(1)-C(5)	115.9(3)	Ir(1)-P(3)-C(8)	110.5(3)
C(4)-Ir(1)-C(5)	35.7(3)	Ir(1)-P(3)-C(51)	117.0(2)
Ir(1)-Ir(2)-S	54.48(4)	Ir(1)-P(3)-C(61)	118.6(3)
Ir(1)-Ir(2)-P(2)	94.01(5)	C(8)-P(3)-C(51)	102.3(3)
Ir(1)-Ir(2)-P(4)	93.08(5)	C(8)-P(3)-C(61)	105.7(4)
Ir(1)-Ir(2)-C(1)	44.6(2)	C(51)-P(3)-C(61)	101.0(3)
Ir(1)-Ir(2)-C(2)	143.5(3)	Ir(2)-P(4)-C(8)	112.8(2)
S-Ir(2)-P(2)	84.27(6)	Ir(2)-P(4)-C(71)	117.9(3)
S-Ir(2)-P(4)	84.36(7)	Ir(2)-P(4)-C(81)	113.7(3)
S-Ir(2)-C(1)	99.1(2)	C(8)-P(4)-C(71)	103.1(4)
S-Ir(2)-C(2)	162.0(3)	C(8)-P(4)-C(81)	105.3(4)

Table 4.5 (Continued)

C(71)-P(4)-C(81)	102.7(4)	C(3)-C(4)-C(5)	139.3(9)
Ir(1)-C(1)-Ir(2)	87.7(3)	Ir(1)-C(5)-C(4)	74.3(5)
Ir(1)-C(1)-O(1)	144.6(7)	Ir(1)-C(5)-C(6)	150.6(9)
Ir(2)-C(1)-O(1)	127.6(6)	C(4)-C(5)-C(6)	135.(1)
Ir(2)-C(2)-O(2)	175.2(8)	F(4)-C(6)-F(5)	103.(1)
F(1)-C(3)-F(2)	99.5(9)	F(4)-C(6)-F(6)	102.(1)
F(1)-C(3)-F(3)	105.(1)	F(4)-C(6)-C(5)	112.(1)
F(1)-C(3)-C(4)	114.(1)	F(5)-C(6)-F(6)	109.(1)
F(2)-C(3)-F(3)	107.(1)	F(5)-C(6)-C(5)	112.6(9)
F(2)-C(3)-C(4)	114.7(9)	F(6)-C(6)-C(5)	117.(1)
F(3)-C(3)-C(4)	116.(1)	P(1)-C(7)-P(2)	113.1(3)
Ir(1)-C(4)-C(3)	150.7(8)	P(3)-C(8)-P(4)	113.7(4)
Ir(1)-C(4)-C(5)	70.0(5)		

bonyl complex and the Ir(2)-C(2) distance is only slightly longer than in the tricarbonyl species (1.860(8) Å *vs* 1.80(1) Å). The C-O distances in both of the carbonyl groups are normal.

At Ir(1) the coordination could be considered somewhat of an average between trigonal bipyramidal and octahedral. Whereas the P-Ir-P angle is bent away from the adjacent metal in the tricarbonyl complex, a compression of the DPM groups along the metal-metal bond in **2** results in a P(1)-Ir(1)-P(3) angle which is almost perfectly linear (179.58(7)°) indicating that the coordinated alkyne forces these phosphorus atoms toward Ir(2). The Ir(1)-P distances (2.350(2) Å, 2.351(2) Å) are slightly longer than those at Ir(2), again a likely result of the increased steric requirements of the alkyne. The sulfido ligand bridges the two metals in an unsymmetrical fashion, with the longer Ir(1)-S distance (2.457(2) Å *vs* 2.381(2) Å for Ir(2)-S) probably arising from steric interactions involving the alkyne CF_3 groups. The opposite situation is evident at C(1), where the distance to Ir(1) (2.032(8) Å) is shorter than that to Ir(2) (2.141(8) Å). This is apparently due to steric effects involving the phenyl group containing C(42), which forces the carbonyl group away from Ir(2). Accordingly, the H(42)-O(1) distance is rather short (2.50 Å) compared to van der Waals radii for these atoms.[16] The Ir(1)-C(1)-Ir(2) angle (87.7(3)°) is not unusual for a bridging carbonyl associated with a metal-metal bond (see also Chapter 2).[14,17] The Ir(1)-Ir(2) separation of 2.8929(4) Å corresponds to a normal single bond and is comparable to other diiridium species which are metal-metal bonded.[1,14,17,18]

The coordinated alkyne moiety lies in the equatorial plane of the molecule, with the midpoint of the C≡C bond almost directly trans to the Ir-Ir bond. The Ir-C distances (2.117(7) Å, 2.065(8) Å) are comparable to those found in diiridium complexes with bridging alkyne groups,[1,10] and in a related triiridium complex, which contains both terminal and bridging HFB groups.[19] The C(5)-C(6) distance (1.28(1) Å) is not unusual for terminal π-bound alkynes in mononuclear Group VIII compounds.[20-25] Typical C-C distances in coordinated alkyne complexes range from 1.19 to 1.32 Å. The angles at which the CF_3 groups are bent back (139.3(9)° and 135.(1)°) are somewhat acute, as typical bend-back angles are in the range 168° to 140°.[25] The slightly greater bending back of the CF_3 group containing C(6) appears to result from a stronger binding of this end of the alkyne, as indicated by the slightly shorter Ir(1)-C(5) distance given above. Stronger π back-donation to C(5) would result in a shorter distance and a greater degree of rehybridization of C(5) toward sp^2. The stronger π back-donation to C(5) than to C(4) is consistent with the former being opposite the good electron-donating sulfido group and C(4) being opposite the π-accepting carbonyl group (C(1)O(1)). Steric factors do not appear to be important, since the shortest non-bonded contact involving the CF_3 groups (F(5)-H(12) = 2.86 Å) is in the direction opposing the observed bending of the CF_3 group. The C-C distance in this terminal alkyne complex is notably shorter than those observed for bridging alkynes in related species such as $[Ir_2Cl_2(CO)_2(\mu\text{-}CH_3O_2CC{\equiv}CCO_2CH_3)(DPM)_2]$ (1.344(8) Å)[1] and $[Rh_2Cl(CNMe)_2(\mu\text{-}F_3CC{\equiv}CCF_3)(DPM)_2]$ (1.32(1) Å),[6] where distances and angles at the unsaturated carbons are very similar to normal alkenes.

Accordingly, the C≡C-CF_3 angles in complex **2** are greater than corresponding angles found in these complexes (av 124.8°). The C-CF_3 distances (1.45(1) Å, 1.47(1) Å) are in the range expected for such bonds adjacent to a carbon-carbon triple bond,[26] slightly shorter than those found in a dirhodium HFB-bridged complex.[6]

(b) Description of Chemistry

The addition of hexafluoro-2-butyne (HFB) to a solution of the A-frame complex, $[Ir_2(CO)_2(\mu\text{-}S)(DPM)_2]$ (**1**), causes a color change from deep purple to yellow. The $^{31}P\{^1H\}$ NMR spectrum of the resulting solution displays two complex multiplets at δ -9.45 and δ -10.91, indicating an unsymmetrical species, **2**, having two sets of chemically inequivalent phosphorus atoms. The infrared spectrum of the solution reveals new bands at 1945, 1771 and 1747 cm^{-1}. The absence of an acetylenic stretch in the region 1645-1490 cm^{-1}, expected for either the parallel or perpendicular bridging modes,[1] suggests a different bonding mode in this species which is confirmed by the structure determination (*vide supra*). The CO stretch at 1945 cm^{-1} is attributed to the terminal carbonyl in complex **2**, while the stretches at 1771 cm^{-1} and 1747 cm^{-1} are attributed to ν(CO) of the bridging carbonyl and ν(C≡C) of the coordinated alkyne, respectively (Δν(C≡C) = 553 cm^{-1} *vs* free alkyne[27]). These bands are unambiguously assigned by preparation of the ^{13}CO enriched product, which displays an IR spectrum in which the carbonyl bands are shifted to 1898 cm^{-1} and approximately 1740 cm^{-1} (underneath the C≡C stretch at 1747 cm^{-1}).

Compound **2** can be compared to the mononuclear HFB complex, diagrammed below, which is formed upon reaction of Vaska's compound, $[IrCl(CO)(PPh_3)_2]$, with HFB.[27] The infrared spectrum of this mononuclear species exhibits a stretch at 1773 cm^{-1} for the coordinated alkyne which is significantly higher than that observed for compound **2**. This is consistent with the sulfido ligand in compound **2** providing a more electron rich

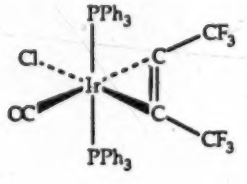

metal, thereby being better able to reduce the C-C bond order through π back-donation (Note that carbonyl stretches in the IR spectrum of the precursor, $[Ir_2(CO)_2(\mu\text{-}S)(DPM)_2]$ (**1**), were found to be rather low (1935, 1920 cm^{-1}), compared to the chloro-bridged analogue, also indicating electron rich metal centers[14]). A C≡C stretch at 1765 cm^{-1} was observed in a related binuclear iridium complex containing a terminal η^2-HFB group, $[Ir_2(CO)_2(\eta^2\text{-}C_4F_6)(P(O\text{-}t\text{-}Bu)_3)_2(\mu\text{-}S\text{-}t\text{-}Bu)_2]$.[13] The relatively high value for ν(C≡C) in **2**, compared to the same stretch in diiridium complexes containing HFB in a bridging position (range 1549-1573 cm^{-1}),[1] is an indication of the significant carbon-carbon triple bond character remaining in the coordinated HFB group of **2**. Accordingly, the bonding between the alkyne and the iridium center of **2** is somewhat weaker than in these cis-dimetallated olefin species, which are rather stable toward alkyne loss.[1] Compound **2** is

stable in solution, even under N_2 purge, but loses HFB upon refluxing in CH_2Cl_2 to regenerate the dark purple color of $[Ir_2(CO)_2(\mu\text{-}S)(DPM)_2]$ (**1**).

The ^{19}F NMR spectrum of **2** displays an interesting temperature dependence. Although only one resonance (singlet, δ -52.62) is observed at 22 °C, lowering the temperature causes this resonance to split and resolve into two multiplets by 5 °C; by -20 °C they are well separated and appear as two partially resolved quartets (δ -52.56, -52.74; $^5J_{F\text{-}F}$ = 4.5 Hz). No broadening or collapse of the resonances is observed, arguing against a fluxional process which averages the environments of the fluorine atoms. It would appear, instead, that the chemical shift of each set of fluorine nuclei is temperature dependent, being accidentally coincident at 22 °C, but moving away from each other at slightly different rates as the temperature is decreased. A similar effect has been observed in the $^{31}P\{^1H\}$ NMR spectra of $[Ir_2Cl(CO)_3(\mu\text{-}H_3CO_2CC{\equiv}CCO_2CH_3)(DPM)_2][BF_4]$.[1]

Compound **1** also reacts with excess dimethylacetylenedicarboxylate (DMA), giving an immediate color change to orange-yellow. The $^{31}P\{^1H\}$ NMR spectrum (δ -8.63(m), -10.06(m)) is very similar to that of the HFB adduct, strongly suggesting an analogous formulation for $[Ir_2(CO)(\eta^2\text{-}DMA)(\mu\text{-}S)(\mu\text{-}CO)(DPM)_2]$ (**3**). This formulation is supported by the solution infrared spectrum of **3** which displays a terminal carbonyl stretch at 1939 cm^{-1}, a bridging CO stretch at 1775 cm^{-1} and a stretch due to the DMA carboxylate groups at 1680 cm^{-1}. The carbonyl stretches are again confirmed by preparation of the complex using ^{13}CO-enriched starting material. The acetylenic stretch for **3** is apparently obscured by the carboxylate band of free DMA in solution, but is clearly visible (at 1753

cm^{-1}) in the infrared spectrum of solid samples of **3**. The higher frequency for this stretch compared to that of compound **2** corresponds to less reduction in the C≡C bond order ($\Delta\nu$(C≡C) = 397 cm^{-1} *vs* free alkyne), caused by less π back-donation by the metal into the π^* orbital of the alkyne. This is not surprising based on the greater electronegativity of the CF_3 group compared to CO_2Me,[28] and is consistent with the ease of reversibility demonstrated by these complexes. As with complex **2**, the formation of **3** is reversible, but in this case alkyne loss is much more facile. A solid sample of **3** which is redissolved in CH_2Cl_2 immediately gives a dark red solution signifying the presence of a large amount of compound **1**. The solution IR spectrum confirms the presence of **1**, along with free DMA, while a small amount of **3** remains. Likewise, reaction of **1** with only one equivalent of DMA results in an equilibrium mixture of **1** and **3**. These results are again consistent with less π back-donation to the DMA group, thus giving weaker metal-alkyne bonding in **3** than in **2**.

The products resulting from the reaction of $[Ir_2(CO)_2(\mu\text{-}S)(DPM)_2]$ (**1**) with HFB and DMA are somewhat surprising based on the virtually exclusive observation of the bridging mode displayed by the products in all previous reactions involving similar DPM-bridged binuclear complexes.[3-9] However, attack of the alkyne at an outside site of the A-frame (as in complexes **2** and **3**) has been proposed[1] (see also Chapter 3) in order to justify the observed products, without having to invoke ligand loss and subsequent recoordination. The rearrangement would then only require movement of the anionic bridge-ligand to a terminal position, and replacement by the coordinated alkyne. In the sulfido-bridged species, the

reluctance of the dianionic sulfide group to move to a terminal site on one metal inhibits such rearrangement and allows the isolation of the presumed initial η^2-alkyne complex. The species isolated reveals that subsequent bridging of the carbonyl ligand adjacent to the alkyne moiety has occurred, which is clearly advantageous sterically, and furthermore provides both metals with stable eighteen-electron configurations. Attempts were made to induce rearrangement to the alkyne bridged form by the addition of polar solvents to CH_2Cl_2 solutions of **2**. This would possibly stabilize a dipolar intermediate such as that shown below, which

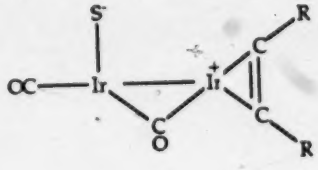

would then allow the alkyne to migrate to the bridge position. These attempts were unsuccessful, leading only to precipitation of the complex. In comparison, conversion of the terminal HFB group in $[Ir_2(CO)_2(\eta^2\text{-}C_4F_6)(P(O\text{-}t\text{-}Bu)_3)_2(\mu\text{-}S\text{-}t\text{-}Bu)_2]$[13] to the bridged form, as was observed in that system, does not require cleavage of a metal-sulfur bond because the molecule is stereochemically nonrigid.

Based on the results of the reactions of the diiridium complex, **1**, with alkynes, an extension to the mixed-metal "RhIr" analogue was expected to give a similar result, except that metal-specific attack of the

alkyne at iridium was anticipated due to its greater ability for π back-bonding.

Solutions of the A-frame complex, $[RhIr(CO)_2(\mu\text{-}S)(DPM)_2]$ (**4**), react immediately with excess HFB, as evidenced by a color change from red to orange-yellow. The resulting compound, **5**, persists in solution only when kept under atmosphere of HFB, rapidly reverting to compound **4** in its absence, as evidenced by a color change to dark red. The $^{31}P\{^1H\}$ NMR spectrum of an HFB-saturated solution of compound **5** is typical of DPM-bridged "RhIr" complexes, having a doublet of multiplets due to the rhodium-bound phosphorus atoms (δ 15.98, $^1J_{Rh\text{-}P}$ = 137.7 Hz) and a multiplet for the iridium-bound phosphorus atoms (δ -10.39). Notably, the chemical shift of the iridium-bound phosphorus atoms in **5** is significantly different from that of the precursor, **4**, whereas the rhodium-bound phosphorus signal is only slightly changed (See Chapter 3). The infrared spectrum of a solution containing **5** displays carbonyl stretches at 1959 cm^{-1} and 1814 cm^{-1}, and a C≡C stretch due to the coordinated alkyne appears at 1753 cm^{-1}. Again, the stretches are unambiguously assigned by preparation of the ^{13}CO enriched species, in which the 1753 cm^{-1} band remains unchanged. The $^{13}C\{^1H\}$ NMR spectrum of **5** displays a doublet of triplets at δ 194.50 ($^1J_{Rh\text{-}C}$ = 71.7 Hz, $^2J_{P\text{-}C}$ = 15.1 Hz), which clearly results from a terminal CO on rhodium, and a partially resolved multiplet at δ 189.92 for the bridging carbonyl group.

The above information suggests a formulation for complex **5** as diagrammed below, quite analogous to the previously discussed diiridium species. Location of the coordinated alkyne on the iridium center is

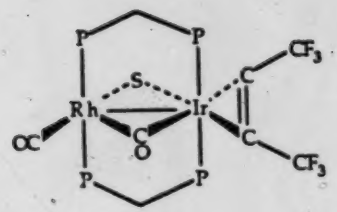

5

consistent with the significant change in chemical shift ($^{31}P\{^1H\}$ NMR) observed for the iridium-bound phosphorus atoms upon reaction with HFB, and with the location of the terminal CO on rhodium established by $^{13}C\{^1H\}$ NMR. The infrared stretch at 1959 cm^{-1} is also consistent with a terminal CO located on the rhodium center, being somewhat higher than the terminal CO stretch associated with the more basic iridium center in compound **2**. Furthermore, the result is not surprising since coordination of the alkyne at iridium should be favored due to an expected stronger bonding through increased π-back donation from the more basic metal. Consistent with the facile reversibility of this reaction compared to the diiridium analogue, the C≡C stretch for the coordinated HFB is several wavenumbers higher than that of compound **2**, again demonstrating less π back-bonding into the alkyne. The difference in lability of the diiridium compound, **2**, and the mixed-metal complex, **5**, is somewhat surprising, given that the alkyne is bound to iridium in both cases, in what is apparently an identical local environment. Clearly, the replacement of the distal iridium by rhodium has a noticeable affect on the Ir-alkyne bonding, such that weaker binding of the alkyne arises from a less basic metal in this position.

The ^{19}F NMR spectrum of compound **5** exhibits one partially resolved quartet (δ -52.04, $^{5}J_{F\text{-}F}$ = 5.0 Hz) and an unresolved resonance (δ -53.74), integrating 1:1. Although the chemical shifts of the two inequivalent CF_3 groups are not coincident as in **2**, the shifts are similarly temperature dependent, however, in this case the resonances gradually move toward one another as the temperature is lowered, such that at -40 °C the resonances occur at δ -52.26 and δ -53.62.

The mixed-metal A-frame, **4**, also reacts with DMA, as evidenced by a color change to light orange in the vicinity of the reagent addition. Although a gradual change in the solution color occurs, after 10 molar equivalents of DMA are added to an 8.7 mM solution of **4** in CH_2Cl_2, the infrared spectrum only displays carbonyl stretches due to **4** (1948, 1920 cm^{-1}) and a strong band at 1725 cm^{-1} due to free DMA. A shoulder on the latter (1680 cm^{-1}) is likely due to the carboxylate of coordinated DMA. The $^{31}P\{^{1}H\}$ NMR spectrum under these conditions reveals a new species at δ 15.82 (Rh-bound phosphorus atoms) and δ -11.71 (Ir-bound phosphorus atoms), similar to the resonances found for **3**. Based on the infrared data, these resonances may represent an average environment for the phosphorus atoms in **4** and the η^2-DMA complex, but the two species do not freeze out in the NMR as the spectrum does not change down to -80 °C. Clearly, the equilibrium established in this case strongly favors reactants. Compared to the stability of complex **5**, this result is not unexpected, given the trend already observed in going from HFB to DMA in complexes **2** and **3**.

Although the sulfido A-frames, **1** and **4**, demonstrate an affinity toward activated alkynes, neither reacts with activated olefins such as tetrafluoroethylene or dimethylmaleate. They also do not react with unactivated alkyne or olefin substrates such as 2-butyne or ethylene.

Conclusions

The intermediacy of terminal π-bound alkyne species has previously been postulated in the reactions of binuclear DPM-bridged complexes with alkynes,[1,29] but until now their characterizations have not been possible due to facile rearrangement to rather stable species in which the alkyne group bridged the two metal centers. The complexes described herein clearly show that the alkyne in each case is coordinated on the outside of the complex, presumably at the initial site of attack. As such, these species function as models for the elusive intermediates which for other A-frames rearrange immediately to the alkyne-bridged species. These observations are consistent with the relative ease by which the monoanionic halide ligand can move to a terminal position relative to the dianionic sulfide group.

Comparison of the "Ir_2"-alkyne complexes to analogous "RhIr"-alkyne complexes suggests that the strength of the metal-alkyne bond is strongly influenced by the nature of the adjacent metal center. Such metal-metal cooperativity may be useful for "tailoring" the electronic environment at a metal center in order to enhance its catalytic activity. Oro and coworkers[30] have found, for example, that certain binuclear

"RuRh" and "RuIr" complexes are more active than their mononuclear parent compounds in catalyzing the reduction of cyclohexene, and that the "RuIr" complex is more active than the "RuRh" complex.

Although binuclear complexes which contain alkynes bound as cis-dimetallated olefins have been observed to give hydrogenated products upon reaction with H_2,[31] somewhat elevated temperatures appear necessary. In DPM-bridged complexes the bridging alkyne is quite stable and similar reactions have generally not been observed, whereas reaction of alkynes with hydride precursors is much more favorable (see Chapter 6). This may be an indication that species containing terminal η^2-alkynes are more important in the hydrogenation of alkynes catalyzed by binuclear complexes. In that case, species of the type discussed in this chapter may be useful since alkyne bridge formation is inhibited, and alkyne coordination is reversible, so that oxidative addition of H_2 can be more competitive, if such a route is favored.

References and Footnotes

1. Sutherland, B. R.; Cowie, M. *Organometallics* **1984**, *3*, 1869.
2. Hoffman, D. M.; Hoffmann, R.; Fisel, C. R. *J. Am. Chem. Soc.* **1982**, *104*, 3858, and references therein.
3. Cowie, M.; Southern, T. G. *J. Organomet. Chem.* **1980**, *193*, C46.
4. Cowie, M.; Southern, T. G. *Inorg. Chem.* **1982**, *21*, 246.
5. Cowie, M.; McKeer, I. R. *Inorg. Chim. Acta* **1982**, *65*, L107.
6. Cowie, M.; Dickson, R. S.; Hames, B. W. *Organometallics* **1984**, *3*, 1879.
7. Mague, J. T.; DeVries, S. H. *Inorg. Chem.* **1982**, *21*, 1632.
8. Mague, J. T. *Inorg. Chem.* **1983**, *22*, 1158.
9. Dickson, R. S.; Cowie, M. *Inorg. Chem.* **1981**, *20*, 2682.
10. Cowie, M.; Vasapollo, G.; Sutherland, B. R.; Ennett, J. P. *Inorg. Chem.* **1986**, *25*, 2648.
11. Mague, J. T. *Organometallics* **1986**, *5*, 918 and references therein.
12. (a) Berry, D. H.; Eisenberg, R. *Organometallics* **1987**, *6*, 1796. (b) McDonald, R.; Cowie, M. manuscript in preparation.
13. Guilmet, E.; Maissonnat, A.; Poilblanc, R. *Organometallics* **1983**, *2*, 1123.
14. Kubiak, C. P.; Woodcock, C.; Eisenberg, R. *Inorg. Chem.* **1980**, *19*, 2733.
15. $R = \Sigma||F_o|-|F_c||/\Sigma|F_o|$; $R_w = [\Sigma w(|F_o|-|F_c|)^2/\Sigma wF_o^2]^{1/2}$.
16. Huheey, J. E. *Inorganic Chemistry*, 3rd ed., Harper and Row, New York, 1983, p 258-259 and references therein.

17. Sutherland, B. R.; Cowie, M. *Inorg. Chem.* **1984**, *23*, 2324.

18. Sutherland, B. R.; Cowie, M. *Organometallics* **1985**, *4*, 1801.

19. Devillers, J.; deMontauzon, D.; Poilblanc, R. *Angew. Chem. Int. Ed. Engl.* **1981**, *20*, 287.

20. Reger, D. L.; Klaeren, S. A.; Lebioda, L. *Organometallics* **1988**, *7*, 189.

21. Barlow, J. H.; Clark, G. R.; Curl, M. G.; Howden, M. E.; Kemmit, D. W.; Russell, D. R. *J. Organomet. Chem.* **1978**, *144*, C47.

22. Glanville, G. O.; Stewart, J. M.; Grim, S. O. *J. Organomet. Chem.* **1967**, *7*, P9.

23. Dickson, R. S.; Ibers, J. A. *J. Organomet. Chem.* **1972**, *36*, 191.

24. Green, M.; Grove, D. M.; Howard, J. A. K.; Spencer, J. L.; Stone, F. G. A. *J. Chem. Soc., Chem. Commun.* **1976**, 759.

25. Ittel, S. D.; Ibers, J. A. *Adv. Organomet. Chem.* **1976**, *14*, 33, and references therein.

26. MacGillavry, C. H.; Rieck, G. D. eds. *International Tables for X-ray Crystallography*; Kynock Press: Birmingham, England, **1968**; *Vol. III*, Table 4.2.2.

27. Parshall, G. W.; Jones, F. N. *J. Am. Chem. Soc.* **1965**, *87*, 5356.

28. Kosower, E. M. *An Introduction to Physical Organic Chemistry*, Wiley, New York, **1968**, p 49.

29. Puddephatt, R. J.; Thompson, M. A. *Inorg. Chem.* **1982**, *21*, 725.

30. Garcia, M. P.; Lopez, A. M.; Esteruelas, M. A.; Lahoz, F. J.; Oro, L. A. *J. Chem. Soc., Chem. Commun.* **1988**, 793.

31. El Amane, M.; Mathieu, R.; Poilblanc, R. *Organometallics* **1983**, *2*, 1618.

CHAPTER 5

FACILE HYDRIDE REARRANGEMENTS IN A-FRAME AND RELATED COMPLEXES AND THE STRUCTURE OF $[RhIr(H)_2(CO)_2(\mu\text{-}Cl)(DPM)_2][BF_4]\cdot CH_2Cl_2$, THE PRODUCT OF H_2 ADDITION AT ONE METAL CENTER IN THE A-FRAME POCKET

Introduction

Homogeneous hydrogenation catalysts based on mononuclear Rh(I) phosphine complexes have been much studied and are reasonably well understood.[1] However, much less is known about catalysts which contain more than one metal center, owing to the added complexity introduced when more than one reactive site is present in the molecule. Reports of catalytic alkyne hydrogenation by the binuclear complexes $[Rh_2(CO)_2(\mu\text{-}Cl)(DPM)_2][BPh_4]$,[2] $[Rh_2H_2(CO)_2(DPM)_2]$,[3] $[Rh_2Cl_2(\mu\text{-}CO)(DPM)_2]$,[4] and $[Ir_2(CO)_2(\mu\text{-}S)(DPM)_2]$[5] and the suggestions[6,7] that the metals may be involved in a cooperative manner, prompted this research group to probe the function of the adjacent metals in hydrogenation reactions catalyzed by $[Rh_2(CO)_2(\mu\text{-}Cl)(DPM)_2]^+$ and related A-frame species.

This chapter concentrates on the binuclear hydrides obtained in reactions with H_2 since such species are pivotal to our understanding of multicenter hydrogenation catalysts. Since the catalytically active dirhodium A-frame species, $[Rh_2(CO)_2(\mu\text{-}Cl)(DPM)_2]^+$, did not yield observable products upon reaction with H_2, studies within this research

group turned to the diiridium analogue, $[Ir_2(CO)_2(\mu\text{-}Cl)(DPM)_2]^+$ (1), as a model catalyst precursor. In the initial study[6] it was found that the thermodynamically favored dihydride product, 2, had the hydrido ligands on the outside of the A-frame complex, as shown. Furthermore, an early

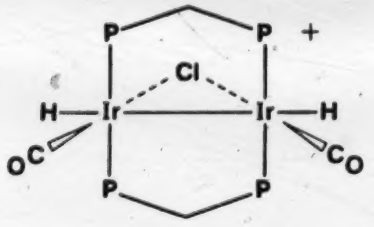

2

study on the reactivity of a similar species, $[Ir_2(CO)_2(\mu\text{-}S)(DPM)_2]$, with H_2 showed the presence of two dihydride species in the 100 MHz ^1H NMR spectrum.[5] One resonance (a quintet) was believed to result from a rapid equilibrium between species **A** and **B**, while the second resonance (analyzed as a triplet of triplets) was believed to be due to **C**, although no

A B C

definitive assignment of structures was possible at that time. It was of interest to establish unequivocally the site of initial attack by H_2 in these A-frames and to determine how a presumed concerted oxidative addition of H_2 at one metal center gave rise to the products containing non-adjacent

hydrido ligands. In this chapter is described a reinvestigation of the reaction of $[Ir_2(CO)_2(\mu\text{-}S)(DPM)_2]$ with H_2 using improved spectroscopic techniques, a continuation of the initial study on $[Ir_2(CO)_2(\mu\text{-}Cl)(DPM)_2]^+$, and similar studies on related A-frame complexes. Also reported are the analogous reactions involving a series of related binuclear complexes which do not contain bridging anionic ligands, since a previous comparison of $[Ir_2(CO)_2(\mu\text{-}Cl)(DPM)_2]^+$ (**1**) and its neutral precursor, *trans*-$[IrCl(CO)(DPM)]_2$, had shown rather dramatic differences[6] which proved useful in establishing the involvement of the bridging halide ligand in **1**.

Experimental Section

General experimental conditions are as described in Chapter 2. The compounds, $[Ir_2(CO)_2(\mu\text{-}Cl)(DPM)_2][BF_4]$,[8] $[Ir_2(CO)_2(\mu\text{-}S)(DPM)_2]$,[5] $[RhCl(CO)_2]_2$,[10] and $[Ir(DPM)_2(CO)][Cl]$,[11] were prepared by the reported procedures. The preparations of $[RhIrCl_2(CO)_2(DPM)_2]$, $[RhIr(CO)_2(\mu\text{-}Cl)(DPM)_2][BF_4]$ and $[RhIr(CO)_2(\mu\text{-}S)(DPM)_2]$ were reported in Chapter 3, whereas those of $[Ir_2I_2(CO)(\mu\text{-}CO)(DPM)_2]$ and $[Ir_2(CO)_2(\mu\text{-}I)(DPM)_2][BF_4]$ appear in Chapter 2. The NMR spectra (^1H, $^1H\{^{31}P\}$, $^{31}P\{^1H\}$) were run on a Bruker WH-400 spectrometer. Spin-saturation-transfer experiments were conducted using a Bruker WH-200 NMR spectrometer. Analyses were not obtained for the hydrides reported here due to facile H_2 loss in most cases.

H/D Exchange Promoted by Compounds 1 and 5c.

Approximately 5 mg of sample was placed in an NMR tube under

N_2 and cooled to liquid nitrogen temperature. Acetone-d_6 which had previously been saturated with H_2/D_2 (1:1) was transferred into this tube and the sample placed under *ca.* 600 torr of H_2/D_2 (1:1 v/v). The NMR tube was flame sealed and the exchange was followed by warming to room temperature and monitoring the H_2 and HD resonances at δ 4.5 in the ^1H NMR spectrum using the Bruker WH-400 spectrometer.

Preparation of Compounds

(a) $[Ir_2(H)_4Cl(CO)_2(DPM)_2][BF_4]$ (Isomers **3a** and **3b**).

An atmosphere of hydrogen was placed over a solution of $[Ir_2(CO)_2(\mu\text{-}Cl)(DPM)_2][BF_4]$ (**1**) (50.0 mg, 0.0376 mmol) in 5 mL of CH_2Cl_2 causing an immediate color change from dark red to pale yellow. The solution was stirred for an additional 15 min and was taken to dryness under a rapid flow of hydrogen, leaving a pale yellow powder. The $^{31}P\{^1H\}$ NMR and ^1H NMR spectra indicated the presence of two species **3a** and **3b** (established as tetrahydrides based on integration of the ^1H resonances) in an approximate 5:1 ratio, respectively. Spectroscopic data for these and all subsequent compounds are given in Table 5.1.

(b) $[RhIr(H)_2(CO)_2(\mu\text{-}Cl)(DPM)_2][BF_4]$ (**8a**).

An atmosphere of hydrogen was placed over a solution of $[RhIr(CO)_2(\mu\text{-}Cl)(DPM)_2][BF_4]$ (**6**) (50.0 mg, 0.0403 mmol) in 8 mL of CH_2Cl_2, causing an immediate color change from orange to yellow-orange. After stirring for 10 min a volume of 20 mL of diethyl ether was added,

Table 5.1. Spectroscopic Data for the Compounds in Chapter 5.[a]

compound	infrared(cm^{-1}) solid[c]	infrared(cm^{-1}) solution[d]	NMR[b] $^{31}P\{^1H\}$ δ[e]	NMR[b] ^1H δ
$[Ir_2(H)_4Cl(CO)_2(DPM)_2][BF_4]$ (3a & 3b)	2059(vs),2022(vs), 1957(med)[f] 2213(w),2130(med)[g]	2071(vs),2036(st), 1965(st)[f] 2146(br, med)[g]	a. -8.83(m) b. -6.58(s)	a. 5.14(m, 2H), 4.85(m, 2H), -10.12(br, 1H), -13.86(br, 1H), -14.75(br, 1H), -16.52(br, 1H)[h], b. 5.78(m, 2H), 3.87(m, 2H), -10.70(br, 2H), -12.88(br, 2H)[h]
$[Ir_2(H)_2(CO)_2(\mu\text{-}S)(DPM)_2]$ (5a)		2012(st),1915(vs)	-4.0(s) (0.9(m),-8.9(m))	5.53(m, 2H), 2.76(m, 2H) -10.46(quintet, 2H, $^2J_{P\text{-}H}$=5.6 Hz) (-10.5(br,1H),-11.3(br,1H))[i]
$[Ir_2(H)_2(CO)_2(\mu\text{-}S)(DPM)_2]$ (5b)		1987(st),1918(sh)	-6.8(m) -13.2(m)	5.31(m, 2H), 3.04(m, 2H) -10.07(t, 1H, $^2J_{P\text{-}H}$=14 Hz) -11.68(t, 1H, $^2J_{P\text{-}H}$=11 Hz)
$[Ir_2(H)_2(CO)_2(\mu\text{-}S)(DPM)_2]$ (5c)	1956(st),1926(st)	1961(vs), 1932 (st)	-8.5(s)	4.82(m, 2H), 2.82(m, 2H) -10.18(m, 2H)
$[RhIr(H)_2(CO)_2(\mu\text{-}Cl)(DPM)_2][BF_4]$ (8a)	2058(st), 2048(st), 1955(vs,br)[f] 2242(w),2215(w)[g]	2070(st), 1973(vs,br)[f] 2225(w)[g]	23.14(dm, $^1J_{Rh\text{-}P}$=109.3 Hz) -7.14(m)	7.0-7.8(m, 40H), 4.29(m,2H), 3.76(m, 2H), -8.62(m, 1H), -17.86(t, 1H, $^2J_{P\text{-}H}$=11.0 Hz)[j]
$[RhIr(H)_2(CO)_2(\mu\text{-}Cl)(DPM)_2][Cl]$ (8b)	2056(st),1980(med), 1946(vs,br)[f] 2245(w),2222(w)[g]	2069(st),1973(vs,br)[f] 2223(w)[g]	23.36(dm, $^1J_{Rh\text{-}P}$=109.2 Hz) -6.96(m)	7.0-7.8 (m, 40H), 4.26(m, 2H), 3.92(m, 2H), -8.62(m, 1H), -17.86(t, 1H, $^2J_{P\text{-}H}$ = 11.0 Hz)[j]

Table 5.1. (Continued)

compound	infrared(cm^{-1}) solid[c]	infrared(cm^{-1}) solution[d]	NMR[b] $^{31}P\{^1H\}$ δ[e]	NMR[b] ^1H δ
$[RhIr(H)_2(CO)_2(\mu\text{-}S)(DPM)_2]$ (9)		2019(st),1924(vs,br)[f]	21.32(dm, $^1J_{Rh\text{-}P}$=151.4 Hz) -4.31(m)	6.7-8.1 (m, 40H), 5.17(m, 2H), 2.90(m, 2H),-9.10(m,1H, $^1J_{Rh\text{-}H}$ = 12.5 Hz) -11.85(t, 1H, $^2J_{P\text{-}H}$ = 12.8 Hz)
$[Ir_2(H)_2(CO)_2(\mu\text{-}I)(DPM)_2][BF_4]$ (11a)	1937(vs)[f]	1942(st)[f]	-8.93(s)	4.96(m, 2H), 4.48(m, 2H), -13.18(quintet, 2H, $^2J_{P\text{-}H}$ = 6.4 Hz)
$[Ir_2(H)_2(CO)_2(\mu\text{-}I)(DPM)_2][I]$ (11b)	1955(vs)[f]	1960(vs,br)[f]	-9.13(s)	4.94(m, 2H), 4.45(m, 2H), -13.26(quintet, 2H, $^2J_{P\text{-}H}$ = 6.4 Hz)[j]
$[Ir_2(H)_4(CO)_2(\mu\text{-}I)(DPM)_2][BF_4]$ (12)		2034(vs),1779(st)[f] 2124(w)[g]	-6.42(s)	7.0-8.0(m, 40H), 6.52(br, 2H), 4.58(br, 2H), -10.62(br, 2H), -13.16(br, 2H)[h]
$[Ir_2(H)_2I_2(CO)_2(DPM)_2]$ (15)	2002(vs),1982(st)[f] 2230(w),2105(w)[g]	2071(vs),2010(vs)[f] 2220(w),2112(w)[g]	-11.19(m), -14.82(m)	5.70(m, 2H), 5.20(m, 2H), -8.90(t, 1H, $^2J_{P\text{-}H}$ = 13.0 Hz), -13.59(t, 1H, $^2J_{P\text{-}H}$ = 8.8 Hz)[j]

[a] Abbreviations used: st = strong, vs = very strong, med = medium, w = weak, s = singlet, m = multiplet, dm = doublet of multiplets, br = broad, t = triplet. [b] CD_2Cl_2 solution except compounds 5a-5c (benzene-d_6) and 11a and 12 (THF-d-$_8$). [c] Nujol mull. [d] CH_2Cl_2 solution except compounds 5a-5c(acetone) and 11a and 12 (THF). [e] Vs 85% H_3PO_4. [f] ν(CO). [g] ν(M-H). [h] -80C. [i] acetone-d_6, -90 °C. [j] -40C.

precipitating a light yellow solid. The solvent was removed, and the solid dried under rapid flow of hydrogen. Isolated yields were approximately 95%. Compound **8a** was determined to be a 1:1 electrolyte in CH_2Cl_2 solutions (Λ_m = 58.0 $\Omega^{-1}cm^2mol^{-1}$).

(c) $[RhIr(H)_2(CO)_2(\mu\text{-}S)(DPM)_2]$ (**9**).

An atmosphere of hydrogen was placed over a solution of $[RhIr(CO)_2(\mu\text{-}S)(DPM)_2]$ (**7**) (20.0 mg, 0.0174 mmol) in 3 mL of CH_2Cl_2. Over a period of 5 to 10 min the color of the solution changed from red to orange. Addition of 10 mL of diethyl ether caused precipitation of a flocculent yellow-brown solid which proved susceptible to decomposition except under a hydrogen atmosphere. For this reason only solution characteristics were obtained for compound **9**.

(d) $[Ir_2(H)_4(CO)_2(\mu\text{-}I)(DPM)_2][BF_4]$ (**12**).

A sample of $[Ir_2(CO)_2(\mu\text{-}I)(DPM)_2][BF_4]$ (10.0 mg, 0.00703 mmol) was dissolved in THF-d_8 in an NMR tube under dinitrogen. Hydrogen was introduced causing an immediate color change from dark orange to yellow. $^{31}P\{^1H\}$ and ^1H NMR spectra, recorded within 10 min of H_2 addition indicated the formation of a single tetrahydride species. Compound **12** was not obtained in solid form due to facile H_2 and HI loss.

(e) $[Ir_2(H)_2(CO)_2(\mu\text{-}I)(DPM)_2][BF_4]$ (**11a**).

Removing the hydrogen atmosphere from the sample of **12**, prepared as in (d), replacing it with dinitrogen, and warming slightly led to

immediate formation of a dihydride species, **11a**, as monitored by $^{31}P\{^1H\}$ and ^1H NMR spectroscopy. Variable amounts of $[Ir_2H(CO)_2(\mu\text{-}H)_2(DPM)_2][BF_4]$, resulting from HI loss from **12**, were also detected by NMR (identified by comparison of the $^{31}P\{^1H\}$ and ^1H NMR spectra with those of an authentic sample[11]) and caused a slight color change from yellow to orange-yellow.

(f) $[RhIr(H)_2(CO)_2(\mu\text{-}Cl)(DPM)_2][Cl]$ (**8b**).

Compound **8b** was prepared by the same method as in (b) for compound **8a**, except that $[RhIrCl_2(CO)_2(DPM)_2]$ (**13**) was used instead of $[RhIr(CO)_2(\mu\text{-}Cl)(DPM)_2][BF_4]$ (**6**). Isolated yield: 95%. Compound **8b** was determined to be a 1:1 electrolyte in CH_2Cl_2 solutions (Λ_m = 44.0 $\Omega^{-1}cm^2$ mol^{-1}).

(g) $[Ir_2(H)_2I_2(CO)_2(DPM)_2]$ (**14**).

Approximately 20 mg of $[Ir_2I_2(CO)(\mu\text{-}CO)(DPM)_2]$ was dissolved in CD_2Cl_2 in an NMR tube under dinitrogen. Hydrogen was introduced, causing the solution to immediately change color from orange to yellow. $^{31}P\{^1H\}$ and ^1H NMR spectra revealed the formation of two dihydride species in a 7:3 ratio. The minor product was identified as $[Ir_2(H)_2(CO)_2(\mu\text{-}I)(DPM)_2][I]$ (**11b**) by comparison of its spectral parameters to that of $[Ir_2(H)_2(CO)_2(\mu\text{-}I)(DPM)_2][BF_4]$ (**11a**). The products were precipitated by the addition of 10 mL of hexanes yielding a yellow powder which proved susceptible to facile H_2 loss unless kept under a hydrogen atmosphere.

Reaction of $[Ir_2(CO)_2(\mu\text{-}S)(DPM)_2]$ (4) with Dihydrogen

The reactions were typically done by suspending 100 mg of compound 1 in approximately 5 mL of solvent under N_2 with stirring. The N_2 atmosphere was displaced by H_2 causing the mixture to turn from dark purple to a light yellow solution almost immediately. Three products were observed with time in the ^1H and $^{31}P\{^1H\}$ NMR spectra, the last of which could be isolated in the solid by precipitation with hexanes; however this solid decomposed rapidly on exposure to air.

X-ray Data Collection

Crystals of $[RhIr(H)_2(CO)_2(\mu\text{-}Cl)(DPM)_2][BF_4]\cdot CH_2Cl_2$ were obtained by slow diffusion of diethyl ether into a saturated CH_2Cl_2 solution of the compound. A suitable crystal was wedged into a capillary tube which was flame-sealed as a precaution against loss of solvent of crystallization. Data were collected on an Enraf-Nonius CAD4 diffractometer at 22 °C using graphite-monochromated MoKα radiation. Unit cell parameters were obtained from a least-squares refinement of the setting angles of 25 reflections in the range $20.0° \leq 2\theta \leq 23.7°$. Automatic peak search and reflection indexing programs established a triclinic crystal system. This system and the lack of systematic absences were consistent with the space groups P1 or $P\bar{1}$; the centrosymmetric space group was chosen and was later verified by successful refinement of the structure.

Intensity data were collected on the CAD4 diffractometer as discussed in Chapter 2. The mean decrease in the intensities of the three

standard reflections was 5.1% and a correction was applied to the data assuming linear decay. Data reduction and absorption corrections were applied as described in Chapter 2. See Table 5.2 for crystal data and details of intensity collection.

Structure Solution and Refinement

The structure was solved in the space group $P\bar{1}$ using Patterson techniques to locate the metal atoms and by successive least-squares and difference Fourier calculations to obtain the other atom positions. All hydrogen atoms were located; the methylene and phenyl protons were placed in their idealized positions by using C-H distances of 0.95 Å whereas those bound to Ir were placed in positions obtained from difference Fourier maps since attempts to refine these atoms failed. The thermal parameters of the iridium-bound hydrogens were fixed at 4.0 $Å^2$ whereas all others were input as 1.2 times the thermal parameter of the attached carbon atom. The BF_4^- anion was badly disordered, displaying only three well defined (although smeared out) maxima in the difference Fourier maps. It appeared that the boron and one fluorine atom were disordered on each side of the plane defined by the three fluorines, so they were input as such. Attempts to refine these two disordered atoms failed, presumably because of the large amount of residual electron density in the vicinity, so these atoms were input and fixed in subsequent refinements, with two half-occupancy fluorine positions and only one boron position.

Table 5.2. Summary of Crystal Data and Details of Intensity Collection

cmpd	$[RhIr(H)_2(CO)_2(\mu\text{-}Cl)(DPM)_2][BF_4]\cdot CH_2Cl_2$
formula	$IrRhCl_3P_4F_4C_{53}BH_{48}$
fw	1286.32
crystal shape	triclinic prism
crystal size, mm	0.484 × 0.375 × 0.315
space group	$P\bar{1}$ (No. 2)
cell parameters	
a, Å	14.171(2)
b, Å	22.638(3)
c, Å	9.642(2)
α, deg	94.18(1)
β, deg	107.38(2)
γ, deg	105.84(1)
V, Å^3	2799.4
Z	2
ρ(calcd), g cm^{-3}	1.578
temp, °C	22
radiation (λ, Å)	graphite monochromated MoKα (0.71069)
receiving aperture, mm	3.00 + (tan θ) wide , 4.00 high, 173 from crystal
scan speed, deg/min	variable between 1.10 and 6.67

Table 5.2 (continued)

scan width, deg	0.50 + (0.347 tan θ) in θ
no. of indep. reflections	9812 (h, ±k, ±l)
no. of observed reflections ($F_o^2 > 3\sigma(F_o^2)$)	7935
linear absorption coeff, μ, cm^{-1}	29.63
range of transmission factors	0.812-1.251
final no. of parameters refined	364
error in observation of unit wt	2.734
R	0.053
R_w	0.081

Refinement was carried out by full-matrix least-squares methods[12] as described in Chapter 2.The final positional and isotropic thermal parameters for the non-hydrogen atoms are given in Table 5.3. Refinement in the space group $P\bar{1}$ converged at R = 0.053 and R_w = 0.081.

Results and Discussion

(a) A-Frame Complexes

It was previously shown[1] that the A-frame complex $[Ir_2(CO)_2(\mu\text{-}Cl)(DPM)_2]^+$ (**1**) reacts readily with H_2 giving first the dihydride $[Ir_2(H)_2(CO)_2(\mu\text{-}Cl)(DPM)_2]^+$ (**2**), which subsequently reversibly adds another equivalent of H_2 to give a tetrahydride species, $[Ir_2(H)_4Cl(CO)_2(DPM)_2]^+$ (**3**). Although only one tetrahydride product was originally observed and reported, subsequent studies (reported herein) indicate that two isomers of **3** are in fact produced. Before discussing the natures and origins of these tetrahydride isomers, however, it is instructive to first consider the dihydride **2** and the facile hydride rearrangements that occur in this and related A-frame dihydrides.

In the initial report,[6] the structure shown earlier for **2** was proposed, in which the hydrido ligands were not adjacent, but instead were located cis to the bridging chloride ligand, one on each metal. Although this is not a structure expected from concerted oxidative addition of H_2 at one Ir center, it is the only dihydride observed, forming essentially instantaneously upon reaction of **1** with H_2. This proposed structure was based on the reluctance of **2** to lose H_2, implying that the hydride ligands were not

Table 5.3. Positional Parameters and Isotropic Thermal Parameters.[a]

Atom	x	y	z	B(Å²)
Ir	0.19224(2)	0.32121(2)	0.09488(4)	2.667(7)
Rh	0.10502(5)	0.17897(3)	0.05200(7)	2.79(1)
Cl(1)	0.2028(2)	0.2414(1)	-0.0886(2)	3.41(5)
Cl(2)[b]	0.3056(5)	0.5594(3)	0.2346(7)	13.9(2)
Cl(3)[b]	0.1866(5)	0.4864(4)	0.3841(8)	14.7(3)
P(1)	0.0294(2)	0.3207(1)	-0.0544(3)	3.06(5)
P(2)	-0.0459(2)	0.1779(1)	-0.1287(3)	3.10(5)
P(3)	0.3434(2)	0.3163(1)	0.2685(2)	2.76(5)
P(4)	0.2619(2)	0.1733(1)	0.2078(3)	2.93(5)
F(1)	0.6223(6)	0.2604(7)	0.350(1)	19.8(4)
F(2)	0.7715(7)	0.2646(5)	0.524(1)	19.8(3)
F(3)	0.633(1)	0.2478(6)	0.556(1)	24.7(5)
F(4)	0.666	0.177	0.430	25.0*
F(5)	0.740	0.322	0.433	25.0*
O(1)	0.3055(6)	0.4357(3)	-0.0051(8)	5.6(2)
O(2)	-0.0076(6)	0.0661(4)	0.1369(9)	5.9(2)
C(1)	0.02651(7)	0.3931(4)	0.028(1)	3.6(2)
C(2)	0.0358(7)	0.1101(5)	0.105(1)	4.0(2)
C(3)	-0.0329(7)	0.2528(4)	-0.197(1)	3.5(2)
C(4)	0.3703(6)	0.2436(4)	0.234(1)	3.3(2)
C(5)[b]	0.235(3)	0.565(1)	0.381(2)	20.(1)
C(11)	-0.0649(7)	0.3248(5)	0.033(1)	3.7(2)*
C(12)	-0.0443(8)	0.3283(5)	0.185(1)	4.6(2)*
C(13)	-0.1182(9)	0.3291(6)	0.252(1)	5.7(3)*
C(14)	-0.2149(9)	0.3269(6)	0.163(1)	5.9(3)*
C(15)	-0.2393(9)	0.3227(6)	0.016(1)	5.9(3)*
C(16)	-0.1656(8)	0.3214(5)	-0.052(1)	4.7(2)*
C(21)	0.0372(7)	0.3865(4)	-0.155(1)	3.5(2)*

Table 5.3. (Continued)

C(22)	0.663(8)	0.4452(5)	-0.078(1)	4.9(2)*
C(23)	0.0858(9)	0.4966(6)	-0.141(1)	5.3(3)*
C(24)	0.077(1)	0.4910(6)	-0.287(1)	6.1(3)*
C(25)	0.052(1)	0.4325(7)	-0.364(2)	7.3(3)*
C(26)	0.0304(9)	0.3794(6)	-0.301(1)	5.4(3)*
C(31)	-0.1659(8)	0.1642(5)	-0.083(1)	4.1(2)*
C(32)	-0.1616(8)	0.1705(5)	0.060(1)	5.0(2)*
C(33)	-0.254(1)	0.1662(7)	0.090(1)	6.6(3)*
C(34)	-0.342(1)	0.1535(8)	-0.016(2)	8.3(4)*
C(35)	-0.351(1)	0.1475(8)	-0.157(2)	9.0(5)*
C(36)	-0.259(1)	0.1527(7)	-0.193(2)	7.0(3)*
C(41)	-0.0781(7)	0.1212(4)	-0.294(1)	3.6(2)*
C(42)	-0.0692(9)	0.0642(6)	-0.280(1)	5.5(3)*
C(43)	-0.092(1)	0.0201(6)	-0.403(1)	6.4(3)*
C(44)	-0.124(1)	0.0326(6)	-0.540(1)	6.5(3)*
C(45)	-0.135(1)	0.0889(7)	-0.563(2)	7.0(3)*
C(46)	-0.112(1)	0.1340(6)	-0.435(1)	6.3(3)*
C(51)	0.3524(6)	0.3240(4)	0.4604(9)	3.1(2)*
C(52)	0.2742(8)	0.3354(5)	0.507(1)	4.3(2)*
C(53)	0.2850(9)	0.3419(6)	0.657(1)	5.1(2)*
C(54)	0.3703(9)	0.3373(6)	0.756(1)	5.3(3)*
C(55)	0.445(1)	0.3254(6)	0.712(1)	6.3(3)*
C(56)	0.4395(8)	0.3196(5)	0.565(1)	5.0(2)*
C(61)	0.4575(6)	0.3773(4)	0.268(1)	3.2(2)*
C(62)	0.5240(8)	0.3682(5)	0.198(1)	4.8(2)*
C(63)	0.600(1)	0.4190(6)	0.182(1)	6.1(3)*
C(64)	0.6124(9)	0.4770(6)	0.244(1)	5.9(3)*
C(65)	0.5439(9)	0.4889(6)	0.313(1)	5.6(3)*
C(66)	0.4684(8)	0.4383(5)	0.325(1)	4.9(2)*
C(71)	0.2671(7)	0.1614(4)	0.393(1)	3.5(2)*
C(72)	0.1862(8)	0.1658(5)	0.443(1)	4.6(2)*

Table 5.3. (Continued)

C(73)	0.1893(9)	0.1553(6)	0.587(1)	5.9(3)*
C(74)	0.269(1)	0.1394(6)	0.678(1)	6.2(3)*
C(75)	0.345(1)	0.1327(7)	0.632(2)	7.3(4)*
C(76)	0.349(1)	0.1447(7)	0.486(2)	6.8(3)*
C(81)	0.3045(7)	0.1130(4)	0.136(1)	3.6(2)*
C(82)	0.235(1)	0.0596(7)	0.051(2)	7.1(3)*
C(83)	0.265(1)	0.0098(8)	0.000(2)	8.4(4)*
C(84)	0.360(1)	0.0176(7)	0.016(2)	7.8(4)*
C(85)	0.438(2)	0.073(1)	0.100(2)	10.9(6)*
C(86)	0.410(1)	0.1211(8)	0.161(2)	8.5(4)*
B	0.692	0.275	0.462	25.0*

[a] Estimated standard deviations in this and subsequent tables are given in parentheses and correspond to the least significant digit. Starred atoms were refined isotropically. Anisotropically refined atoms are given in the form of the isotropic equivalent displacement parameter defined as: (4/3) [$a^2\beta(1,1) + b^2\beta(2,2) + c^2\beta(3,3) + ab(\cos \text{gamma})\ \beta(1,2) + ac(\cos \text{beta})\ \beta(1,3) + bc(\cos \text{alpha})\ \beta(2,3)$].

[b] Atoms Cl(2), Cl(3) and C(5) are those of the CH_2Cl_2 solvent molecule.

mutually adjacent, and on the subsequent reaction of this species with alkyne to yield $[Ir_2(RC{=}C(H)R)_2(CO)_2(\mu\text{-}Cl)(DPM)_2]^+$ ($R = CO_2Me$). The structure determination of the neutral dichloride, obtained by Cl^- addition to this product, confirmed that the metalloolefin moieties were located on the outsides of the complex exactly as proposed for the hydrido ligands in the precursor, compound **2**.[6]

Reaction of the related sulfide-bridged A-frame, $[Ir_2(CO)_2(\mu\text{-}S)(DPM)_2]$ (**4**), with H_2 was also reported to yield a dihydride species [5] having a structure like that of **2**. However, the report of additional, poorly characterized species, which appeared to be intermediates in the reaction, suggested that a reinvestigation of this reaction was warranted. It was also of interest to establish whether the sulfide-bridged complex also yielded tetrahydrides as was the case in the chloride-bridged species.

Initially the reaction of $[Ir_2(CO)_2(\mu\text{-}S)(DPM)_2]$ (**4**) with hydrogen was studied in benzene, although the results are almost identical in toluene or THF and are similar in acetone and CH_2Cl_2. Upon addition of hydrogen, reaction occurs almost immediately as indicated by a change in color of the solution from purple to yellow. The complex initially formed (**5a**) is identified by its $^{31}P\{^1H\}$ and ^1H NMR and IR spectra (see Table 5.1). The $^{31}P\{^1H\}$ NMR spectrum shows a singlet at δ -4.0, indicating a symmetrical species in which all four phosphorus nuclei are chemically equivalent. At the same time the ^1H NMR spectrum of **5a** displays the DPM-methylene resonances at δ 2.76 and 5.53, and a quintet for the hydride resonance at δ -10.50 ($^2J_{P\text{-}H}$ = 5.6 Hz). All three resonances integrate as two protons each, establishing **5a** as a dihydride species in which the hydride ligands are

coupled to four equivalent phosphorus nuclei. The IR spectrum shows two strong bands for the terminal carbonyl ligands (1915, 2012 cm^{-1}) but nothing attributable to an Ir-H stretch. This assignment is confirmed by an almost indistinguishable IR spectrum of the corresponding deuteride, obtained upon reaction of **4** with D_2.

Further reaction for 2 h yields two additional species. One of these species, (**5b**), is present in trace amounts at this stage and displays two multiplets in the $^{31}P\{^1H\}$ NMR spectrum at δ -6.8 and -13.2 and also shows two new hydride resonances (each a triplet) in the ^1H NMR spectrum, at δ -10.10 and -11.70, together with the methylene resonances at δ 5.31, 3.04; again integration indicates that this species, which had not been observed in the previous study,[5] is a dihydride. The $^{31}P\{^1H\}$ NMR results indicate that this species is unsymmetrical, having two chemically different phosphorus environments, and the ^1H NMR parameters indicate that the two hydride ligands are also inequivalent, with each displaying coupling to two phosphorus nuclei. In addition, selective decoupling of each phosphorus resonance of **5b** causes each triplet in the ^1H NMR spectrum to collapse in turn to a singlet, thereby unambiguously establishing that each hydride ligand is coordinated to a different metal.

Also observed together with **5b** is compound **5c**, which after 2 h is present as approximately one tenth the concentration of the initial product **5a**. Complex **5c** is characterized by a singlet in the $^{31}P\{^1H\}$ NMR spectrum, indicating a symmetrical species, and resonances in the ^1H NMR spectrum due to the methylene groups (δ 4.82, 2.82) and two hydride ligands (δ -10.18). Although the hydride resonance was previously identified[5] as a

triplet of triplets in a poorer resolution spectrum, a close inspection of the current spectrum (at 400 MHz) shows that it is a second order pattern in which the second and fourth lines of the pseudo-quintet are broader than the outer and the central lines, having widths at half-height of 8.4 and 3.5 Hz, respectively (see insert in Figure 5.1 for an enlargement of this resonance). This spectrum is invariant with temperature over the range 25 to -80 °C (THF), and has been successfully simulated based on an AA'XX'X''X''' spin system with $^{2}J_{P\text{-}H}$ = 13.4 Hz, $^{3}J_{P\text{-}H}$ =2.4 Hz and $^{3}J_{H\text{-}H}$ = 13.5 Hz. Although the value of $^{3}J_{H\text{-}H}$ appears, at first glance, to be unusually large for 3-bond coupling, it is proposed that effective transmission of coupling through the Ir-Ir bond occurs. In a series of related platinum hydride complexes, $[Pt_2HL(DPM)_2]^+$ (L = phosphine), the three-bond coupling ($J_{H\text{-}Pt\text{-}Pt\text{-}L}$) between the axial H and L groups, which are opposite the Pt-Pt bond, was found to be 3-4 times that of the two-bond coupling between the hydride and the adjacent phosphorus nuclei of the DPM ligands.[13] The hydride-hydride coupling in the present system might also be expected to be large if the H-Ir-Ir-H linkage were also close to being linear.

With time, the concentrations of **5b** and **5c** increase at approximately the same rate at the expense of **2** yielding ratios of the three species **5a**:**5b**:**5c** of *ca.* 15:1:3 after 6 h and *ca.* 2:3:3 after 24 h. After several days under H_2 only compound **5c** remains. Figure 5.1 shows the $^{31}P\{^{1}H\}$ and the ^{1}H NMR spectra of a mixture of all three isomers after approximately 30 h under H_2. Selective phosphorus decoupling unambiguously allows correlation of the species in the ^{1}H and the $^{31}P\{^{1}H\}$ NMR spectra.

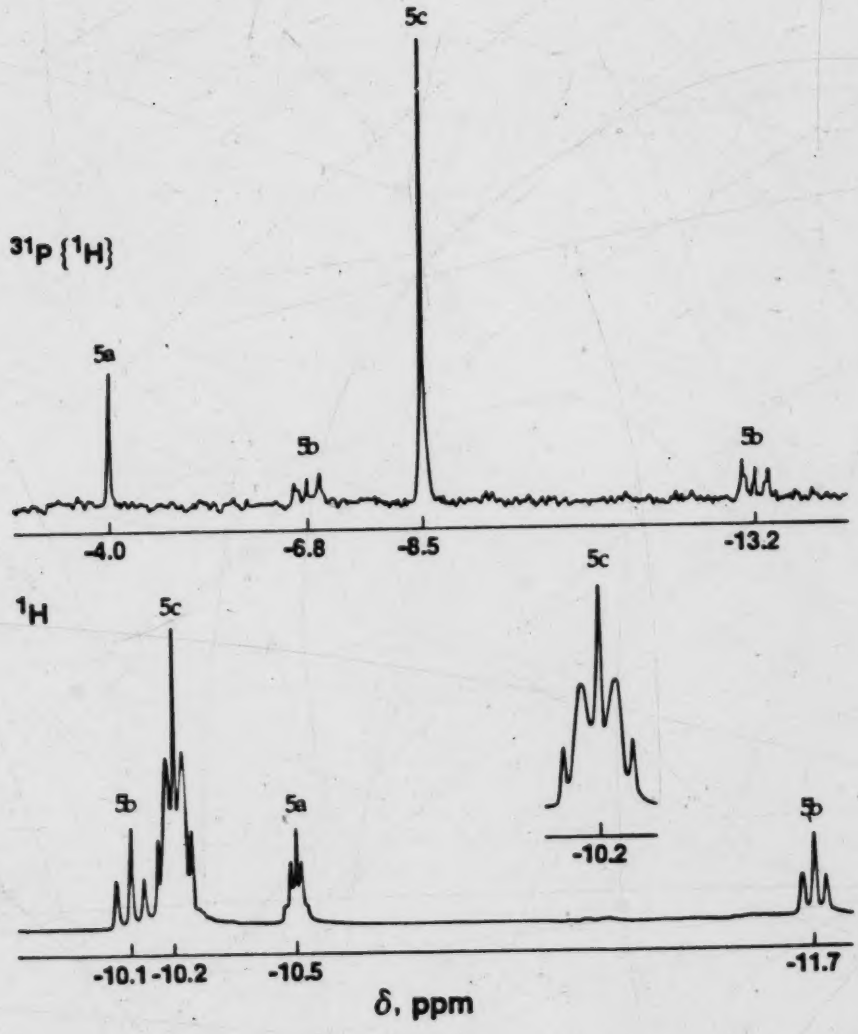

Figure 5.1. The $^{31}P\{^{1}H\}$ NMR (top) and the corresponding hydride region of the ^{1}H NMR spectrum of compound **4** under H_2 showing the three products. An enlargement of the hydride resonance for **5c** is shown as an insert on the ^{1}H NMR spectrum.

The rate of conversion of **5a** to **5c** is enhanced by heating and is also much increased in polar solvents, occurring approximately 16 times faster in a 1:1 (v/v) mixture of nitromethane/CH_2Cl_2 than in CH_2Cl_2 alone, and at approximately the same rate by heating to 40 °C in benzene or CH_2Cl_2. The above reaction of **4** with both H_2 and with D_2 in acetone reveals no evidence, at any stage of the reaction, for Ir-H or Ir-D stretches in the IR spectra; the carbonyl regions in these spectra are essentially superimposable whether under H_2 or D_2. Failure to observe Ir-H stretches is not too surprising however, since the intensities of such stretches can be variable and these bands are often absent.[14]

In the absence of hydrogen, compound **5a** disappears immediately with the reappearance of **4**, while compounds **5b** and **5c** initially remain. Heating this solution to about 60 °C under dinitrogen causes compounds **5b** and **5c** to disappear within approximately 1 h, over which time **5b** is always in significantly lower concentration than **5c** (as monitored by $^{31}P\{^1H\}$ NMR).

Based on the information given above, and on related work involving $[Ir_2(CO)_2(\mu\text{-}Cl)(DPM)_2]^+$,[6] it is now possible to suggest the natures of these hydride species with some confidence. Compound **5a** was previously proposed to be an equilibrium mixture of species such as **A** and **B**, shown earlier. Rapid equilibration of the hydride ligands between the two metal centers would result in a quintet in the ^1H NMR, and a singlet in the $^{31}P\{^1H\}$ NMR spectrum. Upon carrying out the reaction in acetone, the fluxionality of **5a** is now confirmed by the broadening and collapse of the quintet upon cooling, and the emergence of two hydride resonances at δ

-10.5 and -11.3 at -90 °C, leading to a proposed static structure which differs from either of those initially proposed.[5] While a true low temperature

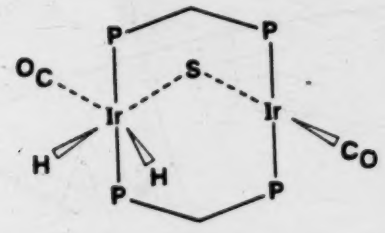

5a

limiting spectrum showing spin-spin coupling is not obtained, the spectrum at -90 °C indicates that the two hydrides are in different chemical environments and are not equivalent as in **A** and **B**. The $^{31}P\{^{1}H\}$ NMR spectrum at this temperature is also consistent with an unsymmetrical species having two chemically inequivalent iridium centers. This structure corresponds to the supposed kinetic product in the reaction of **4** with H_2, and is the result of oxidative addition of H_2 to a single metal center in the binuclear complex. Although equilibration of the two hydrido ligands in **5a** may involve structures such as **A** or **B**, proposed previously,[5] or could occur by intramolecular reductive-elimination / oxidative-addition involving **5a** and a species denoted simply as (**4** + H_2), studies which follow suggest another mechanism (*vide infra*). The I.R. spectrum of **5a**, showing one carbonyl band at 2012 cm^{-1} and the other at 1915 cm^{-1}, is also consistent with the structure above, having one Ir(III) and one Ir(I) center, respectively. The similarities in the I.R. spectra of **5a** and its deuteride are somewhat surprising, considering that the carbonyl stretching frequency in the H_2-adduct of Vaska's complex, $IrCl(CO)(PPh_3)_2$,

is 21 cm^{-1} lower than in the D_2-adduct (1982 vs. 2003 cm^{-1}).[15] This suggests that in compound **5a** neither hydrido ligand is exactly trans to the carbonyl group, such that very little vibronic coupling between the carbonyl and hydrido ligands is observed. Species analogous to **5a** have been observed in at least two cases in which transfer of one hydride ligand to the adjacent metal, with concomitant metal-metal bond formation, was somehow inhibited.[16,17]

The second species observed, **5b**, has two chemically inequivalent hydrido ligands which are on different metals, with each hydrogen showing coupling to only two phosphorus nuclei. The intermediate structure shown for **5b** (in which rearrangement at only one iridium center has taken place) is proposed. This appears to be the most logical

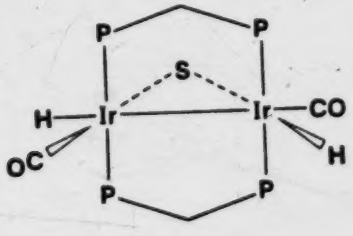

5b

structure which agrees with the spectroscopic parameters, having two chemically different hydride ligands, with one on each metal, resulting in two different phosphorus environments, yielding an AA'BB'-type $^{31}P\{^1H\}$ NMR spectrum. Furthermore a structure such as **5b** represents the intermediate species in the stepwise rearrangement of **5a** to **5c** (vide infra).This species is an Ir(II)/Ir(II) complex having resulted from the transfer of one hydrido ligand in **5a** to the adjacent metal, accompanied by rearrangement

and Ir-Ir bond formation. Such hydride transfer, yielding metals in the same oxidation state, appears to be favored in related binuclear systems in which metal-metal bond formation is not inhibited.[6,18]

It is suggested that the final species (5c) is also an Ir(II)/Ir(II) compound having the symmetric structure, C, as shown earlier, in which rearrangement at both metal centers has occurred to give a species in which the hydrido ligands are no longer adjacent but are on the outside of the complex, and probably almost colinear with the Ir-Ir bond. As noted, such a structure is supported by the ^{1}H NMR spectrum of 5c and the large coupling (13.5 Hz) between the two hydrido ligands, as derived from the NMR simulation. This structure, in which the hydrido ligands are not mutually adjacent, explains the reluctance of 5c to lose H_2 (*vide supra*), although reductive elimination appears more facile than was found for the chloride-bridged analogue.[6] Furthermore, it is worthy of note that although the hydride resonance for the chloride-bridged dihydride species was originally reported to be an unresolved triplet,[6] further studies show it to be a poorly resolved pseudoquintet, not unlike that of 5c. Species 5c appears to be the thermodynamically favoured product and as noted, rearrangement to this isomer is greatly accelerated if the solution is heated under H_2.

The proposed oxidative addition of H_2 at one metal center, followed by transfer of one hydrido ligand to the other metal and concomitant Ir-Ir bond formation is rather similar to a proposal, by Poilblanc and co-workers,[18] for H_2 addition to a binuclear thiolato-bridged complex. Furthermore, the cis-trans isomerism observed in the thiolato-bridged

species is not unlike the isomerism of **5a** to **5c** described in this work. Although Poilblanc proposed a mechanism which did not involve breaking of bonds to the bridging thiolato groups to explain the isomerization, it appears that in the present sulfide-bridged A-frame, cleavage of one Ir-S bond occurs to give a dipolar intermediate (*vide infra*).

Structures **5a-5c** are also consistent with the relative ease of H_2 loss in these species. Species **5a**, in which the hydrido ligands are adjacent and therefore appropriately placed for a concerted reductive elimination, loses H_2 quite readily. Compounds **5b** and **5c** lose H_2 more reluctantly since significant rearrangement at the metal centers to give a species such as **5a**, in which the hydrido ligands are adjacent, is required.

In an attempt to isolate and characterize a species analogous to **5a** having both hydrides associated with one metal, the closely related heterobimetallic compounds, $[RhIr(CO)_2(\mu\text{-}X)(DPM)_2]^{n+}$ (**6**: X = Cl, n = 1; **7**: X = S, n = 0), were synthesized on the assumption that oxidative addition of H_2 should be favored at the Ir center and that because of stronger Ir-H bonds compared to Rh-H,[19] the hydride ligands would remain associated with Ir.

Reaction of compounds **6** and **7** with H_2 yields the dihydrides **8a** and **9**. As anticipated, both hydride ligands have remained coordinated to the iridium center in each case, although NMR and X-ray (*vide infra*) studies indicate that one is also weakly interacting with Rh. The $^{31}P\{^1H\}$ and ^1H NMR spectra for **9**, with and without selective ^{31}P decoupling, are shown in Figure 5.2; those obtained for **8a** are very similar. The $^{31}P\{^1H\}$ NMR spectrum displays a pattern typical of the heterobinuclear rhodium-

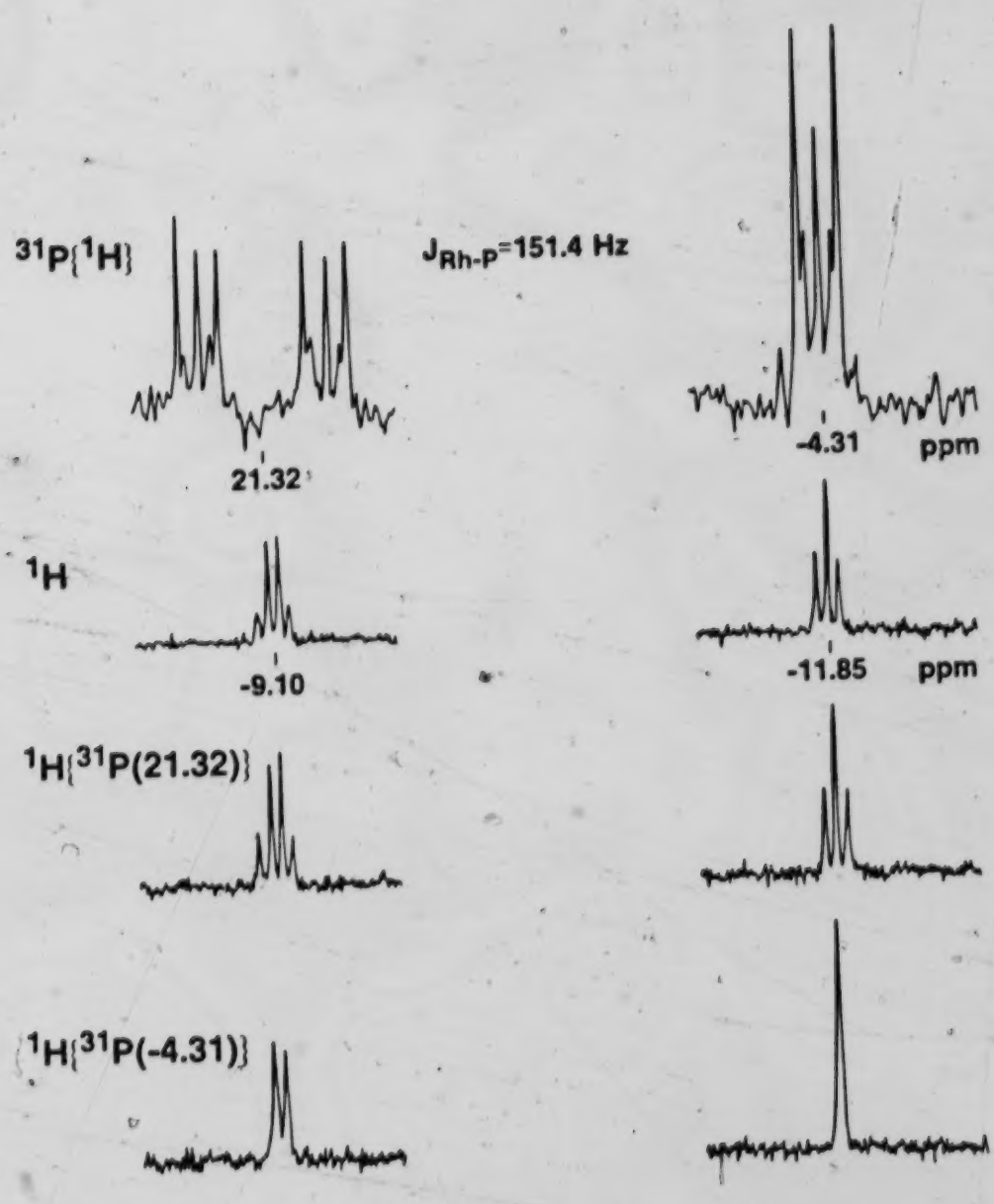

Figure 5.2. The $^{31}P\{^{1}H\}$ NMR spectrum (top) and ^{1}H NMR spectra (hydride region) of compound **9**, including selective ^{31}P decoupling of the ^{1}H NMR spectrum.

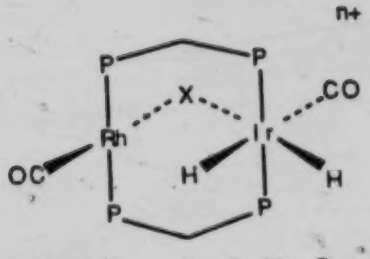

8a: X = Cl, n = 1 ; **9**: X = S, n = 0

iridium complexes; the resonance at δ -4.31 (multiplet) corresponds to the phosphorus nuclei bound to Ir, whereas that at δ 21.32 (doublet of multiplets; $^1J_{Rh\text{-}P}$ = 151.4 Hz) clearly corresponds to the rhodium-bound phosphorus nuclei. The ^1H NMR spectrum displays two high field resonances, each integrating as one hydrogen. The resonance at δ -11.85 is a triplet ($^2J_{P\text{-}H}$ = 12.8 Hz) whereas that at δ -9.10 is an apparent quartet (J = 12.5 Hz). Selective phosphorus decoupling clearly establishes the connectivities involving these hydride ligands. Decoupling the Rh-bound ^{31}P resonance gives rise to no observable change in the ^1H resonance at δ -11.85 and results in only a very slight sharpening of the resonance at δ -9.10, whereas decoupling the Ir-bound ^{31}P resonance causes the triplet ^1H resonance to collapse to a singlet and the quartet to collapse to a doublet, retaining only coupling to rhodium of 12.5 Hz. Clearly both hydride ligands are bound to Ir; however, the hydride ligand giving rise to the low field resonance is also interacting with Rh, as demonstrated by the significant coupling to this nucleus. It appears however that this hydride ligand does not display appreciable coupling to the two phosphorus nuclei on Rh. Although this seems unusual, it should be noted that in somewhat similar complexes, $[M_2(CO)_2(\mu\text{-}H)_2(DPM)_2]$, (M = Rh, Ir) the dirhodium

complex again displayed no coupling of the hydride ligands to phosphorus,[20] whereas obvious coupling ($^2J_{P-H}$ = 6.6 Hz) was observed for the diiridium analogue.[11] It is also significant that the $^1J_{Rh-H}$ value of 12.5 Hz for **9** is somewhat lower than for other bridging hydrides in binuclear species,[20,21] where values of *ca.* 20 to 25 Hz appear typical. In an analogous trinuclear complex, $[Rh_3(H)_2(CO)_2(\mu\text{-}Cl)_2((\mu\text{-}Ph_2PCH_2)_2AsPh)_2]^+$, in which the two hydride ligands are coordinated to the central rhodium while interacting weakly with the terminal ones, the coupling of the hydrides to the central metal was 24.7 Hz but only 10.9 Hz to the terminal rhodium atoms.[22] Moreover, in analogous "Ir_2Rh" and "$IrRh_2$" complexes, coupling constants (J_{Rh-H}) involving the hydride ligands and the weakly interacting Rh nuclei of between 8.7 and 14.1 Hz were reported,[23] much the same as in **8a** and **9**. The high field triplet in **9** therefore results from coupling of the terminal hydride to the two chemically equivalent phosphorus nuclei on iridium, and the apparent quartet is actually a doublet of triplets ($^1J_{Rh-H}$ = 12.5 Hz, $^2J_{P-H}$ = 12.2 Hz) due to coupling to rhodium and the two iridium-bound phosphorus nuclei. As in almost all previous examples of diphosphine-bridged A-frame hydrides of iridium, no H-H coupling is observed.[6,11] In the chloride-bridged analogue (**8a**) the spectra differ only slightly, in that small (but still unresolved) additional coupling to the rhodium phosphines is also observed.

It appears as though oxidative addition of H_2 to the iridium center at the inside or "pocket" of the A-frame occurs in both compounds **6** and **7**, followed by movement of one of the hydride ligands to a semi-bridging position. This supports the earlier proposal of an initial Ir(III)/Ir(I) species

resulting from H_2 attack at one metal center of $[Ir_2(CO)_2(\mu\text{-}S)(DPM)_2]$. The preference of the Ir site of compounds **6** and **7** to oxidatively add H_2 instead of Rh is not surprising in view of previous observations of H_2 addition to the diiridium species,[5,6] but not to the dirhodium analogues. Although the structures of compounds **8a** and **9** can be considered as either of two extremes, involving either a classical hydride bridge or independent Rh(I)/Ir(III) centers having terminal hydride ligands on iridium, the above NMR evidence suggests an intermediate structure having an unsymmetrical Ir-H-Rh bridge, not unlike agostic[24] C-H-M interactions. Such a view is consistent with a recent discussion of interactions of various X-H bonds with transition metals (X = main group or transition metal element) by Crabtree and Hamilton.[25] Furthermore, this proposal is consistent with the X-ray structure as determined for **8a**. A view of the molecule is shown in Figure 5.3. Selected bond distances and angles are given in Tables 5.4 and 5.5, respectively. As shown, both hydride ligands are coordinated to Ir to give a slightly distorted square planar Rh(I) center and an octahedral Ir(III) center. The positions shown for the hydride ligands were derived from a difference Fourier map, but since these atoms did not refine acceptably, their positions are approximate. Therefore the long Ir-H(1) distance (1.81Å), which could in principle reflect the semi-bridging nature of this ligand, may be fortuitous. In any case the positions of these hydride ligands clearly result from H_2 attack at the inside of the complex, between the metals. The Ir-C(1) distance (1.938(6)Å) which is opposite H(1) is significantly longer than the Rh-C(2) distance (1.800(6)Å), consistent with the high trans influence of a

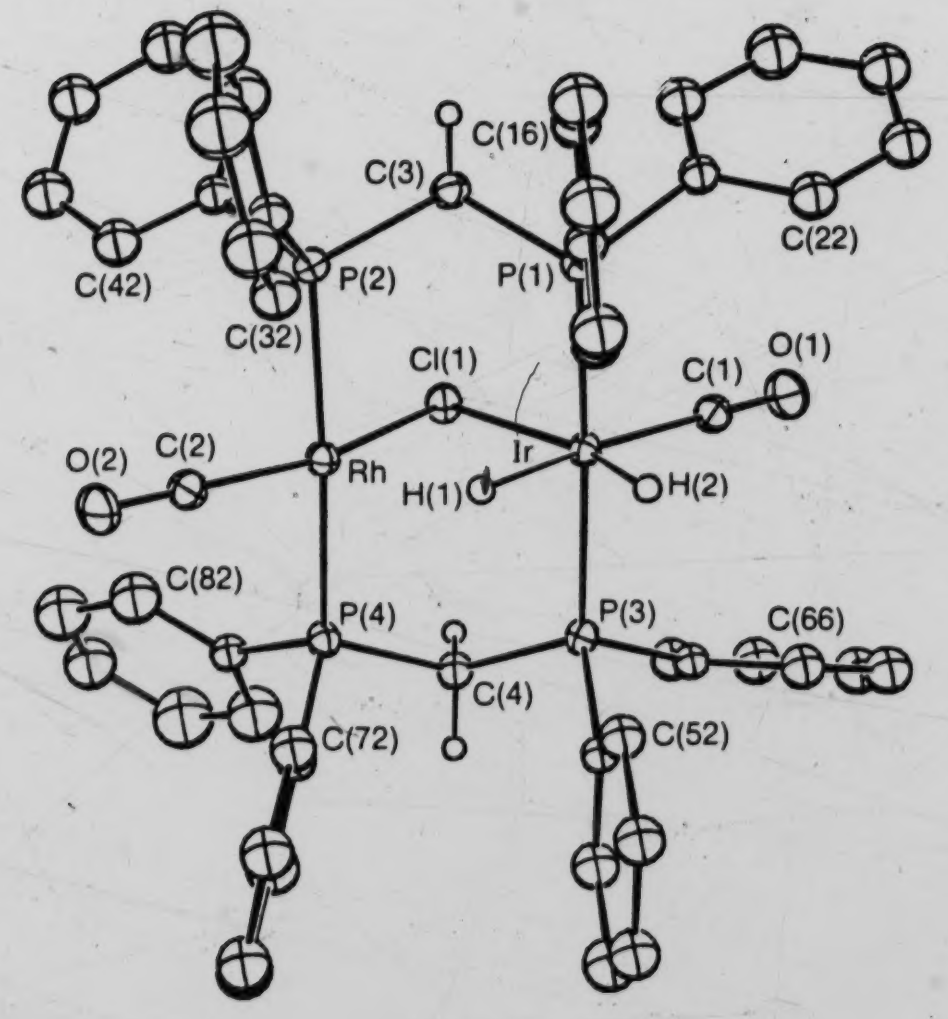

Figure 5.3. A perspective view of the $[RhIr(H)_2(CO)_2(\mu\text{-}Cl)(DPM)_2]^+$ cation showing the numbering scheme. Thermal parameters are shown at the 20% level except for hydrogens, which are artificially small for the methylene and hydride groups but are not shown for other groups.

Table 5.4. Selected Distances (Å) in $[RhIr(H)_2(CO)_2(\mu\text{-}Cl)(DPM)_2][BF_4]$

(a) Bonded

Ir-H(1)	1.81	P(1)-C(21)	1.830(6)
Ir-H(2)	1.56	P(2)-C(3)	1.846(6)
Ir-Cl(1)	2.501(1)	P(2)-C(31)	1.834(7)
Ir-P(1)	2.322(1)	P(2)-C(41)	1.828(6)
Ir-P(3)	2.328(1)	P(3)-C(4)	1.820(6)
Ir-C(1)	1.938(6)	P(3)-C(51)	1.808(6)
Rh-Cl(1)	2.468(1)	P(3)-C(61)	1.820(6)
Rh-P(2)	2.313(1)	P(4)-C(4)	1.825(6)
Rh-P(4)	2.325(1)	P(4)-C(71)	1.810(6)
Rh-C(2)	1.800(6)	P(4)-C(81)	1.806(6)
P(1)-C(3)	1.807(6)	O(1)-C(1)	1.103(7)
P(1)-C(11)	1.801(6)	O(2)-C(2)	1.134(7)

(b) Non-Bonded

Ir-Rh	3.0651(5)
P(1)-P(2)	3.070(2)
P(3)-P(4)	3.073(2)
Rh-H(1)	2.18

Table 5.5. Selected Angles (deg) in $[RhIr(H)_2(CO)_2(\mu\text{-}Cl)(DPM)_2][BF_4]$

Cl(1)-Ir-P(1)	92.55(5)	Rh-P(2)-C(41)	112.4(2)
Cl(1)-Ir-P(3)	91.18(5)	C(3)-P(2)-C(31)	102.9(3)
Cl(1)-Ir-C(1)	96.0(2)	C(3)-P(2)-C(41)	103.7(3)
P(1)-Ir-P(3)	171.67(5)	C(31)-P(2)-C(41)	105.8(3)
P(1)-Ir-C(1)	93.6(2)	Ir-P(3)-C(4)	112.7(2)
P(3)-Ir-C(1)	93.5(2)	Ir-P(3)-C(51)	118.4(2)
Cl(1)-Rh-P(2)	87.70(5)	Ir-P(3)-C(61)	111.8(2)
Cl(1)-Rh-P(4)	88.36(5)	C(4)-P(3)-C(51)	104.0(3)
Cl(1)-Rh-C(2)	157.6(2)	C(4)-P(3)-C(61)	105.3(3)
P(2)-Rh-P(4)	172.09(6)	C(51)-P(3)-C(61)	103.5(3)
P(2)-Rh-C(2)	90.7(2)	Rh-P(4)-C(4)	112.8(2)
P(4)-Rh-C(2)	90.3(2)	Rh-P(4)-C(71)	116.4(2)
Ir-Cl(1)-Rh	76.18(4)	Rh-P(4)-C(81)	113.3(2)
Ir-P(1)-C(3)	112.1(2)	C(4)-P(4)-C(71)	104.3(3)
Ir-P(1)-C(11)	117.6(2)	C(4)-P(4)-C(81)	102.9(3)
Ir-P(1)-C(21)	112.0(2)	C(71)-P(4)-C(81)	105.9(3)
C(3)-P(1)-C(11)	105.8(3)	Ir-C(1)-O(1)	176.7(6)
C(3)-P(1)-C(21)	104.4(3)	Rh-C(2)-O(2)	179.1(7)
C(11)-P(1)-C(21)	103.8(3)	P(1)-C(3)-P(2)	114.4(3)
Rh-P(2)-C(3)	111.9(2)	P(3)-C(4)-P(4)	114.9(3)
Rh-P(2)-C(31)	118.8(2)		

hydride ligand.[14] Analogous differences are also observed for the bridging chloro ligand, although in this case they are less dramatic. Around the Ir center the angles are consistent with octahedral coordination while at Rh the coordination is slightly distorted from square planar, with Rh moving inward towards H(1) slightly, resulting in Cl-Rh-C(2) and P(2)-Rh-P(4) angles of 157.6(2)° and 172.09(6)°, respectively. The resulting Rh-H(1) interaction (approximately 2.18Å) is clearly weak, but is not inconsistent with some interaction, which from the NMR study is clearly established. All parameters involved are closely comparable to the trinuclear rhodium complex alluded to earlier.[22] In particular, the Rh-H distances involving the weak interactions in this "Rh_3" species, are just more than 2.0Å and the corresponding Rh-Rh distances (2.967(1), 2.948(1)Å) are also similar to the present Rh-Ir distance of 3.0651(5)Å, although it appears that, based on the shorter distances in the trirhodium species, the weak Rh-H interactions in the trinuclear species are somewhat stronger than in compound **8a**. The Rh-Ir distance in **8a** is almost exactly equal to the intraligand P-P separations, again suggesting that the interaction between Rh and the "IrH_2" moiety is not strong. Little appears to have changed in the metal inner coordination spheres upon coordination of H_2 (based on a comparison with the structure of $[Rh_2(CO)_2(\mu\text{-}Cl)(DPM)_2][BF_4]$[26]), apart from movement of C(1)O(1) and possibly a slight compression of the Rh-Ir distance.

The infrared spectrum in solution for compound **8a** displays two terminal carbonyl bands at 2070 and 1973 cm^{-1} as well as a weak Ir-H stretch at 2225 cm^{-1}. In the sulfide-bridged analogue, **9**, the corresponding carbonyl

bands are observed at 2019 and 1924 cm^{-1} but no Ir-H stretch is obvious. As observed in the precursors (see Chapter 3), the sulfide-bridged species exhibits lower carbonyl stretching frequencies than the chloride-bridged species. The slight coupling of the bridging hydride ligand to the rhodium-bound phosphines in the chloride-bridged **8a** may suggest that in this case the interaction with rhodium is stronger than in the sulfide-bridged case. Consistent with this suggestion, reductive elimination of H_2 from **8a** occurs less readily than from **9**, requiring prolonged reflux in THF for **8a**, while only a rapid dinitrogen purge under ambient conditions is necessary to induce H_2 loss from **9**.

Based on this work, a feasible mechanism is presented for the hydride rearrangements which occur in the reactions of **1** and **4** with H_2. This is shown in Scheme 5.1. First, oxidative addition of H_2 at one metal center on the <u>inside</u> of the A-frame pocket occurs to yield the Ir(III)/Ir(I) dimer, **II**. This is the species proposed as the initial product (**5a**) observed at low temperature in the reaction of **4** with H_2. Although this adduct has not been unequivocally identified, complexes **8a** and **9** represent models of such a species and are closely related to the next product, **III**, having one hydride ligand in the bridging position. These hydride-bridged species are pivotal to our understanding of the H_2 activation and subsequent hydride rearrangement in the presence of adjacent metals. Not only do these products clearly indicate that H_2 attack occurs on the inside of the A-frame pocket, but they also model a key intermediate in the migration of the hydride ligands over the metal framework in at least two processes. Species **III** presents a possible intermediate in this migration, in which

Scheme 5.1

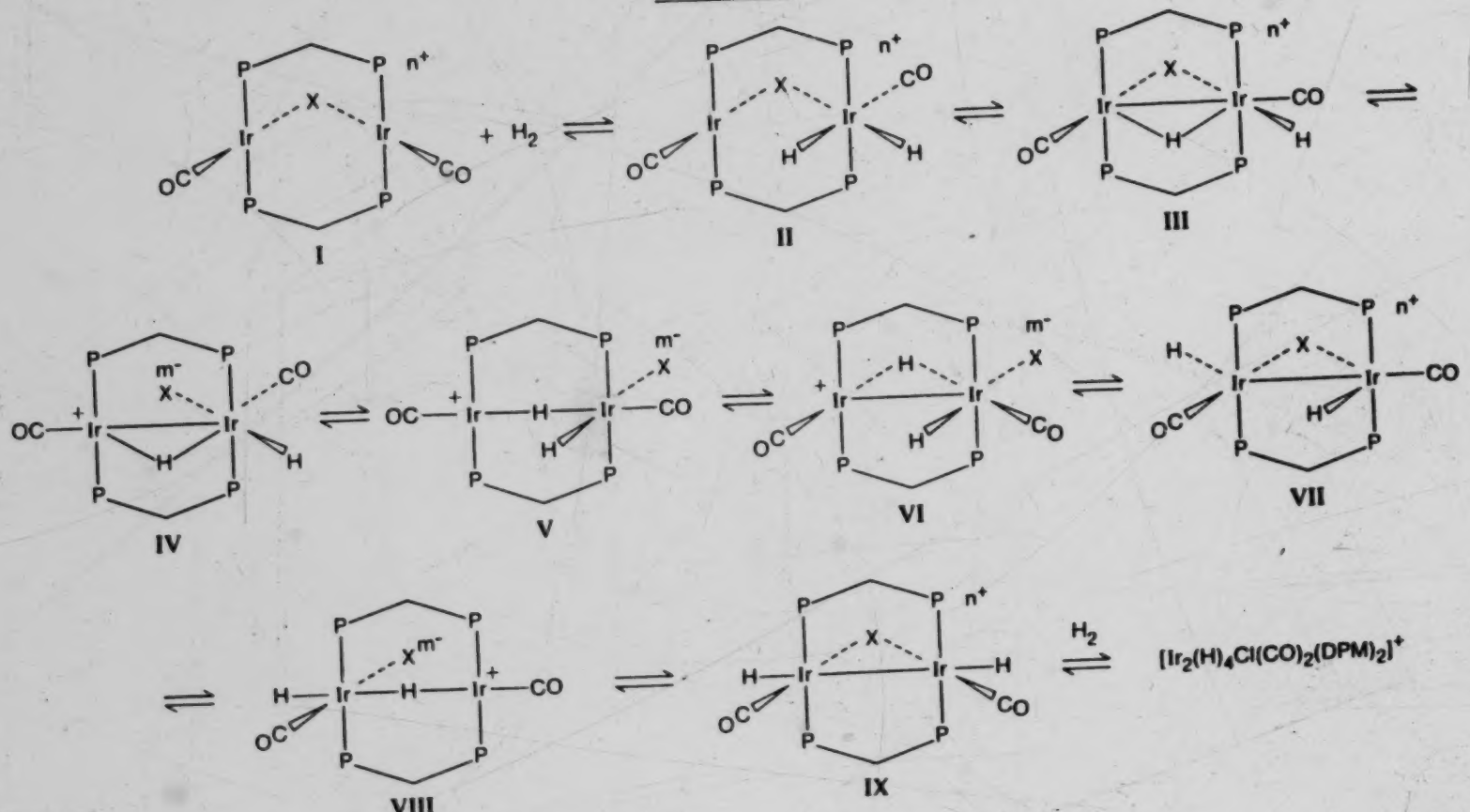

each hydride moves stepwise from one metal to another via a hydride-bridge; it is proposed that the equilibration of the hydride ligands over both metals in **5a** occurs by such a process. This intermediate is also a key species in the movement of the hydride ligands from the face of the dimer opposite the bridging X ligand (X = Cl, S), as in **II**, to that observed in the final species **IX** (complexes **2** and **5c**, respectively) in which both hydrides are adjacent to the bridging X group. It is proposed that this rearrangement also occurs stepwise, via cleavage of one of the Ir-X bonds to give intermediate **IV**. Such a bridge-breaking mechanism has been previously proposed to explain the facile reaction of **2** with alkynes.[6] This step is consistent with the much more facile rearrangement observed for the chloro-bridged dimer compared to the sulfido-bridged analogue, since the latter would involve the formation of a dipolar intermediate by heterolytic cleavage of the covalent Ir-S bond in **5**, whereas formation of **2** involves cleavage of a dative Cl-Ir bond. This proposal is also consistent with the more facile rearrangement of **5** in polar solvents, which would stabilize the dipolar intermediate. Having broken the halide or sulfide bridge the hydrido ligand is now able to "tunnel" between the two metals through an intermediate such as **V** to give **VI** in which the hydride is on the same face of the complex as the ligand X. Such a tunnelling process has been proposed by Puddephatt and coworkers in related "Pt_2" complexes,[27] and should be a reasonably facile process since the flexible DPM ligands can easily accommodate the metal-metal separation of *ca.* 3.2-3.4Å (twice the sum of the Ir and H covalent radii) necessary for a linear Ir-H-Ir intermediate. In support of this proposal, the structure of $[Ir_2(H)(Cl)$-

$(RC{=}C(H)R)_2(CO)_2(\mu\text{-}H)(DPM)_2]^+$ (R = CO_2Me) is shown in Chapter 6, to have an Ir-Ir separation of 3.289Å, and although the hydrides were not located, the NMR study and the dispositions of the other ligands in the X-ray study indicate that one hydride ligand is terminally bound while the other is bridging with an Ir-H-Ir unit which is close to linear. Subsequent transformation of **VI** can occur by movement of the chloro or sulfido group back to the bridging position, displacing the hydride ligand to an adjacent terminal site yielding **VII**, the structure proposed for the intermediate isomer **5b** in the reaction of **4** with H_2. Subsequent rearrangements yielding **IX** are analogous to those already described, but now involve the second hydrido ligand.

It appears, based on the vastly different rates of rearrangement for the chloro and sulfido complexes and on the faster rate for the sulfido species in polar solvents, that the steps involving cleavage of the Ir-X bonds to give intermediates such as **IV-VI** and **VIII**, are rate determining.

As noted earlier, compound **2** (shown as **IX** in Scheme 5.1; X = Cl) reacts further with H_2 to yield two isomers of $[Ir_2(H)_4Cl(CO)_2(DPM)_2]^+$ in a 5:1 ratio. Only the major isomer **3a** had been previously reported and its structure had not been formulated.[6] Based on the present understanding of the reactions of binuclear complexes with H_2, structures for both isomers can now be proposed. Compound **3a** displays a $^{31}P\{^1H\}$ NMR spectrum typical of an unsymmetrical species having an AA'BB' spin system, and the ^1H NMR spectrum shows that all four hydrido ligands are chemically inequivalent. At -60 °C the ^1H NMR spectrum shows four distinct resonances; the two at δ -10.12 ($^2J_{P\text{-}H}$ = 13.2 Hz) and -13.86 ($^2J_{P\text{-}H}$ = 10.4

Hz) are resolved as triplets while the other two are unresolved. Raising the temperature causes the three low field resonances to broaden considerably, while the most upfield resonance resolves into a triplet ($^2J_{P-H}$ = 11.1 Hz) at 0 °C. The fourth resonance is never resolved between +35 °C and -80 °C. At -60 °C selective ^{31}P decoupling of the ^1H NMR spectrum indicates that two hydride atoms are apparently located on each metal. Decoupling the downfield portion of the ^{31}P signal causes the two triplets to become singlets, and decoupling the upfield portion causes the remaining two resonances to sharpen considerably. The minor species (3b) observed in this mixture displays a singlet in the $^{31}P\{^1H\}$ NMR spectrum due to four chemically equivalent phosphorus atoms and the ^1H NMR spectrum displays two different hydride environments (integrating as two protons each), and also exhibits fluxional behavior. At -80 °C the hydride resonances in the ^1H NMR spectrum appear as two broad unresolved peaks, the more upfield of which broadens further and collapses into the baseline as the solution is warmed, and reemerges at -13.5 ppm, but remains broad between +22° and +35°. In the infrared spectrum of the solution, the two tetrahydride species together display three terminal carbonyl bands (2071, 2036, 1965 cm^{-1}) and a broad hydride band (2146 cm^{-1}). The latter was confirmed as such by preparation of the analogous tetradeuterides, by using D_2 instead of H_2. The IR spectrum of the deuterides contains carbonyl stretches at 2063, 1984, and 1960 cm^{-1}, apparently having shifted the previously observed band at 2036 cm^{-1} to a significantly lower frequency (1984 cm^{-1}). Such a shift would suggest strong vibronic coupling between the carbonyl and a hydrido ligand, and is evidence for a trans

relationship between these groups.[14] It is noted that the carbonyl stretch at 1965 cm^{-1} is somewhat low for either of the tetrahydride species, which should contain formally Ir(III) centers.

It is believed that **3a** and **3b** result from oxidative addition of H_2 either in the A-frame pocket of complex **2**, or on the outside of the species.

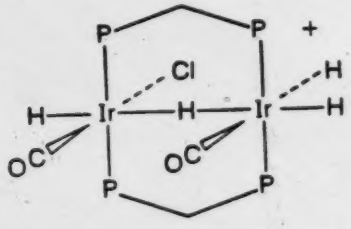

3a

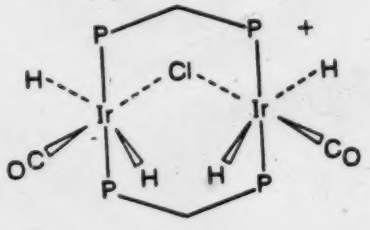

3b

Attack from the outside leads to **3a**, while attack in the pocket leads to the symmetrical species, **3b**. Both proposed structures involve octahedral Ir(III) centers with a bridging hydride ligand in **3a** and a bridging chloride ligand in **3b**. The structure for **3a** has precedent in the structure noted earlier for $[Ir_2(H)(Cl)(RC{=}C(H)R)_2(\mu\text{-}H)(CO)_2(DPM)_2]^+$ (see Chapter 6) in which the hydride ligands opposite the Ir-Ir bond in **3a** are replaced by the alkenyl moieties. Furthermore, this complex resulted from the addition of H_2 to $[Ir_2(RC{=}CHR)_2(CO)_2(\mu\text{-}Cl)(DPM)_2]^+$, a species very reminiscent of **2**. The decoupling study at -60 °C suggests that the bridging hydrido ligand may be bound more strongly to the metal having only one terminal hydride. Formation of both **3a** and **3b** was probably preceded by cleavage of one Ir-Cl bond to yield coordinative unsaturation allowing H_2 attack at one metal. Our failure to observe the analogous tetrahydride in the case of the sulfide-bridged analogue is consistent with its reluctance to cleave one

of the Ir-S bonds. Further support for the structures shown for **3a** and **3b** comes from the reaction of **2** with D_2. The ^1H NMR spectrum shows only one resonance (δ -10.70) for **3b**, consistent with D_2 attack in the pocket of **2**, and displays one strong hydride resonance (δ -16.52) for **3a**, together with three weak ones. In isomer **3a** the three hydride ligands associated with one metal are exchanging with D_2, causing H/D scrambling, whereas the fourth hydride, unable to reductively eliminate as H_2, remains undiluted by deuterium, so it appears as a strong resonance.

Unfortunately, the low temperature limiting spectra for **3a** and **3b** could not be obtained due to instrumental and solvent limitations. The possibility that H_2 loss was involved in the fluxionality was ruled out because placing D_2 above solutions of **3a** and **3b** had no effect on their respective hydride integrations in the ^1H NMR spectrum after 15 min. On a longer timescale however exchange does occur, as observed by monitoring HD formation in the ^1H NMR of a sample of **1** in the presence of H_2/D_2 (1:1 v/v). Although no HD is observed initially upon mixing, after 3 h the H_2:HD ratio is 3:5 while a control sample containing only H_2, D_2 and acetone-d_6 showed no HD formation. This can be compared to the same experiment involving compound **5c** where the H_2:HD ratio is 3:1 immediately after mixing and 1:1 after 3 h. If HD formation is a result of formation of dihydride-dideuteride species, the rate of formation of HD for **5c** would indicate that Ir-S bond cleavage apparently does occur, although not to give a stable product. At the same time the slow rate involving **1** reflects the stability of the coordinatively saturated tetrahydride (or hydride/deuteride) formed.

H/D exchange was similarly found[28] to occur upon reaction of the sulfide A-frame (**4**) itself with 1:1 H_2/D_2, probably indicating that exchange can occur from any of species **5a-5c**. Although formation of HD can be rationalized on the basis of an intermolecular process involving separate dihydride and dideuteride species when starting with **4**, no dideuteride species will be present initially in the experiment done with **5c**. It would therefore appear reasonable to suggest the presence of small, undetected amounts of a single dihydride-dideuteride species analogous to the tetrahydride, $[Ir_2(H)_4(CO)_2(Cl)(DPM)_2][BF_4]$.[6] As noted, both chloride- and sulfide-bridged A-frames react with 1 equivalent of H_2 to give dihydrides having structures like that of **5c**, so it seems reasonable that reaction of **4** with 2 equiv. of H_2, yielding a tetrahydride, should also be possible, as was observed for the chloride analogue. Assuming a tetrahydride intermediate, the H/D exchange can occur in a number of ways. Oxidative addition of H_2 at one metal center and D_2 addition to the other would yield a species analogous to that observed in the reaction of H_2 with $[Ir(\mu\text{-S-t-Bu})(CO)(P(O\text{-t-Bu})_3)]_2$,[16] and ligand scrambling followed by reductive elimination could yield HD. Otherwise, D_2 addition to one of the rearranged species, **5b** or **5c**, could occur with subsequent HD elimination. It is to be noted that the latter mechanism appears to operate for formation of the tetrahydrides from $[Ir_2(CO)_2(\mu\text{-Cl})(DPM)_2]^+$ (*vide supra*) and based on analogies in the two systems we favour this route for the sulfide-bridged species also.

Although one might anticipate that the reaction of the iodo-bridged A-frame, $[Ir_2(CO)_2(\mu\text{-I})(DPM)_2][BF_4]$ (**10**), would parallel that observed with the closely related species, **1** and **4**, this appears not to be the case. As with

the chloro-bridged species **1**, only one dihydride product, **11a**, is observed. It does not appear, however, to be a rearrangement product, but instead appears to be analogous to the initial sulfide-dihydride, **5a**, in which the hydrido ligands occupy the A-frame pocket. The $^{31}P\{^1H\}$ NMR spectrum, which appears as a singlet over the temperature range -80 °C to 22 °C, and the ^1H NMR spectrum, which displays a quintet at δ -13.18 ($^2J_{P\text{-}H}$ = 6.4 Hz), indicate that the hydrido ligands are coupled to four equivalent phosphorus nuclei on the NMR time scale. Unlike the chloro- and sulfido-bridged analogues the IR spectrum for **11a** displays only a single carbonyl stretch at 1937 cm^{-1} This may indicate that a species such as that shown for **11a** may be a better representation for the ground state configuration.

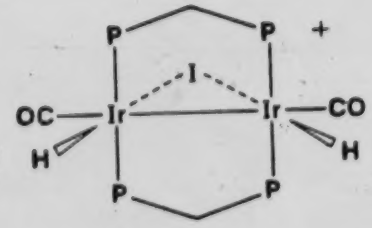

11a

Such a structure, in which the hydride ligands were exchanging metals through an intermediate such as **III** in Scheme 5.1 is consistent with the NMR data. If this species is sufficiently stable it may offer an explanation for the failure of this hydride product to rearrange to a product like **IX**. The reductive elimination of H_2 from **11a** is much more difficult than from **5a**, requiring several hours in refluxing THF under an N_2 purge (compound **5a** merely required an N_2 purge under ambient conditions for 30 min). This appears consistent with the presence of the good electron-

donating iodo group causing a reluctance of the metals in **11a** to undergo reduction.

As with the chloride A-frame, compound **10** also forms a tetrahydride species upon reaction with excess H_2. The ^1H NMR spectrum of the resulting light yellow solution indicates the presence of a single tetrahydride species (**12**) which displays two broad hydride resonances, even at -80 °C, integrating as two protons each. This tetrahydride is fluxional in solution as evidenced by a broadening and collapse into the baseline of the most upfield ^1H resonance as the temperature is raised (at ambient this resonance is barely detectable on the baseline). The $^{31}P\{^1H\}$ NMR spectrum remains a singlet (δ -6.42) at all temperatures studied (-80 to 22 °C) indicating a time-averaged symmetric species. The major species in solution would appear to involve a bridging carbonyl group as evidenced by a low frequency carbonyl stretch in the infrared spectrum (1779 cm^{-1}), however, the structures involved in the fluxionality of **12** are unclear. Additional attack of H_2 in the A-frame pocket of compound **11a** would seem most likely, such that the compound remains symmetric (as indicated by the $^{31}P\{^1H\}$ NMR spectrum). A carbonyl-bridged species could then arise by displacing the iodo group to a terminal position.

Along with extremely facile H_2 loss from **12** to give **11a**, reductive elimination of HI from **12**, forming significant amounts of $[Ir_2H(CO)_2(\mu\text{-}H)_2(DPM)_2]^+$ proved unavoidable. This trihydride was identified by comparison of its $^{31}P\{^1H\}$ and ^1H NMR spectra with those of an authentic sample previously characterized.[11] The presence of this species, and the absence of rearranged products similar to **2** and **5c**, leads one to believe that

tunnelling of the hydrido ligands does indeed occur at some stage, but subsequent reductive elimination of HI is highly favored. It should be noted that reductive elimination of HCl from the chloride tetrahydride **3** has also been observed, but only when **3** is refluxed in THF or higher boiling solvents. Although it is clear that the A-frame iodide complex reacts quite differently from the sulfide and chloride analogues, it is not immediately obvious why this should be so. The steric bulk of the large iodide bridge atom is however expected to be an important factor.

Although the possibility of one or more η^2-H_2 ligands was considered for compound **12**, as well as for the previously discussed tetrahydrides (**3a** and **3b**), the apparent relaxation times (T_1) measured at various temperatures are found to be typical of classical hydrides,[29] so these species are formulated as such. (The apparent relaxation times of the hydride resonances in the ^{1}H NMR were obtained by inversion-recovery at 400 MHz using a 180°-τ-90° pulse sequence, and delay times were varied from 5 to 800 ms. Values were found to be within the range 0.25-0.65 s.)

(b) Neutral, Non-A-frame Complexes

It was previously shown that reactions involving the A-frame (**1**) and the neutral precursor, *trans*-[IrCl(CO)(DPM)]$_2$, differed substantially,[6] and a comparison of these two systems proved to be extremely useful in establishing an understanding of the function of the bridging group in the A-frame species. A study of the neutral precursors to the A-frames, **6** and **10**, namely [$RhIrCl_2(CO)_2(DPM)_2$] (**13**) and [$Ir_2I_2(CO)_2(DPM)_2$] (**14**) was therefore also of interest.

The mixed-metal dichloride, **13**, reacts readily with H_2 yielding **8b**, a species identical to **8a**, discussed earlier, apart from the chloride counter-ion. In addition to almost superimposable spectroscopic parameters, conductivity measurements for **8b** indicate that it is a 1:1 electrolyte (Λ_m = 44.0 $\Omega^{-1}cm^2mol^{-1}$ in CH_2Cl_2).[30] This result differs from that previously reported for the diiridium analogue in which a neutral dihydride was obtained under the same conditions.[1] Compound **8b** loses H_2 somewhat more readily than the BF_4^- salt (requiring only slight warming in CH_2Cl_2 with N_2 purge) probably due to the coordinating ability of the Cl^- ion.

The neutral diiodide complex, **14**, reacts immediately with H_2 to yield two dihydride species in a 7:3 ratio as shown by the NMR spectra in Figure 5.4. This reaction is readily reversed merely by exchanging the H_2 atmosphere by N_2. The minor species **11b** has identical spectroscopic parameters to **11a** and is formulated as such, apart from the I^- counterion. The major product in this reaction displays a $^{31}P\{^1H\}$ NMR spectrum typical of an unsymmetrical species having an AA'BB' spin system. The ^1H NMR spectrum at -40 °C exhibits a triplet for each of two hydride ligands (δ -8.90, $^2J_{P\text{-}H} \doteq$ 13.0 Hz; δ -13.59, $^2J_{P\text{-}H}$ = 8.8 Hz) and selectively decoupling each of the ^{31}P resonances (as revealed in Figure 5.4) establishes that each hydride is coordinated to a different metal. The ease by which H_2 is reductively eliminated from the product suggests mutually adjacent hydride ligands. The infrared bands (ν(CO) 2002, 1982 cm^{-1}; ν(Ir-H) = 2230, 2105 cm^{-1}) are remarkably similar to those of the dichloro complex, $[Ir_2(H)_2Cl_2(CO)_2(DPM)_2]$,[6] which results from reaction of *trans*-$[IrCl(CO)(DPM)]_2$ with hydrogen. It is therefore proposed that compound **15** has the

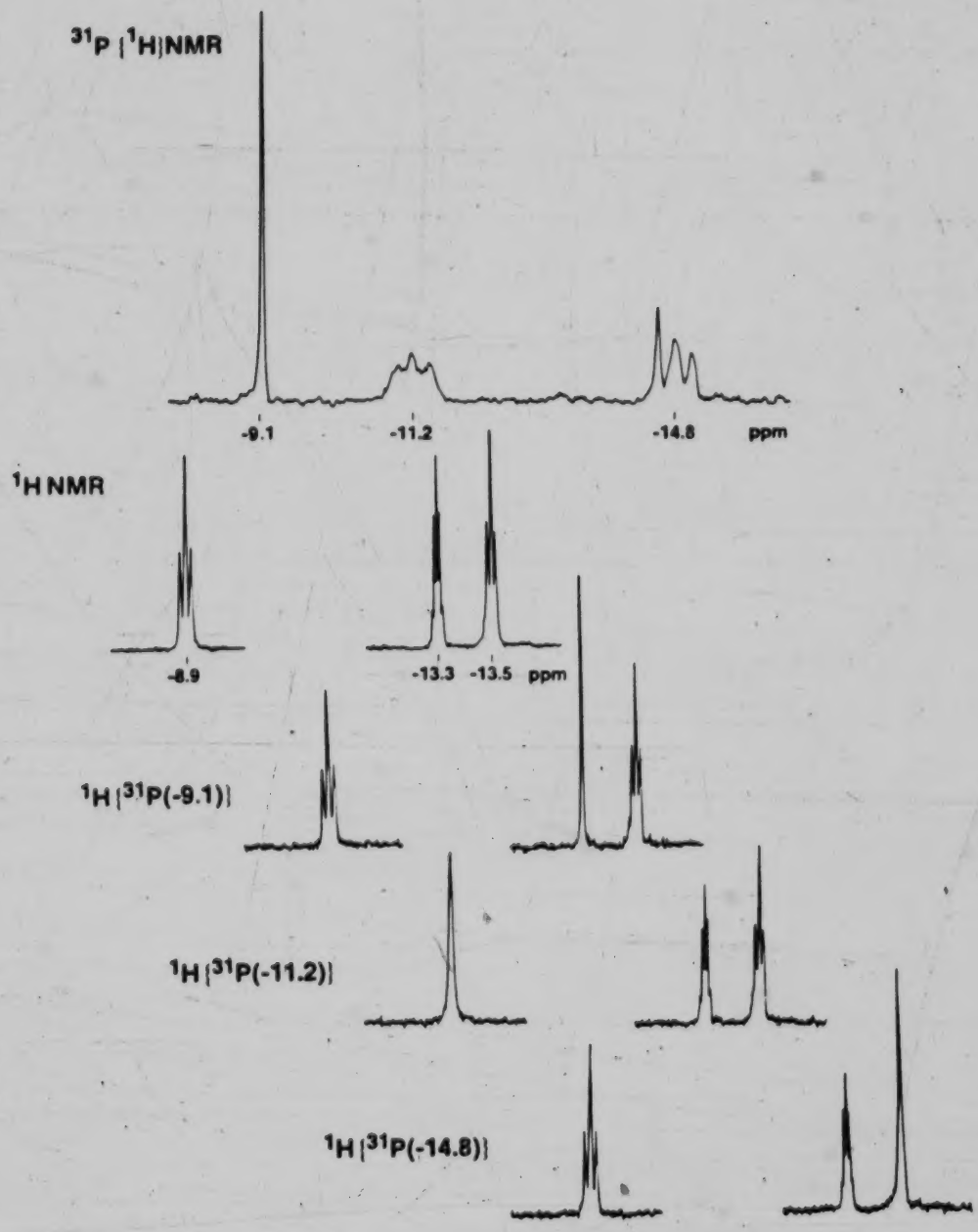

Figure 5.4. The $^{31}P\{^{1}H\}$ NMR spectrum (top) and ^{1}H NMR spectra (hydride region) of compounds **11b** and **15**, also showing selective ^{31}P decoupled ^{1}H NMR spectra.

same geometry, as shown in Scheme 5.2. Note that formation of **15** from **14** requires iodide loss and recoordination in order to go from a cis to a trans arrangement of ligands, suggesting formation of **11b** as an intermediate. Spin saturation transfer experiments on the ^1H NMR signals of the mixture of **11b** and **15** in fact show that both species are in equilibrium. Saturation of the most downfield hydride resonance of **15** causes the intensities of both the high field triplet of **15** and the quintet of **11b** to diminish. It should be noted that the saturation transfer is more pronounced upon the quintet resonance of **11b**, as observed in a greater intensity decrease for this resonance versus that of the upfield triplet of **15**. This suggests species **11b** as the intermediate which exchanges the two hydride environments since site exchange of either of the hydrides in **15** with each other or with the hydrides of **11b** will both involve transfer of

Scheme 5.2

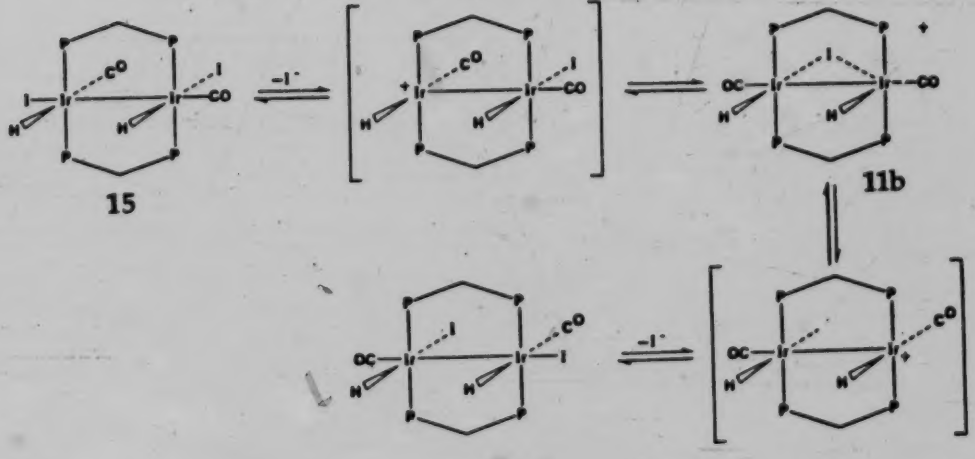

spin information to the quintet resonance of **11b**. This supports the equilibria described in Scheme 5.2, and as proposed for the analogous chloro species.[6] However, the NMR data suggest that the A-frame iodide (**11b**) is significantly more stable than the chloride, since the chloride A-frame was not observed in the NMR spectra above -40 °C. This result again suggests that the stability of this species may be responsible for the failure of **11a** to rearrange (*vide supra*). As one might expect with the presence of compound **11b**, if this solution is left for long periods of time under H_2 the tetrahydride species **12** (iodide salt) and the product of its reductive elimination of HI, $[Ir_2H(CO)_2(\mu\text{-}H)_2(DPM)_2]^+$ (*vide supra*) are observed.

Conclusions

The A-frame complexes $[Ir_2(CO)_2(\mu\text{-}X)(DPM)_2]^{n+}$ ((**1**): X = Cl, n = 1; (**4**): X = S, n = 0) have been shown to react with H_2 to produce dihydrides in which the hydrido ligands are not mutually cis but have rearranged to positions adjacent to the anionic bridging group.[5,6] Based on the intermediates observed in the much slower reaction of $[Ir_2(CO)_2(\mu\text{-}S)(DPM)_2]$ (**4**) with H_2, and on the results involving the mixed-metal analogues $[RhIr(CO)_2(\mu\text{-}X)(DPM)_2]^{n+}$ ((**6**): X = Cl, n = 1; (**7**): X = S, n = 0) in the presence of H_2, a feasible mechanism for the rearrangement of the hydrido ligands is proposed, key features of which include the breakage of one of the bonds between the bridging anionic group and the metal, and subsequent "tunnelling" of the hydride ligands between the two metal centers. Furthermore, it has been established that initial oxidative addition of H_2

occurs at a single metal center in the A-frame pocket of these complexes before stepwise rearrangement takes place. The iodo A-frame $[Ir_2(CO)_2(\mu\text{-}I)(DPM)_2][BF_4]$ (**10**) also undergoes H_2 attack in the pocket, but subsequent rearrangement would appear to result only in reductive elimination of HI upon generation of a species containing mutually adjacent hydrido and iodo ligands. The reaction of the neutral iodo complex $[Ir_2I_2(CO)_2(DPM)_2]$ (**14**) with H_2 leads to a neutral dihydride $[Ir_2(H)_2I_2(CO)_2(DPM)_2]$ (**15**) analogous to that obtained in the reaction of *trans*-$[IrCl(CO)(DPM)]_2$ with H_2. This neutral species is interconverting with $[Ir_2(H)_2(CO)_2(\mu\text{-}I)(DPM)_2][I]$ (**11b**), which is in fact a necessary precursor to **15** in which the iodo and carbonyl groups are no longer mutually cis.

This work has again demonstrated the utility of bridging halide or pseudohalide ligands as a source of incipient coordinative unsaturation, allowing unusual ligand mobility and also allowing for further reaction with incoming substrates.

References and Footnotes

1. (a) James, B. R. *Homogeneous Hydrogenation*; Wiley: New York, 1973. (b) Halpern, J. *Science (Washington, DC)* **1982**, *217*, 401 and references therein. (c) Bosnich, B.; Fryzuk, M. D. *Top. Stereochem.* **1981**, *12*, 119. (d) Kagan, H. B. in *Comprehensive Organometallic Chemistry*; Wilkinson, G., Stone, F. G. A., Eds.; Pergamon: Oxford, 1982; *Vol. 8*. (e) Knowles, W. S.; Chrisopfel, W. S.; Koening, K. F.; Hobbs, C. F. *Adv. Chem. Ser.* **1982**, *196*, 325. (f) Koga, N.; Daniel, C.; Han, J.; Fu, X. Y.; Morokuma, K. *J. Am. Chem. Soc.* **1987**, *109*, 3455 and references therein.
2. Sanger, A. R. *Prepr. -Can. Symp. Catal.* **1979**, *6th*, 37.
3. (a) Kubiak, C. P.; Woodcock, C.; Eisenberg, R. *Inorg. Chem.* **1982**, *21*, 2119. (b) Woodcock, C.; Eisenberg, R. *Inorg. Chem.* **1984**, *23*, 4207.
4. Cowie, M.; Southern, T. G. *Inorg. Chem.* **1982**, *21*, 246.
5. Kubiak, C. P.; Woodcock, C.; Eisenberg, R. *Inorg. Chem.* **1980**, *19*, 2733.
6. Sutherland, B. R.; Cowie, M. *Organometallics* **1985**, *4*, 1801.
7. (a) Kubiak, C. P.; Eisenberg, R. *J. Am. Chem. Soc.* **1977**, *99*, 6129. (b) Poilblanc, R. *Inorg. Chim. Acta* **1982**, *62*, 75.
8. Sutherland, B. R.; Cowie, M. *Inorg. Chem.* **1984**, *23*, 2324.
9. McCleverty, J. A.; Wilkinson, G. *Inorg. Synth.* Vol. VIII, p. 211.
10. Miller, J. S.; Caulton, K. G. *Inorg. Chem.* **1975**, *14*, 1067.
11. McDonald, R.; Sutherland, B. R.; Cowie, M. *Inorg. Chem.* **1987**, *26*, 3333.

12. All computing was carried out on a Digital PDP11/23 PLUS computer using the programs of the Enraf-Nonius Structure Determination Package and some local programs by R.G. Ball.

13. (a) Brown, M. P.; Fisher, J. R.; Hill, R. H.; Puddephatt, R. J.; Seddon, K. R.*Inorg. Chem.* **1981**, *20*, 3516. (b) Kennedy, J. D.; McFarlane, W.; Puddephatt,R. J.; Thompson, P. J. J. Chem. *Soc.., Dalton Trans.* **1976**, 874.

14. Kaesz, H. D.; Saillant, R. B. *Chem. Rev.* **1972**, 72, 231.

15. Vaska, L. *J. Am. Chem. Soc.* **1966**, *88*, 4100.

16. Guilmet, E.; Maisonnat, A.; Poilblanc, R. *Organometallics* **1983**, 2, 1123.

17. Schenck, T. G.; Milne, C. R. C.; Sawyer, J. F.; Bosnich, B. *Inorg. Chem.* **1985**, *24*, 2338.

18. Bonnet, J. J.; Thorez, A.; Maisonnat, A.; Galy, J.; Poilblanc, R. *J. Am. Chem. Soc.* **1979**, *101*, 5940.

19. (a) Pearson, R. G. *Chem. Rev.* **1985**, *85*, 41. (b) Collman, J. P.; Hegedus, L. S. *Principles and Applications of Organotransition Metal Chemistry*; University Science Books, Mill Valley, CA, **1987**; p 82 and references therein.

20. Woodcock, C.; Eisenberg, R. *Inorg. Chem.* **1984**, 23, 4207.

21. (a) Sutherland, B. R.; Cowie, M. *Inorg. Chem.* **1984**, 23, 1290. (b) Lehner, H.; Matt, D.; Togni, A.; Thouvenot, R.; Venanzi, L. M.; Albinati, A. *Inorg. Chem.* **1984**, 23, 4254. (c) Hlatky, G. G.; Johnson, B. F. G.; Lewis, J.; Raithby, P. R. *J. Chem. Soc. Dalton Trans.* **1985**, 1277.

22. (a) Balch, A. L.; Linehan, J. C.; Olmstead, M. M. *Inorg. Chem.* **1986**, *25*, 3937. (b) Balch, A. L.; Linehan, J. C.; Olmstead, M. M. *Inorg. Chem.* **1985**, *24*, 3975.

23. Balch, A. L.; Davis, B. J.; Neve, F.; Olmstead, M. M., *Organometallics*, in press.

24. Brookhart, M.; Green, M. L. H. *J. Organomet. Chem.* **1983**, *250*, 395.

25. Crabtree, R. H.; Hamilton, D. G. *Adv. Organomet. Chem.* **1988**, *28*, 299.

26. Cowie, M.; Dwight, S. K. *Inorg. Chem.* **1979**, *18*, 2700.

27. Puddephatt, R. J.; Azam, K. A.; Hill, R. H.; Brown, M. P.; Nelson, C. D.; Moulding, R. P.; Seddon, K. R.; Grossel, M. C. *J. Am. Chem. Soc.* **1983**, *105*, 5642.

28. Vaartstra, B. A.; O'Brien, K. N.; Eisenberg, R.; Cowie, M. *Inorg. Chem.* **1988**, *27*, 3668.

29. Crabtree, R. H.; Lavin, M.; Bonnevoit, L. *J. Am. Chem. Soc.* **1986**, *108*, 4032.

30. Typically, a 1:1 electrolyte such as $[Rh_2(CO)_2(\mu\text{-}Cl)(\mu\text{-}CO)\text{-}(DPM)_2][BF_4]$, gives a value of *ca.* 45 $\Omega^{-1}cm^2mol^{-1}$ (see reference 6).

CHAPTER 6

MODELLING BINUCLEAR HYDROGENATION CATALYSTS: THE STRUCTURE OF $[Ir_2(H)_2Cl(CH_3O_2CC{=}C(H)CO_2CH_3)_2(CO)_2(DPM)_2][BF_4]\cdot 3THF$, A STABLE COMPLEX CONTAINING MUTUALLY ADJACENT ALKENYL AND HYDRIDO LIGANDS.

Introduction

Preliminary studies done within this research group[1,2] and those described in previous chapters of this thesis have attempted to determine the sites of attack, accessible bonding modes and ligand mobilities involved in reactions of dihydrogen and unsaturated substrates with binuclear DPM-bridged complexes. One of the primary goals of such studies was to gain information relevant to alkyne hydrogenation catalysis in the presence of two or more adjacent metals. As mentioned earlier in this thesis, alkyne hydrogenation was found to be catalyzed by the binuclear complexes $[Rh_2(CO)_2(\mu\text{-}Cl)(DPM)_2][BPh_4]$,[3] $[Rh_2(H)_2(CO)_2(DPM)_2]$,[4,5] and $[Rh_2Cl_2(\mu\text{-}CO)(DPM)_2]$[6], although information about possible intermediates was lacking. Of particular interest were suggestions[1,7,8] that the two adjacent metal centers might be involved cooperatively at some stage of the catalytic cycle in such systems.

Substitution of one or both metals for iridium in these complexes has already proven to be an advantage over the dirhodium systems, yielding isolable and characterizable hydrides upon reaction with H_2

(Chapter 5 and elsewhere[9,10]). These hydride complexes therefore present themselves as potential models of intermediates proposed to be involved in catalytic hydrogenation by binuclear complexes. It has also been shown in previous chapters that the mobility of the anionic bridging group in binuclear diiridium or rhodium-iridium complexes can be instrumental in allowing both hydrides and coordinated alkynes to migrate within the framework of the two-metal systems, and in generating coordinative unsaturation at the metals. These results and a preliminary study[1] of the reactivity of one of these hydrides, $[Ir_2(H)_2(CO)_2(\mu\text{-}Cl)(DPM)_2][BF_4]$ (**1**), with dimethylacetylenedicarboxylate, which resulted in insertion of alkyne moieties into both Ir-H bonds, suggested that further study was warranted.

In this chapter, subsequent steps toward successfully modelling catalytic hydrogenation at adjacent metal centers is investigated by further study into the reaction of **1** and related hydrides with unsaturated substrates.

Experimental Section

General experimental conditions are described in Chapter 2. Dihydrogen and ethylene were obtained from Linde and used as received. Dimethylacetylenedicarboxylate (DMA), 2-butyne and phenylacetylene were purchased from Aldrich Chemical Company. Hexafluoro-2-butyne and tetrafluoroethylene were purchased from PCR Incorporated. The compounds, $[Ir_2(H)_2(CO)_2(\mu\text{-}Cl)(DPM)_2][BF_4]$,[1] $[RhIr(H)_2(CO)_2(\mu\text{-}Cl)(DPM)_2]$-$[X]$ ($X = Cl, BF_4$), $[Ir_2(H)_2(\mu\text{-}I)(DPM)_2][X]$ ($X = I, BF_4$), and $[RhIr(H)_2(CO)_2(\mu\text{-}S)$-

$(DPM)_2$] (Chapter 5) were prepared according to the previously reported procedures. The hydrogenation of 2-butyne was followed by sampling the gases above reaction mixtures with a gas-tight syringe (Hamilton) and analyzing them by gas chromatography on a Perkin-Elmer 8500 Gas Chromatograph using a Chromosorb W-AW column at 25°C. Retention times and approximate quantities of product gases were determined from calibration plots using the pure gases. Attempted catalytic runs for the hydrogenation of ethylene were performed at 22 °C using a hydrogen uptake apparatus (gas buret) to monitor the progress of the reaction. Mass spectroscopy experiments were carried out by the service within the department.

Preparation of Compounds

(a) $[Ir_2(CH_3O_2CC{=}C(H)CO_2CH_3)_2(CO)_2(\mu\text{-}Cl)(DPM)_2][BF_4]$ (**2**).

To a suspension of $[Ir_2(H)_2(CO)_2(\mu\text{-}Cl)(DPM)_2][BF_4]$ (**1**) (200.0 mg, 0.150 mmol) in 15 mL of THF (or acetone) was added an excess of dimethylacetylenedicarboxylate (DMA) (50.0 μL, 0.407 mmol). Within minutes the solution changed color from yellow to orange-yellow. After 1 h the solution was concentrated to a volume of 5 mL under dinitrogen from which a bright yellow microcrystalline solid was precipitated by the addition of 40 mL of diethyl ether. The solid was collected, washed with two 10 mL portions of diethyl ether and dried in vacuo giving typical isolated yields of 80-85%. Anal. calcd for $Ir_2ClP_4F_4O_{10}C_{64}BH_{58}$: C, 47.52%; H, 3.61%; Cl, 2.19%, Found: C, 47.32%; H, 3.55%; Cl, 2.77%. $^{31}P\{^1H\}$ NMR

(THF): δ -13.62(s). ^{1}H NMR (δ, ppm): 5.32(m, 2H), 4.46(m, 2H), 3.52(s, 2H), 3.39(s, 6H), 3.21(s, 6H). IR (cm^{-1}, Nujol): 2028(vs), 2013(vs) (ν(CO)); 1713(vs) (ν(C=O) of CO_2CH_3); 1573 (ν(C=C)).

(b) $[Ir_2(H)_2Cl(CH_3O_2CC{=}C(H)CO_2CH_3)_2(CO)_2(DPM)_2][BF_4]$ (3).

The dinitrogen atmosphere over a solution of 2 (100.0 mg, 0.062 mmol) in 10 mL of THF (or acetone) was displaced by an atmosphere of dihydrogen. Immediately the solution changed color from orange-yellow to pale yellow. The solution was stirred for an additional 30 min under H_2, then concentrated to 5 mL with rapid H_2 flow. Compound 3 was precipitated by the addition of 25 mL of diethyl ether, was collected, and washed with two additional 5-mL volumes of diethyl ether. The resulting colorless microcrystalline solid was dried with a dihydrogen purge giving 3 in 90% yield. Anal. calcd for $Ir_2ClP_4F_4O_{10}C_{64}BH_{60}$: C, 47.46%; H, 3.73%; Cl, 2.19%, Found: C, 47.68%; H, 3.68%; Cl, 2.10%. $^{31}P\{^1H\}$ NMR (acetone-d_6, -40°C): δ -7.90(m), -12.77(m). ^{1}H NMR (δ, ppm): 6.44(m, 2H), 5.24(m, 2H), 4.32(s, 1H), 3.62(s, 1H), 3.52(s, 3H), 3.46(s, 3H), 3.33(s, 3H), 3.10(s, 3H), -8.76 (br, 1H), -19.37(t, 1H, $^2J_{P\text{-}H}$ = 18.4 Hz). IR (cm^{-1}, CH_2Cl_2): 2135(w) (ν(Ir-H); 2051(vs), 2016(med) (ν(CO)); 1709(vs) (ν(C=O) of CO_2CH_3); 1588 (ν(C=C)).

X-ray Data Collection

Crystals of compound 3 suitable for X-ray diffraction studies were obtained by slow diffusion of diethyl ether into a saturated THF solution of the compound. The crystals proved susceptible to loss of both solvent

of crystallization and H_2, so one was selected and wedged into a capillary tube, containing H_2 and solvent vapor, which was then flame sealed. Data were collected on an Enraf-Nonius CAD4 diffractometer at 22 °C using graphite monochromated Mo Kα radiation. Unit cell parameters were obtained from a least-squares refinement of the setting angles of 25 reflections in the range $21.8° \leq 2\theta \leq 25.2°$. A monoclinic crystal system was established by the usual peak search and reflection indexing programs and systematic absences (h0l: l = odd, 0k0: k = odd) in the data were consistent with the space group $P2_1/c$.

Intensity data were collected on the CAD4 diffractometer as described in Chapter 2. The intensities of three standard reflections, measured every hour of exposure time, showed a mean decrease of 9.2% and a correction was applied assuming linear decay. The data were processed in the usual manner on the Digital PDP 11/23 PLUS computer.[11] See Table 6.1 for pertinent crystal data and details of intensity collection.

Structure Solution and Refinement

The structure was solved by using Patterson techniques to locate the metals and by successive least-squares and difference Fourier calculations to obtain the other atom positions. Hydrogen atoms associated with the DPM ligands and carboxylate methyl groups were located but were assigned to idealized positions as described in previous Chapters. Two of the solvent molecules were reasonably well behaved, but electron density associated with them was somewhat smeared out. The third appears

Table 6.1. Summary of Crystal Data and Details of Intensity Collection.

compd	$[Ir_2(H)_2Cl(CH_3O_2CC{=}C(H)CO_2CH_3)_2(CO)_2(DPM)_2][BF_4]\cdot 3THF$
formula	$Ir_2ClP_4F_4O_{13}C_{76}BH_{84}$
fw	1836.09
crystal shape	irregular plate
crystal size, mm	$0.58 \times 0.35 \times 0.056$
space group	$P2_1/c$ (No. 14)
cell parameters	
a, Å	18.675(5)
b, Å	15.775(3)
c, Å	26.371(4)
β, deg	96.38(2)
V, Å^3	7720.6
Z	4
ρ(calcd), g/cm^3	1.517
temp, °C	22
radiation (λ, Å)	graphite monochromated MoKα (0.71069)
receiving aperture, mm	3.00+(tanθ) wide × 4.00 high, 173 from crystal
take off angle, deg	3.00
scan speed, deg/min	variable between 6.67 and 0.95
scan width, deg	0.50 + (0.347 tanθ) in θ

Table 6.1. (Continued)

2θ limits, deg	$1.0 \leq 2\theta \leq 48.0$
no. of unique data collcd	12079 (h, k, ±l)
no. of unique data used ($F_o^2 \geq 3\sigma(F_o^2)$)	5775
linear absorption coeff, μ, cm^{-1}	36.10
range of transmission factors	0.891-1.362
final no. of parameters refined	590
error in observation of unit weight	1.752
R	0.054
R_w	0.062

slightly disordered such that its oxygen and carbon atoms could not be differentiated; all atoms in this ring were therefore refined as carbons. The hydrogen atoms of the solvent molecules were not included in the refinement owing to the high thermal parameters associated with the carbon and oxygen atoms.

Refinement in the space group $P2_1/c$ converged at $R = 0.054$ and $R_w = 0.062$.[12] The final positional and isotropic thermal parameters for all non-hydrogen atoms are given in Table 6.2. The 10 highest peaks in the final difference Fourier map (0.993-0.623 e/Å^3) were in the vicinities of the metals and the THF solvent molecules.

Results and Discussion

(a) Description of Structure

Compound 3 crystallizes in the space group $P2_1/c$ with one complex cation, the BF_4^- anion and three THF solvent molecules in the asymmetric unit. The BF_4^- anion is well-behaved and displays the expected tetrahedral geometry. Although the solvent molecules were found to have high thermal parameters, their geometries are as expected and there are no unusual contacts between the solvent molecules, the BF_4^- anion or the complex cation. A perspective view of the complex cation is shown in Figure 6.1, and a view containing only the metals and equatorial ligands is shown in Figure 6.2. Selected bond distances and angles are given in Tables 6.3 and 6.4, respectively.

Table 6.2. Positional Parameters and Isotropic Thermal Parameters[a]

Atom	x	y	z	B(Å^2)
Ir(1)	0.23047(3)	0.09135(4)	-0.07859(2)	3.55(1)
Ir(2)	0.26816(3)	0.00253(4)	-0.18532(2)	3.71(1)
Cl	0.1051(2)	0.0596(2)	-0.0989(1)	4.27(9)
P(1)	0.1980(2)	0.2179(3)	-0.1261(2)	4.1(1)
P(2)	0.2326(2)	0.1296(3)	-0.2277(2)	4.2(1)
P(3)	0.2351(2)	-0.0479(3)	-0.0429(2)	3.69(9)
P(4)	0.2513(2)	-0.1311(3)	-0.1494(2)	3.8(1)
F(1)	0.9035(5)	0.6415(6)	0.2537(4)	8.1(3)
F(2)	0.9032(7)	0.5182(7)	0.2081(4)	10.9(4)
F(3)	0.8483(7)	0.5261(7)	0.2803(5)	12.0(4)
F(4)	0.9703(8)	0.5307(8)	0.2822(6)	13.7(5)
O(1)	0.3862(6)	0.1322(7)	-0.0576(5)	7.2(3)
O(2)	0.4290(6)	0.0249(7)	-0.1467(5)	7.0(3)
O(3)	0.3162(6)	0.1250(7)	0.0491(4)	7.1(3)
O(4)	0.2928(8)	0.2574(8)	0.0190(5)	9.7(4)
O(5)	0.0734(6)	0.1687(8)	0.0719(4)	7.5(4)
O(6)	0.1879(7)	0.1950(9)	0.0935(5)	9.7(4)
O(7)	0.3668(7)	0.0314(8)	-0.2969(5)	8.7(4)
O(8)	0.4129(6)	-0.0810(9)	-0.2571(5)	8.7(4)
O(9)	0.1940(6)	-0.1742(7)	-0.3563(4)	7.0(3)
O(10)	0.3080(6)	-0.1312(9)	-0.3524(4)	8.7(4)
O(11)[b]	0.439(1)	0.468(2)	0.055(1)	23.(1)
O(12)[b]	0.852(1)	0.444(2)	0.089(1)	25.(1)
C(1)	0.3286(8)	0.1154(9)	-0.0660(5)	4.2(4)
C(2)	0.3685(8)	0.0187(9)	-0.1619(6)	4.4(4)
C(3)	0.1698(7)	0.1875(9)	-0.1922(6)	4.2(4)
C(4)	0.2026(7)	-0.1231(8)	-0.0926(5)	3.7(3)
C(5)	0.377(1)	0.164(2)	0.0804(8)	11.2(8)

Table 6.2. (Continued)

C(6)	0.2745(9)	0.183(1)	0.0216(7)	6.3(5)
C(7)	0.2099(8)	0.1442(9)	-0.0074(6)	4.1(4)
C(8)	0.1493(8)	0.140(1)	0.0108(6)	4.9(4)
C(9)	0.1417(9)	0.173(1)	0.0627(6)	6.0(5)
C(10)	0.063(1)	0.192(1)	0.1247(7)	9.6(6)
C(11)	0.439(1)	0.050(2)	-0.311(1)	13.2(8)
C(12)	0.3627(9)	-0.036(1)	-0.2682(6)	6.3(5)
C(13)	0.2885(8)	-0.052(1)	-0.2551(6)	5.5(4)
C(14)	0.2387(8)	-0.094(1)	-0.2860(6)	5.2(4)
C(15)	0.2519(9)	-0.134(1)	-0.3344(6)	5.9(4)
C(16)	0.203(1)	-0.218(1)	-0.4032(7)	10.6(7)
C(21)	0.1188(7)	0.2705(9)	-0.1065(5)	3.9(3)*
C(22)	0.1295(8)	0.311(1)	-0.0586(6)	5.5(4)*
C(23)	0.067(1)	0.351(1)	-0.0414(7)	6.7(5)*
C(24)	0.0043(9)	0.350(1)	-0.0699(7)	6.7(5)*
C(25)	-0.004(1)	0.311(1)	-0.1149(7)	7.4(5)*
C(26)	0.0531(9)	0.270(1)	-0.1342(6)	6.0(4)*
C(31)	0.2602(8)	0.3042(9)	-0.1290(6)	4.5(4)*
C(32)	0.237(1)	0.376(1)	-0.1514(8)	8.6(6)*
C(33)	0.283(1)	0.445(1)	-0.1610(8)	9.1(6)*
C(34)	0.350(1)	0.444(1)	-0.1397(8)	9.4(6)*
C(35)	0.379(2)	0.370(2)	-0.117(1)	17.(1)*
C(36)	0.328(1)	0.300(1)	-0.1138(9)	10.8(7)*
C(41)	0.2948(8)	0.2094(9)	-0.2451(6)	4.4(3)*
C(42)	0.365(1)	0.202(1)	-0.2280(7)	7.1(5)*
C(43)	0.415(1)	0.269(1)	-0.2412(8)	10.1(6)*
C(44)	0.386(1)	0.337(1)	-0.2692(7)	7.8(5)*
C(45)	0.316(1)	0.343(1)	-0.2839(7)	7.6(5)*
C(46)	0.2689(9)	0.278(1)	-0.2719(7)	6.5(4)*
C(51)	0.1738(8)	0.1064(9)	-0.2864(6)	4.5(4)*
C(52)	0.1095(9)	0.069(1)	-0.2855(6)	5.8(4)*

Table 6.2. (Continued)

C(53)	0.069(1)	0.042(1)	-0.3306(7)	7.7(5)*
C(54)	0.099(1)	0.053(1)	-0.3753(7)	7.0(5)*
C(55)	0.164(1)	0.090(1)	-0.3771(7)	7.4(5)*
C(56)	0.2046(9)	0.116(1)	-0.3340(6)	5.6(4)*
C(61)	0.3205(7)	-0.0957(8)	-0.0148(5)	3.6(3)*
C(62)	0.3861(9)	-0.070(1)	-0.0271(6)	6.3(4)*
C(63)	0.4497(9)	-0.114(1)	-0.0074(7)	6.6(5)*
C(64)	0.443(1)	-0.182(1)	0.0245(7)	6.9(5)*
C(65)	0.3776(9)	-0.207(1)	0.0359(7)	7.1(5)*
C(66)	0.3144(9)	-0.164(1)	0.0157(6)	5.6(4)*
C(71)	0.1755(7)	-0.0636(9)	0.0063(5)	3.8(3)*
C(72)	0.1064(8)	-0.098(1)	-0.0038(6)	5.0(4)*
C(73)	0.0624(9)	-0.102(1)	0.0362(7)	6.7(4)*
C(74)	0.0876(9)	-0.073(1)	0.0835(6)	5.9(4)*
C(75)	0.1562(9)	-0.040(1)	0.0955(7)	6.1(4)*
C(76)	0.1993(8)	-0.036(1)	0.0561(6)	4.8(4)*
C(81)	0.1879(8)	-0.1984(9)	-0.1902(6)	4.2(3)*
C(82)	0.1179(8)	-0.1737(9)	-0.2002(6)	4.6(4)*
C(83)	0.0678(9)	-0.227(1)	-0.2298(6)	5.9(4)*
C(84)	0.091(1)	-0.300(1)	-0.2480(7)	7.1(5)*
C(85)	0.163(1)	-0.325(1)	-0.2388(7)	7.9(5)*
C(86)	0.2124(9)	-0.274(1)	-0.2077(6)	5.9(4)*
C(91)	0.3302(7)	-0.1991(9)	-0.1328(5)	3.9(3)*
C(92)	0.3895(9)	-0.190(1)	-0.1550(6)	6.0(4)*
C(93)	0.449(1)	-0.246(1)	-0.1441(7)	6.8(5)*
C(94)	0.444(1)	-0.308(1)	-0.1115(7)	7.3(5)*
C(95)	0.3860(9)	-0.322(1)	-0.0888(7)	7.0(5)*
C(96)	0.3260(9)	-0.265(1)	-0.0968(6)	5.8(4)*
C(100)[b]	0.418(2)	0.561(2)	0.054(1)	18.(1)*
C(101)[b]	0.342(2)	0.543(2)	0.027(1)	23.(1)*
C(102)[b]	0.331(2)	0.457(3)	0.032(2)	26.(2)*

Table 6.2. (Continued)

C(103)[b]	0.402(3)	0.426(3)	0.015(2)	33.(2)*
C(104)[b]	0.897(2)	0.423(2)	0.041(1)	20.(1)*
C(105)[b]	0.892(1)	0.318(2)	0.047(1)	14.2(9)*
C(106)[b]	0.825(1)	0.332(2)	0.050(1)	13.9(9)*
C(107)[b]	0.880(2)	0.352(2)	0.102(2)	21.(1)*
C(108)[b]	0.616(2)	0.433(2)	0.343(1)	19.(1)*
C(109)[b]	0.572(2)	0.352(2)	0.317(1)	17.(1)*
C(110)[b]	0.635(2)	0.321(2)	0.283(1)	27.(1)*
C(111)[b]	0.674(2)	0.418(2)	0.311(1)	22.(1)*
C(112)[b]	0.617(3)	0.407(3)	0.270(2)	22.(2)*
B	0.907(1)	0.553(2)	0.2566(9)	7.7(6)*

[a] Estimated standard deviations in these and subsequent tables are given in parentheses and correspond to least significant digits. Starred atoms were refined isotropically. Anisotropically refined atoms are given in the form of the isotropic equivalent displacement parameter defined as: $(4/3)[a^2\beta(1,1) + b^2\beta(2,2) + c^2\beta(3,3) + ab(\cos \text{gamma})\beta(1,2) + ac(\cos \text{beta})\beta(1,3) + bc(\cos \text{alpha})\beta(2,3)]$.

[b] The THF solvent molecules are labelled as follows:
THF(1): O(11), C(100), C(101), C(102), C(103).
THF(2): O(12), C(104), C(105), C(106), C(107).
THF(3): C(108), C(109), C(110), C(111), C(112); see text regarding disorder of this molecule.

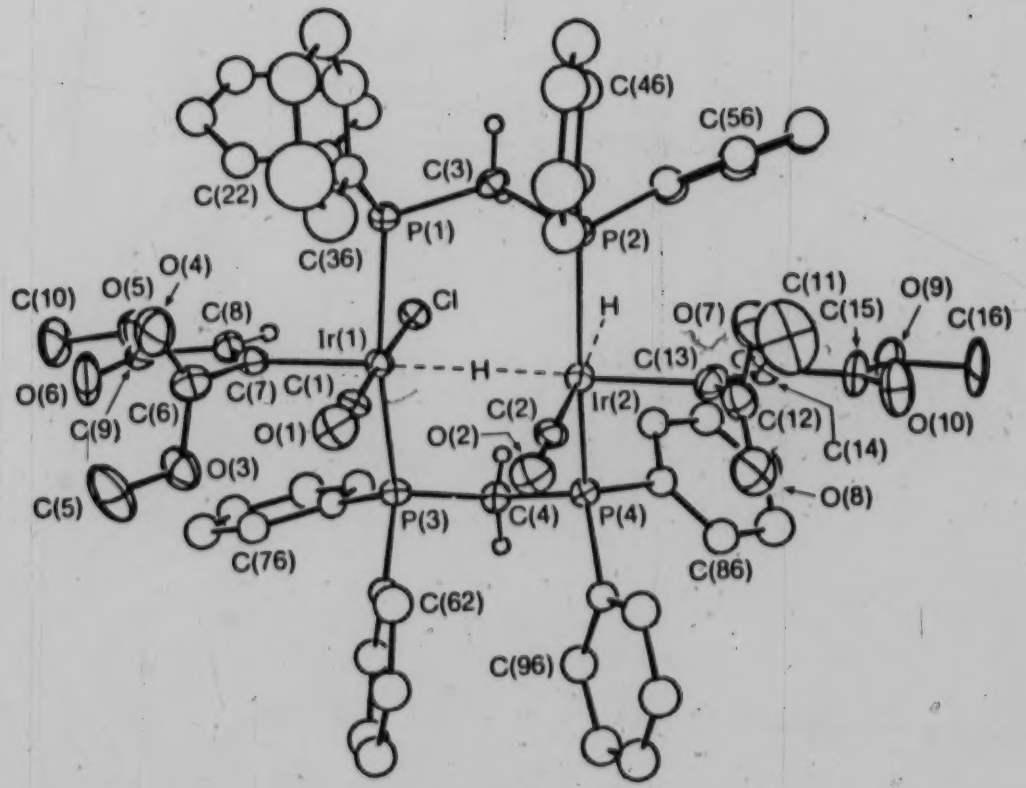

Figure 6.1 Perspective view of the $[Ir_2(H)_2Cl(CH_3O_2CC{=}C(H)CO_2CH_3)_2(CO)_2(DPM)_2]^+$ cation showing the numbering scheme. Thermal parameters are shown at the 20% level except for the methylene hydrogens, which are shown artificially small. The hydrido ligands, which were not located, are shown in their idealized positions.

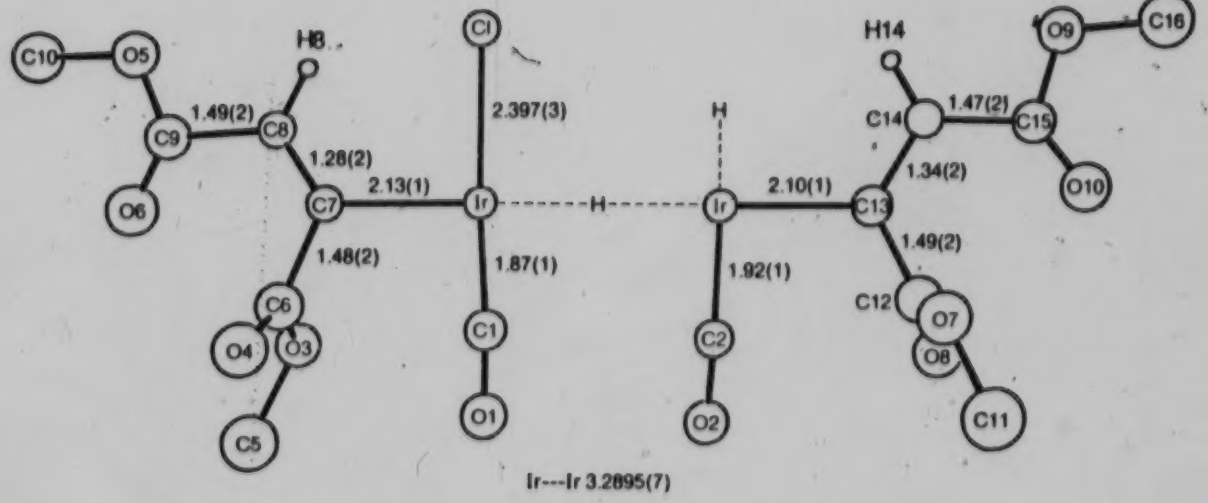

Figure 6.2. View of the approximate equatorial plane of the complex, including some relevant bond distances.

Table 6.3. Distances (Å) in $[Ir_2(H)_2Cl(CH_3O_2CC{=}C(H)CO_2CH_3)_2(CO)_2(DPM)_2]^+$

(a) Bonded

Ir(1)-Cl	2.397(3)	O(1)-C(1)	1.11(1)
Ir(1)-P(1)	2.399(3)	O(2)-C(2)	1.16(1)
Ir(1)-P(3)	2.388(3)	O(3)-C(5)	1.46(2)
Ir(1)-C(1)	1.87(1)	O(3)-C(6)	1.35(2)
Ir(1)-C(7)	2.13(1)	O(4)-C(6)	1.23(2)
Ir(2)-P(2)	2.354(3)	O(5)-C(9)	1.33(2)
Ir(2)-P(4)	2.346(3)	O(5)-C(10)	1.48(2)
Ir(2)-C(2)	1.92(1)	O(6)-C(9)	1.17(2)
Ir(2)-C(13)	2.10(1)	O(7)-C(11)	1.46(2)
P(1)-C(3)	1.83(1)	O(7)-C(12)	1.32(2)
P(1)-C(21)	1.83(1)	O(8)-C(12)	1.19(2)
P(1)-C(31)	1.80(1)	O(9)-C(15)	1.33(1)
P(2)-C(3)	1.83(1)	O(9)-C(16)	1.45(1)
P(2)-C(41)	1.81(1)	O(10)-C(15)	1.20(1)
P(2)-C(51)	1.83(1)	C(6)-C(7)	1.48(2)
P(3)-C(4)	1.82(1)	C(7)-C(8)	1.28(2)
P(3)-C(61)	1.84(1)	C(8)-C(9)	1.49(2)
P(3)-C(71)	1.82(1)	C(12)-C(13)	1.49(2)
P(4)-C(4)	1.84(1)	C(13)-C(14)	1.34(2)
P(4)-C(81)	1.84(1)	C(14)-C(15)	1.47(2)
P(4)-C(91)	1.84(1)		

(b) Non-Bonded

Ir(1)-Ir(2)	3.2895(7)	O(1)-O(2)	3.07(1)
P(1)-P(2)	3.151(5)	C(1)-C(2)	3.11(2)
P(3)-P(4)	3.143(5)	O(1)-H(36)	2.26
Cl-H(8)	2.49	O(2)-H(42)	2.57

Table 6.4. Angles (deg) in $[Ir_2(H)_2Cl(CH_3O_2CC{=}C(H)CO_2CH_3)_2(CO)_2(DPM)_2]^+$

Cl-Ir(1)-P(1)	82.7(1)	Ir(1)-P(3)-C(61)	121.9(4)
Cl-Ir(1)-P(3)	83.5(1)	Ir(1)-P(3)-C(71)	114.1(4)
Cl-Ir(1)-C(1)	177.3(4)	C(4)-P(3)-C(61)	103.2(5)
Cl-Ir(1)-C(7)	90.(3)	C(4)-P(3)-C(71)	104.1(5)
P(1)-Ir(1)-P(3)	165.4(1)	C(61)-P(3)-C(71)	103.2(5)
P(1)-Ir(1)-C(1)	96.3(4)	Ir(2)-P(4)-C(4)	111.6(4)
P(1)-Ir(1)-C(7)	94.3(3)	Ir(2)-P(4)-C(81)	112.9(4)
P(3)-Ir(1)-C(1)	97.1(4)	Ir(2)-P(4)-C(91)	118.8(4)
P(3)-Ir(1)-C(7)	90.9(3)	C(4)-P(4)-C(81)	99.8(5)
C(1)-Ir(1)-C(7)	91.9(5)	C(4)-P(4)-C(91)	107.6(5)
P(2)-Ir(2)-P(4)	155.9(1)	C(81)-P(4)-C(91)	104.5(5)
P(2)-Ir(2)-C(2)	104.6(4)	C(5)-O(3)-C(6)	112.(1)
P(2)-Ir(2)-C(13)	90.1(4)	C(9)-O(5)-C(10)	113.(1)
P(4)-Ir(2)-C(2)	99.2(4)	C(11)-O(7)-C(12)	115.(1)
P(4)-Ir(2)-C(13)	91.8(4)	C(15)-O(9)-C(16)	116.(1)
C(2)-Ir(2)-C(13)	94.1(6)	Ir(1)-C(1)-O(1)	178.(1)
Ir(1)-P(1)-C(3)	108.0(4)	Ir(2)-C(2)-O(2)	177.(1)
Ir(1)-P(1)-C(21)	113.4(4)	P(1)-C(3)-P(2)	119.2(6)
Ir(1)-P(1)-C(31)	121.8(4)	P(3)-C(4)-P(4)	118.4(5)
C(3)-P(1)-C(21)	103.6(5)	O(3)-C(6)-O(4)	122.(2)
C(3)-P(1)-C(31)	106.1(5)	O(3)-C(6)-C(7)	113.(1)
C(21)-P(1)-C(31)	102.6(6)	O(4)-C(6)-C(7)	125.(2)
Ir(2)-P(2)-C(3)	110.3(4)	Ir(1)-C(7)-C(6)	113.(1)
Ir(2)-P(2)-C(41)	123.9(4)	Ir(1)-C(7)-C(8)	124.(1)
Ir(2)-P(2)-C(51)	110.0(4)	C(6)-C(7)-O(8)	122.(1)
C(3)-P(2)-C(41)	104.4(5)	C(7)-C(8)-C(9)	121.(1)
C(3)-P(2)-C(51)	100.1(5)	O(5)-C(9)-O(6)	123.(2)
C(41)-P(2)-C(51)	105.5(6)	O(5)-C(9)-C(8)	111.(1)
Ir(1)-P(3)-C(4)	108.8(4)	O(6)-C(9)-C(8)	127.(2)

Table 6.4 (Continued)

O(7)-C(12)-O(8) 122.(2)	C(12)-C(13)-C(14)123.(1)
O(7)-C(12)-C(13) 113.(1)	C(13)-C(14)-C(15)125.(1)
O(8)-C(12)-C(13) 125.(2)	O(9)-C(15)-O(10) 124.(1)
Ir(2)-C(13)-C(12) 113.(1)	O(9)-C(15)-C(14) 112.(1)
Ir(2)-C(13)-C(14) 124.(1)	O(10)-C(15)-C(14)124.(1)

The complex exhibits a geometry in which each metal has a distorted octahedral coordination with the hydrido ligands situated as shown in the figures. The major distortion from octahedral geometries at the metal centers is due to the DPM ligands. As was found in the complex obtained from Cl^- addition to **2**, $[Ir_2Cl_2(CH_3O_2CC{=}C(H)CO_2CH_3)_2(CO)_2(DPM)_2]$,[1] both DPM ligands in complex **3** are tilted away from the side of the molecule containing the carbonyl ligands and the carboxylate groups which are nearest the metals. The resulting angles at Ir(1) (P(1)-Ir(1)-C(1) = 96.3(4)° and P(3)-Ir(1)-C(1) = 97.1(4)°) are very similar to those found in the dichloro complex. At Ir(2), however, the angles are slightly greater (P(2)-Ir(2)-C(2) = 104.6(4)° and P(4)-Ir(2)-C(2) = 99.2(4)), indicating less steric congestion opposite C(2). Although the Ir-P distances at Ir(2) (2.354(3), 2.346(3)) are similar to those found in the neutral dichloro complex, those at Ir(1) are slightly longer (2.399(3), 2.388(3)) owing to the greater steric congestion caused by the larger chloro ligand on Ir(1). The congestion at this metal results in some rather close non-bonded contacts between phenyl hydrogens and the carbonyl oxygen atoms (O(1)-H(36) = 2.26 Å, O(2)-H(42) = 2.57 Å). These distances are rather short compared to the sums of the van der Waals radii involved.[13]

Although the hydrido ligands were not located crystallographically, their approximate positions are assigned on the basis of ^1H NMR spectroscopic data (*vide infra*) and the positions of the other ligands in the structure. The position of the terminal hydride is obvious from the vacant coordination site opposite C(2), and the bridging hydride is suggested to be part of a nearly colinear Ir-H-Ir linkage. Such positions are

consistent with the octahedral geometry of the complex, and furthermore, the Ir-Ir separation of 3.2895(7) Å is almost exactly what would be predicted based on sums of covalent radii for the Ir atoms and the bridging hydrido ligand (3.27 Å).[13] It should be pointed out that for all cases of hydride-bridged metal complexes in which the hydrido ligand was located (either by X-ray or neutron diffraction), the M-H-M linkage is bent, with angles ranging from 85° to 159°.[14] It is expected that the same is true in compound **3**, although the arrangement of the other ligands suggests this linkage may be almost linear.

The carbonyl and chloro ligands in complex **3** are normal, with parameters involving these ligands comparable to values previously reported.[1,9,15-16] The Ir(2)-C(2) distance is marginally longer than that of Ir(1)-C(1) (1.92(1) Å vs. 1.87(1) Å) and is similar to the Ir-CO distance in another cationic hydride complex, $[IrH(CO)_2(\mu\text{-}H)_2(DPM)_2][Cl]$,[9] in which the carbonyl is located opposite a hydrido ligand. This is taken as further support for the presence of a hydrido ligand opposite C(2), based on the known "trans-influence" that is exhibited by this ligand.[17]

Parameters within the metallated olefin groups are essentially the same as in the neutral dichloro species,[1] however, it should be noted that the carboxylate group involving C(6) is oriented with its methoxy substituent below the plane shown in Figure 6.2, while that involving C(12) has its methoxy group above the plane. This was not the case in the neutral dichloro complex, which contained an approximate mirror plane perpendicular to the Ir-Ir bond. Such a difference is, no doubt, a consequence of the differing steric requirements in these compounds.

(b) Description of Chemistry

The reaction of $[Ir_2(H)_2(CO)_2(\mu\text{-}Cl)(DPM)_2][BF_4]$ (1) with 2 equivalents of dimethylacetylenedicarboxylate (DMA) in CH_2Cl_2 was previously found[1] to give a mixture of products, from which the neutral complex, $[Ir_2Cl_2(CH_3O_2CC{=}C(H)CO_2CH_3)_2(CO)_2(DPM)_2]$, was separated and structurally characterized. The X-ray structure determination of this neutral species offered support for the structure proposed for **1**, due to the positions of the metallated olefin groups on the outsides of the complex, opposite the Ir-Ir bond. Since the source of an additional chloride ion was attributed to the CH_2Cl_2 solvent, it was anticipated that the mixture obtained in the reaction did contain the analogous cationic species but that it was sensitive to the solvent. It is now confirmed that the cationic di-inserted species, $[Ir_2(CH_3O_2CC{=}C(H)CO_2CH_3)_2(CO)_2(\mu\text{-}Cl)(DPM)_2][BF_4]$ (2) is exclusively

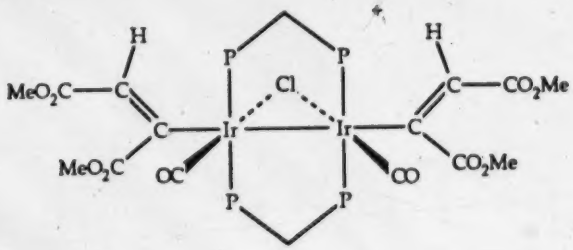

2

obtained when the reaction is performed in either THF or acetone; the reaction occurs rapidly upon addition of DMA, causing a color change from yellow to orange-yellow. Addition of only one equivalent of DMA to **1** merely yields one half of an equivalent of **2**, and unreacted **1**, as shown by $^{31}P\{^1H\}$ NMR. The symmetric nature of this species is evidenced

by a singlet in the $^{31}P\{^1H\}$ NMR spectrum (δ -13.62), and the ^1H NMR spectrum which reveals only two carboxylate methyl resonances (δ 3.39 (s, 6H), 3.21 (s, 6H)) and one resonance for the two equivalent hydrogen atoms (3.52 (s, 2H)) on the metallated olefin moieties. This contrasts the solution asymmetry found in the case of the neutral dichloro complex,[1] which was presumed to be due to steric crowding in the equatorial plane. The infrared spectrum of the isolated bright yellow solid displays two carbonyl stretches at 2028 and 2013 cm^{-1}, a DMA carboxylate stretching band at 1713 cm^{-1}, a band at 1573 cm^{-1} attributed to the C=C stretch of the metallated olefins, and a broad band at 1050 cm^{-1} characteristic of the BF_4^- counterion. Both carbonyl bands are higher than those of the dichloro species, as expected by the cationic nature of **2**.

Clearly, the reaction of the dihydride complex, **1**, with alkyne is rather facile, in spite of the coordinative saturation at both metals in **1**. The mechanism proposed for the hydride rearrangement, yielding **1** (Chapter 5), suggests a route to coordinative unsaturation at each metal center, allowing subsequent reaction with alkyne. As previously proposed, the bridging chloride ligand can swing into a terminal position on one metal, providing a site at the other metal for alkyne attack. Subsequent hydride migration, transfer of the chloride to the other metal and a repeat of the above sequence at the second metal center must be very rapid since the reaction is immediate with no intermediate observed, even at low temperature. Note that the diinserted product, **2**, is again equipped to generate coordinative unsaturation at either metal center by the same mechanism since it is quite analogous to **1**. This would appear to be a

viable route to oxidative addition of H_2 adjacent to the alkenyl ligand and subsequent reductive elimination of the free olefin. Such a route was not available to the neutral dichloro species apparently preventing further reaction with H_2. Furthermore, the similarity between compound **2** and its precursor, **1**, suggested that **2** should also react with H_2.

As anticipated, solutions of compound **2** react immediately under an atmosphere of H_2 causing a color change to very pale yellow, reminiscent of the pale coloration of the tetrahydrides formed when **1** is reacted with H_2 (see Chapter 5). The $^{31}P\{^1H\}$ NMR spectrum reveals a single unsymmetrical species, **3** (δ -7.90 (m), -12.77 (m)), and the ^1H NMR spectrum displays two broad hydride resonances (δ -8.76, -19.37) at 22 °C, integrating as one proton each. However, at -40 °C the more downfield hydride resonance appears as a triplet ($^2J_{P\text{-}H}$ = 18.4 Hz) and by -80 °C the upfield hydride resonance is also somewhat better resolved into a multiplet. The ^1H NMR spectra, with and without the appropriate selective ^{31}P decoupling are shown in Figure 6.3, along with the $^{31}P\{^1H\}$ NMR spectrum. It is clear that the triplet at δ -8.76 represents a hydride which is terminally bound to one iridium center as evidenced by collapse of this resonance to a singlet upon selective decoupling of the ^{31}P resonance at δ -7.90. It is also evident that the hydride represented at δ -19.37 bridges both metals as observed in the partial collapse of this resonance during each selective decoupling. Although this resonance approaches the appearance of a pure triplet upon selective decoupling, the multiplicity is not very clear due to the poor resolution. Broad-band decoupling of both ^{31}P resonances from the ^1H NMR spectrum causes both

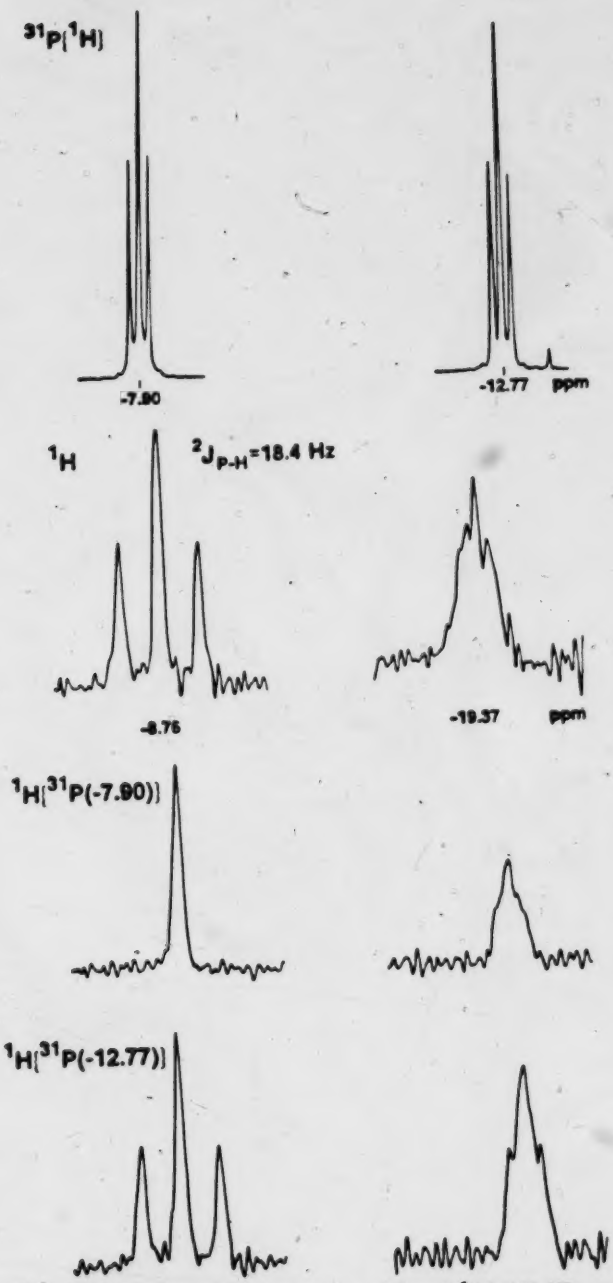

Figure 6.3 $^{31}P\{^{1}H\}$ NMR spectrum (top) and ^{1}H NMR spectra (hydride region) for compound **3** at -80 °C, also showing selective ^{31}P decoupled ^{1}H NMR spectra.

hydride resonances to collapse to singlets (not shown). It is these NMR data, as well as the observed positions of the other ligands found in the X-ray structure which suggest the locations of the two hydrido ligands as indicated in Figures 6.1 and 6.2.

The infrared spectrum of **3** displays two carbonyl stretches (2051, 2016 cm^{-1}) consistent with carbonyl groups on Ir(II) centers, and a weak band at 2135 cm^{-1} assigned to ν(Ir-H) by comparison of this spectrum to that of the analogous dideuteride, prepared by addition of D_2 to compound **2**. Additonal bands due to the carboxylate groups (1709 cm^{-1}) and the C=C stretch of the metallated olefin (1588 cm^{-1}) are also present. In the IR spectrum of the deuterated analogue (ν(CO): 2060, 2018 cm^{-1}) one of the two CO bands has shifted to higher frequency, consistent with this CO stretch having been coupled to the ν(Ir-H) at 2135 cm^{-1}, and supporting the location of a hydrido ligand opposite a carbonyl group.

The significance of compound **3** is appreciated when it is recognized that reports of characterized dihydrido-alkyl (-alkenyl) complexes are quite rare, even among the ever-increasing number of products of C-H activation.[18] Such species, which are often proposed as intermediates in hydrogenation catalyzed by monohydride transition-metal complexes, are usually very unstable toward elimination of the hydrogenated product.[19] Furthermore, the structure of **3** is concrete evidence that the chloride ligand can easily move to a terminal position, giving support to the mechanism by which hydride rearrangements occur, and also by which coordinative unsaturation is generated to allow further reaction with alkynes or H_2.

Attempts to reductively eliminate the expected hydrogenated product, dimethylmaleate, from **3** have been unsuccessful. No reaction is observed upon addition of substitutive ligands such as CO or PMe_3 to compound **3**. Neither is the olefin removed by heating solutions of **3** under N_2 purge, and instead, prolonged reflux in THF causes eventual H_2 loss. Such vigorous conditions required for H_2 loss suggests a high degree of stability, perhaps associated with exceptionally strong Ir-H bonds. This factor, as well as the presence of the electron withdrawing carboxylate groups in the organic moiety to cause strong Ir-C bonding,[20] appear to inhibit reductive elimination of the free olefin.

Reaction of compound **1** with another activated alkyne, hexafluoro-2-butyne (HFB), and subsequent reaction with H_2, yields analogous results to that found for DMA. The NMR and IR data in each case are almost identical apart from slight differences resulting from the change in substituents on the alkyne.

Although compound **1** reacts easily with activated alkynes, no reaction is observed upon exposure of **1** to activated olefins such as dimethylmaleate and tetraflouroethylene. These attempts were followed by monitoring the $^{31}P\{^1H\}$ NMR spectra over several hours in the presence of excess olefin. In each case compound **1** was found to be the only phosphorus-containing species present in solution.

Due to the stability of complex **3** toward olefin loss, which is attributed, in part, to the stronger Ir-C bonds in the activated alkenyl group, it was of interest to investigate the result of using unactivated alkynes for reaction with **1** and subsequent reaction with H_2. When

phenylacetylene is reacted with **1**, in the absence of H_2, the immediate appearance of small amounts of styrene and $[Ir_2(CO)_2(\mu\text{-}Cl)(DPM)_2][BF_4]$ as monitored by ^1H and $^{31}P\{^1H\}$ NMR spectra, respectively, indicates that hydrogenation is occurring by another mechanism (*vide infra*). However, the major product, **4**, appears to be one which is analogous to the di-inserted DMA product, **2**, as evidenced by a singlet in the $^{31}P\{^1H\}$ NMR spectrum (δ -13.48) at nearly the same chemical shift as **2**. The major bands in the infrared spectrum at 2004 and 1969 cm^{-1} are also consistent with those of **2**. Upon addition of excess H_2 to the sample mixture, the major species, **5**, is an unsymmetrical one as revealed by $^{31}P\{^1H\}$ NMR (δ -11.97 (m), -18.21 (m)). The ^1H NMR spectrum (-40 °C) of **5** displays methylene resonances at δ 3.93 (m, 2H) and δ 2.88 (m, 2H) and high field hydride resonances at δ -12.07 (m, 1H) and δ -13.15 (t, 1H, $^2J_{P\text{-}H}$ = 16.5 Hz). Selective ^{31}P decoupling of the ^1H NMR spectrum indicates that the hydride at δ -13.15 is terminal on one iridium center, while the hydride at δ -12.07 bridges the two metals. Decoupling the ^{31}P resonance at δ -11.97 causes collapse of the triplet hydride resonance (δ -13.15) into a singlet, and collapse of the multiplet hydride resonance (δ -12.07) into a triplet ($^2J_{P\text{-}H}$ = 11.5 Hz). Decoupling the ^{31}P resonance at δ -18.21 only affects the multiplet hydride resonance, resulting in a slightly broadened singlet. The results of the selective decoupling experiment suggest that complex **5** is rather analogous to complex, **3**, and a similar geometry is proposed for this complex, as shown below (DPM groups omitted for clarity).

Unfortunately, due to the presence of the additional products in the reactions, the hydrogen nuclei resulting from migration to the organic

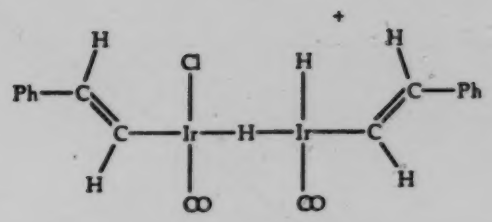

5

moieties in both **4** and **5** could not be located in the ^1H NMR experiment. It would appear reasonable, by steric arguments, to expect that the phenyl substituents are as far from the metals as possible.

It should be noted that the $^{31}P\{^1H\}$ NMR spectrum containing **5** as the major product also revealed the formation of the complex, $[Ir_2H(CO)_2(\mu\text{-}H)_2(DPM)_2]^+$ which has been previously characterized.[9] Its formation may be the result of HCl loss from species **5**, followed by consecutive H_2 additions and olefin eliminations at each metal center. Reductive elimination of HCl from **5** might not be difficult (compared to the same for **3**) since the bridging hydrido ligand appears to already be primarily bound to the same metal as the chloro ligand, and adjacent to it. Such a proposal is also consistent with the previous observation of HCl and HI elimination from tetrahydride complexes which are structurally analogous to **3** and **5** (see Chapter 5); again the resulting species in each case is $[Ir_2H(CO)_2(\mu\text{-}H)_2(DPM)_2]^+$.

Leaving the sample containing **5** under H_2 for approximately 24 h results in an increase in the concentration of styrene, as monitored by ^1H NMR, and essentially complete conversion of all phosphorus-containing species into the two isomeric tetrahydrides (resulting from addition of

excess H_2 to the A-frame complex $[Ir_2(CO)_2(\mu\text{-}Cl)(DPM)_2][BF_4]$) as monitored by $^{31}P\{^1H\}$ NMR.

Based upon the observations previously described, and on the DMA chemistry leading up to the structure determination of **3**, the mechanism outlined in Scheme 6.1 is proposed as the major pathway by which phenylacetylene is hydrogenated to styrene. This mechanism is related to that previously proposed (Chapter 5) for the hydride rearrangements leading to species **1** in that cleavage of one Ir-Cl bond yielding a sixteen-electron metal center is important. The steps leading to the doubly-inserted chloro-bridged species have already been described earlier in this chapter. Reaction of the doubly-inserted product with H_2 yields the species analogous to **3**, which is a stable species for **3** itself, but for the inserted phenylacetylene case goes on to reductively eliminate one equivalent of styrene. A "windshield-wiper" motion of the chloro ligand again generates a site for H_2 attack next to the other metallated olefin group, and subsequent elimination of the second olefin molecule regenerates the dihydride, **1**.

As noted, the reaction of **1** with phenylacetylene yields small amounts of styrene in the absence of H_2. It is found that reactions of **1** with 2-butyne and ethylene also lead to direct hydrogenation of the substrate. The reaction of excess 2-butyne with 50.0 mg of the dihydride compound **1** (in CH_2Cl_2 or THF) causes an immediate color change from yellow to orange-yellow. Over a period of 20 min the orange color intensifies and after this time the $^{31}P\{^1H\}$ NMR spectrum reveals that the only phosphorous-containing species remaining is the A-frame complex,

Scheme 6.1

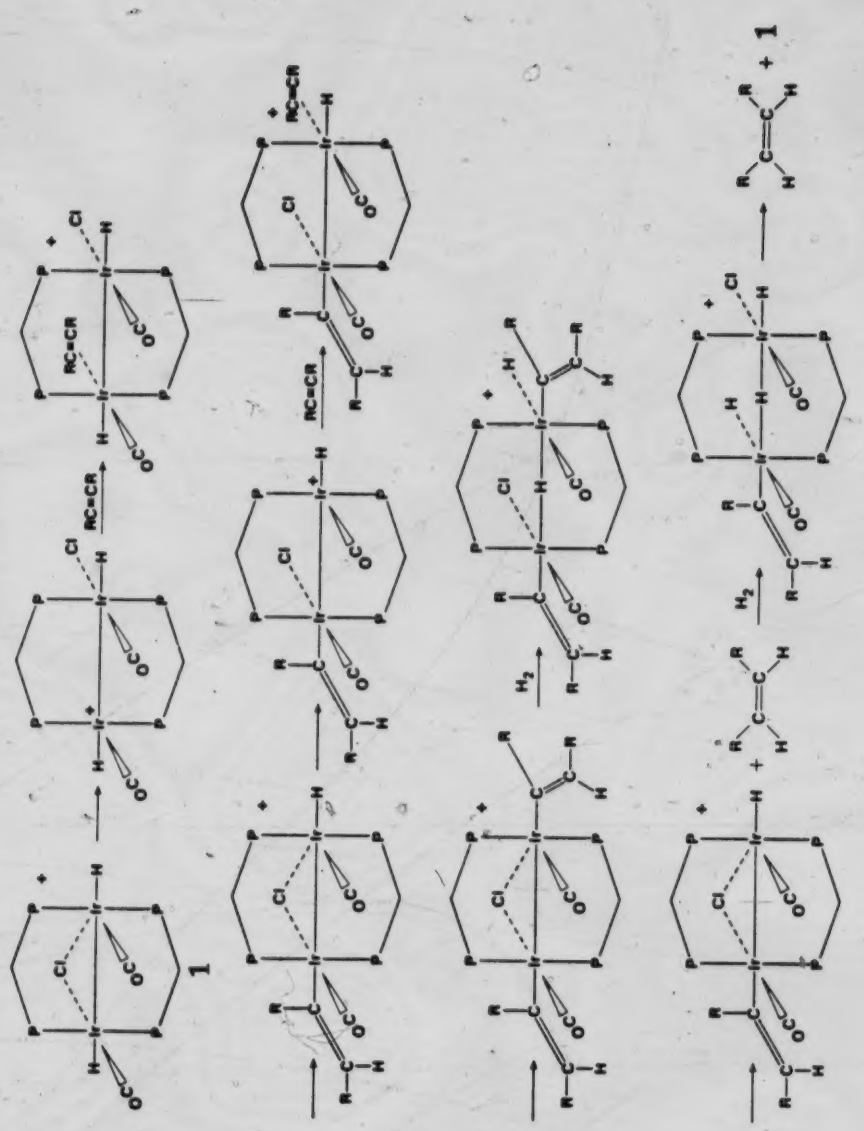

$[Ir_2(CO)_2(\mu\text{-}Cl)(DPM)_2][BF_4]$, which is identified by comparing the $^{31}P\{^1H\}$ NMR spectrum with that of an authentic sample. An infrared spectrum of the solution confirms that complete conversion to the A-frame complex has occurred. Analysis of a sample of the gas above the solution by gas chromatography reveals nearly equal concentrations of cis-2-butene and trans-2-butene as well as residual 2-butyne and a small amount of 1-butene. Note that H_2 is excluded from this reaction and therefore direct butyne hydrogenation by **1** is occurring; clearly the route suggested by the DMA chemistry is not involved with this substrate. Similarly, the reaction of compound **1** with excess ethylene causes the solution to become orange in approximately the same time as the reaction with 2-butyne. Analysis of the gases above the solution by mass spectrometry verifies the presence of ethane. Removal of the ethylene/ethane atmosphere followed by recording of the infrared and $^{31}P\{^1H\}$ NMR spectra of the solution again reveals only the A-frame complex, $[Ir_2(CO)_2(\mu\text{-}Cl)(DPM)_2][BF_4]$.

Since the hydrido ligands in **1** are not mutually adjacent, an intramolecular mechanism for the hydrogenation of 2-butyne and ethylene appears unlikely. In order to provide support for an intermolecular reaction, a 1:1 mixture of $[Ir_2(H)_2(CO)_2(\mu\text{-}Cl)(DPM)_2][BF_4]$ (**1**) and its analogous dideuteride, $[Ir_2(D)_2(CO)_2(\mu\text{-}Cl)(DPM)_2][BF_4]$ was reacted with excess ethylene and the products analyzed by high resolution mass spectrometry. The mass spectrum revealed that an approximate 1:2:1 ratio of C_2H_6, C_2H_5D and $C_2H_4D_2$ had resulted, which is consistent with an intermolecular reaction. The same mechanism would appear reasonable for rationalizing the observation of trans-2-butene in reactions of **1** with 2-butyne, however,

isomerization of an initially formed cis-product by unreacted **1** could also explain its formation, along with the production of 1-butene (see Chapter 1 for a description of alkene isomerization).

The involvement of an intermolecular mechanism in the case of unactivated substrates is no doubt related to the iridium-carbon bond strengths in the metallated-olefin intermediates. For 2-butyne and ethylene (and to some degree for phenylacetylene) these bonds are evidently weak and perhaps undergo homolytic bond cleavage such that the hydrogenation proceeds by a radical pathway. A radical mechanism has been supported in other hydrogenation reactions by the observation of Chemically Induced Dynamic Nuclear Polarization (CIDNP) in the NMR experiment (see also Chapter 1).[21] However, no such CIDNP effects were evident in the ^{1}H NMR signal of the butenes when the reaction of **1** with 2-butyne was closely monitored by NMR.

Although the reaction of **1** with both 2-butyne and ethylene proceed at attractive rates, **1** is not an effective catalyst for the hydrogenation of these substrates (at least under ambient conditions) due to very effective competition for the dihydride complex by H_2 to yield the coordinatively saturated tetrahydride isomers described in Chapter 5. Consequently, even under conditions of high substrate concentration and low H_2 concentration needed to circumvent this problem, the catalysis is slow. Using substrate:H_2 mole ratios near 10:1, over solutions of the A-frame precursor of **1**, caused no apparent H_2 uptake in the the case of ethylene, and less than 1 turnover per hour was observed in the case of 2-butyne. Although an extensive study into this mechanism has not yet been undertaken, it is

potentially very important in catalytic hydrogenation by these systems, and clearly should be investigated further. Studies of these reactions at elevated temperatures, where the tetrahydrides may be less likely to quench the reaction, would be of interest.

The reactions of several related hydrides (described in Chapter 5) with unsaturated substrates were also studied, in order to further ascertain those factors which promote hydrogenation by binuclear complexes and to substantiate some of the above conclusions. In the following cases the hydride complexes did not undergo rearrangement, neither was substrate hydrogenation observed.

The iodo A-frame complex $[Ir_2(CO)_2(\mu\text{-}I)(DPM)_2][BF_4]$ was found to react with excess H_2, yielding a single tetrahydride species which subsequently underwent facile HI loss and H_2 loss (see Chapter 5) to give $[Ir_2H(CO)_2(\mu\text{-}H)_2(DPM)_2][BF_4]$ (6) and $[Ir_2(H)_2(CO)_2(\mu\text{-}I)(DPM)_2][BF_4]$ (7), respectively. Addition of DMA to the mixture of 6 and 7 results in the immediate reaction of 6 to form a symmetrical species, 8, as observed by $^{31}P\{^1H\}$ NMR (δ -13.79 (s)), while less than 5% of 7 has reacted to yield an unsymmetrical species, 9 ($^{31}P\{^1H\}$ NMR: δ -10.80 (m), -16.37 (m)). After 30 min, 90% conversion of 7 to 9 has occurred. Complex 8 is characterized in the ^1H NMR spectrum by two complex multiplets for the DPM methylene protons (δ 4.73, 2H; 4.44, 2H), a singlet for the coordinated DMA carboxylate methyl protons (δ 3.10, 6H) and two hydride resonances (δ -11.29 (m), -17.80 (quintet), $^2J_{H\text{-}P}$ = 9.5 Hz) integrating 2:1, respectively. Selective decoupling of the ^{31}P resonance at δ -13.79 confirms the proton assignments (the methylene resonances become an AB quartet and the hydride signals

collapse to singlets), indicating that the three hydrido ligands have been retained upon reaction of compound **6** with DMA. A structure for **8** consistent with the NMR studies is shown below. The hydride resonance at δ -11.29 looks very similar to that observed for the two protons of

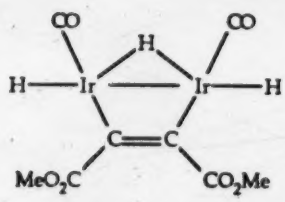

8

$[Ir_2(H)_2(CO)_2(\mu\text{-}S)(DPM)_2]$, the rearranged sulfide dihydride (Chapter 5), which was also suggested to have a colinear H-Ir-Ir-H linkage. The splittings of this resonance indicate that the couplings involved here are slightly less than those derived for the sulfide dihydride. The bridging DMA moiety is likely to be bound as shown, based on the exclusive observation of this mode in such complexes containing Ir(II) or Ir(III) centers.[22] Note that addition of the alkyne across the two metals of **6** requires a shift of one bridging hydride to a terminal position. This would appear to be very facile based on spin-saturation-transfer experiments on **6**,[9] which have revealed that the two hydrides on the same face of the dimer undergo site exchange. Therefore, the result of DMA addition to **6** strongly suggests that the site exchange occurs in a stepwise fashion, involving an intermediate containing a terminal hydrido ligand on each metal. Via this intermediate the DMA can undergo coordination in the site between the two hydrido ligands yielding **8**, as shown.

The product, **8**, is nevertheless a surprising result based on the reaction of **6** with CO which simply causes H_2 elimination.[9] A reasonable explanation for these results is that CO addition takes place by attack at an outside site of the complex, leaving two hydrido ligands adjacent and therefore susceptible to reductive elimination, while DMA attack occurs between the two adjacent hydrido ligands. Thus, in the case of DMA, the hydrido ligands are no longer adjacent and reductive elimination of H_2 is prevented. Evidently, formation of the alkyne bridge precludes hydride migration to the substrate and once formed, is rather stable in this coordination mode.

The other product in this reaction, compound **9**, is characterized in the ^1H NMR spectrum by two multiplets for the DPM methylene protons (δ 4.90, 2H; 4.73, 2H), two singlets for the DMA carboxylate methyl protons (δ 3.38, 3H; 3.16, 3H) and a triplet in the upfield hydride region (δ -14.49, 1H, $^2J_{H\text{-}P}$ = 11.8 Hz). Integrations are consistent with a single DMA moiety incorporated and only one hydrido ligand. An additional singlet at δ 3.90, integrating as one proton, would appear to arise from the hydrogen which has migrated to the unsaturated substrate. Consistent with the coupling to only two phosphorus nuclei, selective decoupling of the ^{31}P resonance at δ -10.80 causes the upfield triplet in the ^1H NMR spectrum to collapse to a singlet, while selective decoupling at δ -16.37 has no effect on this resonance. This evidence suggests the structure shown below for **9** in which alkyne insertion into one Ir-H bond has occurred. This result is reminiscent of the reaction of $[Ir(H)_2Cl_2(CO)_2(DPM)_2]$ with DMA.[1] As with this neutral chloro complex, **9** has not been induced to react further with

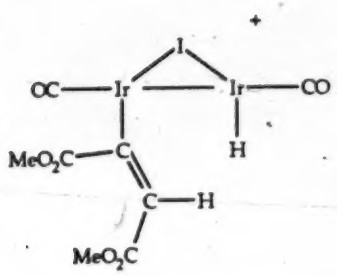

9

DMA to yield insertion into the remaining Ir-H bond, nor is there any indication for reductive elimination of the olefin. By comparison with the A-frame complexes which contain doubly-inserted alkynes (*vide supra*), it would appear that the low reactivity of **9**, as well as that of the singly-inserted dichloro complex,[1] may be a function of the steric crowding in the A-frame pocket after the first insertion has occurred. It has previously been suggested by this research group[1] that the DPM phenyl groups may play a role in this regard. Notably, the neutral diiodo-dihydride species, $[Ir_2(H)_2I_2(CO)_2(DPM)_2]$ does not react with DMA, even though it exists in equilibrium with the cationic form, $[Ir_2(H)_2(CO)_2(\mu\text{-}I)(DPM)_2][I]$ (see Chapter 5). Competition for a coordination site by the counterion evidently precludes coordination of the alkyne. Reactions of either the neutral or cationic iodo complexes with 2-butyne or ethylene also reveal no obvious reaction and no hydrogenated products are detected.

Another related diiridium A-frame complex, $[Ir_2(CO)_2(\mu\text{-}S)(DPM)_2]$, was previously described (Chapter 5) to react with H_2, yielding three isomeric dihydrides over time. Although the system was found[16] to catalyze the hydrogenation of acetylene, ethylene and propylene at high temperatures, it was of interest to investigate the possibility of inter-

mediates arising from insertion of unsaturated substrates into Ir-H bonds of the dihydrides observed in this system.

Isolation of the sulfide-dihydride, $[Ir_2(H)_2(CO)_2(\mu\text{-}S)(DPM)_2]$ (**10**), analogous to the rearranged chloro species **1** and addition of excess DMA, causes no reaction as monitored over a period of 2h. Allowing the reaction mixture to stir for approximately 2 days, however, did result in conversion of all starting material to a variety of products. No attempts were made to separate the products, however one of the species is identified as the product observed upon reaction of the sulfide A-frame complex alone with DMA (Chapter 4). Furthermore, the time allowed for the reaction to occur is clearly sufficient to allow reverse rearrangement of the hydrides and even H_2 loss, increasing the number of possible reacting species. The failure of the rearranged dihydride to react with DMA is consistent with the mechanism outlined in Scheme 6.1 since cleavage of one Ir-S bond to create coordinative unsaturation is probably short lived, and reformation of that bond is likely to preclude coordination of the alkyne.

If one equivalent of DMA is added to a solution containing predominantly the <u>initially</u> formed dihydride in the reaction of $[Ir_2(CO)_2(\mu\text{-}S)(DPM)_2]$ with H_2, the major species observed, **11**, is unsymmetrical ($^{31}P\{^1H\}$ NMR: δ -16.50 (br,m), -24.32 (br,m)). This species has retained its two hydrido ligands (^1H NMR: δ -10.91 (t, 1H, $^2J_{P\text{-}H}$ = 15.0 Hz), -16.44 (quintet, 1H, $^2J_{P\text{-}H}$ = 8.3 Hz)), although their environments are significantly different from those of the precursor, which suggests that insertion has not occurred, at least for this major species. Unfortunately the presence of

minor species also apparently containing coordinated DMA prevent unambiguous assignment of the DMA carboxylate protons belonging to **11**. However, due to the obvious change in hydride environments, DMA is assumed to be involved with the complex. The ^{31}P resonances which appear broad at room temperature both collapse to the baseline as the sample is cooled, but do not sufficiently reemerge even down to -80 °C. At the same time the hydride signals in the ^{1}H NMR spectrum are seemingly unaffected by temperature. At +40 °C, however, while the ^{31}P resonances lose their broadness and resemble a typical AA'BB' spin system, the hydride resonances are broad and unresolved. Selective ^{31}P decoupling of the ^{1}H NMR spectrum at this temperature does not resolve the hydride resonances, and at lower temperatures the ^{31}P signals are too broad to selectively decouple. Broad-band decoupling the ^{31}P resonances at lower temperature causes both hydride resonances in the ^{1}H NMR spectrum to collapse into singlets. These results strongly suggest a fluxional process which is relatively fast on the NMR timescale, especially at high temperature. It is suggested that this may simply be exchange between free DMA and that which is π-coordinated to a single metal center. This is not inconsistent with the result of DMA and HFB addition to $[Ir_2(CO)_2(\mu\text{-}S)(DPM)_2]$, which gives a stable terminal η^2-alkyne species with HFB, for which a crystal structure has been determined (Chapter 4). It was found that HFB attacks the complex adjacent to the sulfide bridge and causes a shift of one carbonyl group into a bridging position. A similar reaction could be forming **11**, which might lead to the structure shown below where one hydrido ligand occupies a bridge position.

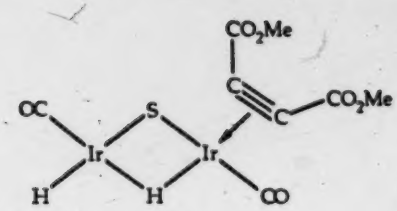

11

Another set of hydrides of interest in reactions with alkyne are the mixed-metal complexes, $[RhIr(H)_2(CO)_2(\mu\text{-}X)(DPM)_2]^{n+}$ (**12**: X = Cl, n = 1; **13**: X = S, n = 0). The chloro A-frame complex, $[RhIr(H)_2(CO)_2(\mu\text{-}Cl)(DPM)_2][Cl]$ (**12a**), derived from the neutral precursor, $[RhIrCl_2(CO)_2(DPM)_2]$, was found (Chapter 5) to lose H_2 very readily compared to the analogous BF_4^- salt (**12b**). Consequently, compound **12a** immediately loses H_2 upon reaction with DMA, even when the reaction is done under an H_2 atmosphere. This is evidenced by an ^1H NMR spectrum which no longer contains high field hydride resonances, nor is there evidence for insertion of the alkyne. Furthermore, the $^{31}P\{^1H\}$ NMR and IR spectra of the single product formed, **14**, are consistent with the previously identified product (Chapter 3) of direct addition of DMA to $[RhIrCl_2(CO)_2(DPM)_2]$. Upon attempts to induce alkyne insertion at elevated temperatures the product of CO loss

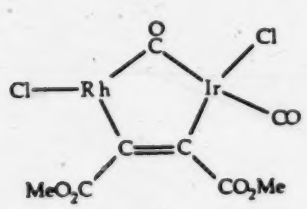

14

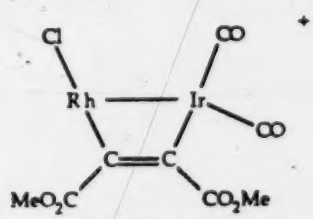

15

from this dimetallated olefin complex is identified, as well as the product of chloride loss, (15) (see Chapter 3 and elsewhere[23]).

The analogous mixed-metal A-frame, $[RhIr(H)_2(CO)_2(\mu\text{-}Cl)(DPM)_2][BF_4]$ (12b), does not react with DMA under ambient conditions, even in the absence of H_2. This is consistent with the lack of reactivity of 12a (noted above) toward insertion and the more severe conditions required to remove H_2 from 12b. Refluxing CH_2Cl_2 solutions of 12b in the presence of excess DMA for 3 h yields at least 3 other mixed-metal species as evidenced by $^{31}P\{^1H\}$ NMR. The major species is identified as 15 (see Chapter 3). This compound has also been characterized as the perchlorate salt,[23] for which NMR parameters are very similar. Minor products observed after reflux include hydride species, as evidenced by several high field resonances in the ^1H NMR, however, there is no evidence for insertions and the mixture was not investigated further. It is expected that some of these products may arise from simple π-coordination of the alkyne at one metal with concomitant transfer of ligands to the other metal or to bridging positions, as described previously for the homobinuclear iridium sulfide-dihydride species.

The mixed-metal sulfide-dihydride complex, 13, undergoes an immediate color change from light orange to blue-violet upon reaction with HFB. The ^1H NMR spectrum again indicates total loss of hydrides from the complex and no evidence for insertion of HFB into the metal-hydride bonds. This is not surprising since 13 is known to lose H_2 extremely readily (Chapter 5). $^{31}P\{^1H\}$, ^1H, and ^{19}F NMR all indicate the formation of two distinct mixed-metal species in nearly equal concen-

trations, with each containing a single HFB moiety. One of these products is identical to the single product formed by HFB addition to the precursor, $[RhIr(CO)_2(\mu\text{-}S)(DPM)_2]$ (Chapter 4). The other is likely an isomer, however no conversion of one to the other occurs over several hours. It may be that this isomer results from attack in the pocket of the A-frame complex rather than at the outside, which may be possible due to the open site left by the H_2 molecule immediately after it reductively eliminates.

The mixed-metal dihydrides **12** and **13** do not react under ambient conditions with the activated alkenes, tetraflouroethylene and dimethyl-maleate, nor do they react with the unactivated substrates, 2-butyne and ethylene.

Conclusions

It has become clear from the previously discussed reactivity of the A-frame complexes that the rearrangement of the hydrido ligands such that they are no longer adjacent but instead are on the outside of the complexes is an important feature. In those complexes which do not undergo rearrangement, either H_2 elimination or attack of the unsaturated substrate at a location which is non-adjacent to the hydrido ligands prevents the possibility of alkyne insertion into the Ir-H bond and eventual completion of the hydrogenation sequence. It is also evident that the success of both the hydride rearrangement and the subsequent insertion of the unsaturated substrate are dependent on the nature of the anionic bridging group for the creation of coordinative unsaturation at

each metal center, in turn. Equally important is the condition that reductive elimination of HX not be too facile and that the size of the anionic bridge-atom not deter coordination of substrates adjacent to it; both appear to be problems with the iodo A-frame system. Lastly, it is evident that hydrogenation of unsaturated substrates can occur by at least two pathways in these systems: a pathway comprised purely of oxidative addition, hydride migration and reductive elimination steps, and an intermolecular pathway, probably involving radical intermediates.

Although there are significant differences between the chemistry of the rhodium and iridium A-frame complexes, a study of the diiridium and mixed-metal "RhIr" complexes has provided useful insights into the catalysis by $[Rh_2(CO)_2(\mu\text{-}Cl)(DPM)_2]^+$. In particular, the crystal structure of 3 clearly establishes the ability of the bridging chloro ligand to open up a coordination site on one metal center by taking a terminal position on the other. This provides a great deal of support for the mechanism of hydride rearrangement described in Chapter 5, as well as the proposed mechanism for phenylacetylene hydrogenation described in Scheme 6.1, for which "windshield wiper" movement of the anionic group is pivotal. It appears that the diiridium A-frame complex is an effective model for the dirhodium catalyst, with Scheme 6.1 representing a feasible mechanism by which alkynes could be hydrogenated by $[Rh_2(CO)_2(\mu\text{-}Cl)(DPM)_2]^+$. One should be cautious, however, in assigning this mechanism to the catalysis exclusively, as indicated by the intermolecular pathway shown here to be very facile for 2-butyne and ethylene hydrogenation. Such pathways are, no doubt, available to the dirhodium system as well, and perhaps through

other hydride species in addition to the rearranged analogue of 1.

An important realization has come from these studies regarding metal-metal cooperativity in catalysis by these systems. Although the metals do cooperate by virtue of the coordinative unsaturation which is generated by the "windshield wiper" mechanism, the actual hydrogenation occurs independently at each metal center. There is no evidence for interaction of the substrate with the adjacent metal during its insertion into the Ir-H bond; neither is a hydride on one metal ever observed to migrate to the unsaturated substrate on an adjacent metal. This does not say, however, that transmission of electronic effects of one metal upon the other is not a factor. There is evidence that such electronic communication is easily transmitted through bridging ligands in iridium pyrazolate complexes.[24] Particularly of relevance to this thesis is the observation by Oro and coworkers[25] of the enhancement of catalysis by a second metal center in binuclear "RuRh" and "RuIr" complexes, which are more active than their mononuclear parent compounds in catalyzing the hydrogenation of cyclohexene. Further studies on these systems will hopefully determine whether such effects are involved, and to what extent one metal can be tailored to enhance activity at the other.

References and Footnotes

1. Sutherland, B. R.; Cowie, M. *Organometallics* **1985**, *4*, 1801.
2. Sutherland, B. R.; Cowie, M. *Organometallics* **1984**, *3*, 1869.
3. Sanger, A. R. *Prepr. -Can. Symp. Catal.* **1979**, *6th*, 37.
4. Kubiak, C. P.; Woodcock, C.; Eisenberg, R. *Inorg. Chem.* **1982**, *21*, 2119.
5. Woodcock, C.; Eisenberg, R. *Inorg. Chem.* **1984**, *23*, 4207.
6. Cowie, M.; Southern, T. G. *Inorg. Chem.* **1982**, *21*, 246.
7. Kubiak, C. P.; Woodcock, C.; Eisenberg, R. *J. Am. Chem. Soc.* **1977**, *99*, 6129.
8. Poilblanc, R. *Inorg. Chim. Acta* **1982**, *62*, 75.
9. McDonald, R.; Sutherland, B. R.; Cowie, M. *Inorg. Chem.* **1987**, *26*, 3333.
10. McDonald, R.; Cowie, M. manuscript in preparation.
11. Programs used were those of the Enraf-Nonius Structure Determination Package by B. A. Frenz, in addition to local programs by R. G. Ball.
12. $R = \Sigma| |F_o| - |F_c| | / \Sigma |F_o|$; $R_w = [\Sigma w(|F_o| - |F_c|)^2 / \Sigma w F_o^2]^{1/2}$.
13. Huheey, J. E. *Inorganic Chemistry*, 3rd ed., Harper and Row, New York, **1983**, p 258-259 and references therein.
14. Teller, R. G.; Bau, R. *Struct. Bonding(Berlin)* **1981**, *44*, 1.
15. (a) Sutherland, B. R.; Cowie, M. *Inorg. Chem.* **1984**, *23*, 2324. (b) Sutherland, B. R.; Cowie, M. *Organometallics* **1985**, *4*, 1637.

16. Kubiak, C. P.; Woodcock, C.; Eisenberg, R. *Inorg. Chem.* **1980**, *19*, 2733.

17. Kaesz, H. D.; Saillant, R. B. *Chem. Rev.* **1972**, *72*, 231.

18. A leading review containing many references is: Crabtree, R. *Chem. Rev.* **1985**, *85*, 245.

19. James, B. R. in *Comprehensive Organometallic Chemistry*, Wilkinson, G.; Stone, F. G. A.; Abel, E. W. eds., Pergammon Press, Oxford, **1982**, Vol. 8, p 285.

20. (a) Lukehart, C. M. *Fundamental Transition Metal Organometallic Chemistry*, Wadsworth, Belmont CA, **1985**, p 220. (b) Collman, J. P.; Hegedus, L. S.; Norton, J. R.; Finke, R. G. *Principles and Applications of Organotransition Metal Chemistry*, University Science Books, Mill Valley, California, **1987**, p 100.

21. Sweany, R. L.; Halpern, J. *J. Am. Chem. Soc.* **1977**, *99*, 8335.

22. See Chapters 2-4 and references therein.

23. Mague, J. T. *Organometallics* **1986**, *5*, 918.

24. Bushnell, G. W.; Fjeldsted, D. O. K.; Stobart, S. K.; Zaworotko, M. J.; Knox, S. A. R.; Macpherson, K. A. *Organometallics* **1985**, *4*, 1107.

25. Garcia, M. P.; Lopez, A. M.; Esteruelas, M. A.; Lahoz, F. J.; Oro, L. A. *J. Chem. Soc., Chem. Commun.* **1988**, 793.

CHAPTER 7

CONCLUSIONS

The objective of the studies of this thesis was to obtain a better understanding of how adjacent metals are capable of interacting with substrate molecules during catalytic hydrogenation. The results of these studies indicate that this objective has been met to a significant extent. Evidence for facile ligand migration, characterization of model intermediates and observed variations in reactivity caused by different ligands and metals, have been successful in extending our understanding of the possible reaction paths available to binuclear systems.

The approach used was one in which model complexes of known dirhodium catalysts were designed and synthesized and their reactivities under conditions relevant to hydrogenation were studied. Although it is recognized that the models chosen may not perfectly mimic the systems being modelled, the studies reported herein do indicate that facile rearrangement processes can occur about the two metal centers, in spite of the stereochemical rigidity imposed by the bridging DPM ligands, and that more than one pathway is possible for the hydrogenation of unsaturated substrates using binuclear complexes. Furthermore, the applicability of these studies is supported by the fact that at least one of the model systems operated catalytically under more forcing conditions.

Studies on the primary model complex, $[Ir_2(CO)_2(\mu\text{-}Cl)(DPM)_2][BF_4]$, which was selected by analogy to the catalytically active dirhodium

congener, suggested that the mobility of the bridging chloro ligand was instrumental in several processes. This was particularly evident in its reactivity with H_2 compared to that of the sulfide-bridged complex, as described in Chapter 5. Further studies into the effects of the anionic bridge-ligand were therefore initiated, by preparation of the neutral and cationic iodo complexes described in Chapter 2. Since these compounds had not been investigated previously, it was of interest to examine some chemistry comparable to the established diiridium complexes, before proceeding to the hydrogenation studies. This research group's interest in the reactivity of binuclear complexes with small molecules led to an initial investigation of the reactions of the iodocarbonyl complexes with carbon monoxide and activated alkynes, and later with molecular oxygen and subsequent reactivity of an oxygen adduct which will be discussed in the Appendix. The iodocarbonyl complexes proved to be somewhat different from the analogous chlorocarbonyl complexes, apparently affected by both the size and the greater electron-donating ability of the iodo ligands. These features allowed coordination of no more than three carbonyl ligands in the complexes and the electronic factors were evident in generally lower carbonyl stretches in the infrared spectra. The alkyne, dimethylacetylenedicarboxylate (DMA), coordinated to the complexes in the expected cis-dimetallated olefin geometry, but again, the situation of the iodo ligands produced somewhat different results compared to the chloro analogues.

Reaction of the iodocarbonyl species with H_2 (Chapter 5) was also found to be slightly different from that of the chloro and sulfido species, as

the isolated dihydride maintained mutually adjacent hydrido ligands, and when rearrangement apparently did occur, facile reductive elimination of HI yielded a cationic trihydride species. Reaction of the A-frame dihydride, $[Ir_2(H)_2(CO)_2(\mu\text{-}I)(DPM)_2][BF_4]$, with DMA resulted in insertion of the alkyne into one of the Ir-H bonds, but no further reaction could be induced. This reactivity at only one of the Ir-H units was reminiscent of a similar reaction with the neutral dichloro species, $[Ir_2(H)_2Cl_2(CO)_2(DPM)_2]$.

In an attempt to bridge the gap between the chemistries of the catalytically active dirhodium complexes and the model diiridium complexes, the mixed-metal "RhIr" chlorocarbonyl complexes were synthesized (Chapter 3). Again, it was of interest to examine some comparative chemistry in order to assess the behavior of complexes containing two different metals in close proximity. In general, the reactions of these complexes with carbon monoxide and activated alkynes gave results which were cognizant of the chemistries of both homobinuclear analogues. Accordingly, reaction of the mixed-metal complexes with H_2 yielded products in which the hydrido ligands were primarily bound to the iridium center. However, the presence of both iridium and rhodium did not appear conducive to further modelling of the steps involved in hydrogenation of unsaturated substrates, presumably due to either facile reductive elimination of H_2 from these species, or to exceptionally strong Ir-H bonds and reluctance of the species to mobilize ligands.

Overall, the comparative studies of the chloro, iodo and sulfido complexes and the mixed-metal complexes were instructive in demonstrating the sensitivity of binuclear species of this type to the steric and

electronic effects of the ligands and the metal centers themselves. The terminal η^2-alkyne complexes described in Chapter 4 were further indication of these effects, where the bridging sulfido ligand did not allow rearrangement to give a species having the alkyne bridging the two metals, as had been observed in all analogous compounds. Furthermore, the bonding of the alkyne to one iridium center was strongly influenced by the nature of the adjacent metal, as observed in stronger binding of the alkyne in the diiridium complex compared to the mixed-metal "RhIr" analogue.

As stated in Chapter 1, one of the goals of this thesis was to account for the rearrangement of hydrido ligands to non-adjacent positions in the A-frame complex, $[Ir_2(H)_2(CO)_2(\mu\text{-}Cl)(DPM)_2][BF_4]$. With major contributions coming from a study of the much slower rearrangement in the reaction of $[Ir_2(CO)_2(\mu\text{-}S)(DPM)_2]$ with H_2, a feasible mechanism was proposed in Chapter 5. Initial attack of H_2 in the pocket of the A-frame was established, followed by stepwise tunnelling of each hydrido ligand between the metals to positions on either side of the anionic bridging group. Involvement of a bridge-to-terminal ("windshield-wiper") movement of the anionic group was consistent with the observed rates for hydride rearrangement in the chloro and sulfido species, and also supported by some of the chemistry described in previous chapters.

A related mechanism was proposed in Chapter 6 to describe the pathway leading to alkyne hydrogenation by the rearranged dihydride species. The structure determination of $[Ir_2(H)_2Cl(CH_3O_2CC{=}C(H)\text{-}CO_2CH_3)_2(CO)_2(DPM)_2][BF_4]$ provided concrete evidence for the important

bridge-to-terminal step to generate coordinative unsaturation in these mechanisms. Although the mechanism relies on the windshield-wiper movement of the bridging group from one metal to the other, the hydrogenation itself appears to proceed at each metal center independently, rather reminiscent of the olefin route described for $HRhCO(PPh_3)_3$ in Chapter 1. It is therefore concluded that metal-metal cooperativity does not occur in the hydrogenation steps themselves, while the method by which coordinative unsaturation is generated at each metal to allow these steps to occur might well be described as a cooperativity between the metals.

In conclusion, the model catalyst, $[Ir_2(CO)_2(\mu\text{-}Cl)(DPM)_2][BF_4]$, in conjunction with related species, appear to have provided a feasible mechanism by which catalytic hydrogenation could occur in the dirhodium complex, $[Rh_2(CO)_2(\mu\text{-}Cl)(DPM)_2]^+$. However, the observation of an additional intermolecular pathway in the model system, which was evident in reactions of $[Ir_2(H)_2(CO)_2(\mu\text{-}Cl)(DPM)_2][BF_4]$ with 2-butyne and ethylene (Chapter 6), would suggest that such a mechanism could also be effective in the dirhodium catalysis, perhaps even involving other hydride species. There is clearly evidence that a number of possible paths may be responsible for catalytic hydrogenation by the binuclear dirhodium species.

There are obviously some aspects involved in hydrogenation at adjacent metal centers that look attractive, such as the facile activation of H_2 and separation of the hydrido ligands from one another by rearrangement, and the potential for electronic communication between metal

centers as discussed in the conclusions of Chapters 4 and 6. It has yet to be shown however, that two metals can both be directly involved in the hydrogenation itself and thereby be advantageous over mononuclear systems. Further studies into the possibility of metal-metal cooperativity in these types of complexes might concentrate on the use of other ligands and different homo- and hetero-binuclear metal centers in order to "tailor" the electronic and steric factors to the conditions necessary for cooperativity to be favored. Current studies are underway, for example, using less sterically encumbered diphosphine ligands such as bis(dimethylphosphino)methane instead of DPM.

APPENDIX I

REACTION OF A BINUCLEAR IODOCARBONYL COMPLEX WITH MOLECULAR OXYGEN: THE STRUCTURE OF $[Ir_2I_2(CO)_2(\mu\text{-}O_2)(DPM)_2]$, A COMPOUND CONTAINING A PEROXO-BRIDGED METAL-METAL BOND.

Introduction

Transition metal dioxygen complexes have attracted a great deal of interest, especially due to their relevance to biological oxygen transport proteins such as hemoglobin and myoglobin,[1] and to oxidations of organic substrates by metalloenzymes. The study of biomimetic chemical models has therefore been extensive, particularly since the early sixties,[1-5] and synthetic dioxygen complexes have also been under investigation due to their industrial potential as catalytic intermediates in chemical oxidations.[1,7]

The coordination of molecular oxygen to transition metal complexes can be reversible or irreversible, and the O_2 molecule can bind to metals in a variety of bonding modes;[8] those more commonly observed are diagrammed below. Single metal centers can undergo formal one-

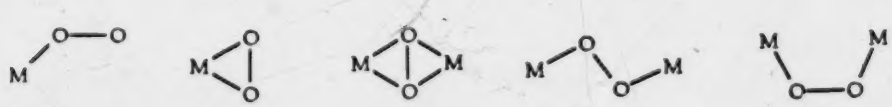

I II III IV V

electron oxidations in which the complexes contain a superoxide (O_2^-) ligand, or two-electron oxidations to yield peroxide (O_2^{2-}) complexes, whereas binuclear dioxygen complexes are normally peroxo-bridged and of the types IV and V above.

Binuclear dioxygen complexes have attracted interest within the bioinorganic field due to evidence that two metal centers are involved per active site, in proteins such as hemerythrin and hemocyanin, and oxygenase enzymes such as tyrosinase and dopamine-beta-hydroxylase.[1-5] Outside of the biological interests, binuclear dioxygen complexes are synthetically attractive due to the potential for the two adjacent metal centers to act in a cooperative manner for substrate oxidation. Interesting reactivities at adjacent metal centers have been discussed previously in this thesis and have also been reported in connection with a variety of metal-metal bonded species.[9] As part of an ongoing study in this research group into the reactivity of small molecules at adjacent metal centers, it was of interest to investigate an anticipated rich chemistry of binuclear DPM-bridged rhodium and iridium dioxygen complexes. Herein is reported the first known binuclear complex containing a peroxo-bridged metal-metal bond and a preliminary study of the reactivity of this complex.

Experimental Section

All solvents used were routinely dried and distilled and stored under dinitrogen. Reactions were carried out under Schlenk conditions except where noted. The compound, $[Ir_2I_2(CO)(\mu\text{-}CO)(DPM)_2]$ (**1**), was

prepared as described in Chapter 2. Carbon monoxide, carbon dioxide, sulfur dioxide and nitrogen dioxide were obtained from Matheson. Dihydrogen was obtained from Linde (Union Carbide). Dimethyl-acetylenedicarboxylate (DMA), silver tetrafluoroborate, tetrafluoroboric acid and trimethylphosphine were purchased from Aldrich Chemical Company. The $^{31}P\{^{1}H\}$ NMR spectra were run on Bruker HFX-90 (with Fourier transform capability) and Bruker WH-400 NMR spectrometers. Infrared spectra were recorded on a Nicolet 7199 Fourier transform IR spectrometer or on a Perkin-Elmer 883 IR spectrometer, either as solids in Nujol mulls on KBr plates or as solutions in KCl cells with 0.5 mm window path lengths. Elemental analyses were performed by the micro-analytical service within the department.

Preparation of Compounds

(a) $[Ir_2I_2(CO)_2(\mu\text{-}O_2)(DPM)_2]$ (**2**).

A sample of $[Ir_2I_2(CO)(\mu\text{-}CO)(DPM)_2]$ (**1**) (100.0 mg, 0.078 mmol) was dissolved in 25 mL of CH_2Cl_2 in a flask which was open to the atmosphere. The solution was left to stir for several hours, during which time a dark purple microcrystalline solid precipitated. The orange colored solution was transferred to another flask, while the purple solid was washed with two 5 mL portions of CH_2Cl_2 and the washings added to the mother liquor. The colored solution was again stirred for 2-3 h and a second crop of the purple solid collected in the same manner as the first. This process was repeated several times, until the total isolated yield of **2** was approximately

70%. Anal. calcd for $Ir_2I_2P_4O_4C_{52}H_{44}$: C, 41.78%; H, 2.97%, Found: C, 41.44%; H, 2.91%. $^{31}P\{^1H\}$ NMR (CH_2Cl_2, vs 85% H_3PO_4): δ -24.40 (s). Infrared (cm^{-1}): 2005 (vs), 1979 (st) (Nujol); 2000 (vs), 1975 (st) (CH_2Cl_2).

(b) $[Ir_2I_2(CO)_2(\mu\text{-}SO_4)(DPM)_2]$ (3).

A sample of $[Ir_2I_2(CO)_2(\mu\text{-}O_2)(DPM)_2]$ (2) (45.0 mg, 0.030 mmol) was suspended in 5 mL of CH_2Cl_2 under dinitrogen. Sulfur dioxide gas was bubbled into the solution causing an immediate color change to bright yellow and complete dissolution of the starting material. The solution was left under SO_2 atmosphere for 30 min, then concentrated to half of its original volume with rapid dinitrogen flow. The product was precipitated by the addition of 10 mL of diethyl ether, collected and dried *in vacuo*. The isolated orange-yellow solid was obtained in 96% yield. Anal. calcd for $Ir_2I_2SP_4O_6C_{52}H_{44}$: C, 40.06%; H, 2.84%; I, 16.28%; S, 2.06%, Found: C, 38.48%; H, 2.86%; I, 15.13%; S, 2.47%. $^{31}P\{^1H\}$ NMR (CH_2Cl_2, vs 85% H_3PO_4): δ -17.69 (s). Infrared (cm^{-1}): 2085 (med), 2037 (vs), 2028 (vs) (Nujol); 2079 (st), 2039 (vs) (CH_2Cl_2).

X-ray Data Collection

Single crystals of $[Ir_2I_2(CO)_2(\mu\text{-}O_2)(DPM)_2]$ (2) suitable for X-ray crystallography were obtained by allowing slow diffusion of atmospheric oxygen into a CH_2Cl_2 solution of $[Ir_2I_2(CO)(\mu\text{-}CO)(DPM)_2]$ (1). Although the crystals appeared as well-formed tertragonally distorted octahedral prisms, most did not diffract well; even the crystal chosen was of poorer diffraction

quality than desired. The crystal was wedged into a capillary tube which was flame sealed. Data were collected on an Enraf-Nonius CAD4 diffractometer at 22 °C using MoKα radiation. Unit cell parameters were determined from a least-squares refinement of the setting angles of 25 reflections in the range $19.9° \leq 2\theta \leq 23.7°$. Automatic peak search and reflection indexing programs, in addition to a cell reduction program, established a tetragonal crystal system. The data revealed systematic absences (00l, $l \neq 4n$; h00, $h \neq 2n$) which were consistent with the space groups $P4_12_12$ and $P4_32_12$.

Intensity data were collected on the CAD4 diffractometer as described in Chapter 2. The mean decrease in the intensity of three standard reflections was 11.3% and a correction was applied assuming linear decay. The data were processed with a value of 0.04 for p to downweight intense reflections,[10] and corrections for Lorenz and polarization effects and for absorption[11] were applied. See Table A.1 for pertinent crystal data and details of intensity collection.

Structure Solution and Refinement

The crystal structure was solved in the space group $P4_12_12$ by using direct methods to locate the iridium and iodine atoms and by successive least-squares and difference Fourier calculations to obtain the other atom positions. The hydrogen atoms associated with the phenyl and methylene groups were assigned idealized positions by using C-H distances of 0.95 Å and thermal parameters fixed at 1.2 times those of their attached carbon

Table A.1. Summary of Crystal Data and Details of Intensity Collection.

compd	$[Ir_2I_2(CO)_2(\mu\text{-}O_2)(DPM)_2]$
formula	$Ir_2I_2P_4O_4C_{57}H_{44}$
fw	1495.03
crystal shape	tetragonally distorted octahedron
crystal size, mm	0.47 × 0.32 × 0.32
space group	$P4_12_12$ (No. 92)
cell parameters	
a, Å	14.647(2)
c, Å	27.973(4)
Z	4
V, Å^3	6001.4
ρ(calcd), g/cm^3	1.655
temp, °C	22
radiation (λ, Å)	graphite monochromated MoKα (0.71069)
receiving aperture, mm	3.00+(tanθ) wide × 4.00 high, 173 from crystal
take-off angle, deg	3.00
scan speed, deg/min	variable between 6.67 and 1.11
scan width, deg	0.60 + (0.347 tanθ) in θ
2θ limits, deg	$1.0 \leq 2\theta \leq 50.0$
no. of unique data collcd	4751 (h, k, l)

Table A.1. (Continued)

no. of unique data used ($F_o^2 \geq 3\sigma(F_o^2)$)	3585
linear absorption coeff, μ, cm^{-1}	55.73
range of transmission factors	0.815-1.157
final no. of parameters refined	169
error in observation of unit weight	2.587
R	0.061
R_w	0.093

atoms. Subsequent refinements allowed the hydrogen atoms to "ride" on their attached carbons.

The structure was refined as described in previous chapters, and converged at R = 0.061 and R_w = 0.093.[12] Attempts to refine in the enantiomorphic space group $P4_32_12$ resulted in somewhat higher residuals of R = 0.080 and R_w = 0.115, suggesting that $P4_12_12$ was the correct choice, so all subsequent calculations were performed in this space group. In the final difference Fourier map the 10 highest peaks were in the range 1.788-1.188 e/Å^3 and were primarily located near carbon atoms in the phenyl groups. The positions and isotropic thermal parameters for the atoms of the final model are given in Table A.2.

Results and Discussion

(a) Description of Structure

Compound **2** crystallizes in the tetragonal space group $P4_12_12$ with the molecule occupying the crystallographic 2-fold axis. An Ortep plot of the molecule, viewed approximately along the 2-fold axis of rotation, is shown in Figure A.1. A view of the equatorial plane, omitting the DPM ligands, is shown in Figure A.2. Bond distances and angles are given in Tables A.3 and A.4, respectively.

The complex has the usual trans arrangement of the DPM ligands[13] with parameters within the diphosphine ligands and the Ir-P distances (2.377(4), 2.367(4) Å) consistent with previous structures of this type

Table A.2. Positional Parameters and Isotropic Thermal Parameters

Atom	x	y	z	B(Å^2)
Ir	0.34160(6)	0.24514(6)	0.03266(3)	2.62(1)
I	0.3907(1)	0.1077(1)	0.09538(7)	3.96(4)
P(1)	0.2884(4)	0.3308(4)	0.0993(2)	2.8(1)
P(2)	0.1518(4)	0.4023(4)	0.0288(3)	3.0(1)
O(1)	0.516(1)	0.356(2)	0.0294(8)	6.7(6)
O(2)	0.216(1)	0.187(1)	0.0264(6)	3.9(4)
C(1)	0.448(2)	0.309(2)	0.034(1)	5.3(7)
C(2)	0.226(2)	0.433(2)	0.0841(8)	3.5(6)
C(11)	0.376(2)	0.385(2)	0.1339(8)	2.7(5)*
C(12)	0.427(2)	0.342(2)	0.138(1)	5.1(7)*
C(13)	0.531(3)	0.382(3)	0.159(2)	9.(1)*
C(14)	0.522(2)	0.465(2)	0.186(1)	6.6(9)*
C(15)	0.427(2)	0.510(2)	0.180(1)	4.9(7)*
C(16)	0.357(2)	0.469(2)	0.153(1)	4.5(6)*
C(21)	0.213(2)	0.273(2)	0.1402(8)	3.2(5)*
C(22)	0.171(2)	0.196(2)	0.130(1)	4.7(6)*
C(23)	0.114(2)	0.153(2)	0.162(1)	4.9(6)*
C(24)	0.099(2)	0.196(2)	0.205(1)	6.1(7)*
C(25)	0.139(2)	0.279(2)	0.217(1)	5.7(7)*
C(26)	0.205(3)	0.311(3)	0.177(1)	7.7(9)*
C(31)	0.100(2)	0.514(2)	0.0162(9)	3.6(5)*

Table A.2. (Continued).

C(32)	0.150(2)	0.595(2)	0.015(1)	4.3(6)*
C(33)	0.109(3)	0.668(3)	-0.002(2)	9.(1)*
C(34)	0.027(3)	0.678(3)	-0.011(1)	7.2(9)*
C(35)	-0.030(2)	0.608(2)	-0.009(1)	5.8(7)*
C(36)	0.011(2)	0.523(2)	0.004(1)	5.5(7)*
C(41)	0.059(2)	0.337(2)	0.055(1)	4.2(6)*
C(42)	0.019(2)	0.263(2)	0.0278(9)	3.9(5)*
C(43)	-0.059(2)	0.218(2)	0.048(1)	4.7(6)*
C(44)	-0.095(2)	0.249(3)	0.090(1)	6.5(8)*
C(45)	-0.063(2)	0.319(2)	0.116(1)	4.8(7)*
C(46)	0.019(2)	0.372(2)	0.098(1)	6.9(9)*

Estimated standard deviations in these and subsequent tables are given in parentheses and correspond to least significant digits. Starred atoms were refined isotropically. Anisotropically refined atoms are given in the form of the isotropic equivalent displacement parameter defined as:
$(4/3)[a^2\beta(1,1) + b^2\beta(2,2) + c^2\beta(3,3) + ab(\cos \text{gamma})\beta(1,2) + ac(\cos \text{beta})\beta(1,3) + bc(\cos \text{alpha})\beta(2,3)]$.

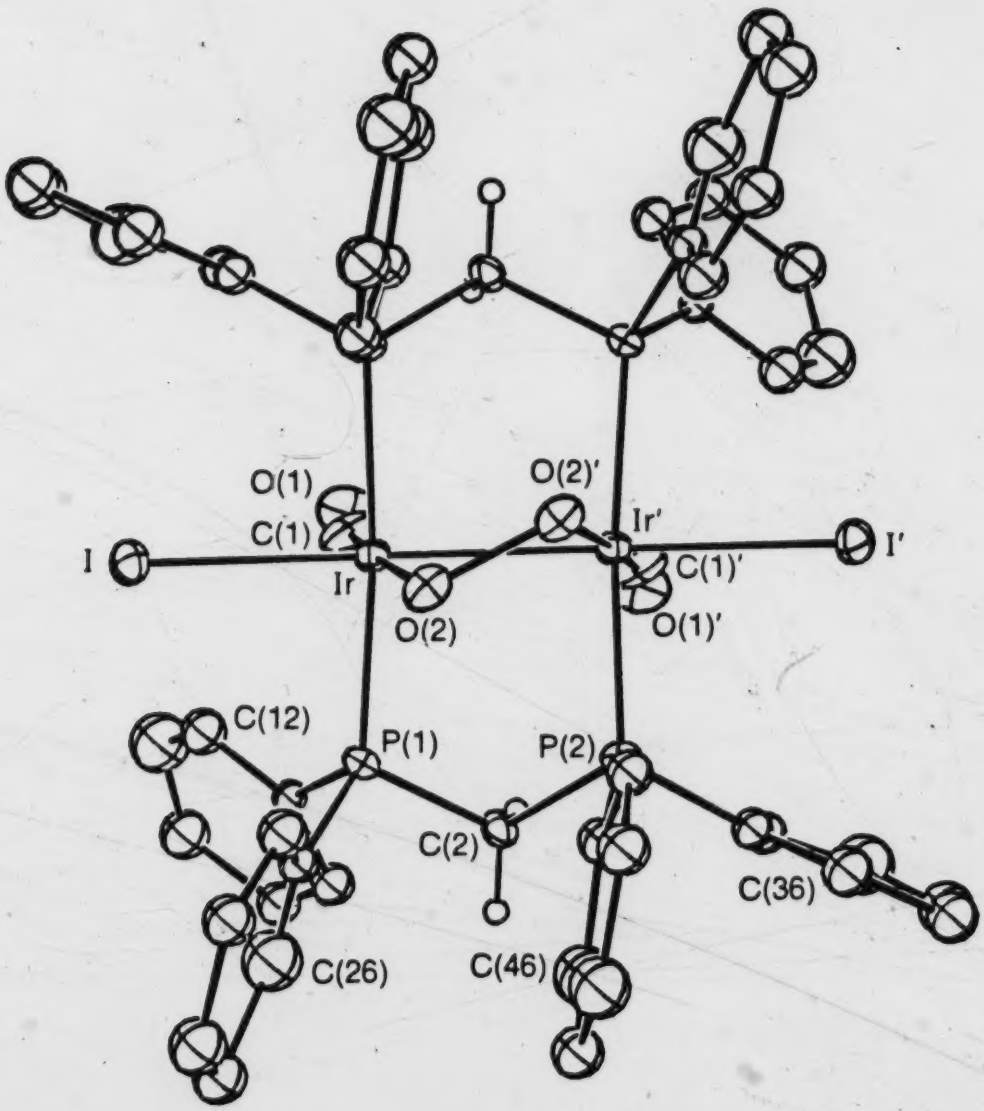

Figure A.1. Ortep plot of $[Ir_2I_2(CO)_2(\mu\text{-}O_2)(DPM)_2]$ showing the numbering scheme. Thermal parameters are shown at the 20% level except for hydrogen atoms, which are shown artificially small for the methylene groups and omitted for the phenyl groups.

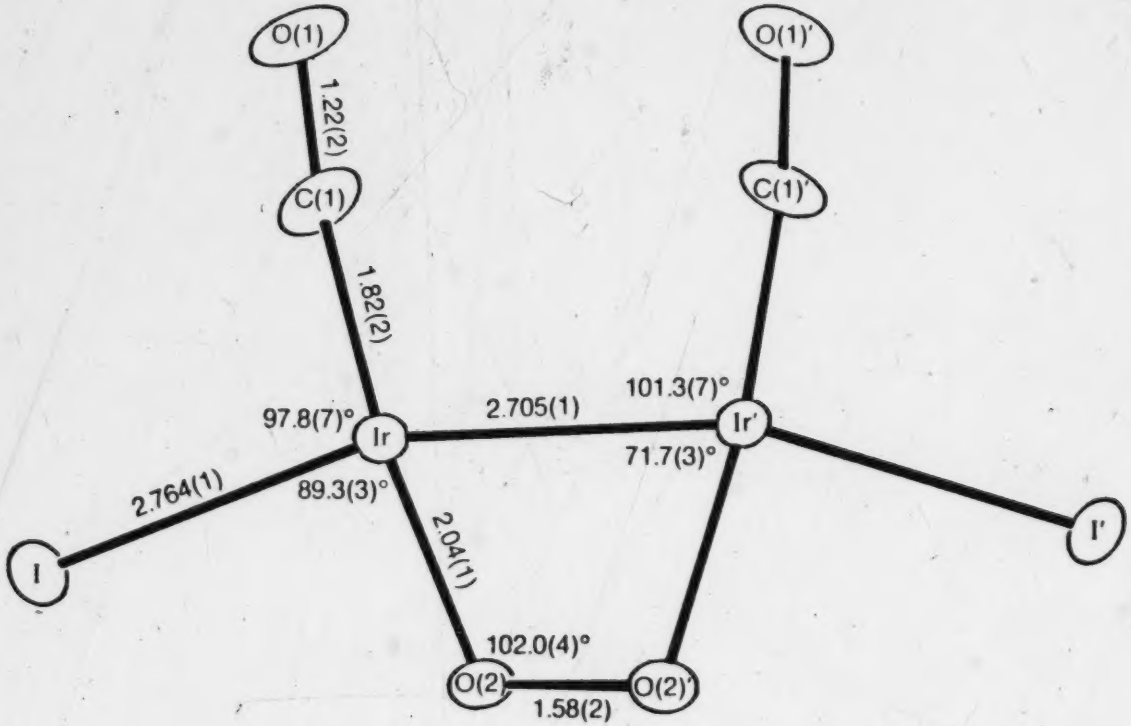

Figure A.2. A view of the approximate equatorial plane of the complex, including some relevant parameters.

Table A.3. Bond Distances (Å) in $[Ir_2I_2(CO)_2(\mu\text{-}O_2)(DPM)_2]$.

Ir-Ir'	2.705(1)	C(15)-C(16)	1.41(2)
Ir-I	2.764(1)	C(21)-C(22)	1.31(2)
Ir-P(1)	2.377(4)	C(21)-C(26)	1.18(3)
Ir'-P(2)	2.367(4)	C(22)-C(23)	1.36(3)
Ir-O(2)	2.04(1)	C(23)-C(24)	1.38(3)
Ir-C(1)	1.82(2)	C(24)-C(25)	1.39(3)
P(1)-C(2)	1.81(2)	C(25)-C(26)	1.55(3)
P(1)-C(11)	1.79(2)	C(31)-C(32)	1.41(2)
P(1)-C(21)	1.80(2)	C(31)-C(36)	1.35(3)
P(2)-C(2)	1.95(2)	C(32)-C(33)	1.31(3)
P(2)-C(31)	1.84(2)	C(33)-C(34)	1.24(3)
P(2)-C(41)	1.82(2)	C(34)-C(35)	1.32(3)
O(1)-C(1)	1.22(2)	C(35)-C(36)	1.44(3)
O(2)-O(2)'	1.58(2)	C(41)-C(42)	1.45(2)
C(11)-C(12)	1.35(2)	C(41)-C(46)	1.42(3)
C(11)-C(16)	1.37(2)	C(42)-C(43)	1.43(2)
C(12)-C(13)	1.36(3)	C(43)-C(44)	1.36(3)
C(13)-C(14)	1.44(3)	C(44)-C(45)	1.34(3)
C(14)-C(15)	1.54(3)	C(45)-C(46)	1.53(3)

Table A.4. Angles (deg) in $[Ir_2I_2(CO)_2(\mu\text{-}O_2)(DPM)_2]$.

Ir'-Ir-O(2)	71.7(3)	Ir-O(2)-O(2)'	102.0(4)
I-Ir-P(1)	88.5(1)	Ir-C(1)-O(1)	171.(2)
I-Ir-O(2)	89.4(3)	P(1)-C(2)-P(2)	106.0(8)
Ir'-Ir-C(1)	101.3(7)	P(1)-C(11)-C(12)	118.(1)
I-Ir-C(1)	97.8(7)	P(1)-C(11)-C(16)	117.(1)
P(1)-Ir-Ir'	94.6(1)	C(12)-C(11)-C(16)	125.(2)
P(1)-Ir-O(2)	89.5(3)	C(11)-C(12)-C(13)	122.(2)
P(1)-Ir-C(1)	89.6(6)	C(12)-C(13)-C(14)	121.(2)
O(2)-Ir-C(1)	172.7(7)	C(13)-C(14)-C(15)	113.(2)
Ir-Ir'-P(2)	90.5(1)	C(14)-C(15)-C(16)	122.(2)
Ir-P(1)-C(2)	114.8(5)	C(11)-C(16)-C(15)	116.(2)
Ir-P(1)-C(11)	114.9(5)	P(1)-C(21)-C(22)	124.(1)
Ir-P(1)-C(21)	116.5(5)	P(1)-C(21)-C(26)	113.(2)
C(2)-P(1)-C(11)	97.1(7)	C(22)-C(21)-C(26)	124.(2)
C(2)-P(1)-C(21)	103.3(7)	C(21)-C(22)-C(23)	122.(2)
C(11)-P(1)-C(21)	108.0(7)	C(22)-C(23)-C(24)	118.(2)
Ir'-P(2)-C(2)	110.0(5)	C(23)-C(24)-C(25)	123.(2)
Ir'-P(2)-C(31)	115.7(5)	C(24)-C(25)-C(26)	110.(2)
Ir'-P(2)-C(41)	121.9(5)	C(21)-C(26)-C(25)	124.(2)
C(2)-P(2)-C(31)	100.1(7)	P(2)-C(31)-C(32)	123.(1)
C(2)-P(2)-C(41)	102.4(8)	P(2)-C(31)-C(36)	122.(1)
C(31)-P(2)-C(41)	103.7(8)	C(32)-C(31)-C(36)	116.(2)

Table A.4. (Continued)

C(31)-C(32)-C(33)117.(2)	C(42)-C(41)-C(46) 123.(2)
C(32)-C(33)-C(34) 128.(3)	C(41)-C(42)-C(43) 118.(2)
C(33)-C(34)-C(35) 121.(3)	C(42)-C(43)-C(44) 119.(2)
C(34)-C(35)-C(36) 115.(2)	C(43)-C(44)-C(45) 126.(2)
C(31)-C(36)-C(35) 124.(2)	C(44)-C(45)-C(46) 120.(2)
P(2)-C(41)-C(42) 119.(1)	C(41)-C(46)-C(45)114.(2)
P(2)-C(41)-C(46) 118.(2)	

(Chapters 2, 4, 6 and references therein). Each metal center has a distorted octahedral geometry comprised of the two trans phosphorus atoms, a carbonyl group, an iodo ligand, one oxygen atom of the peroxo group and the Ir-Ir bond. The major distortion appears to arise due to the binding of the small O_2 molecule between the metals, resulting in an acute Ir'-Ir-O(2) angle of 71.7(3)°.

The O-O distance of the bridging O_2 moiety is extremely long, at 1.58(2) Å; this is much longer than the distance of 1.2074 Å in molecular oxygen[14] and is even longer than the typical peroxide bond distance (1.49 Å).[15] For dioxygen bound to Group VIII transition metals, O-O distances tend to be between these two values, with terminal η^2-bound peroxo complexes exhibiting O-O bond lengths in the range 1.30-1.52 Å.[1,15,16] Binuclear peroxo-bridged complexes usually display bond lengths in the upper portion of the same range. Apparently, the only other dioxygen complex having an O-O bond distance in the range of that found in **2** is a hydroxy-bridged diplatinum complex, $[Pt_2(O_2)(OH)(PPh_3)_4]^+$ (1.547(21) Å).[17] One longer distance reported (1.625(23) Å) for $[Ir(O_2)(Ph_2PCH_2CH_2PPh_2)_2]$-$[PF_6]$[18] was later shown to be incorrect,[19] and a distance of 1.52(1) Å was subsequently established. Such a long distance in this molecule is presumably due to significant reduction in O-O bond order through back-bonding from the electron rich metal into the π^* molecular orbital of O_2. Enhancement of the backbonding is no doubt a function of the basicity of the third-row metal, compared to the dicobalt complexes for which most structural information is available,[1] as well as the presence of the π-basic iodo ligands. It is to be emphasized here, that this complex is an unprece-

dented example of a peroxo-bridged metal-metal bond, and appears to be one of the longest O-O bond distances reported.

The overall geometry of the complex is rather reminiscent of the first dimetallacyclobutane, $[Os_2(\mu\text{-}C_2H_4)(CO)_8]$ reported by Norton et al.[20] In this diosmium species a twist of 27° about the Os-Os bond was attributed to deviation from an eclipsed conformation of the $Os(CO)_4$ units. The C-C distance of the bridging ethylene group (1.53(3) Å) corresponded to a normal single bond.

Coordination of the peroxo ligand is skewed such that the torsion angle, Ir-O(2)-O(2)'-Ir' is 34.6°, with the geometry at the oxygen atom thus resembling that of hydrogen peroxide and related derivatives.[21] Such a torsion angle is still not as severe as is normally found for cis-dimetallated O_2 in cobalt species which are unrestricted by metal-metal bonds or bridging ligands.[22,23] Associated with this geometry, the entire complex is twisted about the Ir-Ir axis such that the P(1)-Ir-Ir'-P(2) torsion angle is 16.4°. Similarly, the torsion angles C(1)-Ir-Ir'-C(1)' and O(2)-Ir-Ir'-O(2)' are 17.2° and 20.7°, respectively. The Ir-O(2)-O(2)' angle (102.0(4)°) is similar to the analogous angle found in $[Pt_2(O_2)(OH)(PPh_3)_4]^+$ (101.5(13)°),[17] but is rather acute compared to peroxo-bridged dicobalt complexes, where values of 110-120° are typical.[1] The Ir-O(2) bond distance (2.04(1) Å) is in agreement with typical Ir-O bond lengths of 2.00-2.07 Å found in terminal η^2-peroxo complexes,[15] and similar to those found in the platinum complex noted above.[17] A related binuclear diiridium species, $[Ir_2(CO)_2Cl_2(\mu\text{-}Ph_2P(CH_2)_3PPh_2)_2]$, was also found to react with dioxygen, but at one or both metal centers independently.[24] The X-ray structure of $[Ir_2(CO)_2Cl_2$-

$(O_2)(\mu\text{-}Ph_2P(CH_2)_3PPh_2)_2]$ revealed a terminally-bound η^2-dioxygen ligand with an O-O bond length of 1.477(11) Å and Ir-O bond lengths of 2.029(8) and 2.035(8) Å. A bridging dioxygen ligand is apparently not favored in this species due to the large distance between the metals (a result of the longer-chain bridging diphosphine ligand).

The Ir-I bond distance (2.764(1) Å) is longer than that of the Ir-I bond opposite the metal-metal bond in the precursor, compound **1** (2.6811(7) Å) (Chapter 2), but is still shorter than the Ir-I distance at the more crowded Ir center of **1**. The Ir-Ir' bond distance (2.705(1) Å) is significantly shorter than the metal-metal bond in **1** (2.8159(5) Å), which may be a consequence of the dioxygen bridge holding the metals closer together, as well as the positions of the iodo ligands which are both directed away from the congested sites between the metals in **2**.

(b) Description of Chemistry

Solutions of the diiodo complex, $[Ir_2I_2(CO)(\mu\text{-}CO)(DPM)_2]$ (**1**) are found to be sensitive to atmospheric oxygen, causing tetragonal prisms of the compound, $[Ir_2I_2(CO)_2(\mu\text{-}O_2)(DPM)_2]$ (**2**) to precipitate. The isolated dark purple solid proves to be relatively insoluble in a variety of solvents. Nevertheless, solution characteristics are obtained from *in situ* preparations of the complex. The $^{31}P\{^1H\}$ NMR spectrum of **2** displays a singlet (δ -24.40) indicating that all four phosphorus nuclei are equivalent, consistent with the symmetry revealed by the solid state structure. Infrared spectra indicate only terminal carbonyl stretches (2005, 1979 cm^{-1}) which

are shifted to higher frequency compared to the terminal carbonyl band (1948 cm^{-1}) of the precursor, **1**. This shift is consistent with the increase in the oxidation state of each metal to Ir(II), and the frequencies are similar to those of the Ir(II) dihydride complex, $[Ir_2(H)_2I_2(CO)_2(DPM)_2]$ (Chapter 5).

Oxygen addition to **1** is irreversible (no evidence for O_2 loss upon prolonged reflux in toluene), as was found in a related mononuclear iodoiridium complex, $[Ir(O_2)I(CO)(PPh_3)_2]$.[25] This is perhaps not surprising based on the degree of Ir-O bonding that is implied by the long O-O distance; however, it has been pointed out[26] that there seems to be no obvious correlation between this distance and O_2 lability.

Preliminary studies have been carried out on the reactivity of compound **2**. Dioxygen complexes have been observed to react with a wide variety of small molecules such as SO_2, NO_2, NO, CO_2, CO and activated alkynes.[8] Most of these reactions are well documented for mononuclear peroxo complexes, but much less has been done in the case of binuclear peroxo complexes.

Upon addition of excess SO_2 to a suspension of **2**, an immediate reaction occurs as evidenced by a color change to bright yellow and complete dissolution of the starting material. The $^{31}P\{^1H\}$ NMR spectrum of the solution indicates a single, symmetric species (δ -17.69(s)), and infrared stretches at 2079 cm^{-1} and 2039 cm^{-1} indicate retention of both carbonyl ligands. Additional absorbances in the infrared spectrum at 1260, 1140, 952 and 800 cm^{-1}, which are absent from the spectrum of **2**, are consistent with bands expected for a coordinated sulfate group.[27] The spectroscopy, along with elemental analyses which indicates one sulfur

are shifted to higher frequency compared to the terminal carbonyl band (1948 cm^{-1}) of the precursor, **1**. This shift is consistent with the increase in the oxidation state of each metal to Ir(II), and the frequencies are similar to those of the Ir(III) dihydride complex, $[Ir_2(H)_2I_2(CO)_2(DPM)_2]$ (Chapter 5).

Oxygen addition to **1** is irreversible (no evidence for O_2 loss upon prolonged reflux in toluene), as was found in a related mononuclear iodoiridium complex, $[Ir(O_2)I(CO)(PPh_3)_2]$.[25] This is perhaps not surprising based on the degree of Ir-O bonding that is implied by the long O-O distance; however, it has been pointed out[26] that there seems to be no obvious correlation between this distance and O_2 lability.

Preliminary studies have been carried out on the reactivity of compound **2**. Dioxygen complexes have been observed to react with a wide variety of small molecules such as SO_2, NO_2, NO, CO_2, CO and activated alkynes.[8] Most of these reactions are well documented for mononuclear peroxo complexes, but much less has been done in the case of binuclear peroxo complexes.

Upon addition of excess SO_2 to a suspension of **2**, an immediate reaction occurs as evidenced by a color change to bright yellow and complete dissolution of the starting material. The $^{31}P\{^1H\}$ NMR spectrum of the solution indicates a single, symmetric species (δ -17.69(s)), and infrared stretches at 2079 cm^{-1} and 2039 cm^{-1} indicate retention of both carbonyl ligands. Additional absorbances in the infrared spectrum at 1260, 1140, 952 and 800 cm^{-1}, which are absent from the spectrum of **2**, are consistent with bands expected for a coordinated sulfate group.[27] The spectroscopy, along with elemental analyses which indicates one sulfur

per binuclear unit, leads to the formulation below for compound **3** (DPM ligands are omitted for clarity).

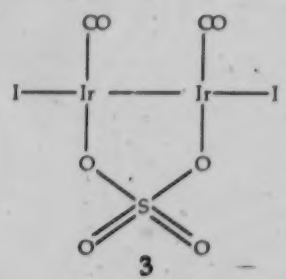

3

Compound **2** is also reactive toward NO_2, and IR evidence suggests the presence of coordinated nitrate in the final product (excess NO_2) with bands at 1503, 1259, 967 and 780 cm^{-1}. Further studies may show that the final species formed contains terminal nitrato ligands on each metal, analogous to reactions of mononuclear peroxo complexes that yield $M(NO_3)_2$ species,[28,29] however, studies remain incomplete at this time.

Preliminary studies on the reaction of **2** with $HBF_4 \cdot Et_2O$ indicate that more than one proton can be accepted by the peroxo complex. The ^1H NMR spectra reveal that hydrides are not involved, suggesting protonation at the peroxo oxygens, but these protons have not yet been found in the ^1H NMR spectrum. Addition of one and a half equivalents of $HBF_4 \cdot Et_2O$ to a suspension of **2** in CH_2Cl_2 causes an immediate color change to orange and dissolution of all the starting material (the extra half equivalent is necessary in order to react with all of **2**). The $^{31}P\{^1H\}$ NMR spectrum reveals two new symmetric species (δ -12.62(s), -16.74(s)) in nearly equal concentrations, and the infrared spectrum displays two sets of carbonyl stretches at 2081, 2044 cm^{-1} and 2023, 2001 cm^{-1}. Upon addition of excess $HBF_4 \cdot Et_2O$ the $^{31}P\{^1H\}$ NMR spectrum displays one singlet at δ -12.62

and only the carbonyl bands at 2081 and 2044 cm^{-1} remain. After each addition, an IR band at approximately 3400 cm^{-1} increases in intensity, which is further evidence for formation of O-H bonds in the reaction. Furthermore, the infrared stretches for the carbonyl groups corresponding to each of the new species are consistent with initial formation of a cationic species and excess H^+ finally yielding a dicationic species.

Compound **2** does not undergo addition reactions with CO or CO_2 to give the expected bridging carbonate complex.[8] It is also unreactive toward the activated acetylene, dimethylacetylenedicarboxylate (DMA). It was anticipated that this reaction might cleave the O-O bond in **2** and leave each oxygen bonded to one metal and one carbon of the alkyne, as occurs in a mononuclear platinum complex.[30] Attempts to remove one of the oxygen atoms with PMe_3 were also unsuccessful.

It is anticipated that reaction with weaker electrophiles might be possible upon removal of one iodo ligand from **2**, in order to create coordinative unsaturation. In this way the substrates might be further activated by the metal center, and not be required to react directly with the peroxo group. Further studies are underway to investigate these possibilities and to further characterize the products in the reaction of **2** with NO_2 and H^+.

References and Footnotes

1. Niederhoffer, E. C.; Timmons, J. H.; Martell, A. E. *Chem. Rev.* **1984**, *84*, 137 and references therein.
2. Sigel, H. ed. *Metal Ions in Biological Systems*, Dekker, New York, **1981**.
3. Collman, J. P. *Acc. Chem. Res.* **1977**, *10*, 265.
4. Gelling, O. J.; vanBolhuis, F.; Meetsma, A.; Feringa, B. L. *J. Chem. Soc., Chem. Commun.* **1988**, 552.
5. Karlin, K. D.; Cruse, R. W.; Gultneh, Y.; Farooq, A.; Hayes, J. C.; Zubieta, J. *J. Am. Chem. Soc.* **1987**, *109*, 2668.
6. Karlin, K. D.; Gultneh, Y. *J. Chem. Ed.* **1985**, *62*, 983.
7. Sheldon, R. A.; Kochi, J. K. *Metal-Catalyzed Oxidations of Organic Compounds*; Academic Press, New York, **1981**.
8. Gubelmann, M. H.; Williams, A. F. *Struct. Bonding (Berlin)* **1983**, *55*, 1.
9. Chisholm, M. H. ed., *Reactivity of Metal-Metal Bonds*, ACS Symposium Series 155, Washington DC, **1981**.
10. Doedens, R. J.; Ibers, J. A. *Inorg. Chem.* **1967**, *6*, 204.
11. Programs used were those included in the Enraf-Nonius Structure Determination Package by B. A. Frenz, in addition to local programs by R. G. Ball.
12. $R = \Sigma | |F_o| - |F_c| | / \Sigma |F_o|$; $R_w = [\Sigma w(|F_o| - |F_c|)^2 / \Sigma w F_o^2]^{1/2}$.
13. Puddephatt, R. J. *Chem. Soc. Rev.* **1983**, *12*, 98.

14. Cromer, D. T.; Waber, J. T. *International Tables for X-ray Crystallography*; Kynock Press, Birmingham, England, **1968**, *Vol. III*, Table 4.1.1.

15. Vaska, L. *Acc. Chem. Res.* **1976**, *9*, 175.

16. Cotton, F. A.; Wilkinson, G. *Advanced Inorganic Chemistry*, 4th ed., Wiley, New York, **1980**, p 156.

17. Bhaduri, S.; Casella, L.; Ugo, R.; Raithby, P.; Zuccaro, C.; Hursthouse, M. B. *J. Chem. Soc., Dalton Trans.* **1979**, 1624.

18. McGinnety, J. A.; Payne, N. C.; Ibers, J. A. *J. Am. Chem. Soc.* **1969**, *91*, 6301.

19. Nolte, M. J.; Singleton, E.; Laing, M. *J. Am. Chem. Soc.* **1975**, *97*, 6396.

20. Motyl, K. M.; Norton, J. R.; Schauer, C. K.; Anderson, O. P. *J. Am. Chem. Soc.* **1982**, *104*, 7325.

21. Reference 15, p 496.

22. Bouwman, E.; Driessen, W. L. *J. Am. Chem. Soc.* **1988**, *110*, 4440.

23. Lever, A. B. P.; Gray, H. B. *Acc. Chem. Res.* **1978**, *11*, 348.

24. Wang, H. -H.; Pignolet, L. H.; Reedy, P. E. Jr.; Olmstead, M. M.; Balch, A. L. *Inorg. Chem.* **1987**, *26*, 377.

25. McGinnety, J. A.; Doedens, R. J.; Ibers, J. A. *Inorg. Chem.* **1967**, *6*, 2243.

26. Laing, M.; Nolte, M. J.; Singleton, E. *J. Chem. Soc., Chem. Commun.* **1975**, 660.

27. Horn, R. W.; Weissberger, E.; Collman, J. P. *Inorg. Chem.* **1970**, *9*, 2367.

28. Cook, C. D.; Jauhal, G. S. *J. Am. Chem. Soc.* **1967**, *89*, 3066.

29. Critchlow, P. B.; Robinson, S. D. *Coord. Chem. Rev.* **1978**, *25*, 69.

30. Clark, H. C.; Goel, A. B.; Wong, C. S. *J. Am. Chem. Soc.* **1978**, *100*, 6241.

APPENDIX II

SOLVENTS AND DRYING AGENTS

$(CH_3)_2CO$	$CaSO_4$
CH_2Cl_2	P_2O_5
THF	Na/benzophenone
CH_3OH	Na
Et_2O	Na/benzophenone
C_6H_6	Na
C_7H_7	Na
hexanes	Na/K

All solvents were distilled from their respective drying agents under an atmosphere of dinitrogen in order to exclude oxygen.